

**In Vitro-In Silico Methods For Risk  
Assessment Of Organophosphate Pesticides  
(OPs) As Found In Commonly Consumed  
Vegetables In Kenya**



**Isaac Mokaya Omwenga**

## **Propositions**

1. The presence of organophosphate pesticide residues in vegetables from Peri-urban Nairobi, Kenya requires risk management actions.  
(this thesis)
2. Physiologically based kinetic modeling is essential for a novel approach in risk assessment of organophosphate pesticides.  
(this thesis)
3. Antimicrobial resistance poses an existential threat to humanity.
4. Epigenetics holds the key in unraveling the possible factors behind health and disease.
5. The wellbeing of a society is largely dependent on consistent political decisions made.
6. Persistence and endurance are the most essential virtues in a PhD journey.

Propositions belonging to the thesis, entitled

In vitro-in silico methods for risk assessment of organophosphate pesticides (OPs) as found in commonly consumed vegetables in Kenya

Isaac Mokaya Omwenga

Wageningen, 7 January 2022

**In vitro-in silico methods for risk assessment of  
organophosphate pesticides (OPs) as found in  
commonly consumed vegetables in Kenya**

**Isaac Mokaya Omwenga**

**Thesis committee:****Promotor**

Prof. Dr. I.M.C.M. Rietjens

Professor of Toxicology

Wageningen University & Research

Wageningen, The Netherlands

**Co-promotors**

Dr. J. Louisse

Scientific Researcher Toxicology

Wageningen Food safety Research

Wageningen, The Netherlands

Dr. Hans Mol

Senior Scientist pesticides, natural toxins, food safety & exposure

Wageningen Food safety Research

Wageningen, The Netherlands

**Other members**

Prof. Dr. Violette Geissen, Wageningen University & Research

Dr. Jessica Broeders, Board for the Authorization of Plant Protection Products and Biocides (CTGB)

Dr. Paul Scheepers, Radboud University Medical Center, Nijmegen

Dr. Remco Westerink, Utrecht University

This research was conducted under the auspices of the Graduate School VLAG (Advanced studies in Food Technology, Agrobiotechnology, Nutrition and Health Sciences).



**In vitro-in silico methods for risk assessment of  
organophosphate pesticides (OPs) as found in  
commonly consumed vegetables in Kenya**

**Isaac Mokaya Omwenga**

**Thesis**

submitted in fulfilment of the requirements for the degree of doctor

at Wageningen University

by the authority of the Rector Magnificus,

Prof. Dr. A.P.J. Mol,

in the presence of the

Thesis Committee appointed by the Academic Board

to be defended in public

on Friday 7 January 2022

at 13:30 p.m. in the Aula.

Isaac Mokaya Omwenga

In vitro-in silico methods for risk assessment of organophosphate pesticides (OPs) as found in commonly consumed vegetables in Kenya

296 pages

PhD thesis, Wageningen University, Wageningen, the Netherlands (2022)

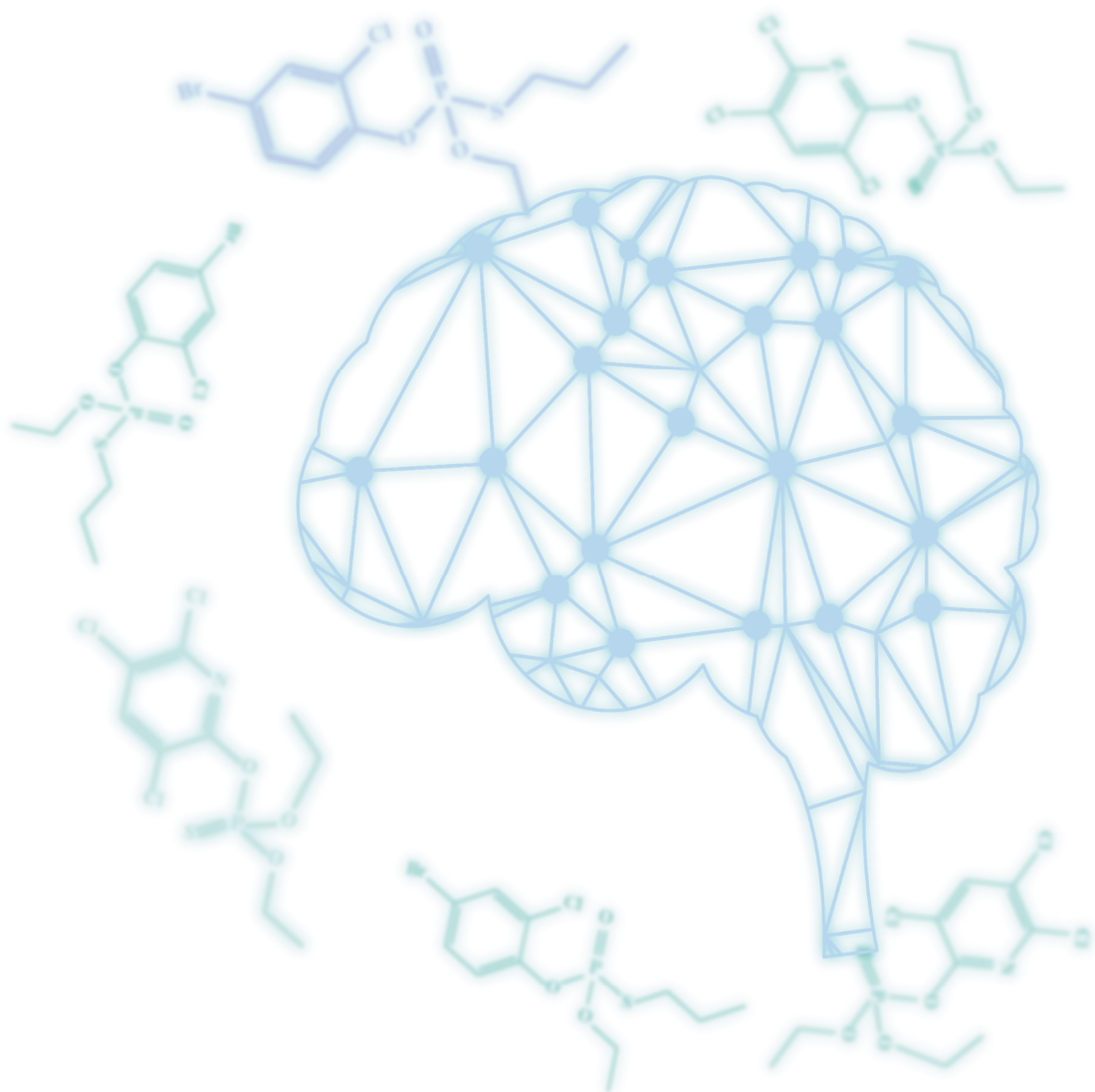
With references, with summary in English

ISBN: 978-94-6395-987-2

DOI-link: <https://doi.org/10.18174/553680>

# Contents

<b>Chapter 1.....</b>	<b>7</b>
<b>General Introduction</b>	
<b>Chapter 2.....</b>	<b>55</b>
<b>Organophosphate and Carbamate Pesticide Residues and accompanying risks in Commonly Consumed Vegetables in Kenya</b>	
<b>Chapter 3.....</b>	<b>95</b>
<b>Prediction of dose-dependent in vivo acetylcholinesterase inhibition by profenofos in rats and humans using physiologically based kinetic (PBK) modeling-facilitated reverse dosimetry</b>	
<b>Chapter 4.....</b>	<b>147</b>
<b>Prediction of in vivo acetylcholinesterase inhibition upon acute combined exposure to profenofos and chlorpyrifos by using a combined in vitro and in silico approach</b>	
<b>Chapter 5.....</b>	<b>189</b>
<b>Predicting interindividual differences in profenofos detoxification based on in vitro kinetic data and a physiologically based kinetic (PBK) and Monte Carlo modelling approach</b>	
<b>Chapter 6.....</b>	<b>221</b>
<b>General Discussion and Future Perspectives</b>	
<b>Chapter 7.....</b>	<b>281</b>
<b>Summary</b>	
<b>Appendices .....</b>	<b>289</b>
<b>Acknowledgements, About the Author, Overview of Completed Training Activities</b>	



# CHAPTER 1.

General Introduction

## GENERAL INTRODUCTION, AIM AND OUTLINE OF THE THESIS

### 1.1 Background

Pesticides are indispensable in improving the efficiency of food production processes, increasing crop yields, reducing the costs of food, as well as providing high-quality produce for the ever increasing world population. Previous reports have indicated that up to 40% of food production globally is lost annually due to pests, weeds and diseases (Oerke, 2006). In addition, pesticide use has shown to be beneficial in controlling pests of infrastructural and public health significance such as termites, mosquitoes, ants, roaches, rats, and other pests (Suratman et al., 2015). Pesticides distribution from targeted sites may follow different routes during spraying, allowing toxic chemicals access to beneficial and non-target organisms in the environment (Ngolo, 2019). Organophosphate pesticides (OPs) are esters of phosphoric acid, thiophosphoric acid, or other phosphoric acids and are applied in many insecticides, certain herbicides, and nerve agents (Edwards, 1973; Kushwaha et al., 2016). These chemicals were introduced to replace persistent and hazardous organochlorine pesticides (Chapalamadugu and Chaudhry, 1992; Pogačnik and Franko, 2003), becoming popular initially in the United States (Bonner et al., 2007) and then globally. However, most OPs have been classified by the World Health Organization (WHO) Food and Agriculture Organisation (FAO) and US Environmental Protection Agency (EPA) to be moderately or highly hazardous to non-target organisms including humans (WHO, 2009). OPs have been extensively used for the control of agricultural and household pests globally (Kumari and John, 2019). Exposure to these pesticides has been reported for various segments of the population, including agriculture workers and their families, house hold members during home application of pesticides, people that live in proximity to farms, or the general public via residues on food (Bradman et al., 2011; Lu et al., 2010). Studies worldwide reveal that infants and adults are exposed to OPs and carbamate pesticide residues as a consequence of their presence in food (Amaroli et al., 2013).

Furthermore, several studies have demonstrated that maternal exposure to food containing pesticides residues in the neonatal period as well as early infancy exposure can alter the development and function of the immune, nervous, endocrine and reproductive systems (Glynn et al., 2008; Grandjean et al., 2008; Borchers et al., 2010). In all these events, acetylcholinesterase (AChE) has been found to play a role in the modulation of cell proliferation (Angelini et al., 2004), apoptosis (Aluigi et al., 2010), cell-substrate interaction and messages mediated by ion changes (Aluigi et al., 2005). Recent studies provide insights on the mechanisms underlying the toxicity of neurotoxic pesticides, including, for example, AChE inhibitors (organophosphorus and carbamates) (Aardema et al., 2008) found in the environment and food from agricultural sites (Abdel Rasoul et al., 2008). A particular example is chlorpyrifos, whose exposure during the neonatal period and early infancy have been reported to alter the development and function of the nervous, immune, endocrine and reproductive systems (Glynn et al., 2008; Grandjean et al., 2008; Borchers et al., 2010), and has been shown to increase the risk of delays in mental and motor development and to cause an increased occurrence of pervasive developmental disorders such as Attention Deficit Hyperactivity Disorder (ADHD) (Rauh et al., 2006) following exposure of children while in the womb (Amaroli, 2013). Epidemiological studies have linked chronic OP exposure to reproductive disorders, developmental toxicity, birth defects, cancer, Parkinson's disease, Alzheimer's disease, diabetes, chronic respiratory disease, cardiovascular diseases, chronic nephropathies and amyotrophic lateral sclerosis (ALS) (Mostafalou & Abdollahi, 2013). The critical effects of OPs in animal studies are related to neurotoxicity (acute and chronic), of which some are mediated through inhibition of AChE, the enzyme that terminates the action of the neurotransmitter acetylcholine (ACh) within neuromuscular junctions and nerve tissue, leading to overstimulation of the post-synaptic membrane (Timchalk and Poet, 2008). Whereas acute OP toxicity is generally thought to be mediated by overstimulation of nicotinic and muscarinic

acetylcholine receptors due to AChE inhibition, chronic OP neurotoxicity is hypothesized to be due to receptor down-regulation. This leads to long-term neurological and neurobehavioral deficits (Costa, 2006; Costa, 2018), called organophosphorus ester-induced delayed neurotoxicity (OPIDN) or organophosphorus ester-induced chronic neurotoxicity (OPICN). OPs have not been found to be genotoxic, nor carcinogenic or teratogenic in chronic studies in rats (Ghorab and Khalil, 2015).

In the hazard and risk assessment of OPs, *in vivo* animal studies on OP-induced inhibition of brain or red blood cells (RBC) AChE have been used for various OPs to derive a point of departure (POD) such as a BMDL10 to set safe exposure levels, such as an Acute Reference Dose (ARfD). In these *in vivo* studies, AChE activity is usually measured in blood and sometimes also brain tissue after OP exposure. ARfDs for, for example, profenofos, chlorpyrifos, acephate, methamidofos and omethoate as reported by organizations as the European Food Safety Authority (EFSA), the United States Environmental Protection Authority (EPA), and the Joint FAO/WHO Meeting on Pesticide Residues (JMPR), have been derived from data on OP-induced AChE inhibition from animal studies (JMPR, 2007; EPA, 2006; EPA, 2011; EPA, 2016; EFSA, 2019). For example, PODs for profenofos and chlorpyrifos have been derived by estimation of exposure levels resulting in 10% RBC AChE inhibition following acute (single day, 24 hours) exposure. However, the reliance on approaches consisting of live animal experimentation has its drawbacks in terms of economical, ethical and scientific considerations (Van Norman, 2020; Wang et al., 2020; Huang et al., 2021). Consequently, the so-called principles of the 3Rs have been propagated in the later 1950s and reinforced in the European Union (Directives of the European Parliament), with the aim to Replace, Reduce and Refine (3Rs) the use of animals in scientific research (Russell and Burch, 1959; Flecknell, 2002; Amaroli et al., 2013; Kendall et al., 2018; Arck, 2019; Huang et al., 2021). Besides aiming for a reduction of animal use for toxicity testing, application of the 3Rs



are moving the field of chemical risk assessment to more mechanism-based *in vitro* and *in silico* approaches (Flecknell, 2002; Amaroli et al., 2013; Arck, 2019; Kendall et al., 2018). Furthermore, based on available data on pharmaceuticals, there have been concerns about the lack of concordance between animal and human toxicity and efficacy studies, which led scientists to question the value of animal studies requirement in determining drugs that should enter the last stage of trials (USFDA, 2006; Ewert et al., 2014; Milman, 2015; Van Norman, 2019; Abi-Gerges et al., 2019; Greenfieldboye, 2019; Van Norman, 2020). Although human data are in general lacking for non-pharmaceuticals, it can be expected that also for these chemicals, toxicity data obtained in animals may not always be representative for the human situation. Consequently, *in vitro* human tissue-based and *in silico* models have been developed as a replacement for animal *in vivo* models in testing of various compounds (Yang and Xiong, 2012). Indeed, *in vitro* approaches with cell cultures, organs-on-a-chip, organoids, 3D printed tissues (additive manufacturing), *in silico* computational biomodelling, and *ex vivo* tests using tissue from dead animals and humans have been developed to replace the use of live animals (Taylor, 2019; Huang et al., 2021; Van Norman, 2020). These models offer promise in overcoming the lack of correlation between animal and human toxicity studies (MacGregor et al., 2001; Thasler et al., 2006; Yang and Xiong, 2012). Moreover, *in vitro* studies facilitate exploration of cellular and molecular mechanisms underlying toxicity (Kendall, 2018). Consequently, the term “new approach methodologies” (NAMs) has emerged as a descriptive reference to these *in silico* or *in vitro* methods that can be utilized to predict data required for chemical hazard and risk assessment (Parish et al., 2020). These new approaches include integrated approaches to testing and assessment (IATAs), defined approaches for data interpretation, and performance-based evaluation of test methods (Parish et al., 2020).

With this view in mind, the present thesis aimed to assess whether *in vivo* dose-dependent OP-induced AChE inhibition can be predicted by a combined *in vitro*-*in silico* approach, allowing

to set an ARfD for OPs by an animal-free approach. To estimate the amount of OP that reaches the target (AChE), so-called physiologically based kinetic (PBK) models can be used. A PBK model is a set of mathematical equations that describe the absorption, distribution, metabolism, and excretion (ADME) characteristics of a chemical within an organism (Krewski et al., 1994; Chiu et al., 2007; Louisse et al., 2017). It is based on physiological and anatomical, physicochemical, and kinetic parameters (Louisse et al., 2017). A PBK model permits the simulation of the chemical's *in vivo* kinetics (ADME) and can relate external exposure to internal exposure at the target sites. Translating effect concentrations of chemicals obtained in relevant *in vitro* models representing *in vivo* target sites (internal exposure) with a PBK model allows the prediction of dose levels that cause toxicity (external exposure), also referred to as quantitative *in vitro* to *in vivo* extrapolation (QIVIVE) or PBK modelling facilitated reverse dosimetry. Indeed, the quantitative interpretation of toxic effects of compounds in *in vitro* studies, using *in silico* approaches including PBK modelling is a necessary component of the American National Academy of Sciences' vision on toxicity testing in the 21st century (Krewski et al., 2010).

Besides the use of PBK models for QIVIVE, PBK models are also of use for the interpretation of human biomonitoring data (Brown et al., 2015; Clewell et al., 2008; Campbell et al., 2011) and to better understand possible species differences in toxicokinetics and related differences in sensitivity to the chemical of interest. Only a handful of PBK models have been built for commonly used OPs (chlorpyrifos (Timchalk et al., 2002; Bouchard et al., 2005; Mosquin et al., 2009; Lu et al., 2010), malathion (Bouchard et al., 2003; Bogen and Singhal, 2017; Bouchard et al., 2017), parathion (Sultatos, 1990) and diazinon (Poet et al., 2004)), while for many more OPs PBK models are lacking.

The current thesis aimed at developing a non-animal approach for OP hazard assessment, that can be applied in next generation risk assessment (NGRA). The novel method developed allows

to quantitatively predict the potential of OP pesticides to inhibit AChE in vivo upon acute exposure, also taking combined exposure into account. Furthermore, this thesis aimed to obtain data on the occurrence of OPs on commonly consumed vegetables in Kenya, as such data, and related estimations of human exposure, are lacking. Kenya, a member of the East Africa community in the African continent, is a middle income country whose economy relies heavily on agricultural produce (including horticulture where vegetables are grown and floriculture). The use of chemical pesticides is indispensable in Kenya due to the hot and humid tropical environmental conditions that are conducive to the development of pests, weeds, and disease vectors (Omwenga et al., 2016).

## **1.2 Human exposure to OPs**

Exposure to OPs may be through the gastrointestinal tract following consumption of residues in food, via skin, or inhalation (Risher and Navarro, 1997; Smegal, 2000). Exposure to these pesticides has been reported for various segments of the population, including agricultural workers and their families, house hold members during home application of pesticides, people that live in proximity to farms, or the general public via residues on food (Quandt et al., 2004; Bradman et al., 2011). Consequently, OPs and their metabolites have been found in human blood, serum, urine, and breast milk (Hardt and Angerer, 2000; Liu et al., 2014; Zhang et al., 2014; Naksen et al., 2016; Nishihama, et al., 2021).

Consumption of conventionally grown fruits and vegetables provides the major pesticide exposure route for the general population (Bradman et al., 2015). In order to monitor the risk and adverse effects following exposure to pesticides, various pesticide monitoring programs have been implemented by various authorities in different countries and regions of the world. While the developed countries such as the USA, Canada and countries in the EU have implemented pesticide monitoring programs, providing information that can be used to estimate human exposure, in developing countries such information is lacking and health risk

assessments cannot be performed (Ecobichon, 2001). Furthermore, recent studies have shown that people of all ages especially in developing countries are increasingly being exposed to higher levels of OP pesticides as a consequence of the increased quantity of pesticide residues in food (Amaroli et al., 2013). Indeed, exponential increase in the use of these pesticides over the last 40 years has been reported globally, with an average rise up from 0.49 kg per hectare in 1961 to 2 kg in 2004, leading to the presence of these substances in the daily diet (Amaroli et al., 2013; Zhang, 2018). In other regions of the world such as the EU, there has been a reduction in pesticide use, accompanied by a decline in regulatory approvals of chemical substances used as pesticides, while the demand is increasing in many developing countries, which together account for a quarter of global pesticide use (UNICEF, 2018). Various studies have reported on the levels of pesticide residues in various food products, including milk products (Golge et al., 2018; Muhammad Arif et al., 2021), other animal products such as poultry and sheep fat (EFSA, 2019), cereals (Lozowicka et al., 2014; EFSA, 2019), olive oils (Razzaghi et al., 2018), fish (Sapozhnikova, 2014) and fruit and vegetables from various countries including Korea (Lee and Lee 2012) Chile (Elgueta et al., 2019) Indonesia ( Bhandari et al., 2019), China (Wang et al., 2019; Jiang et al., 2021), EU (EFSA, 2019), Turkey (Hepsağ and Kizildeniz, 2021), Canada (Wang et al., 2019) and USA (Baker et al., 2002; Hu et al., 2016; Chiu et al., 2018). However, few data are available on the presence and levels of pesticide residues on vegetables consumed in African countries, including Kenya. This thesis therefore includes a study on the levels of organophosphate and carbamate pesticide residues and accompanying calculated risks in commonly consumed vegetables in Kenya.

### **1.3 The model compounds of the present thesis: profenofos and chlorpyrifos**

In the present thesis two OPs, profenofos and chlorpyrifos (Figure 1) were studied to develop the proof-of-concept regarding the development of non-animal approaches to predict in vivo

dose-dependent effects on AChE activity upon single and combined exposure. These OPs were selected based on the findings of the study on the presence of OPs (and carbamates) on commonly consumed vegetables in Kenya (Chapter 2). Profenofos and chlorpyrifos are members of the OP group that have been extensively used for the control of agricultural and household pests globally (Kumari & John, 2019). They have been used extensively in agriculture and their residues have been detected concurrently in various vegetables (Kunyanga et al., 2018; Omwenga et al., 2021), indicating their relevance for consideration of combination effects. Generally, the toxicity of OPs and especially their oxon forms is related to phosphorylation of the serine residue of the AChE enzyme at the active site, leading to diminished ability to hydrolyze the neurotransmitter, acetylcholine (ACh).

Profenofos (O-(4-bromo-2-chlorophenyl) O-ethyl S-propyl phosphorothioate) is a thiophosphate OP pesticide (O=P-S-C) that exists in an active oxon form. The pesticide was developed for pest strains resistant to chlorpyrifos and other OPs (Gotoh et al., 2001). Profenofos has been classified as a moderately hazardous (Toxicity Class II) pesticide by the WHO with a moderate level of acute toxicity (LD<sub>50</sub> of 358 to 1178 mg/kg in rat) following oral administration (Reported in JMPR (2007)) (Table 1). Dietary intake of profenofos is the primary exposure route for humans (Greish et al., 2011) and residue levels exceeding EU maximum residue levels (MRLs) have been found in various vegetables in Kenya (Karanja et al., 2012).

Chlorpyrifos (chlorpyrifos, O, O-diethyl O-3,5,6-trichloropyridin-2-yl phosphorothioate, O, O-diethyl O-3,5,6-trichloro-2-pyridyl phosphorothioate, chlorpyrifos-ethyl) is a widely used thionophosphate OP (S=P-O-C) pesticide (Eaton et al., 2018). It has an LD<sub>50</sub> of 82–270 mg/kg bw (Qiao, 2010) following oral administration (Table 1). Chlorpyrifos's in vivo toxicity is a result of its bioactivation by cytochrome P450 (CYP)-mediated monooxygenases to a more potent AChE inhibitor, chlorpyrifos-oxon (CPO). This oxidation reaction, which proceeds

through a possible phosphooxythiiran intermediate, can result in either a desulfuration reaction that generates the oxon or a dearylation reaction that degrades the parent compound (Chambers, 1992; Timchalk et al., 2001).

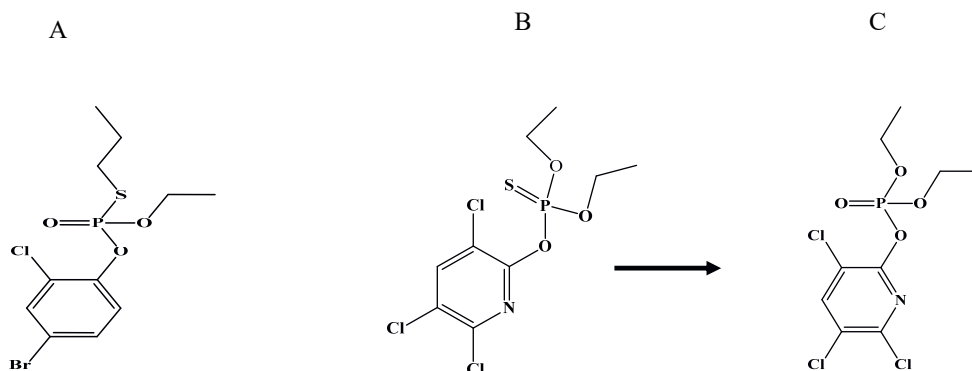


Figure 1. Chemical structures of profenofos (A), chlorpyrifos (B) and chlorpyrifos' toxic metabolite chlorpyrifos oxon (C).

#### 1.4 Absorption, Distribution, Metabolism and Excretion (ADME) of profenofos and chlorpyrifos

Following exposure, organophosphate pesticides such as chlorpyrifos require bioactivation by cytochrome P-450s (CYPs) to form the (more) active oxon metabolites which are potent AChE inhibitors, with the exception of a few OPs including profenofos which are already in an oxon form (Figure 1) (Ma and Chambers, 1994). Therefore, unlike other OPs that require metabolic activation, the parent compound profenofos is itself responsible for the AChE inhibition activity.

In general, profenofos exhibits rapid absorption and distribution with extensive metabolism and no accumulation in tissues (EPA, 2016). In a profenofos kinetic study in rats, recovery of radioactivity in fecal and urine samples ranged from 97-108% of the administered dose, with >97% of the radioactivity excreted in the urine within 48 hours (EPA, 2016, JMPR, 2007). Only less than 0.2% of the radioactivity was expired through air in volatile form. Furthermore, analysis of fecal material revealed that <4% of the parent compound or its metabolites remained unabsorbed or were excreted via the biliary system into the intestinal tract (JMPR, 2007). As shown in Figure 2 profenofos appears to be metabolized primarily by hydrolysis of its thiophosphate ester followed by dephosphorylation to form 4-bromo-2-chlorophenol (BCP), which undergoes sulfate or glucuronide conjugation (FAO, 2012; Dadson et al., 2013; EPA, 2016). Previous in vivo studies in rat identified conjugated and unconjugated 4-bromo-2-chlorophenol (BCP), *O*-ethyl-*O*-(2-chloro-4-bromo-phenyl)-phosphate, and thiophosphoric acid *O*-(4-bromo-2-chloro-phenyl) ester *O*'-ethyl ester (Figure 2) (Cho et al., 2002; EPA, 2016). Currently, no apparent sex or dose related differences in the absorption, distribution, metabolism, or excretion of profenofos have been demonstrated. In in vitro studies, also CYP-mediated formation of other metabolites has been reported (in the presence of inhibitors of hydrolysis enzymes) (Dadson et al., 2013), but these are considered less relevant, since based on these in vitro studies the hydrolysis reaction is expected to be more efficient than the CYP-mediated oxidations.

In a kinetic study involving young adult male rhesus monkeys, approximately 0.5 mg/kg bw of profenofos was administered and the results showed rapid profenofos absorption with significant concentrations measured in the blood and plasma at the first blood measurement (30 minutes post-dose) (EPA, 2016). The time to reach maximum concentration in the blood (T<sub>max</sub>) was 1 hour post-dose with a rapid decline in the blood concentration thereafter. In that study, the terminal phase elimination half-life (t<sub>1/2</sub>) was approximately 4 hours. Up to 68% of

the administered dose was recovered in the excreta (urine, faeces, and cage wash after 168 hours) with the majority recovered in the urine (49%) (US EPA, 2016), with ultimately complete excretion following treatment. The glucuronide conjugate of BCP was the main metabolite.

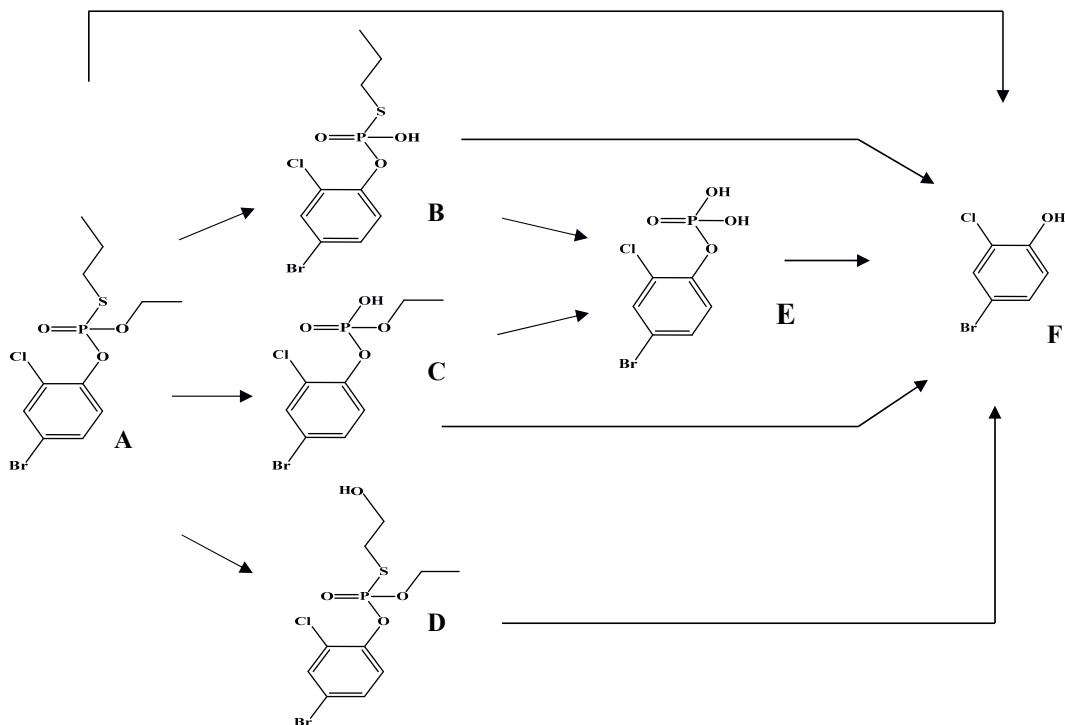


Figure 2. Metabolic pathways for metabolism of profenofos (A) based on data reported in previous studies (Gotoh et al., 2001; Dadson et al., 2013). Metabolites include desethylated profenofos (B), desthiopropylprofenofos (C), hydroxypropyl profenofos (D), 4-bromo-2-chlorophenyl dihydrogen phosphate (E), and 4-bromo-2-chlorophenyl (BCP) (F).



Chlorpyrifos kinetic data in experimental animals indicate that following oral exposure absorption is rapid. About 70% of the administered dose is absorbed following oral administration. Metabolism is complete, with 3,5,6-trichloro-2 pyridinol and its glucuronide and possibly sulfate conjugates being excreted. As shown in figure 3, once absorbed into the body, chlorpyrifos can be metabolized by CYP enzymes through diarylation (oxidative ester cleavage), forming 3,5,6-trichloro-2-pyridinol (TCPy) and diethylthiophosphate (DETP), or oxidative desulfuration, forming CPO which is the active form inhibiting AChE (Kamataki et al., 1976; Timchalk et al., 2002). These conversions are catalyzed by CYP enzymes, with CYP2B6 being the most active CYP for conversion of chlorpyrifos into CPO, and CYP2C19 being the most active CYP for conversion of chlorpyrifos into TCPy and DETP, whereas CYP3A4 is involved in both pathways (Foxenberg et al., 2007; Tang et al., 2001). CPO is converted by A-esterases, with paraoxonase 1 (PON1) as the main A-esterase involved, resulting in formation of TCPy and diethyl phosphate (DEP) (Furlong et al., 1989; Timchalk et al., 2002).

In general, chlorpyrifos has a short biological half-life of approximately 18 h in plasma and 62 h in fat tissue (Qiao, 2010). However, due to its very wide use, chlorpyrifos metabolites are commonly found in human tissue (fat tissue) (Bakke et al., 1976; Eaton et al., 2008). Excretion of chlorpyrifos metabolites as well as traces of chlorpyrifos occurs mainly through urine. In a chlorpyrifos kinetic study, a single dose of radioactive chlorpyrifos administered to rats (unspecified strain) at a dose of 50 mg/kg bw by gavage showed a 90.1% excretion of the administered radioactivity in 26 h, with 90% of the excreted material being in urine and 10% in feces. The metabolites excreted were [ $^{36}\text{Cl}$ ]-3,5,6-trichloro-2-pyridyl phosphate (75–80%)(DETP), 3,5,6-trichloro-2-pyridinol (TCPy) (15–20%), and traces of unmetabolized chlorpyrifos, indicating that deethylation is the main metabolic pathway in rats (Figure 3).

Furthermore, tissue residues of chlorpyrifos with a radioactive half-life of about 62 h were found mainly in fat tissue (Smith et al., 1967).

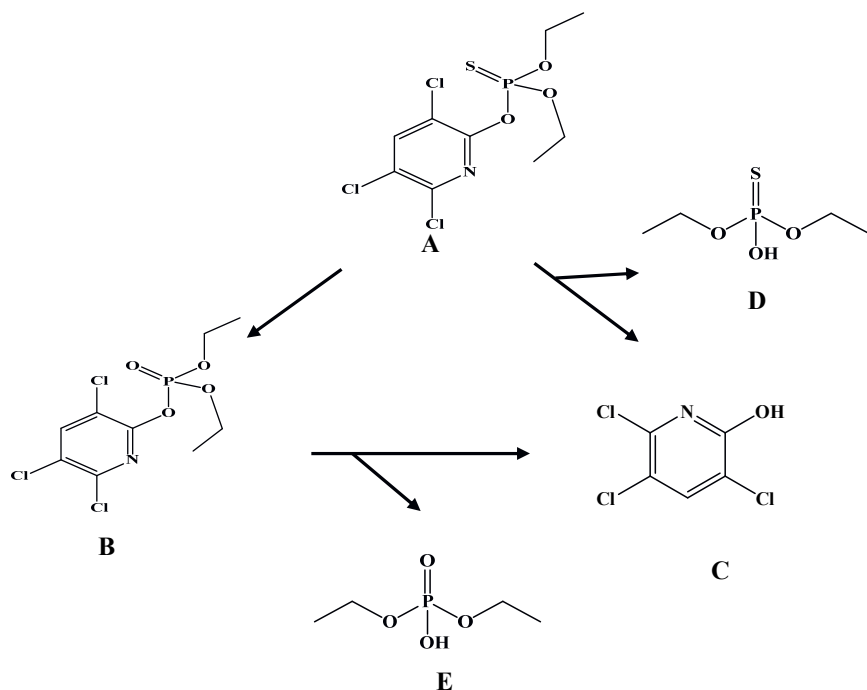


Figure 3. Metabolic pathways for metabolism of chlorpyrifos (A) based on data reported in previous studies (Eaton et al., 2008; Tang, et al., 2001). Metabolites include chlorpyrifos oxon (CPO) (B), 3,5,6-trichloro-2-pyridinol (TCPy) (C), diethyl thiophosphate (DETP) (D) and diethyl phosphate (DEP) (E).

## 1.5 Organophosphate Toxicity

OPs are primarily neurotoxicants, and exert their toxicity on the nervous systems of the target species (Casida, 2009). The OPs are non-species specific in their toxic effect, hence a wide range of mammals, humans included, are susceptible to their adverse effects. OP neurotoxicity can be broadly classified into two types: acute cholinergic toxicity and, in few instances, delayed neurotoxicity (Aldridge, 1981). A possible third type that falls in between acute and delayed neurotoxicity, referred to as the intermediate syndrome, characterised by muscular weakness, and developing once acute cholinergic symptoms have subsided, has been described in humans following severe OP poisoning.

The critical effects of OPs in animal studies are related to neurotoxicity, which has been reported to be related to, amongst others, inhibition of acetylcholinesterase (AChE), neuropathy target esterase (NTE) (Costa, 2018), acylpeptide hydrolase (APH) (Richards et al., 2000), fatty acid amide hydrolase (FAAH) (Quistad et al., 2001; Buntyn et al., 2017) muscarinic M2 receptors (Costa, 2006), and a variety of lipases (Quistad et al., 2006). Inhibition of AChE is one of the mechanisms by which OPs cause acute neurotoxicity (Jamal et al., 2002; Farahat et al., 2003). AChE inhibition occurs following hydroxyl group phosphorylation of the serine-OH in the enzyme active site by the P=O moiety of the OP, thus impeding its action on the physiological substrate. The hydrolysis of the phosphorylated enzyme proceeds at a very slow rate. Although some hydroxylamine derivatives have been found to facilitate reactivation of AChE, and hence are clinically used in the therapy of OP poisoning (Eyer, 2003), the dephosphorylation of the phosphorylated AChE fails once the enzyme-inhibitor complex loses one of the 2 alkyl (R) groups (by nonenzymatic hydrolysis) otherwise referred to as aging (Figure 4) (Quinn et al., 2017). The aged phosphorylated AChE is considered to be irreversibly inhibited, and de novo synthesis is the only possibility of replacing its activity, a process that takes days to occur (Sultatos, 2006).

AChE inhibition is characterized by decreased hydrolysis of acetylcholine in both central and peripheral cholinergic synapses, resulting initially in overstimulation of nicotinic and muscarinic receptors, followed by receptor down-regulation on post-synaptic membranes (Costa, 2006). Acute or repeated exposure to OPs can lead to a delayed neurotoxicity referred to as organophosphate ester-induced polyneuropathy (OPIDP), a neurodegenerative disorder caused by inhibition and aging of at least 70% of the activity of the neuropathy target esterase (NTE) present in nerve tissues as well as other tissues (e.g., lymphocytes, testis) (Johnson and Glynn, 1995; Johnson and Glynn, 2001; Costa, 2018). OPIDP is characterized by tingling of the feet and hands, followed by sensory loss, flaccidity of the distal skeletal muscles and upper extremities resulting from progressive muscle weakness and ataxia (Lotti and Moretto, 2005). These effects are encountered 2–3 weeks following OP exposure, mostly when eventual cholinergic toxicity signs have subsided.

Pathologically, OPIDP can be designated as a distal sensorimotor axonopathy, characterized by bilateral degenerative lesions in distal levels of axons and their terminals as the primary lesions, mainly affecting longer myelinated peripheral and central nerve fibers, eventually resulting in breakdown of myelin sheaths and neuritic segments (Ehrich and Jortner, 2010). Furthermore, OPs whose chemical structure leads to aging of phosphorylated NTE (by a chemical process similar to that for AChE) can cause OPIDP, implying that the aging of NTE is a key event in the initiation of OPIDP. Moreover, OPIDP is only initiated following phosphorylation and subsequent aging of at least 70% of NTE, a two-step pathway occurring hours following poisoning.

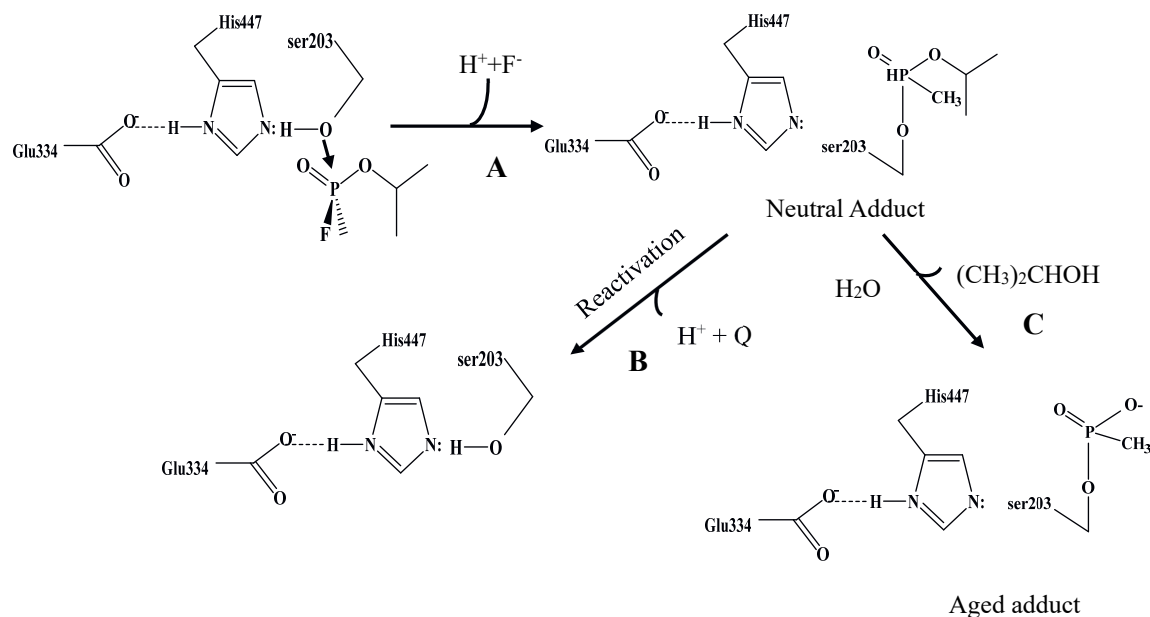


Figure 4. AChE inhibition by the organophosphorus nerve agent sarin based on previous studies (Quinn et al., 2017). The figure shows phosphorylation of the AChE enzyme (A), AChE enzyme reactivation (B) and AChE aging (Loss of one alkyl group through dealkylation) (C)

### 1.6 Hazard assessment of OPs

In the hazard assessment of OPs, in vivo animal studies on OP-induced inhibition of RBC AChE have been used to derive a point of departure (POD) to set safe exposure levels, such as an Acute Reference Dose (ARfD) (Table 1). ARfDs for chlorpyrifos, acephate, methamidofos, omethoate and profenofos as reported by organizations as the European Food Safety Authority (EFSA), United States Environmental Protection Authority (EPA), and the Joint FAO/WHO Meeting on Pesticide Residues (JMPR) have been derived from data on OP-induced RBC or brain AChE inhibition from animal studies (EPA, 2006; JMPR, 2007; EPA, 2011; EPA, 2016;

EFSA, 2019). For chronic exposure, in vivo animal studies with repeated-dosing have been conducted, with measurement of OP induced AChE inhibition as the end point (EPA, 2016). Although these in vivo studies do not measure complex neurotoxicity endpoints, the information on OP-induced inhibition of AChE in vivo is considered adequate in the hazard characterization to assess acute effects. In risk assessment of profenofos, JMPR used a NOAEL value of 100 mg/kg bw to derive an ARfD, based on a dataset on profenofos-induced inhibition of brain AChE in rats (upon a single exposure to profenofos). This NOAEL was then divided by a default uncertainty factor of 100 (10 for interspecies differences and 10 for intraspecies difference) to derive an ARfD of 1 mg/kg bw. Furthermore, the US EPA considered erythrocyte (RBC) AChE inhibition to be more suitable to derive a POD for human safety assessment, since it is more sensitive than brain AChE inhibition in case of profenofos exposure (EPA, 2016). A 10% RBC inhibition of AChE has been adopted by the US EPA to obtain a POD to define the ARfD for profenofos (EPA, 2016). The US EPA reported a BMDL10 of 1.99 mg/kg bw for profenofos-induced RBC AChE inhibition in adult rats upon a single exposure to profenofos. This BMDL10 was divided by a default uncertainty factor of 100 (10 for interspecies differences and 10 for intraspecies difference) to derive an ARfD of 0.0199 mg/kg/day. Furthermore, recent epidemiological studies have consistently identified associations between OP exposure and neurodevelopmental outcomes, for example attention problems, autism spectrum disorder in early childhood, delays in mental development in infants (24-36 months) as well as intelligence decrements in school age children. Consequently, there is a need for protection of children from OP exposures that could cause these effects. Based on this consideration the Food Quality Safety Act (FQPA) safety factor of 10 for interindividual variability has been added by the US EPA for some OPs including chlorpyrifos and profenofos for the population subgroups consisting of infants, children, women of childbearing age and youth for all exposure scenarios, resulting to an ARfD of 0.00199 mg/kg bw/day (EPA, 2016).

However, the FQPA safety factor does not apply in dietary exposures for the adult population subgroup 50-99 years old where the FQPA safety factor does not apply (total uncertainty factor = 100).

In a recent report from EFSA (EFSA, 2019), an ARfD for profenofos of 0.005 mg/kg bw was reported, based on a German evaluation in 2001 that defined an ARfD based on a NOAEL in a dog study using inhibition of brain cholinesterase activity as critical effect. Unfortunately, no further information (e.g. NOAEL) on that particular dog study is publicly available.

For chronic toxicity testing of profenofos, EPA (2016) conducted a 91-day repeated-dose study with RBC AChE inhibition as the end point in rats. In this study, data were obtained for both chronic effects as well as for tests on the ability of profenofos to induce carcinogenicity. A BMDL10 of 0.12 mg/kg bw/day associated with RBC AChE inhibition in male and female adult rats at the 13 week interim measurement was selected as a suitable POD for the steady-state dietary exposure scenario for all populations (Table 2). In the next step, an uncertainty factor of 1000 (10 to account for interspecies extrapolation, 10 for intraspecies variation, and 10 as an extra FQPA safety factor to account for uncertainty in the human dose-response relationship for neurodevelopmental effects) was applied to the BMDL10 to obtain a steady-state population-adjusted dose (ssPAD) of 0.00012 mg/kg bw/day for exposure scenarios with infants, children, youths, and women of childbearing age. Again, the FQPA safety factor does not apply in dietary exposures for the adult population subgroup 50-99 years old where the FQPA safety factor does not apply (total uncertainty factor = 100), hence the ssPAD for this population subgroup is 0.0012 mg/kg bw/day (EPA, 2016).

On the other hand, JMPR (2007) established an ADI of 0.03 mg/kg bw/day based on an overall NOAEL of 2.9 mg/kg bw/day derived from inhibition of brain AChE activity in three short-term studies in dogs and using a safety factor of 100. This ADI was supported by the NOAEL of 5.1 mg/kg bw/day identified based on inhibition of maternal and pup brain AChE activity in

a study of developmental neurotoxicity in rats and a NOAEL of 4.5 mg/kg bw per day identified on the basis of inhibition of brain AChE activity in a 2-year study in mice (JMPR, 2007).

For chlorpyrifos risk assessment, 20% inhibition of AChE has initially been described by EFSA to derive a suitable POD to define the acute reference dose for chlorpyrifos (EFSA, 2014). However, EPA in its risk assessment of chlorpyrifos derived a BMDL10 of 0.36 mg/kg bw resulting in 10% RBC AChE inhibition as POD (BfR, 2012; Koshlukova and Reed, 2014; Fan, 2014) (Table 1). Moreover, in the recent past, EPA indicated that 10% RBC AChE inhibition may not be adequately protective for human health since several studies suggest that adverse effects could occur even at lower levels of RBC AChE inhibition (EPA, 2016).

EFSA adopted an ARfD value of 0.005 mg/kg bw/ day based on a NOAEL of 0.5 mg/kg bw derived from rat RBC AChE inhibition, and applying an uncertainty factor of 100 (EFSA, 2014). On the other hand, US EPA used the Benchmark Dose (BMDL10) approach to derive reference values resulting in slightly lower values of 0.36 mg/kg bw using inhibition of RBC AChE as the critical effect (BfR, 2012; Fan, 2014; Koshlukova and Reed, 2014). Using the default factor of 100, the resulting ARfD is 0.0036 mg/kg bw/day.

For chronic exposure, the Acceptable Daily Intake (ADI) and Acceptable Operator Exposure Level (AOEL) were derived to be 0.01 mg/kg bw per day, based on long- and short-term studies respectively, in all species tested, with the application of an uncertainty factor (UF) of 100. The most sensitive end point the inhibition of RBC AChE was used to derive the ADI. In order to derive the Acceptable operator exposure levels (AOEL), a repeated dose study in juvenile and adult rats was used. In this study a NOAEL of 0.1 mg/kg bw per day based on RBC AChE inhibition was identified and an UF of 100 applied, resulting in an AOEL of 0.001 mg/kg bw per day, similar to the ADI.



As discussed above, the PODs for OPs including profenofos and chlorpyrifos have been derived by estimation of exposure levels resulting in 10% RBC AChE inhibition following acute oral exposure (single day, 24 hours). However, repeated exposures generally result in more AChE inhibition at a given administered dose compared to single exposures. Moreover, AChE inhibition in repeated dosing toxicological studies with OPs exhibit a consistent pattern of inhibition that reaches a steady state at approximately 2-3 weeks of exposure in adult laboratory animals (U.S. EPA, 2016). This phenomenon observed in repeated dosing results from the equilibrium achieved between the inhibited enzyme and the de novo synthesis of new enzyme. Consequently, AChE short term studies of 2-3 weeks generally exhibit inhibition activity similar to those of longer duration (i.e., up to 2 years of exposure)

Table 1. PODs as derived by various regulatory bodies.

Study type	Species	LD50 (mg/kg bw)	NOAEL (mg/kg bw/day)	LOAEL (mg/kg bw/day)	Endpoint used	References
<b>Chlorpyrifos</b>						
Short term			0.5		RBC AChE	EFSA, 2014
2 year	Rat, dog		0.1		RBC AChE	EFSA, 2014
Short term, oral	Rat	82–155	1.0	5	Sings of Cholinergic poisoning	Clegg and Gemert, 1999
	females					
Short term, oral	Rat		1		RBC AChE inhibition	JMPR, 1999
Short term, oral	human		0.5		RBC AChE inhibition	Clegg and Gemert, 1999
Repeated dosing	human		0.1		RBC AChE inhibition	Clegg and Gemert, 1999
<b>Profenofos</b>						
Short term, oral	Rat	358–1178			Sins of Cholinergic poisoning	JMPR, 2007
Short term	Rat		100		Brain AChE inhibition	JMPR, 2007
2 year toxicity	Rat		5.7			JMPR, 2007

Table 2. Profenofos and chlorpyrifos BMD10 and BMDL10 results (mg/kg bw/day) for RBC AChE inhibition over time in adult rats (profenofos data are taken from EPA, 2016 while data for chlorpyrifos are from BfR, 2012 and EFSA, 2014)

Dosing days	Males		Females	
	BMD10 (mg/kg bw/day)	BMDL10 (mg/kg bw/day)	BMD10 (mg/kg bw/day)	BMDL10 (mg/kg bw/day)
<b>Profenofos</b>				
1	13.49	11.24	3.17	1.99
10	NMF	NMF	0.38	0.17
35	NA	NA	0.32	0.19
90	0.33	0.29	0.66	0.54
91	0.14	0.12	0.13	0.12
364	0.17	0.15	0.22	0.18
<b>Chlorpyrifos</b>				
1 (BfR, 2012) 10% RBC AChE inhibition				0.36
1 (EFSA, 2014) 20% RBC AChE inhibition				0.5
NMF- No model fit				
NA- Not applicable				

## 1.7 PBK modelling-based reverse dosimetry

The concentration-response curves obtained from in vitro models are inadequate for human risk and safety assessment because risk assessment requires in vivo dose-response curves from which points of departure (PODs) can be derived for defining safe exposure levels. Consequently, the use of current non-animal based testing strategies requires a method to translate the in vitro concentration-response curves to in vivo dose-response curves that can replace the data from animal bioassays (Archibald et al., 2011). As earlier discussed (see background section), experimental animals may not be good models to predict toxicity effects in humans (Shanks et al., 2009; Crump et al., 2010) hence the vivo dose-response curves defined should relate closely to humans rather than to rodents (Louisse et al., 2017). To bridge the gap between in vitro alternative testing strategies and the needs of modern risk assessment for in vivo data, the application of so-called physiologically based kinetic (PBK) modeling-

based reverse dosimetry provides the solution. The principle is based on the use of PBK models to translate in vitro concentration-response curves to in vivo dose-response curves for various species including human. This approach can provide dose-response curves for toxicity in human provided that the PBK models used, and preferably also the cell models used, relate to the human situation.

The PBK model is used in the reverse order when the PBK modeling-based reverse dosimetry is applied. In that case the PBK model is used to calculate the dose level that would be needed to obtain the concentration of a compound or of its metabolite in the blood or in a tissue of interest. Reverse dosimetry has been successfully used to estimate exposure using biomonitoring data (e.g. chemical levels in blood and urine). Examples include estimation of exposure to chlorpyrifos in rats and humans (Timchalk et al., 2002), and chlorpyrifos in children (Rigas et al., 2001). Furthermore, these models can be used for reverse dosimetry of in vitro toxicity data, thereby translating in vitro effect concentrations to in vivo doses, enabling prediction of in vivo dose-dependent toxicity, as has been shown for the OP chlorpyrifos (Zhao et al., 2019). Such PBK modeling-facilitated reverse dosimetry of in vitro toxicity data is considered crucial in the transition to non-animal based new approach methodologies (NAMs) for the safety assessment of chemicals (Louisse et al., 2017). Scientific approaches for risk assessment prefer the use of human data, and this requires the development of novel human in vivo testing strategies (Krewski et al., 2010). Therefore, this thesis also aims to develop an approach using in vitro toxicity data combined with PBK modelling facilitated reverse dosimetry to predict in vivo acute AChE inhibition. For the reverse dosimetry approach to be performed, in vitro concentrations of the chemical need to be set equal to a relevant dose metric in the PBK model, such as a maximal blood concentration or the area under the concentration-time curve (AUC) in the blood or in a specific target tissue (Rietjens et al., 2019; USEPA, 2014b). Since the aim here is to predict OP-induced RBC AChE inhibition upon acute exposure,

the relevant dose metric chosen for reverse dosimetry in this thesis was the maximum concentration in blood. This is in line with previous studies that have demonstrated that PBK modeling-facilitated reverse dosimetry of OP in vitro toxicity data may adequately predict inhibition of OP based RBC AChE, as demonstrated for the OP chlorpyrifos (Zhao et al., 2019).

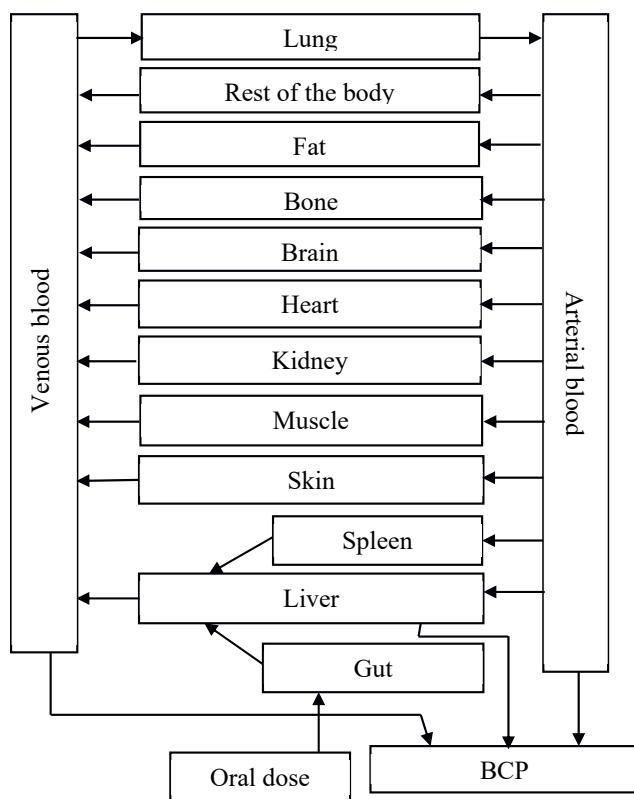


Figure 5. Schematic diagram of the PBK model for profenofos for rats and humans as developed in this thesis (Chapter 3).

### 1.8 Taking combination exposure into account in risk assessment

Since a variety of pesticides is being used, environmental, occupational and dietary exposures are primarily to pesticide mixtures. As a result, there is lifelong combined exposure to various pesticides from, for example, one food item containing multiple compounds or combinations of food items, each containing different residues (Boobis et al., 2008). If these pesticides have a similar mode of action and toxic end point, assessing the dietary risk of exposure for each pesticide separately may lead to underestimation of the health risk (Boon et al., 2008). Also, the EU Scientific Committees on Health and Environmental Risks (SCHER), on Consumer Safety (SCCS), and on Emerging and Newly Identified Health Risks (SCENIHR) have recently indicated that the health effect from combination exposure could be greater than the effect from individual compound exposure (SCCS, SCHER, SCENIHR, 2012). For this reason, current approaches in pesticide risk assessment include cumulative and probabilistic approaches in order to include the amount and variety of pesticide residues likely to be present in the vegetable sample (Jensen et al., 2015; Boon et al., 2015; Elgueta et al., 2019). The first step in assessing effects of combined exposure to pesticide mixtures is to identify substances with a similar mode of toxicity (Gallagher et al., 2015; EFSA, 2019). For example, AChE inhibitors, such as OPs and carbamates have been assigned the same cumulative assessment group (CAG) by the United States Environmental Protection Agency (US EPA) as well as by the European Food Safety Authority (EFSA) (USEPA, 2006, 2007, 2011; EFSA, 2019). For chemicals in the same CAG, the current scientific and regulatory recommendations for the risk assessment of mixtures follows a test strategy based on a component-based assessment, a concept with dose addition as the default model (Kortenkamp et al., 2009; EFSA et al., 2013; Bopp et al., 2015; EFSA et al., 2019).

On the other hand, substances with a different mode of action are assumed to have independent action since these substances induce effects through different modes of action devoid of

interaction with each other (Drescher and Boedeker, 1995; Medlock Kakaley et al., 2019). Therefore, response addition principles can be applied, hence it is assumed that there is no need for a combined risk assessment if exposure of the respective chemicals is for each chemical in the mixture below levels that cause adverse effects when testing the chemical in isolation. However, when no information on the mode of action is available, dose/concentration addition should be considered (Staal and van der Ven, 2016). When the dose additivity approach is used, the hazard index (HI) and toxic equivalency factor (TEF) are commonly applied to facilitate the combined risk assessment (Staal and van der Ven, 2016). The HI is the sum of the hazard quotients (HQs) for compounds that affect the same target organ or organ system. HQs are defined as the ratio of the exposure (for example, EDI) and a safe dose (an acceptable or tolerable daily intake (ADI or TDI) for chronic exposure (te Biesebeek et al., 2021) or an ARfD for acute exposure (Boobis et al., 2008; OECD, 2018). If the HI is lower than 1, it implies that the levels of the toxicants are not likely to elicit the adverse effect even during a lifetime exposure (when based on an ADI/TDI), whereas a HI higher than 1, implies that adverse effects cannot be excluded and should therefore be evaluated case by case to see which exposure adds the most to the HI and exceedance of relevant health based guidance values (HBGVs) and to direct potential risk management actions (Boobis et al., 2008; te Biesebeek et al., 2021).

For evaluation of combined exposure by dose addition also the so-called toxic equivalency (TEQ) approach applying toxic equivalency factors (TEFs) is preferred to evaluate the combined exposure to structurally related compounds with a similar mode of action but different potency (Delistraty, 1997). The TEQ method takes into consideration the differences in toxicity between congeners. The TEF for each individual congener is expressed as the ratio of the dose or concentration inducing a defined level of toxicity, such as for example the EC50, from the compound of interest and from the reference compound;

$$\text{TEF} = \text{EC50 reference compound} / \text{EC50 compound X}$$

The total value called the toxic equivalency (TEQ) value for a mixture is calculated by the sum of each compound's dose or concentration multiplied by its corresponding TEF value. Both profenofos and chlorpyrifos share a similar mode of toxicity, hence belong to the same CAG related to brain and/or RBC AChE inhibition (EFSA et al., 2019). Therefore, a dose additivity approach can be used. For this dose additivity approach, the hazard index (HI) and toxic equivalency factor (TEF) may also be used to perform the combined risk assessment (Staal and van der Ven, 2016).

### 1.9 Goal of the research and thesis overview

The main aim of the research was to develop a non-animal based combined in vitro and in silico approach to predict in vivo AChE inhibition upon acute exposure to single pesticides as well as to a combined exposure to pesticides. To define the model compounds for the studies, first organophosphate and carbamate pesticide residues were determined in commonly consumed vegetables in Kenya. Only OP pesticides were detected of which profenofos was most abundant in the samples assessed. Therefore, profenofos PBK models were developed based on in silico and in vitro input data for rats and humans, and the models were applied for reverse dosimetry of in vitro data on profenofos-induced AChE inhibition. Chlorpyrifos was found to be present on some of the vegetable samples together with profenofos. In a next step, a combined in vitro-in silico approach was developed to predict the effects of combined acute exposure to profenofos and chlorpyrifos on in vivo AChE activity. Finally, human interindividual differences in profenofos detoxification were assessed in vitro and these data were combined with a Monte Carlo simulation approach, to predict human interindividual differences in internal profenofos exposure and related consequences on AChE activity, all without the need for in vivo studies.

**Chapter 1** of the thesis (this chapter) starts with providing background information on OP use in agriculture, the exposure of non-target species to OPs and a description of the characteristics

and toxicity of the OPs studied in this thesis, profenofos, and chlorpyrifos. This chapter also presents background information on the hazard assessments for profenofos and chlorpyrifos and presents the concepts of PBK modelling-based reverse dosimetry and approaches used to assess combined exposure.

**Chapter 2** analyses the occurrence of OPs in commonly consumed vegetables in Kenya and assesses the accompanying exposure and health risks. A total of 90 samples were analysed by liquid chromatography/high-resolution tandem mass spectrometry. Exposure analysis and risk characterization was conducted using the acute/short-term hazard quotient (aHQ) for potential health risks emanating from short term intake and the chronic/long-term hazard quotient (cHQ) for potential health risks from long term consumption of contaminated vegetables. The risk assessment of the cumulative chronic exposure to residues was performed by summing the chronic Hazard Quotients (cHQ) for the individual pesticide residues as Hazard Index (HI) =  $\Sigma$ cHQ.

**Chapter 3** proposes a combined in vitro-in silico approach to predict AChE inhibition by the OP profenofos in rats and humans by applying PBK modelling-facilitated quantitative in vitro to in vivo extrapolation (QIVIVE). A PBK model was developed for both species. Parameter values for profenofos conversion to 4-bromo-2-chlorophenol (BCP) were derived from in vitro incubations with liver microsomes, liver cytosol, and plasma from rats and humans whereas other chemical-related parameter values were derived using in silico calculations. The PBK model predictions were evaluated by comparison to literature data on profenofos kinetics in rats following oral exposure (Cho et al., 2002). Following model evaluation, the concentration-dependent inhibition of rat and human AChE was determined in vitro and these data were translated with the PBK models to predicted dose-dependent AChE inhibition in rats and humans in vivo.



**Chapter 4** investigates the combination effects of two selected OPs (profenofos and chlorpyrifos), by studying the combined effects of profenofos and chlorpyrifos's toxic metabolite chlorpyrifos oxon (CPO) on AChE inhibition *in vitro*, as well as the effects of chlorpyrifos and CPO on profenofos biotransformation (detoxification) by human liver microsomes, cytosol, and human plasma. The profenofos physiologically based kinetic (PBK) model developed in chapter 3 was extended to include the description of chlorpyrifos kinetics, using also *in vitro* kinetic data from the literature and *in silico* calculations. The profenofos concentrations in the model are expressed as CPO-equivalents (i.e., using a TEF/RPF approach) allowing prediction of total internal CPO-equivalents (and related effects on AChE activity) upon combined exposure to profenofos and chlorpyrifos.

**Chapter 5** aimed to predict human interindividual differences in profenofos detoxification based on a combined *in vitro-in silico* approach to account for human variability in toxicokinetics. To that end, profenofos conversion to BCP was studied in *in vitro* incubations with S9 liver fractions of 25 different Caucasian donors and with plasma samples of 25 different Caucasian donors. The obtained information on the variation in the *in vitro* kinetic constants  $V_{max}$  and  $K_m$ , was applied in the PBK model developed in Chapter 3 using a Monte Carlo simulation modelling approach. Internal concentrations were estimated for the geometric mean (GM), the 90<sup>th</sup>, 95<sup>th</sup> and 99<sup>th</sup> percentiles of the simulated virtual population. The model was then used for reverse dosimetry of the *in vitro* data on profenofos-induced AChE inhibition of Chapter 3. Also, the interindividual variability in profenofos toxicokinetics was quantified by dividing the internal  $C_{max}$  concentrations of profenofos for the 90<sup>th</sup> or 99<sup>th</sup> percentile by that of the GM, which was compared to the default uncertainty factor for interindividual differences in kinetics (IPCS 2005). The predicted BMDL10 for the 99<sup>th</sup> percentile was compared to PODs of the regulatory bodies.

Finally, **Chapter 6** summarizes the main outcomes of this thesis and compiles the overall discussion. The chapter discusses: (i) the potential health concerns raised by OP exposure through consumption of vegetables contaminated by OP pesticide residues in peri-urban Nairobi, Kenya, (ii) the benefits and challenges of using PBK modelling-based reverse dosimetry to predict OP-derived neurotoxicity endpoints, (iii) OPs and long term effects considering neurodegenerative diseases including Parkinsonism and (iv) risk assessment of combined exposure to OPs and to OPs and other types of pesticides. Finally, the chapter provides further considerations for further studies on OPs and their effects in humans and assessment of exposure through contaminated foodstuff such as vegetables globally as well as locally (i.e., Kenya).

## REFERENCES

- Aardema, H., Meertens, J.H., Ligtenberg, J.J., Peters-Polman, O.M., Tulleken, J.E., and Zijlstra, J.G. (2008). Organophosphorus pesticide poisoning: cases and developments. *The Netherlands Journal of Medicine* 66, 149–153.
- Abi-Gerges, N., McMahon, C., Vargas, H., et al. (2019). The west coast regional safety pharmacology society meeting update: filling in the translational gaps in safety assessment. *J Pharmacol Toxicol Methods* 2019;98:106582.
- Arck, P.C. (2019). When 3 Rs meet a forth R: Replacement, reduction and refinement of animals in research on reproduction. *J Reprod Immunol.* 132:54-59.
- Aldridge, W. N. (1981). Organophosphorus compounds: Molecular basis for their biological properties. *Sci. Prog.* 67, 131–147.
- Aluigi, M.G., Angelini, C., Falugi, C., Fossa, R., Genever, P., Gallus, L., Layer, P.G., Prestipino, G., Rakonczay, Z., Sgro, M., Thielecke, H., and Trombino, S. (2005). Interaction between organophosphate compounds and cholinergic functions during development. *Chemical Biological Interaction* 157–158, 305–316.
- Aluigi, M.G., Guida, C., and Falugi, C. (2010). Apoptosis as a specific biomarker of diazinon toxicity in NTERA2-D1 cells. *Chemical Biological Interaction* 187, 299–303.
- Amaroli, A., Aluigi, M.G., Falugi, C., and Chessa, M.G. (2013). Effects of the neurotoxic thionophosphate pesticide chlorpyrifos on differentiating alternative models. *Chemosphere.* 90(7):2115-22.
- Angelini, C., Baccetti, B., Piomboni, P., Trombino, S., Aluigi, M.G., Stringara, S., Gallus, L., and Falugi, C. (2004). Acetylcholine synthesis and possible functions during sea urchin development. *European Journal of Histochemistry* 48:235–243.
- Archibald, K., Coleman, R., Foster, C., and Signatories, O. (2011). Open letter to UK Prime Minister David Cameron and Health Secretary Andrew Lansley on safety of medicines. *Lancet*, 377, 1915-1915.
- Baker, B.P., Benbrook, C.M., Groth, E., and Lutz Benbrook, K. (2002). Pesticide residues in conventional, integrated pest management (IPM)-grown and organic foods: insights from three US data sets. *Food Addit Contam.* 19(5):427-46.
- Bakke, J.E., Feil, V.J., and Price, C.E. (1976). Rat urinary metabolites from O,O-diethyl-O-(3,5,6-trichloro-2-pyridyl) phosphorothioate. *J. Environ. Sci. Health Bull.* 3:225–230.
- BfR., 2012. Reconsideration of the human toxicological reference values (ARfD, ADI) for

- chlorpyrifos—BfR opinion No 026/2012, 1 June. Available at: <https://www.bfr.bund.de/cm/349/reconsideration-of-the-human-toxicological-referencevalues-arfd-adi-for-chlorpyrifos.pdf>. Accessed January 23, 2021.
- Bhandari, G., Zomer, P., Atreya, K., Hans G.J. m., Yang, X., and Geissen, V. (2019). Pesticide residues in Nepalese vegetables and potential health risks. *Environmental Research*, <https://doi.org/10.1016/j.envres.2019.03.002>
- Bradman, A., Quiros-Alcala, L., Castorina, R., Aguilar Schall, R., Camacho, J., Holland, N.T., Barr, D.B., and Eskenazi, B. (2015). Effect of organic diet intervention on pesticide exposures in young children living in low-income urban and agricultural communities. *Environ Health Perspect.* 123:1086–1093. doi: doi:10.1289/ehp.1408660
- Bradman, A., Castorina, R., Barr, D.B., Chevrier, J., Harnly, M.E., Eisen, E.A., et al. (2011). Determinants of organophosphorus pesticide urinary metabolite levels in young children living in an agricultural community. *Int J Environ Res Public Health* 8(4):1061–1083
- Brown, K., Phillips, M., Grulke, C., Yoon, M., Young, B., McDougall, R., Leonard, J., Lu, J., Lefew, W., and Tan, Y.M. (2015). Reconstructing exposures from biomarkers using exposure-pharmacokinetic modeling - A case study with carbaryl. *Regul. Toxicol. Pharmacol.*, 73, 689-698.
- Bonner, M.R., Coble, J., Blair, A., Beane Freeman, L.E., Hoppin, J.A., Sandler, D.P., and Alavanja, M.C. (2007). Malathion exposure and the incidence of cancer in the agricultural health study. *Am J Epidemiol.* 166(9):1023-34.
- Borchers, A., Teuber, S.S., Keen, C.L., and Gershwin, M.E. (2010). Food safety. *Clinical Reviews in Allergy and Immunology* 39, 95–141.
- Boobis, A.R., Ossendorp, B.C., Banasiak, U., Hamey, P.Y., Sebestyen, I., and Moretto, A. (2008). Cumulative risk assessment of pesticide residues in food. *Toxicol Lett.* 180:137–150.
- Boon, P.E., Van der Voet, H., Van Raaij, M.T., and Van Klaveren, J.D.. 2008. Cumulative risk assessment of the exposure to organophosphorus and carbamate insecticides in the dutch diet. *Food Chem Toxicol.* 46:3090–3098.
- Boon, P.E., van Donkersgoed, G., Christodoulou, D., Crepet, A., D'Addezio, L., Desvignes, V., Ericsson, B.G., Galimberti, F., Ioannou-Kakouri, E., Jensen, B.H., et al. (2015). Cumulative dietary exposure to a selected group of pesticides of the triazole group in different European countries according to the EFSA guidance on probabilistic modelling. *Food Chem Toxicol.* 79:13–31.

- Bopp, S., Berggren, E., Kienzler, A., Van der Linden, S., and Worth, A. (2015). Scientific methodologies for the assessment of combined effects of chemicals - a survey and literature review. EUR 27471 EN 1–64. <https://doi.org/10.2788/093511>. Scientific methodologies for the assessment of combined effects of chemicals - a survey and literature review. EUR 27471 EN 1–64. <https://doi.org/10.2788/093511>.
- Bouchard, M., Gosselin, N.H., Brunet, R.C., Samuel, O., Dumoulin, M.J., and Carrier, G. (2003). A toxicokinetic model of malathion and its metabolites as a tool to assess human exposure and risk through measurements of urinary biomarkers. *Toxicol Sci* 73:182-194.
- Bouchard, M., Carrier, G., Brunet, R.C., Bonvalot, Y., and Gosselin, N.H. (2005). Determination of biological reference values for chlorpyrifos metabolites in human urine using a toxicokinetic approach. *J Occup Environ Hyg* 2:155-168.
- Bouchard, M., Gosselin, N.H., Brunet, R.C., Samuel, O., Dumoulin, M., and Carrier, G. (2017). A toxicokinetic model of malathion and its metabolites as a tool to assess human exposure and risk through measurements of urinary biomarkers. *Toxicol Sci* 73:182-194.
- Buntyn, R.W., Alugubelly, N., Hybart, R.L., Mohammed, A.N., Nail, C.A., Parker, G.C., Ross, M.K., and Carr, R.L. (2017). Inhibition of endocannabinoid-metabolizing enzymes in peripheral tissues following developmental chlorpyrifos exposure in rats. *Int J Toxicol* 36:395-402.
- Campbell, J., Clewell, R., Andersen, M., and Clewell, H. (2011). Interpreting biomonitoring data for di-n-butyl and di-(2-ethylhexyl) phthalate metabolites in urine using a physiologically based pharmacokinetic model and reverse dosimetry: Estimation of cumulative in utero exposure. *Toxicol. Lett.*, 205, S210-S210.
- Casida, J. E. (2009). Pest toxicology: The primary mechanisms of pesticide actions. *Chem. Res. Toxicol.* 22, 609–619.
- Chambers, R., and Conway, R. (1992). Sustainable rural livelihoods: Practical concepts for the 21st century. IDS discussion paper, No. 296. pp.127-130.
- Chapalamadugu, S., and Chaudhry, G.R. (1992). Microbiological and biotechnological

- aspects of metabolism of carbamates and organophosphates. *Crit. Rev. Biotechnol.* 12:357–389.
- Chiu, W.A., Barton, H.A., DeWoskin, R.S., Schlosser, P., Thompson, C.M., Sonawane, B., Lipscomb, J.C., and Krishnan, K. (2007). Evaluation of physiologically based pharmacokinetic models for use in risk assessment. *Journal of Applied Toxicology: An International Journal* 27:218-237.
- Chiu, Y.H., Williams, P.L., Gillman, M.W., Hauser, R., Rifas-Shiman, S.L., Bellavia, A., Fleisch, A.F., Oken, E., and Chavarro, J.E. (2018). Maternal intake of pesticide residues from fruits and vegetables in relation to fetal growth. *Environ Int.* 119:421-428
- Cho, Y., Min, K., Lee, I., and Cha, C. (2002). Determination of urinary metabolite of profenofos after oral administration and dermal application to rats. *J. Fd Hyg. Safety* 17(1):20–25
- Clegg, D.J., and Gemert, M. V. (1999). Determination Of The Reference Dose For Chlorpyrifos: Proceedings Of An Expert Panel, *Journal of Toxicology and Environmental Health, Part B: Critical Reviews*, 2(3): 211-255
- Clewell, H.J., Tan, Y.M., Campbell, J.L., and Andersen, M.E. (2008). Quantitative interpretation of human biomonitoring data. *Toxicol. Appl. Pharmacol.*, 231, 122-133.
- Crump, K.S., Chen, C., and Louis, T.A. (2010). The future use of in vitro data in risk assessment to set human exposure standards: challenging problems and familiar solutions. *Environ. Health Perspect.*, 118, 1350-1354.
- Costa, L.G. (2006). Current issues in organophosphate toxicology. *Clin Chim Acta* 366:1-13.
- Costa, L.G. (2018). Organophosphorus Compounds at 80: Some Old and New Issues. *Toxicol Sci.* 2018; 162(1):24–35.
- Dadson, O.A., Ellison, C.A., Singleton, S.T., Chi, L., McGarrigle, B.P., Pamela J. Lein, J.P., Farahat, F.M., Farahat, T., and Olson, J.R. (2013). Metabolism of profenofos to 4-bromo-2-chlorophenol, a specific and sensitive exposure biomarker. *Toxicology* 306 (2013) 35– 39
- Delistraty, D. (1997). Toxic equivalency factor approach for risk assessment of polycyclic aromatic hydrocarbons. *Toxicological environmental chemistry* 64(1-4):81-108
- Drescher, K., and Boedeker, W. (1995). Assessment of the combined effects of substances: the relationship between concentration addition and independent action. *Biometrics*:716-730
- Eaton, D.L., Daroff, R.B., Autrup, H., Bridges, J., Buffler, P., Costa, L.G., Coyle, J., McKhann,

- G., Mobley, W.C., Nadel, L., Neubert, D., Schulte-Hermann, R., and Spencer, P.S. (2008). Review of the toxicology of chlorpyrifos with an emphasis on human exposure and neurodevelopment. *Crit Rev Toxicol.* 38 Suppl 2:1-125. doi: 10.1080/10408440802272158.
- Ecobichon, D.J. (2001). Pesticide use in developing countries. *Toxicology.* 160:27–33. doi:10.1016/S0300-483X(00)00452-2
- Edwards, C.A. (1973). Environmental pollution by pesticides. Plenum Press, London. p. 78–79.
- Ehrich, M., and Jortner, B. S. (2010). Organophosphorus-induced delayed neuropathy. In Hayes' Handbook of Pesticide Toxicology (R. Krieger, Ed.), pp. 1479–1504. Academic Press, San Diego
- European Food Safety Authority (EFSA). (2014). Panel on Plant Protection Products and their Residues (PPR). Scientific Opinion on the identification of pesticides to be included in cumulative assessment groups on the basis of their toxicological profile (2014 update). *EFSA Journal* 2013;11(7):3293, 131 pp. doi:10.2903/j.efsa.2013.3293 o
- European Food Safety Authority (EFSA) (2019). Scientific report on the 2017 European Union report on pesticide residues in food. *Efsa J.* 17(6):5743.
- European Food Safety Authority, (EFSA) (2014). Conclusion on the peer review of the pesticide human health risk assessment of the active substance chlorpyrifos. *EFSA J.* 12, 3640.
- European Food Safety Authority (EFSA) (2014b). Scientific Opinion on good modelling practice in the context of mechanistic effect models for risk assessment of plant protection products *EFSA Journal* 12:3589
- European Food Safety Authority (EFSA) (2019). Scientific Report on scientific support for preparing an EU position in the 51st Session of the Codex Committee on Pesticide Residues(CCPR). *EFSA Journal* 17(7):5797
- Elgueta, S., Fuentes, M., Valenzuela, M., Zhao, G., Liu, S., Lu, H., and Correa, A. (2019). Pesticide residues in ready-to-eat leafy vegetables from markets of Santiago, Chile and consumer's risk. *Food Addit Contam Part B.* 12:259–267.
- EPA. (2016). Profenofos: Human health draft risk assessment(DRA) for registration review. [https://www3.epa.gov/pesticides/chem\\_search/cleared\\_reviews/csr\\_PC-111401\\_19-Oct-16.pdf](https://www3.epa.gov/pesticides/chem_search/cleared_reviews/csr_PC-111401_19-Oct-16.pdf). (accessed on 12/3/2020).
- EPA. (2016). Chlorpyrifos: Revised Human Health Risk Assessment for Registration Review.

- Available at: [https:// www.regulations.gov/document? D/4EPA-HQ-OPP-2015-0653-0454](https://www.regulations.gov/document?D%2F4EPA-HQ-OPP-2015-0653-0454). file ID: EPA-HQ-OPP-2015-0653-0454. Accessed July 23, 2021.
- Ewert, L., Aylott, M., Deurinck, M., et al. (2014). The concordance between nonclinical and phase I clinical cardiovascular assessment from a crosscompany data sharing initiative. *Toxicol Sci* 2014; 142:427–35.
- Eyer, P. (2003). The role of oximes in the management of organophosphorus pesticide poisoning. *Toxicol Rev.* 2003;22(3):165-90. doi: 10.2165/00139709-200322030-00004.
- FAO. (2012). Food and Agriculture Organization of the United Nations (2012) [http://www.fao.org/fileadmin/templates/agphome/documents/Pests\\_Pesticides/JMPR/Evaluation08/Profenofos.pdf](http://www.fao.org/fileadmin/templates/agphome/documents/Pests_Pesticides/JMPR/Evaluation08/Profenofos.pdf). Accessed 2021/08.
- Fan, A. M. (2014). Biomarkers in toxicology, risk assessment, and environmental chemical regulations. In *Biomarkers in Toxicology* (pp. 1057–1080). <https://doi.org/10.1016/B978-0-12-404630-6.00064-6>
- Farahat, T.M., Abdelrasoul, G.M., Amr, M.M., Shebl, M.M., Farahat, F.M., and Anger, W.K. (2003). Neurobehavioral effects among workers occupationally exposed to organophosphorous pesticides. *Occup Environ Med* 60:279-286.
- Flecknell, P. (2002). “Replacement, Reduction, Refinement”, *ALTEX - Alternatives to animal experimentation*, 19(2), pp. 73-78. Available at: <https://www.altex.org/index.php/altex/article/view/1106> (Accessed: 3September 2021).
- Foxenberg, R. J., McGarrigle, B. P., Knaak, J. B., Kostyniak, P. J., and Olson, J. R. (2007). Human hepatic cytochrome p450-specific metabolism of parathion and chlorpyrifos. *Drug Metab. Dispos.* 35, 189–193
- Furlong, C. E., Richter, R. J., Seidel, S. L., Costa, L. G., and Motulsky, A. G. (1989). Spectrophotometric assays for the enzymatic hydrolysis of the active metabolites of chlorpyrifos and parathion by plasma paraoxonase/arylesterase. *Anal. Biochem.* 180, 242–247.
- Gallagher, S.S., Rice, G.E., Scarano, L.J., Teuschler, L.K., Bolleweg, G., and Martin, L. (2015). Cumulative risk assessment lessons learned: a review of case studies and issue papers. *Chemosphere*.120:697–705.
- Ghorab, M. A., and Khalil, M.S. (2015). Toxicological Effects of Organophosphates



- Pesticides, *International Journal of Environmental Monitoring and Analysis*. Vol. 3, No. 4, 2015, pp. 218-220. doi: 10.11648/j.ijema.20150304.13
- Glynn, A., Thuvander, A., Aune, M., Johannisson, A., Darnerud, P.O., Ronquist, G., and Cnattingius, S. (2008). Immune cell counts and risks of respiratory infections among infants exposed pre- and postnatally to organochlorine compounds: a prospective study. *Environmental Health Perspectives* 4, 7–62.
- Golge, O., Koluman, A., and Kabak, B. (2018). Validation of a modified QuEChERS method for the determination of 167 pesticides in milk and milk products by LC-MS/MS. *Food Anal Methods*. 11:1122–1148.
- Gotoh, M., Sakata, M., Endo, T., Hayashi, H., Seno, H., and Suzuki, O. (2001). Profenofos metabolites in human poisoning. *Forensic Sci Int* 116: 221-226.
- Grandjean, P., Bellinger, D., Bergman, A., Cordier, S., Davey-Smith, G., Eskenazi, B., Gee, D., Gray, K., Hanson, M., van den Hazel, P., Heindel, J.J., Heinzow, B., Hertz-Picciotto, I., Hu, H., Huang, T.T., Jensen, T.K., Landrigan, P.J., McMillen, I.C., Murata, K., Ritz, B., Schoeters, G., Skakkebaek, N.E., Skerfving, S., and Weihe, P. (2008). The Faroes statement: human health effects of developmental exposure to chemicals in our environment. *Basic and Clinical Pharmacology Toxicology* 102:73–75.
- Greenfieldboye, N. (2019). EPA Chief Pledges to Severely Cut Back on Animal Testing of Chemicals. *NPR Health News*. September 10, 2019. Available at: <https://www.npr.org/sections/health-shots/2019/09/10/759435118/epa-chief-pledges-to-severely-cut-back-on-animal-testing-of-chemicals>. Accessed July 16, 2021.
- Greish, S., Ismail, S.M., Mosleh, Y., Loutfy, N., Dessouki, A.A., and Ahmed, M.T. (2011). Human risk assessment of profenofos: A case study in Ismailia, Egypt. *Polycyclic Aromat Compd* 31:28-47.
- Hardt, J., and Angerer, J. (2000). Determination of dialkyl phosphates in human urine using gas chromatography-mass spectrometry. *J Anal Toxicol* 24:678-684.
- Hepsağ, F., and Kizildeniz, T. (2021). Pesticide residues and health risk appraisal of tomato cultivated in greenhouse from the Mediterranean region of Turkey. *Environ Sci Pollut Res Int*. 2021 May;28(18):22551-22562. doi: 10.1007/s11356-020-12232-7.
- Huang, H.J., Lee, Y.H., Hsu, Y.H., Liao, C.T., Lin, Y.F., and Chiu, H.W. (2021). Current Strategies in Assessment of Nanotoxicity: Alternatives to In Vivo Animal Testing. *Int J Mol Sci*. 22(8):4216. doi: 10.3390/ijms22084216.
- Hu, Y., Chiu, Y.H., Hauser, R., Chavarro, J., and Sun, Q. (2016). Overall and class-specific

- scores of pesticide residues from fruits and vegetables as a tool to rank intake of pesticide residues in United States: A validation study. *Environ Int.* 2016 Jul-Aug;92-93:294-300.
- Jamal, G.A., Hansen, S., and Julu, P.O.O. (2002). Low level exposures to organophosphorus esters may cause neurotoxicity. *Toxicology* 181-182: 23-33.
- Jensen, B.H., Petersen, A., Nielsen, E., Christensen, T., Poulsen, M.E., and Andersen, J.H. (2015). Cumulative dietary exposure of the population of Denmark to pesticides. *Food Chem Toxicol.* 83:300– 307.
- Jiang, M., Gao, H., Liu, X., Wang, Y.U., Lan, J., Li, Y., Lv, S., Zhu, K., and Gong, P. (2021). Detection of Pesticide Residues in Vegetables Sold in Changchun City, China. *J Food Prot* 84(3):481-489.
- Joint Meeting on Pesticide Residues (JMPR) (2007).  
[http://www.fao.org/fileadmin/templates/agphome/documents/Pests\\_Pesticides/JMPR/Evaluation08/Profenofos.pdf](http://www.fao.org/fileadmin/templates/agphome/documents/Pests_Pesticides/JMPR/Evaluation08/Profenofos.pdf). Accessed on 5/9/2021.
- Johnson, M.K., and Glynn, P. (1995). Neuropathy target esterase (NTE) and 675 organophosphorus induced delayed polyneuropathy (OPIDP): recent 676 advances. *Toxicol Lett* 82-83: 459-463.
- Johnson, M.K., and Glynn, P. (2001). Neuropathy target esterase In *Handbook of Pesticide Toxicology*, (Krieger R., Ed.), 953–965. Academic Press, San Diego.
- International Programme on Chemical Safety (IPCS) (2005). Chemical- specific adjustment factors for interspecies differences and human variability: guidance document for use of data in dose/ concentration-response assessment. WHO, Geneva
- Kamataki, T., Lee Lin, M.C., Belcher, D.H., and Neal, R.A. (1976). Studies of the metabolism of parathion with an apparently homogeneous preparation of rabbit liver cytochrome P-450. *Drug Metab Dispos.* 4(2):180-9.
- Krewski, D., Acosta Jr, D., Andersen, M., Anderson, H., Bailar III, J.C., Boekelheide, K., Brent, R., Charnley, G., Cheung, V.G., and Green Jr, S. (2010). Toxicity testing in the 21st century: a vision and a strategy. *Journal of Toxicology and Environmental Health, Part B* 13:51-138.
- Krewski, D., Withey, J. R., Ku, L. F., and Andersen, M. E. (1994). Applications of physiologic pharmacokinetic modeling in carcinogenic risk assessment. *Environmental health perspectives*, 102:11(Suppl 1), 37–50.
- Karanja, N.K., Njenga, M., Mutua, G.K., Lagerkvist, C.J., Kutto, E., and Okello, J.J. (2012).

- Concentrations of heavy metals and pesticides residues in leafy vegetables and implications for peri-urban farming in Nairobi, Kenya. *J Agric Food Syst Commun Dev.* 3:255–267.
- Kendall, P. (2018). Replacing the replacements: Animal model alternatives *Science.* 362 (6411): 246-246
- Kortenkamp, A., Backhaus, T., and Faust, M.J.C. (2009). State of the Art Report on Mixture Toxicity, vol. 70307. pp. 94–103.
- Koshlukova, S. E., and Reed, N. R. (2014). Chlorpyrifos. <https://doi.org/10.1016/B978-0-12-386454-3.00115-9>
- Kumari, D., and John, S. (2019). Health risk assessment of pesticide residues in fruits and vegetables from farms and markets of Western Indian Himalayan region. *Chemosphere.* 224:162-167.
- Kunyanga, C., Amimo, J., Kingori, L.N., and Chemining'wa, G. (2018). Consumer risk exposure to chemical and microbial hazards through consumption of fruits and vegetables in Kenya. *Food Sci Qual Manage.* 78. ISSN 2225-0557 (Online).
- Kushwaha, M., Verma, S., and Chatterjee, S. (2016). Profenofos, an Acetylcholinesterase-Inhibiting Organophosphorus Pesticide: A Short Review of Its Usage, Toxicity, and Biodegradation. *J Environ Qual.* 2016 Sep;45(5):1478-1489.
- Lee, K.G., and Lee S.K. (2012). Monitoring and risk assessment of pesticide residues in yuza fruits (*Citrus junos* Sieb. Ex Tanaka) and yuza tea samples produced in Korea. *Food Chem.* 135:2930–2933.
- Liu, P., Wu, C.H., Chang, X.L., Qi, X.J., Zheng, M.L., and Zhou, Z.J. (2014). Assessment of chlorpyrifos exposure and absorbed daily doses among infants living in an agricultural area of the Province of Jiangsu, China. *Int Arch Occup Environ Health* 87:753-762.
- Lotti, M., and Moretto, A. (2005). Organophosphate-induced delayed polyneuropathy. *Toxicol Rev.* 2005;24(1):37-49.
- Louisse, J., Beekmann, K., and Rietjens, I.M. (2017). Use of physiologically based kinetic modeling-based reverse dosimetry to predict in vivo toxicity from in vitro data. *Chemical Research in Toxicology* 30:114-125.
- Lozowicka, B., Kaczynski, P., Paritova, A.E., Kuzembekowa, G.B., Abzhaliyeva, A.B.,

- Sarsembayeva, N.B., and Alihan, K. (2014). Pesticide residues in grain from Kazakhstan and potential health risks associated with exposure to detected pesticides. *Food Chem Toxicol.* 64:238–248.
- Lu, C., Holbrook, C.M., and Andres, L.M. (2010). The implications of using a physiologically based pharmacokinetic (PBPK) model for pesticide risk assessment. *Environ Health Perspect* 118:125-130
- MacGregor, J.T., Collins, J.M., Sugiyama, Y., Tyson, C.A., Dean, J., Smith, L., Andersen, M., Curren, R.D., Houston, J.B., Kadlubar, F.F., Kedderis, G.L., Krishnan, K., Li, A.P., Parchment, R.E., Thummel, K., Tomaszewski, J.E., Ulrich, R., Vickers, A.E., and Wrighton, S.A. (2001). In vitro human tissue models in risk assessment: report of a consensus-building workshop. *Toxicol Sci.* 59(1):17-36.
- Ma, T., and Chambers, J.E. (1994). Kinetic parameters of desulfuration and dearylation of parathion and chlorpyrifos by rat liver microsomes. *Food Chem. Toxicol.* 32:763–767.
- Medlock Kakaley, E., Cardon, M.C., Gray, L.E., Hartig, P.C., and Wilson, V.S. (2019). Generalized concentration addition model predicts glucocorticoid activity bioassay responses to environmentally detected receptor ligand mixtures. *Toxicological Sciences* 168(1):252-263
- Milman, O. (2015). National Institutes of Health announces end to chimpanzee research. *The Guardian*. November 19, 2015. Available at: <https://www.theguardian.com/us-news/2015/nov/19/national-institutes-health-end-chimpanzee-research>. Accessed September 26, 2020.
- Mostafalou, S., and Abdollahi, M. (2013). Pesticides and human chronic diseases: evidences, mechanisms, and perspectives. *Toxicol Appl Pharmacol* 268:157–77.
- Mosquin, P.L., Licata, A.C., Liu, B., Sumner, S.C., and Okino, M.S. (2009). Reconstructing exposures from small samples using physiologically based pharmacokinetic models and multiple biomarkers. *J Expo Sci Environ Epidemiol* 19:284-297.
- Muhammad Arif, A., Javed, I., Ayaz, M., Abdullah, M., Imran, M., Shahbaz, M., Aslam Gondal, T., Ali, M., Iqbal, Z., Iqbal, Z., Salehi, B., Sharifi-Rad, J., and Martins, N. (2021). Organochlorine pesticide residues in raw milk samples collected from dairy farms and urban areas of Lahore district, Pakistan. *J Food Sci Technol.* 2021 Jan;58(1):129-137.
- Ngolo, P., Nawiri, M., Machochi, A., and Oyieke, H. (2019). Pesticide Residue Levels in Soil, Water, Kales and Tomatoes in Ewaso Narok Wetland, Laikipia, County, Kenya. *Journal of Scientific Research and Reports*, 24(5):1-11.

- Naksen, W., Prapamontol, T., Mangklabruks, A., Chantara, S., Thavornyutikarn, P., Robson, M.G., and Panuwet, P. (2016). A single method for detecting 11 organophosphate pesticides in human plasma and breastmilk using GC-FPD. *J Chromatogr B Analyt Technol Biomed Life Sci* 1025:92-104.
- Nishihama, Y., Nakayama, S.F., Isobe, T., Jung, C.-R., Iwai-Shimada, M., Kobayashi, Y., Michikawa, T., Sekiyama, M., Taniguchi, Y., Yamazaki, S., et al. (2021). Urinary Metabolites of Organophosphate Pesticides among Pregnant Women Participating in the Japan Environment and Children's Study (JECS). *Int. J. Environ. Res. Public Health* 18:5929.
- OECD. (2018). Considerations for assessing the risks of combined exposure to multiple chemicals. Series on Testing and Assessment No. 296. Paris Cedex 16, France
- Omwenga, I., Kanja, L., Nguta, J., Mbaria, J., and Irungu, P. (2016). Organochlorine pesticide residues in farmed fish in Kiambu and Machakos Counties, Kenya. *Cogent Environmental Science*, 2:1, 1153215,
- Omwenga, I., Kanja, L., Zomer, P., Louisse, J., Rietjens, I.M.C.M., and Mol, H. (2021). Organophosphate and carbamate pesticide residues and accompanying risks in commonly consumed vegetables in Kenya. *Food Addit Contam Part B Surveill.* 2021 Mar;14(1):48-58.
- Omwenga, I., Zhao, S., Kanja, L., Mol, H., Rietjens, I.M.C.M., and Louisse, J. (2021). Prediction of dose-dependent in vivo acetylcholinesterase inhibition by profenofos in rats and humans using physiologically based kinetic (PBK) modeling-facilitated reverse dosimetry. *Arch Toxicol.* 95(4):1287-1301.
- Parish, S.T., Aschner, M., Casey, W., Corvaro, M., Embry, M.R., Fitzpatrick, S., Kidd, D., Kleinstreuer, N.C., Lima, B.S., Settivari, R.S., Wolf, D.C., Yamazaki, D., and Boobis, A. (2020). An evaluation framework for new approach methodologies (NAMs) for human health safety assessment. *Regul Toxicol Pharmacol.* 112:104592.
- Poet, T.S., Kousba, A.A., Dennison, S.L., and Timchalk, C. (2004). Physiologically based pharmacokinetic/pharmacodynamic model for the organophosphorus pesticide diazinon. *Neurotoxicology* 25:1013-1030.
- Pogačnik, L., and Franko, M. (2003). "Detection of organophosphate and carbamate

- pesticides in vegetable samples by a photothermal biosensor,” *Biosensors and Bioelectronics*, vol. 18:1–9.
- Qiao D. (2010). Development of health criteria for school site risk assessment pursuant to health and safety code section 901(g): child-specific reference dose (chRD) for school site risk assessment – chlorpyrifos. Integrated Risk Assessment Branch Office of Environmental Health Hazard Assessment, California, USA: California Environmental Protection Agency 2010.
- Quandt, S.A., Arcury, T.A., Rao, P., Snively, B.M., Camann, D.E., Doran, A.M., Yau, A.Y., Hoppin, J.A., and Jackson, D.S. (2004). Agricultural and residential pesticides in wipe samples from farmworker family residences in North Carolina and Virginia. *Environ Health Perspect* 112:382–387.
- Quinn, D.M., Topczewski, J., Yasapala, N., and Lodge, A., (2017). Why is Aged Acetylcholinesterase So Difficult to Reactivate? *Molecules*. 2017 Sep 4;22(9):1464
- Quistad, G.B., Sparks, S.E., and Casida, J.E. (2001). Fatty acid amide hydrolase inhibition by neurotoxic organophosphorus pesticides. *Toxicol Appl Pharmacol* 173: 48-55.
- Quistad, G.B., Liang, S.N., Fisher, K.J., Nomura, D.K., and Casida, J.E., (2006). Each lipase has a unique sensitivity profile for organophosphorus inhibitors. *Toxicol Sci* 91:166-172.
- Rietjens, I.M.C.M., Ning, J., Chen, L., Wesseling, S., Strikwold, M., and Louisse, J., (2019). Selecting the dose metric in reverse dosimetry based QIVIVE Archives of toxicology 93:1467-1469
- Russell, W.M.S., and Burch, R.L. (1959). *The Principles of Humane Experimental Technique*. Potters Bar, Hertfordshire, England: Universities Federation for Animal Welfare. [online] Available at: [http://altweb.jhsph.edu/pubs/books/humane\\_exp/het-toc](http://altweb.jhsph.edu/pubs/books/humane_exp/het-toc) [Accessed 12 May 2021].
- Taylor, K. (2019). " Recent Developments in Alternatives to Animal Testing". In *Animal Experimentation: Working Towards a Paradigm Change*. Leiden, The Netherlands: Brill. doi: [https://doi.org/10.1163/9789004391192\\_025](https://doi.org/10.1163/9789004391192_025)
- Thasler, W.E., Schlott, T., Kalkuhl, A., Plän, T., Irrgang, B., Jauch, K.W., and Weiss, T.S., (2006). Human tissue for in vitro research as an alternative to animal experiments: a charitable "honest broker" model to fulfil ethical and legal regulations and to protect research participants. *Altern Lab Anim*. 34(4):387-92.

- Timchalk, C., and Poet, T.S., (2008). Development of a physiologically based pharmacokinetic and pharmacodynamic model to determine dosimetry and cholinesterase inhibition for a binary mixture of chlorpyrifos and diazinon in the rat. *Neurotoxicology*. 29(3):428-43.
- Timchalk, C., Trease, H.E., Trease, L.L., Minard, K.R., and Corley, R.A., (2001). Potential technology for studying dosimetry and response to airborne chemical and biological pollutants. *Toxicol Ind Health*. 2001 Jun;17(5-10):270-6.
- Timchalk, C., Nolan, R.J., Mendrala, A.L., Dittenber, D.A., Brzak, K.A., and Mattsson, J.L. (2002). A physiologically based pharmacokinetic and pharmacodynamic (PBPK/PD) model for the organophosphate insecticide chlorpyrifos in rats and humans. *Toxicol Sci* 66:34-53.
- Rauh, V.A., Garfinkel, R., Perera, F.P., Andrews, H.F., Hoepner, L., Barr, D.B., Whitehead, R., Tang, D., and Whyatt, R.W., (2006). Impact of prenatal chlorpyrifos exposure on neurodevelopment in the first 3 years of life among inner-city children. *Pediatrics* 118: 1845–1859.
- Risher, J., and Navarro, H.A., (1997). Toxicological profile for chlorpyrifos. Washington, DC: US Department of Health and Human Services, Agency for Toxic Substance and Disease Registry. <https://www.atsdr.cdc.gov/toxprofiles/tp84.pdf> accessed on 6/9/2021
- Richards, P.G., Johnson, M.K., Ray, and D.E., (2000). Identification of acylpeptide hydrolase as a sensitive site for reaction with organophosphorus compounds and a potential target for cognitive enhancing drugs. *Mol Pharmacol* 58:577-583.
- Rietjens, I.M., Louisse, J., and Punt, A., 2011. Tutorial on physiologically based kinetic modeling in molecular nutrition and food research. *Molecular Nutrition & Food Research* 55: 941-956.
- Rigas, M.L., Okino, M.S., and Quackenboss, J.J., (2001). Use of a pharmacokinetic model to assess chlorpyrifos exposure and dose in children, based on urinary biomarker measurements. *Toxicol Sci* 61:374-381.
- Razzaghi, N., Ziarati, P., Rastegar, H., Shoeibi, S., Amirahmadi, M., Conti, G.O., Ferrante,

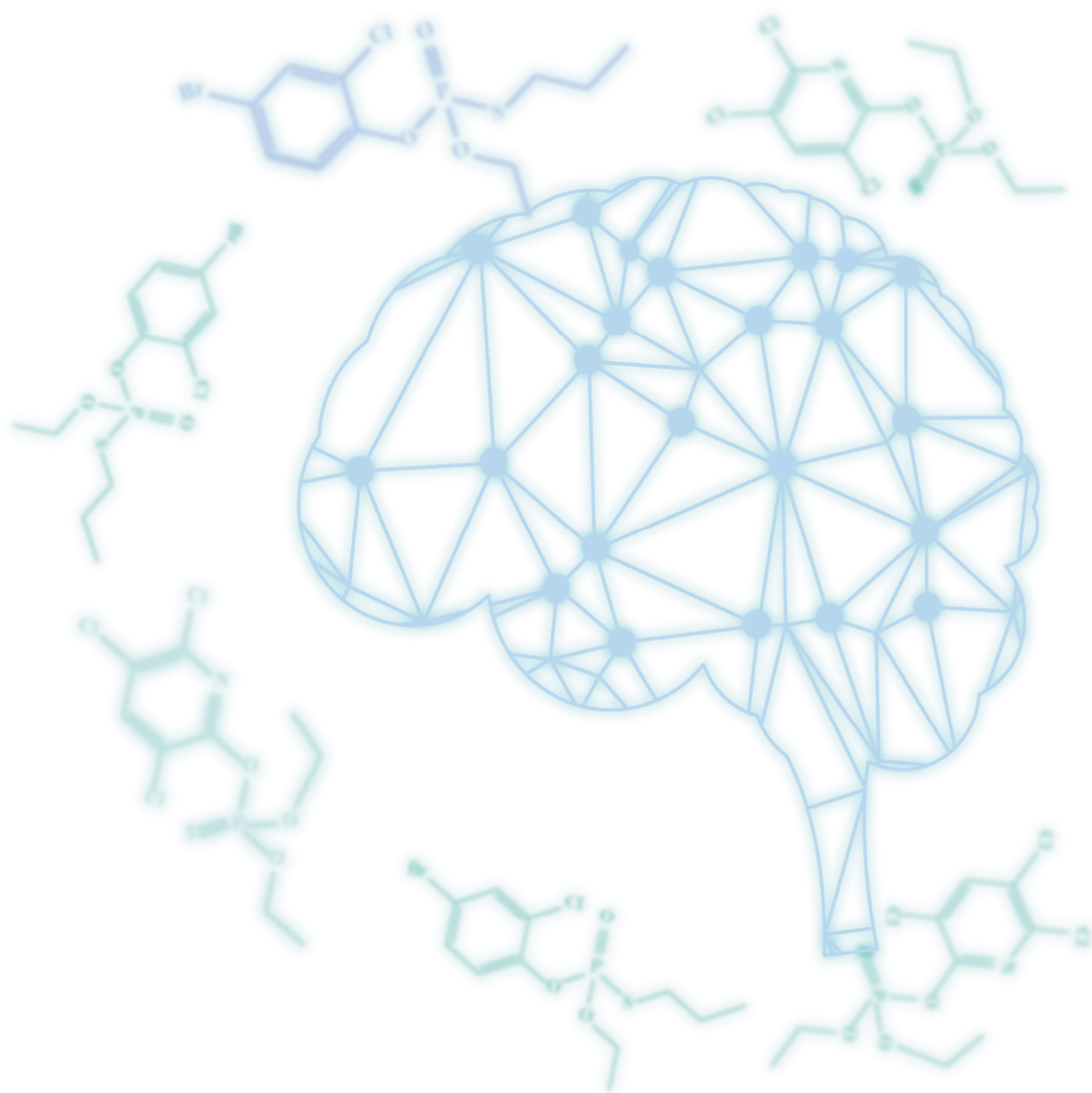
- M., Fakhri, Y., and Khaneghah, A.M. (2018). The concentration and probabilistic health risk assessment of pesticide residues in commercially available olive oils in Iran. *Food Chem Toxicol.* 120:32–40.
- Sapozhnikova, Y. (2014). Evaluation of low-pressure gas chromatography-tandem mass spectrometry method for the analysis of > 140 pesticides in fish. *J Agric Food Chem.* 62:3684–3689.
- Shanks, N., Greek, R., and Greek, J., (2009). Are animal models predictive for humans? *Philos. Ethics Humanit. Med.*, 4:2.
- Smegal, D.C., (2000). Human health risk assessment chlorpyrifos. USA: U.S. Environmental Protection Agency.
- Smith, G.N., Watson, B.S., and Fischer, F.S. (1967). Investigations on Dursban insecticide. Metabolism of (36Cl) O,O-diethyl O-3,5,6-trichloro-2-pyridyl phosphorothioate in rats. *J. Agr. Fd. Chem.*, 15(1): 132-138.
- Staal, Y., and Van der ven, L., (2016) “Risk assessment of substances in combined exposures (mixtures).” . RIVM Letter report 2015-0189
- Sultatos, L. G., (2006). Interactions of organophosphorus and carbamate compounds with cholinesterases. In *Toxicology of Organophosphate and Carbamate Compounds* (R.C. Gupta, Ed.), pp. 209–218. Elsevier, Amsterdam.
- Sultatos, L.G., (1990). A physiologically based pharmacokinetic model of parathion based on chemical-specific parameters determined in vitro. *J Amer Coll Toxicol* 9:611-619.
- Suratman, S., Edwards, J.W., and Babina, K., 2015. Organophosphate pesticides exposure among farmworkers: pathways and risk of adverse health effects. *Rev Environ Health.* 30(1):65-79.
- Tang, J., Cao, Y., Rose, R. L., Brimfield, A. A., Dai, D., Goldstein, J. A., and Hodgson, E., 2001. Metabolism of chlorpyrifos by human cytochrome P450 isoforms and human, mouse, and rat liver microsomes. *Drug Metab. Dispos.* 29:1201–1204.
- te Biesebeek, J.D., Sam, M., Sprong, R.C., van Donkersgoed, G., Kruisselbrink, J.W., de Boer, W.J., van Lenthe, M., van der Voet, H., and van Klaveren, J.D., (2021). Potential impact of prioritisation methods on the outcome of cumulative exposure assessments of pesticides. EFSA supporting publication 2021:EN-6559. 91 pp.
- Timchalk, C., Nolan, R. J., Mendrala, A. L., Dittenber, D. A., Brzak, K. A., and Mattsson, J.



- L., (2002). A physiologically based pharmacokinetic and pharmacodynamic (PBPK/PD) model for the organophosphate insecticide chlorpyrifos in rats and humans. *Toxicological Sciences*, 66(1):34-53.
- United Nations Children's Fund (UNICEF), Understanding the Impacts of Pesticides on Children: A discussion paper, (2018). [http://www.ounipestiziden.lu/uploads/2/2/4/8/22480338/2018\\_01\\_xx\\_understanding\\_the\\_impact\\_of\\_pesticides\\_on\\_children-unicef.pdf](http://www.ounipestiziden.lu/uploads/2/2/4/8/22480338/2018_01_xx_understanding_the_impact_of_pesticides_on_children-unicef.pdf)
- US EPA., (2006). Organophosphorus cumulative risk assessment (2006). [accessed 2019 Dec]. [www.epa.gov/pesticides/cumulative](http://www.epa.gov/pesticides/cumulative).
- US EPA., (2011). Pyrethrins/pyrethroid cumulative risk assessment (2011). [accessed 2019 Dec]. [www.epa.gov/pesticides/cumulative](http://www.epa.gov/pesticides/cumulative).
- US EPA., (2016). US EPA-Pesticides; Profenofos [https://www3.epa.gov/pesticides/chem\\_search/cleared\\_reviews/csr\\_PC-111401\\_19-Oct-16.pdf](https://www3.epa.gov/pesticides/chem_search/cleared_reviews/csr_PC-111401_19-Oct-16.pdf). Accessed on 3/9/2021
- U.S. Food and Drug Administration., (2006). Press release: FDA issues advice to make earliest stages of clinical drug development more efficient. January 12. Washington DC: U.S. Food and Drug Administration.
- Van Norman, G.A., (2019). Limitations of Animal Studies for Predicting Toxicity in Clinical Trials: Is it Time to Rethink Our Current Approach? *JACC Basic Transl Sci*. 25;4(7):845-854. doi: 10.1016/j.jacbts.2019.10.008. PMID: 31998852; PMCID: PMC6978558.
- Van Norman, G.A., (2020). Limitations of Animal Studies for Predicting Toxicity in Clinical Trials: Part 2: Potential Alternatives to the Use of Animals in Preclinical Trials. *JACC Basic Transl Sci*. 5(4):387-397. doi: 10.1016/j.jacbts.2020.03.010. Epub 2020 Apr 27. PMID: 32363250; PMCID: PMC7185927.
- WHO., (2009). The WHO recommended classification of pesticides by hazard and guidelines to classification. World Health Organization, Geneva.
- Wang, F., Ren, C., Ma, H., Li, P., Hao, J., Chen, L., and Sun, M., (2019). [Determination of pesticide residues in wolfberry using QuEChERS-gas chromatography-tandem mass spectrometry]. *Se Pu*. 8;37(10):1042-1047. Chinese. doi: 10.3724/SP.J.1123.2019.04014..
- Wang, J., Chow, W., Wong, J.W., Leung, D., Chang, J., and Li, M., (2019). Non-target data

- acquisition for target analysis (nDATA) of 845 pesticide residues in fruits and vegetables using UHPLC/ESI Q-Orbitrap. *Anal Bioanal Chem.* 2019 Mar;411(7):1421-1431.
- Yang, Z., and Xiong, H., (2012). In vitro, Tissue-Based Models as a Replacement for Animal Models in Testing of Drugs at the Preclinical Stages Available in <https://www.intechopen.com/chapters/40245> (accessed on 6/9/2021)
- Wang, Y., Zhao, Z., and Song, F., (2020). The Ethical Issues of Animal Testing in Cosmetics Industry. *Humanities and Social Sciences.* 8(4): 112-116.
- Zhang, Y., Han, S., Liang, D., Shi, X., Wang, F., Liu, W., Zhang, L., Chen, L., Gu, Y., and Tian, Y., (2014). Prenatal exposure to organophosphate pesticides and neurobehavioral development of neonates: a birth cohort study in Shenyang, China. *PloS one*, 9:88491.
- Zhang, WenJun, (2018). Global pesticide use: Profile, trend, cost / benefit and more. *Proceedings of the International Academy of Ecology and Environmental Sciences*, 2018, 8(1): 1-27 IAEES
- Zhao, S., Kamelia, L., Boonpawa, R., Wesseling, S., Spenkelink, B., and Rietjens, I.M.C.M., (2019). Physiologically based kinetic modelling-facilitated reverse dosimetry to predict in vivo red blood cell acetylcholinesterase inhibition following exposure to chlorpyrifos in the Caucasian and Chinese population. *Toxicol Sci* 171: 69–83.





# CHAPTER 2.

Organophosphate and Carbamate Pesticide Residues  
and accompanying risks in Commonly Consumed  
Vegetables in Kenya

Isaac Omwenga  
Laetitia Kanja  
Paul Zomer  
Jochem Louisse  
Ivonne M.C.M. Rietjens  
Hans Mol

*Published in: Food Additives & Contaminants: Part B (2021)*  
*14(1):48-58*

## **ABSTRACT**

The current study was conducted to assess the levels of organophosphates and carbamates in vegetables in Kenya, and to examine potential consumer health risks. A total of 90 samples were analysed by liquid chromatography/high resolution tandem mass spectrometry. Residues of acephate, chlorpyrifos, methamidophos, omethoate and profenofos were found in 22% of the samples, ranging from 10 to 1343 µg/kg. The EU MRL was exceeded in 21%, 10%, 8% and 22% of the samples of French beans, kales, spinach, and tomatoes respectively. Chlorpyrifos in spinach had an acute HQ of 3.3 and 2.2 for children and adults, respectively, implying that potential health risks with respect to acute dietary exposure cannot be excluded. For chronic dietary exposure, all chronic HQs were below 1. The HI for the pesticides was 0.54 and 0.34 for children and adults. Routine monitoring of OPs and carbamates in vegetables is recommended to minimize consumer's health risks.

## 2.1 Introduction

Pesticide use is essential for control of pests in horticultural crops and adequate production of food supplies for the ever increasing world population as well as for control of vector-borne diseases. Most developing countries with a rapidly growing population require pesticides to improve food production (Akoto et al., 2015). However, the extensive use of pesticides has led to adverse effects to human health as well as other non-target species and the environment (Bravo et al., 2011; Stadlinger et al., 2013; Li et al., 2017; Bhandari et al., 2019).

Organophosphates (OPs) and carbamates were considered safer than their predecessors, the persistent organochlorine insecticides like aldrin, dieldrin and DDT (Fernández et al., 2000; Pogačnik and Franko, 2003). However, over 40 OP pesticides, including the most commonly used ones such as chlorpyrifos have been classified by the WHO Food and Agriculture Organization and US Environmental Protection Agency (EPA) to be moderately or highly hazardous to human health (WHO, 2009; Roberts and Reigart, 2013). The intensive use of OP pesticides in various crops may lead to accumulation of levels higher than those permitted, and subsequently affect quality of agricultural products, and raise concerns with respect to human health and international trade (EC, 2005; Boobis et al., 2008). The OPs and carbamates produce their effects by inhibiting acetylcholinesterase (AChE), the enzyme that terminates the action of the neurotransmitter acetylcholine (ACh) within neuromuscular junctions and nerve tissue, leading to overstimulation of the post-synaptic membrane (Timchalk and poet, 2008). Reported effects related to exposure to OPs vary from mild short-term impacts such as nausea and headaches to chronic effects such as infertility, birth defects, blood disorders, nerve disorders, endocrine disruption and reproductive effects (Mansour, 2004; Alavanja et al., 2013). Consumption of conventionally grown fruits and vegetables provide the major pesticide exposure route for the general population (Bradman et al., 2015). Consequently, biomonitoring

studies have found pesticides and their metabolites in biospecimens in several countries including USA and Canada (CDC, 2017; Haines et al., 2017).

Despite regulation of pesticides through maximum residues limits (MRLs), there is lifelong combined exposure to low amounts of hundreds of various pesticides from one food item containing multiple compounds or combinations of food items, each containing different residues (Boobis et al. 2008). If these pesticides have a similar mechanism of action and end point, assessing the dietary risk of exposure differently may lead to underestimation of the health risk (Boon et al., 2008). Consequently, recent approaches in pesticide risk assessment include cumulative and probabilistic approaches in order to include the amount and variety of pesticide residues likely to be present in the vegetable sample (Boon et al., 2015; Jensen et al., 2013, 2015; Elgueta et al., 2019). The initial step in assessing pesticide mixtures is to identify substances with a similar mechanism of toxicity (Gallagher et al., 2015). For example, acetylcholinesterase inhibitors such as OPs and carbamates have been assigned the same cumulative assessment group by the United States Environmental Protection Agency (USEPA, 2006, 2007, 2011) hence their choice in this study.

The use of chemical pesticides is still indispensable in Kenya due to the hot and humid tropical environmental conditions that are conducive to the development of pests, weeds, and disease vectors (Omwenga et al., 2016). There is increased use of chemicals, especially fertilizers, veterinary chemicals and pesticides, since agriculture accounts for 60% of Kenya's foreign exchange earnings and provides raw materials for the industries (NIP, 2006). Many small-scale farmers are not aware of the hazards associated with these chemicals. For example, a previous study in Ghana revealed that up to 45% and 20 % of farmers wore partial or no personal protective equipment at all when applying pesticides to cocoa plants hence increasing their risks of exposure to pesticides (Okoffo et al., 2016). In addition, the study reported other poor operational habits such as talking, eating, drinking, stirring pesticides with bare hands and



smoking among others during the process of pesticides application (Okoffo et al., 2016). Other indiscreet practices, such as application of higher than recommended doses of pesticides on crops and failure to implement the pre-harvest time frame after application, may lead to consumers' exposure to pesticides at levels of concern (Akoto et al., 2015). Furthermore, OP pesticides of environmental and human health concern that have been banned in developed countries such as EU, USA and Canada are still used in developing countries (Picciotto et al., 2018). For example, pesticides such as chlorpyrifos, profenofos, acephate, metamidophos, dimethoate and omethoate which are banned in Europe and other countries are still in use in developing countries such as Costa Rica, Guatemala (Bravo et al., 2011), Mexico (Gonzales et al., 2018) and Kenya (PCPB, 2019). The focus of occupational and public health institutions in developing countries have been on acute poisonings, as delayed and chronic effects remain undetermined (Wesseling et al., 2005; Toe, 2010; Bravo et al., 2011).

Vegetables provide vitamins, minerals and active compounds known to reduce the effect of cardiovascular diseases (Ivey et al. 2015). According to the WHO, vegetables and fruits constitute on average 30% of food consumption (WHO, 2003). However, in Kenya, it is estimated that fresh fruits and vegetables constitute 25% and >80% of the diets in the urban and the rural areas, respectively (Mungai et al., 2000; Kunyanga et al., 2018). Among them, kales (*Brassica oleraceae var acephala*), spinach (*Spinacia oleracea*), tomatoes (*Solanum lycopersicum*) and to a lesser extent French beans (*Phaseolus vulgaris*) are the most common vegetables used in various dishes (Karanja et al., 2012; Okello et al., 2012; Mutai et al., 2015; RSA, 2015; Njuguna et al., 2019). In general, it is reported that the amounts of pesticides used in vegetable crops are three times higher than what is used for cereal crops (Fan et al., 2015), which are staple foods in many other countries. Consequently, it is expected that vegetables contain higher pesticide residue levels as compared to cereal-based foodstuffs, not only because of the large amount of pesticide usage but also because some, like tomatoes, are eaten raw in

salads (Baig et al., 2009; Knežević et al., 2012). Monitoring pesticide residues in vegetables is therefore key in determining and mitigating possible risks to human health from daily dietary pesticide exposure of consumers (Curl et al., 2003).

Developed countries such as USA, Canada and in the EU have implemented pesticide monitoring programmes. However, little effort has focused on long-term adverse health effects of pesticides on the agricultural workers and local consumers in developing countries (Ecobichon, 2001). Many studies have reported on the levels of pesticide residues in various food products, including milk products (Golge et al., 2018), poultry and sheep fat (EFSA 2019), cereal (Lozowicka et al., 2014; EFSA, 2019), olive oils (Razzaghi et al., 2018), fish (Sapozhnikova, 2014), and fruit and vegetables from various countries (Lee and Lee, 2012; Jensen et al., 2013; Zhao et al., 2014; Quijano et al., 2016; Muñoz et al., 2017; EFSA, 2019). However, few data are available on the presence and levels of pesticide residues in vegetables consumed in Kenya (Ngatia and Kabaara, 1976; Karembu, 1991; Karanja et al., 2012; Mutai et al., 2015; Kunyanga et al., 2018).

The objective of this study was therefore to determine OP pesticides and carbamates in tomatoes, kales, spinach and French beans and evaluate the associated dietary exposure and the associated potential health risks to children and adults upon acute and chronic exposure.

## **2.2 Materials and Methods**

### **2.2.1 Chemicals and Reagents**

Pesticide reference standards for organophosphate pesticides were obtained from Restek (Restek Corporation, Bellefonte, USA) while carbamate standards were from LGC standards (Teddington UK) and Sigma Aldrich (Zwijndrecht, the Netherlands) with certified purity ranging from 97% to 99%. Acetonitrile and acetic acid were obtained from Rankem (New

Delhi, India), and anhydrous magnesium sulfate, primary and secondary amine from Phenomenex (Phenomenex Inc, California, USA). All the other organic solvents used were high performance liquid chromatography (HPLC) grade.

### 2.2.2 Study site and Study design

This study was conducted in urban and peri-urban Nairobi. Nairobi is the capital city of Kenya and is very likely to reflect what is anticipated in other counties in the country. With an altitude of 1,670 meters (5,480 feet) above the sea level, urban and peri-urban Nairobi receive 1,050 millimeters of rainfall, twice a year with the long rains between March and May. The short rains occur between October and December. The mean annual temperature is 62.6 F (17°C), with mean daily maximum and minimum temperatures of 73.4 F (23°C) and 53.6 F (12°C), respectively.

A total of 90 vegetable samples consisting of 19 French beans, 29 kales, 24 spinach and 18 tomatoes samples were collected from Mkulima, Kangemi, Kawangware, Limuru, N-market and Kiambu open air markets in the months of April, May and June 2018. The selection of these vegetables for this study was based on their high consumption and commercial significance in Kenya (Karanja et al., 2012; Okello et al., 2012; Mutai et al., 2015; RSA, 2015; Njuguna et al., 2019).

The sampling was performed in accordance with the general principles and methods of the European Commission (EC) directive 2002/63/EC (EC, 2002) for compliance verification with MRLs in food commodities. Dust from the samples was removed with light brushing, without washing prior to placing them into the collection bags. Only fresh, high-quality vegetables that were free from blemishes or rot were sampled. Samples were double packed and transported on ice from the markets to the Department of Public health, Pharmacology and Toxicology,

University of Nairobi, Kenya. In the laboratory, samples were placed in the refrigerator at 4°C and extracted within 5 days of collection.

### **2.2.3 Extraction Procedure**

The extraction and clean-up method used was based on QuEChERS (quick easy cheap effective rugged and safe) sample preparation method for pesticides (Anastassiades et al., 2003). About 1 kg of each vegetable sample was homogenized in a blender (SM1030 SANYO Electric Co., Ltd. Japan) and 15 g of the homogenized sample was accurately weighed and transferred into a 50-mL polypropylene centrifuge tube with screw cap. Extraction was conducted according to the AOAC Official Method 2007.01. Briefly, a 15-mL volume of 1% acetic acid in acetonitrile was added as an extraction solvent and the tube was tightly capped and vigorously mixed for 5 min by hand shaking. The tube was opened and 6 g of anhydrous MgSO<sub>4</sub> and 1.5 g sodium acetate were added. The tube was closed immediately after addition and vigorously mixed by hand for 1 minute to avoid formation of salt lump. The mixture was centrifuged at 4000 rpm (Sorvall ST 16, Thermo scientific, MA, USA). The acetonitrile phase was transferred into cryotubes and stored in the freezer (-80°C). Samples were transported at ambient temperature to the Netherlands for instrumental analysis.

After centrifugation, an aliquot of the acetonitrile phase was diluted 1:1 with water and filtered. The final extract contained 0.5 g of matrix equivalent per ml.

### **2.2.4 LC-hrMS screening**

Applying the method described by Zomer and Mol (2015), the extracts were first analysed using LC-hrMS. Following a non-targeted measurement, the extracts were screened in a targeted manner for a total of 118 cholinesterase-inhibiting compounds (organophosphate and carbamate pesticides) including some of their metabolites. Suspect screening was done based on expected retention time, a protonated molecule (NH<sub>4</sub><sup>+</sup> or Na-adduct in some cases) and a

fragment ion. The compound specific parameters that were used for data processing during the pesticide screening can be made available upon request. As quality control, a mix solution of pesticides at 10 ng/ml was included in the sample batch to verify the detection capabilities of the method. These QC samples confirmed that similar detection limits were obtained as described by Zomer and Mol (2015) (typically  $\leq 10$   $\mu\text{g/kg}$ ). The sample extracts in which pesticides were detected during screening were re-analysed for confirmation and quantification, using an LC-MS/MS method.

### 2.2.5 LC-MS/MS confirmation and quantification

An Acquity UPLC system (Waters, Millford, MA, USA) was coupled to a TQ-S triple quad MS system (Waters). Chromatography was performed on a HSS-T3 C18 column (1.7  $\mu\text{m}$ , 2.1x100 mm, Waters) using water (eluent A) and MeOH:H<sub>2</sub>O 95:5 (eluent B), both containing 5 mM ammonium formate and 0.1 % formic acid. The LC flow rate was 0.4 ml/min, column temperature 45°C, and injection volume 5  $\mu\text{l}$ . The LC gradient started with 100% A for 1 min, followed by a two-step linear increase to eluent B (45% B at 2.5 min, 100% B at 8.5 min), which was maintained 3 min and then back initial conditions in 30 s, allowing a equilibration for 2 min before the next injection.

The MS was used in positive MRM mode with the following source parameters; capillary (3 kV), source offset (50 V), source temperature (150 °C), desolvation temperature (590 °C), cone gas flow (150 L/Hr), desolvation gas flow (1000 L/Hr) and nebuliser gas flow (7 bar). The transitions were grouped into two scan events to enable use of longer dwell times for each transition. Table 1 shows the two transitions measured for each compound. The second transition (Q1) was used to calculate an ion ratio between Qn and Q1. In positive samples this value was compared to the average ratio in the standards and used for identification. The linear range was established by injecting a calibration curve in solvent. Positive samples were

quantified by 1-point bracketed calibration using a standard in matrix prepared from a blank sample from the corresponding matrix. As QC samples the same spiked samples as used in the LC-hrMS screening were measured.

### **2.2.6 Data processing**

For suspect screening by LC-hrMS, the software package Tracefinder (version 3.2 SP1, Thermo Scientific) was used to process the data. For confirmatory LC-MS/MS analysis, Masslynx was used. Calculations were further conducted using Microsoft Excel 2010.

### **2.2.7 Exposure analysis and risk characterisation**

Exposure to pesticide residues through the consumption of tomatoes, kales, spinach and French beans was estimated by multiplying the residue concentration detected in the vegetables by food consumption data.

Dietary exposure ( $\mu\text{g}/\text{kg}$  bw/day)

$$= \frac{\text{Concentration of chemical in food } (\mu\text{g}/\text{kg}) \times \text{Food consumption } (\text{kg}/\text{person}/\text{day})}{\text{Body weight } (\text{kg bw}/\text{person})}$$

Consumption of vegetables contaminated with pesticides can have acute and chronic risks which can be quantified using hazard quotient (HQ) and hazard index (HI) approaches. The following equations were used for determination of HQs:

#### **2.2.7.1 Acute/short-term Hazard Quotient (aHQ)**

The aHQ was calculated based on the estimated short-term intake (ESTI) and the acute reference dose (ARfD) as follows:

$$\text{ESTI} = (\text{the highest level of residue} \times \text{the highest large portion of food consumption per day/body weight})$$

$$\text{aHQ} = \text{ESTI}/\text{ARfD}$$

### 2.2.7.2 Chronic/long-term Hazard Quotient (cHQ)

The cHQ was calculated based on the estimated daily intake (EDI) and the acceptable daily intake (ADI) as follows:

$$\text{EDI} = \frac{\text{mean level of residue} \times \text{average portion of food consumption per day}}{\text{body weight}}$$

$$\text{cHQ} = \text{EDI/ADI}$$

Information on ARfDs and ADIs was obtained from the EU pesticides database.

([https://ec.europa.eu/food/plant/pesticides/eu-pesticides-](https://ec.europa.eu/food/plant/pesticides/eu-pesticides-database/public/?event=activesubstance.selection&language=EN)

[database/public/?event=activesubstance.selection&language=EN](https://ec.europa.eu/food/plant/pesticides/eu-pesticides-database/public/?event=activesubstance.selection&language=EN) )

When HQs exceed 1, a health risk cannot be excluded.

## 3. Results and discussion

In Kenya, vegetables play an important role in the nutrition and health of both the urban and rural population and their intake is estimated to constitute up to 80% of the diets (Mungai et al., 2000; Kunyanga et al., 2018). Therefore, potential exposure to vegetable contaminants such as pesticide residues is likely to be high. The mean consumptions of kales, spinach, tomatoes and French beans per day are 200, 100, 200 and 10 g/day respectively (Karanja et al., 2012; Kariathi et al., 2016; Kunyanga et al., 2018; Njuguna et al., 2019). As data of Kenyan large portion consumption of the vegetables were not available, for aHQ, the maximum consumption value was assumed to be 560 (g/day) for tomatoes, kales and spinach based on a study conducted in Tanzania (Kariathi et al., 2016) and an estimate of 50 g/day for French beans was made. The dietary exposure was calculated for both the consumer groups of adults (aged above 18 years) and children (3–10 years old). For dietary exposure assessment, a body weight of 70 kg for adults (aged above 18 years) and 23 kg for children (aged 3–10 years) was applied as recommended by EFSA (EFSA, 2012). In children, the vegetables consumption (g/day) was assumed to be half that of an adults' daily vegetable consumption.

Major sources of uncertainties in the exposure assessment are food consumption rate, body weight, sampling, processing factors, analytical bias and variation, and left-censored data (non detects) (EFSA, 2006c). Processing factors were not considered during exposure assessment in this study.

The substitution method was applied for non-detects as described in the EFSA scientific report (EFSA, 2010b). The non-detect results were replaced with zero and the value of the LOQ (10 µg/kg), according to a Lower and Upper Bound (LB and UB) scenario, respectively.

The risk assessment of the cumulative chronic exposure to residues was performed by using the Hazard Index (HI) method, which is calculated by summing the chronic Hazard Quotients (cHQ) for the individual pesticide residue as described by Reffstrup et al., (2010):

$$\text{Hazard Index (HI)} = \sum \text{cHQ}$$

An HI exceeding 1 indicates that a health risk related to the combined exposure cannot be excluded.



**Table 1: Compound specific parameters LC-MS/MS measurement**

Name	Precursor ion	Product ion	Cone [V]	Coll. En [V]	Dwell [s]
Methamidophos Qn	142.2	94	20	13	0.05
Methamidophos Ql	142.2	125	20	13	0.05
Acephate Ql	184	125	10	20	0.1
Acephate Qn	184	143	10	17	0.1
Omethoate Ql	214	155	22	17	0.05
Qmethoate Qn	214	183	22	10	0.05
Fenthion Qn	279	169	30	18	0.01
Fenthion Ql	279	247	30	12	0.01
Pirimiphos-methyl Ql	306	108	30	25	0.01
Pirimiphos-methyl Qn	306	164	30	25	0.01
Triazophos Qn	314	119	25	35	0.01
Triazophos Ql	314	162	25	20	0.01
Azinphos-ethyl Qn	346	132	10	15	0.01
Azinphos-ethyl Ql	346	160	10	10	0.01
Chlorpyrifos Qn	350	198	20	17	0.01
Chlorpyrifos Ql	352	200	20	17	0.01
Profenofos Ql	373	97	30	33	0.01
Profenofos Qn	373	303	30	18	0.01

### 3.1 Occurrence of OP pesticides and carbamates in Kenyan vegetables

In this survey, 118 organophosphate and carbamate pesticides were screened in vegetable samples comprising of French beans, kales, spinach, and tomatoes to assess health risk. After the screening, acephate, azinphos-ethyl, chlorpyrifos, fenthion, methamidophos, omethoate, pirimiphos-methyl, profenofos, triazophos, aldicarb, carbaryl, carbetam, carbofuran,

ethiofencarb, methiocarb and pirimicarb were tentatively detected. However, during confirmatory quantitative analysis, only chlorpyrifos, profenofos, acephate, methamidophos and omethoate had levels above the default limit of quantification of 10 µg/kg. Out of 90 vegetable samples analysed, 20 (22 %) were found to contain residues of the targeted pesticide.

The most frequently detected pesticides in the positive samples were profenofos (40%) (only in tomatoes), followed by chlorpyrifos (35%), acephate (30%), methamidophos (30%), and omethoate (15%). The concentration of profenofos in tomato ranged from 10 to 958 µg/kg (44 % of samples) while chlorpyrifos had a range of 78 to 107 µg/kg in tomato (11 % of samples), 26 to 315 µg/kg in kales (7% of samples), and 24-1,343 µg/kg (8% of samples) in spinach respectively (Table 2). Concentrations of omethoate ranged from 11 to 98 µg/kg in tomato while acephate was found between 41 to 66 µg/kg (21% of samples). The methamidophos concentration ranged from 20 to 25 µg/kg (21% of samples), 182 µg/kg, and 13 µg/kg in French beans, tomato and kales respectively. The findings are summarised in Table 2.

The presence of multiple residues in French beans and tomatoes were 17%. Acephate and methamidophos were found in three French beans while the fourth had acephate, methamidophos and chlorpyrifos (Table 2). Methamidophos can be used as an insecticide as such, but is also a metabolite of acephate. Since it was always found together with acephate (in a ratio of 0.3 - 0.5) it was concluded that its presence was the result of acephate applications. Omethoate is another OP pesticide that can be applied as such but also is a degradation product of dimethoate. Dimethoate was not detected, indicating that it might have been applied as such or it was a metabolite of dimethoate as observed in a previous study (Bhandari et al, 2018; Kunyanga et al., 2018). Most of the pesticide residues were found in tomatoes followed by French beans, kales and lastly spinach.

Chlorpyrifos is one of the most used pesticides worldwide due to its effectiveness against a wide range of pests and rapid action (Angioni et al., 2011) and also still registered for use in

vegetable crops as well as soil treatment in Kenya (Mutai et al., 2015; PCPB, 2019). It is registered for use in pineapples, roses, cotton, coffee, barley and wheat to control various pests. Its presence in French beans, kales, spinach, and tomatoes could be due to plant uptake from the soil where it is applied to control soil based pests (Zhang et al., 2015), spray drift, or direct application on vegetables. Poor compliance of the pre-harvest interval due to high market demand for the vegetables has also been reported to result in high residue levels as observed in Ghana (Ntow et al., 2006; Darko & Akoto, 2008; Akoto et al., 2015). Ngigi et al. (2011) made a similar observation in Kenya among 85 percent of peri-urban farmers. Furthermore, other studies have indicated that farmers with low perception of harmful effects of pesticides may use them at higher than recommended doses on crops leading to higher pesticide residues (Horna et al., 2008).

In the current study, OP pesticides were detected in 22% of the screened vegetables. These prevalence is lower compared to published reports from other developing countries such as Chile, where pesticide screening in 118 leafy vegetable samples found 72% of spinach samples to contain pesticide residues at higher concentrations than the current study (Elgueta, et al., 2017). In Tanzania, Kiwango et al., (2018) found 31% of sampled vegetables to contain detectable levels of OP residues including dimethoate, acephate, profenofos, dichlorvos and malathion at a mean of 8,560 µg/kg, 2,900 µg/kg, 8,440 µg/kg 20,800 and 5,470 µg/kg respectively. In Algeria, Mebdoua, et al., (2017) found OP pesticide residues in 58% of the 120 vegetable analyzed. Another study by Elgueta et al., (2019) reported a higher frequency of chlorpyrifos detection at 21% and a mean of 10 µg/kg in lettuce, while the detection frequency in spinach and chard was 13% and a mean of 130 µg/kg for both leafy vegetables. Furthermore, methamidophos was found in spinach, chard and lettuce with a frequency of 8% and a mean of 60 µg/kg. The levels of pesticide residues in vegetables in this study were higher than those reported in India (Bhanti and Taneja, 2007).

Profenofos and chlorpyrifos were the most frequently detected pesticide residues in vegetables followed by acephate, and its metabolite methamidophos. These results are in agreement with previous studies involving pesticide screening in vegetables in peri urban Nairobi that reported profenofos (Karanja et al., 2012) and chlorpyrifos (Kunyanga et al., 2018) as the most frequently detected pesticides among others. Although omethoate is restricted for use in fruits and vegetables, it was detected in 15% of the vegetable samples. This might be due to spray drifting from neighboring farmers' fields, or cross contamination by different vectors since it is registered for use as insecticide for coffee and ornamental flowers (PCPB, 2019). Its presence could also be due to illegal use or its persistent nature (Xu et al., 2015). A previous study by Mutai et al. (2015) found kales and French beans in peri urban Nairobi to contain up to 100 and 700  $\mu\text{g/kg}$  of chlorpyrifos and dimethoate residues, respectively. Furthermore, the pesticide levels were reported to be higher during the dry period than during the wet period in that study, though there was no significant difference. Seasonal variability in pesticide residues has been observed, a phenomenon that leads to inadequate assessment of total exposure to pesticides (Mtashobya, 2017). In the same study, significant pesticide residues were found in French beans as compared to kales, an observation that Mutai et al. (2015) related to the coarse nature and dense texture of French beans that slow down the rate of volatilization, a process by which pesticides dissipate in contrast to smooth texture of kales (Bedos et al., 2002). Other factors that could affect the occurrence of pesticides and their residues in different matrices include lipid content, rainfall, temperature, soil properties, and soil organisms (Bento et al., 2016).

Pesticide residues need to comply with maximum residue levels (MRLs) which are based on Good Agricultural Practice (GAP). Since GAP may differ in different countries, also MRLs can differ. Exceedance of local MRLs are an indication that local GAP is not well followed. There are no national MRLs in Kenya. Therefore, codex MRLs were used instead as benchmark. For

the five OPs found in the four crops in this study, Codex MRLs were available for only five OP/crops combinations, thus most vegetables in this study had no established codex MRL for comparison with the measured OP levels. Chlorpyrifos exceeded the codex MRL of 10 µg/kg in French beans. Profenofos and acephate were below codex MRLs in tomatoes. Similarly, methamidophos was below the codex MRL in French beans. In lack of Codex MRLs, findings were also compared to EU-MRLs. EU-MRLs were exceeded in 8-33% of the vegetable samples. Acephate/methamidophos and omethoate have no registration in the EU, and for their residues no import tolerances apply. Hence, an EU-MRL set at the default LOQ of 10 µg/kg applies and may obviously be exceeded when these pesticides are applied in the field. Several exceedances were observed for chlorpyrifos, banned in the EU since January 2020, but at the time of collecting and analyzing the samples it was still having MRLs above the 10 µg/kg default for certain crops (e.g. tomatoes). With a relatively high MRL for profenofos in tomatoes, no exceedances were observed for this OP pesticide although it was the most frequently detected pesticide in this study. In a previous study, Karanja et al. (2012) reported levels of profenofos, diazinon, cypermethrin and bitertanol above EU permissible limits in kales in peri urban Nairobi.

Table 2: Frequency and levels of organophosphate residues detected in/on various vegetables

Pesticides	French beans n=19			Kales n=29			Spinach n=24			Tomatoes n=18		
	number	Min-	EU-	Number	Min-	EU-	number	Min-	EU	number	Min-	EU
	detected	max	MRL	detected	max	MRL	detected	max	MRLS	detected	max	MRL
	(%)	(µg/kg)		(%)	(µg/kg)	(µg/kg)	(%)	(µg/kg)	(µg/kg)	(%)	(µg/kg)	(µg/kg)
Profenofos	0	-	10	0	-	10	0	-	10	8(44)	10-958	10000
Omethoate	0	-	10	0	-	10	0	-	10	3(17)	36100	10
Chlorpyrifos	1(5.3)	117	10	2(6.9)	26-315	10	2(8.3)	24- 1343	10	2(11)	78-107	100
Acephate	4(21)	41-66	10	1(3.4)	43	10	0	-	10	1(5.6)	409	10
Methamidophos	4(21)	20-25	10	1(3.4)	13	10	0	-	10	1(5.6)	182	10

### 3.2 Risk characterisation of the detected pesticides

The HQs related to exposure via dietary intake of the investigated vegetables contaminated with OPs for children and adults are presented in Table 3. Table 4 shows acute reference dose and acceptable daily intake values used in this study. The consumption of spinach was found to imply an acute risk in children and adults with an aHQ of 3.3 and 2.2 for chlorpyrifos in children and adults, respectively. In all other cases, the aHQ and cHQ for the individual pesticides were below 1, implying no risk. Chlorpyrifos, methamidofos and omethoate contributed most to chronic HQs with 0.32, 0.13 and 0.04 in children, and 0.21, 0.09 and 0.03 in adults, respectively. The aHQs for the individual pesticides for children and adults varied from 0.05 to 3.27, and from 0.03 to 2.15, while the cHQ varied from 0.00 to 0.25 for children and 0.00 to 0.14 for adults at the UB, respectively. The HQ for each residue is higher for children than for adults, due to the fact that exposure per kilogram body weight is highest for children.

Due to extensive use of OPs to control pests in vegetable farming, one expects consumer exposure to insecticide mixtures. Indeed, a number of biomonitoring studies have reported the presence of several organophosphate metabolites in urine and inhibition of acetylcholinesterase in plasma of agricultural workers (Timchalk & Poet, 2008). Therefore, many studies begin to characterize the toxicological effects of exposures to concurrent or sequential OP pesticide mixtures (Timchalk & Poet, 2008; Reffstrup et al., 2010). In this study, some vegetables showed more than one type of pesticide residue. The presence of multiple residues could be a result of plant uptake of persistent pesticides (Zhang et al., 2015), spray drift (Coronado et al., 2011) and poor agricultural practices that involve mixing of more than one kind of pesticides during application based on the conception that as a mixture they will be more potent, as has been observed among Nepalese farmers (Bhandari et al., 2018). Indeed, the practice of using pesticide cocktails that sometimes include unapproved or banned pesticides is worrying but in practice among some farmers in Africa.

Exposure to two or more pesticides may result in additive and/or interactive effects (Reffstrup et al., 2010; Saha and Zaman 2012). We used the hazard index method proposed by the US EPA to assess risk posed by a group of pesticides that act by a common mechanism (i.e. AChE inhibition) or that are toxicologically similar, assuming additive effects (US EPA, 2000; Reffstrup et al., 2010). Chronic HIs for OPs in all vegetables sampled were  $< 1$  in both children and adults, implying no health risks upon long-term combined exposure.



Table 3: HQs for detected pesticides in French beans, kales, spinach and tomatoes

Long-term Risk																
Short-term Risk																
		Children					Adult					Children			Adult	
	Pesticide	ARfD	ESTI	aHQ	ESTI	aHQ	HR	ADI	Mean	EDI	cHQ	EDI	cHQ	HR		
F. beans	Methamidophos	3	0.03	0.01	0	0	no	1	LB	2.47	0	0	0	no		
									UB	11.42	0	0	0	no		
	Acephate	100	0.07	0	0.05	0	no	30	LB	11.84	0	0	0	no		
Kales									UB	19.74	0	0	0	no		
	Chlorpyrifos	5	0.13	0.03	0.08	0.02	no	1	LB	8.32	0	0	0	no		
									UB	16.74	0	0	0	no		
	Acephate	100	0.12	0	0.08	0	no	30	LB	1.48	0.01	0	0	no		
									UB	11.14	0.05	0	0.03	no		
	Chlorpyrifos	5	3.83	0.77	2.52	0.5	no	1	LB	11.76	0.05	0.05	0.03	no		
Spinach									UB	21.07	0.09	0.09	0.06	no		
	Methamidophos	3	0.16	0.05	0.1	0.03	no	1	LB	0.45	0	0	0	no		
									UB	10.1	0.04	0.03	0.03	no		
Tomatoes	Chlorpyrifos	5	16.35	<b>3.27</b>	10.74	<b>2.15</b>	yes	1	LB	56.96	0.12	0.12	0.08	no		
									UB	66.13	0.14	0.14	0.09	no		
	Acephate	100	4.98	0.05	3.27	0.03	no	30	LB	22.72	0.1	0	0.06	no		
									UB	32.17	0.14	0	0.09	no		
	Chlorpyrifos	5	1.3	0.26	0.86	0.17	no	1	LB	5.94	0.03	0.03	0.02	no		
									UB	19.17	0.08	0.08	0.05	no		
	Methamidophos	3	2.23	0.74	1.46	0.49	no	1	LB	10.17	0.09	0.09	0.03	no		
									UB	20.06	0.09	0.09	0.06	no		
	Omethoate	2	1.19	0.6	0.78	0.39	no	2	LB	9.67	0	0	0.03	no		
									UB	18.61	0.08	0.04	0.03	no		
	Profenofos	1000	11.66	0.01	7.66	0.01	no	30	LB	100.22	0.44	0.01	0.29	no		
									UB	105.78	0.92	0.03	0.01	no		

ESTI = Estimated short-term intake ( $\mu\text{g kg b.w.}^{-1}$ )

aHQ = acute/short term Hazard Quotient

cHQ = Chronic/long-term Hazard Quotient

ARfD ( $\mu\text{g kg b.w.}^{-1}$ ) and ADI ( $\mu\text{g kg b.w.}^{-1} \text{ day}^{-1}$ ) values were extracted from the EU pesticides database (<http://ec.europa.eu/food/plant/pesticides/eu-pesticides-database/public/?event=homepage&language=EN>)

HR = Health risk can no longer be excluded

EDI = Estimated daily intake ( $\mu\text{g kg b.w.}^{-1} \text{ day}^{-1}$ )

LB = lower bound, LOQ is replaced by 0;

UB = upper bound, LOQ was replaced by LOQ-value = 10  $\mu\text{g/kg}$

The aHQ values in bold represent a potential risk upon exposure to the pesticides via dietary exposure in adolescents and adults

### 3.4 Uncertainties related to dietary exposure assessment

Scientific uncertainties affect dietary exposure assessments and therefore should be considered during interpretation of the results. Due to paucity of data on Kenyan large portion consumption of the vegetables for aHQ determination, the maximum consumption value was assumed to be 560 (g/day) for tomatoes, kales and spinach based on a study conducted in Tanzania (Kariathi et al., 2016). Though the dietary habits of the two countries are similar to a large extent, there is a possibility to under- or over-estimate the consumption and therefore in future a dietary recall questionnaire should be used to assess large portion consumption of vegetables in Kenya. In addition, processing factors such as washing, peeling and cooking were not considered during exposure assessment in this study. Generally, inclusion of processing factors could have led to lower estimated exposure. Finally, the high proportion of left-censored data may have introduced uncertainties in the overall estimate. The substitution method applied for non-detects as described in the EFSA scientific report (EFSA, 2010b) could lead to an over-estimation of the exposure (substitution of non detects with LOQ (10  $\mu\text{g/kg}$ )) or under-estimation (substitution of non detects with zero). Nevertheless, given that all individual cHQs and His, even with the worst-case approach, were below 1, indicates no risk resulting from long term consumption of the vegetables.

Since the dietary pesticide intakes determined in the current study considered only exposures from the major vegetables, it did not cover the total dietary exposure to OP pesticides. Other

food products such as fish, meats, dairy, grains, and drinking water, and exposure due to occupational or residential sources may add to the overall exposure.

Table 4: Acute reference dose and acceptable daily intake values used in this study

Pesticide	ARfD (mg/kg bw/day)	ADI (mg/kg bw/day)	Year
Chlorpyrifos	0.005	0.001	EFSA 2014
Profenofos	1	0.03	JMPR 2007
Acephate	0.1	0.03	JMPR 2005
Omethoate	0.002	0.0003	EFSA 2013
Methamidofos	0.003	0.001	EFSA Dir 06/131

## Conclusion

This study revealed the occurrence of several organophosphate pesticide residues in French beans, kales, spinach and tomatoes, sampled from peri-urban Nairobi. Chlorpyrifos, acephate, omethoate and methamidophos exceeded the Codex and/or EU MRLs. However, only the aHQ of chlorpyrifos in spinach revealed that a potential acute risk to both children and adult consumers could not be excluded. There were no indications for chronic risks, not for the individual OPs found, and also not for the combined chronic exposure assessed through the HI. Routine monitoring of OPs and carbamates in vegetables is recommended to minimize consumer's health risks.

## Acknowledgements

This work is supported by the Netherlands Universities Foundation for International Cooperation (Nuffic) via scholarship granted to Isaac Omwenga (NFP - PhD.17/0019). The authors would like to thank the county government of Nairobi for consenting to this study as well as the local farmers and traders for their cooperation and support during the sample collection.

## Conflict of interest statement

The authors declare that there are no conflicts of interest.

**REFERENCES**

- Akoto, o., Gavor, s., Appah, M.K., Apau, K., 2015. Estimation of human health risk associated with the consumption of pesticide-contaminated vegetables from Kumasi, Ghana, *Environ Monit Assess* (2015) 187:244 DOI 10.1007/s10661-015-4471-0
- Alavanja, M.C.R., Ross, M.K., Bonner, M.R., 2013. Increased cancer burden among pesticide applicators and others due to pesticide exposure. *Cancer J. Clin.* **2013**, 63, 120–142
- Anastassiades, M., Lehotay, S.J., Stajnbaher, D., Schenck, F.J., 2003. Fast and easy multiresidue method employing acetonitrile extraction/partitioning and “dispersive solid-phase extraction” for the determination of pesticide residues in produce. *J. AOAC Int.* 2003, 86, 412–431. [PubMed]AOAC Official Method 2007.01, Pesticide Residues in Foods by Acetonitrile Extraction and Partitioning with Magnesium Sulfate.
- Angioni, A., Dedola, F., Garau, A., Sarais, G., Cabras, P., Caboni, P. 2011. Chlorpyrifos residues levels in fruits and vegetables after field treatment. *J Environ Sci Health B* 46:544–549
- Baig, S. A., Akhtera, A. N., Ashfaq, M., & Asi, R. M., 2009. Determination of the organophosphorus pesticide in vegetables by high performance liquid chromatography. *American- Eurasian Journal of Agricultural and Environmental Sciences*, 6(5), 513–519
- Bhanti, M., Taneja, A., 2007. Contamination of vegetables of different seasons with organophosphorous pesticides and related health risk assessment in northern India. *Chemosphere* 69: 63–68. <https://doi.org/10.1016/j.chemosphere.2007.04.071> PMID: 17568651
- Bedos, C., Cellier P., Calvet, R., Barriuso, E, and Gabrielle, B., 2002. Mass transfer of pesticides into the atmosphere by volatilization from soils and plants. *Agronomie*. **22**: 21-23
- Bento, C.P.M, Yang, X., Gort, G., Xue, S., van Dam, R., Zomer, P., et al, 2016. Persistence of glyphosate and aminomethylphosphonic acid in loess soil under different combinations of temperature, soil moisture and light/darkness. *Sci Total Environ* 2016; 572: 301-311.
- Bhandari, G., Atreya, K., Yang, X., Fan, L., Geissen, V., 2018. Factors affecting pesticide

- safety behaviour: The perceptions of Nepalese farmers and retailers. *Science of The Total Environment* 2018; 631-632: 1560-1571.
- Bhandari, G., Zomer, P., Atreya, K., Hans G.J. m., Yang, X., Geissen, V., 2019. Pesticide residues in Nepalese vegetables and potential health risks. *Environmental Research*, <https://doi.org/10.1016/j.envres.2019.03.002>
- Bradman, A., Quiros-Alcala, L., Castorina, R., et al., 2015. Effect of organic diet intervention on pesticide exposures in young children living in low-income urban and agricultural communities. *Environ. Health Perspect.* 123, 1086–1093. <https://doi.org/10.1289/ehp.1408660>.
- Bravo, V., Rodriguez, T., van Wendel de Joode, B., Canto, N., Calderon, G.R., Turcios, M., et al., 2011. Monitoring pesticide use and associated health hazards in Central America. *Int J Occup Environ Health.* 2011; 17 (3):258–69. Epub 2011/09/13. <https://doi.org/10.1179/107735211799041896> PMID: 21905395.
- Boobis, A.R., Ossendorp, B.C., Banasiak, U., Hamey, P.Y., Sebestyen, I., Moretto, A., (2008). Cumulative risk assessment of pesticide residues in food. *Toxicol Lett* 180:137–150
- Boon, P.E., Van der Voet, H., Van Raaij, M.T., Van Klaveren, J.D. 2008. Cumulative risk assessment of the exposure to organophosphorus and carbamate insecticides in the dutch diet *Food Chem. Toxicol.*, 46 (9) (2008), pp. 3090-3098
- Centers for Disease Control and Prevention. Fourth National Report on Human Exposure to Environmental Chemicals, Updated Tables, January 2017. Atlanta, GA: National Center for Environmental Health; 2017
- Curl C. L., Fenske R.A., and Elgethum, K., 2003. “Organophosphorus pesticide exposure of urban and suburban preschool children with organic and conventional diets,” *Environmental Health Perspectives*, vol. 111, no. 3, pp. 377–382, 2003.
- Coronado, G.D., Holte, S., Vigoren, E., Griffith, W.C., Barr, D.B., Faustman, E., Thompson, B. 2011. Organophosphate pesticide exposure and residential proximity to nearby fields: evidence for the drift pathway. *J Occup Environ Med* 2011; 53: 884-891.
- Darko, G., Akoto, O., 2008. Dietary intake of organophosphorus pesticide residues through vegetables from Kumasi, Ghana. *Food Chem Toxicol* 2008; 46: 3703-3706.
- Dixon, G. R. (1985). *Vegetable crop diseases* (p. 404). London: The Macmillan Press Ltd.
- EC (European Commission), 2002. Establishing Community Methods of Sampling for the

- Official Control of Pesticide Residues in and on Products of Plant and Animal Origin and Repealing Directive. OJEU L 2002, 187, 30–43.
- EC (European Commission), 2005. Regulation No. 396/2005 on maximum residue levels of pesticides in products of plant and animal origin. Annex II ([http://ec.europa.eu/food/plant/protection/pesticides/pesticide\\_res\\_annex\\_ii.xls](http://ec.europa.eu/food/plant/protection/pesticides/pesticide_res_annex_ii.xls)).
- Ecobichon, D.J. (2001) Pesticide Use in Developing Countries. *Toxicology*, 160, 27-33.  
[http://dx.doi.org/10.1016/S0300-483X\(00\)00452-2](http://dx.doi.org/10.1016/S0300-483X(00)00452-2)
- EFSA, 2012. Guidance on selected default values to be used by the EFSA scientific committee, scientific panels and units in the absence of actual measured data. *EFSA Journal* 10 (3), 2579.
- EFSA, 2006c. Guidance of the scientific committee on a request from EFSA related to uncertainties in dietary exposure assessment. *The EFSA Journal* 438, 1–54.
- EFSA, 2010b. Management of left-censored data in dietary exposure assessment of chemical substances. *EFSA Journal* 8 (3), 1557.
- EFSA, (2018). The 2018 European Union report on pesticide residues in food. *EFSA Journal* 14: e04611.
- Elgueta, S., Moyano S., Sepúlveda P., Quiroz C., Correa A., 2017. Pesticide residues in leafy vegetables and human health risk assessment in North Central agricultural areas of Chile. *Food Addit Contam Part B Surveill.* 10:105–112.  
[doi:10.1080/19393210.2017.1280540](https://doi.org/10.1080/19393210.2017.1280540).
- Elgueta, S., Fuentes, M., Valenzuela, M., Zhao, G., Liu, S., Lu, H., Correa, A., 2019. Pesticide residues in ready-to-eat leafy vegetables from markets of Santiago, Chile, and consumer's risk, *Food Additives & Contaminants: Part B*, DOI: [10.1080/19393210.2019.1625975](https://doi.org/10.1080/19393210.2019.1625975)
- EFSA (European Food Safety Authority), 2019. Scientific report on the 2017 European Union report on pesticide residues in food. *EFSA Journal* 2019;17(6):5743, 152 pp. <https://doi.org/10.2903/j.efsa.2019.5743>

- Fan, L., Niu, H., Yang, X., Qin, W., Bento, C.P., Ritsema, C.J., Geissen, V., 2015. Factors affecting farmers' behaviour in pesticide use: Insights from a field study in northern China. *Sci. Total Environ.* 537, 360-368.450  
<http://doi.org/10.1016/j.scitotenv.2015.07.150>
- Fernández, M., Picó, Y., Mañes, J., 2000. “Determination of carbamate residues in fruits and vegetables by matrix solid-phase dispersion and liquid chromatography-mass spectrometry,” *Journal of Chromatography A*, vol. 871, no. 1-2, pp. 43–56, 2000.
- Gallagher, S.S., Rice, G.E., Scarano, L.J., Teuschler, L.K., Bolleweg, G., Martin, L. 2015. Cumulative risk assessment lessons learned: a review of case studies and issue papers *Chemosphere*, 120 (2015), pp. 697-705
- Glat, R. 2010. Scaling up political ecology: the case of non-authorized pesticides on fresh vegetables imported into the United States, 1996-2006. *Ann Assoc Am Geogr.* 100:327–355. [Taylor & Francis Online], [Web of Science ®], [Google Scholar]
- Golge, O., Koluman, A., Kabak, B., 2018. Validation of a modified QuEChERS method for the determination of 167 pesticides in milk and milk products by LC-MS/MS. *Food Anal. Methods* 11, 1122–1148
- Gonzales, B.F., editor. *Highly Hazardous Pesticides in Mexico*. 1st English Edition. RAPAM; 2018. Texcoco, Mexico. Available from:  
[http://www.academia.edu/36923833/Highly\\_Hazardous\\_Pesticides\\_in\\_Mexico01.pdf](http://www.academia.edu/36923833/Highly_Hazardous_Pesticides_in_Mexico01.pdf)
- Haines, D.A., Saravanabhavan, G., Werry, K., Khoury, C., 2017. An overview of Human biomonitoring of environmental chemicals in the Canadian Health Measures Survey:2007–2019. *Int. J. Hyg. Environ. Health* 220, 13–28.  
<https://doi.org/10.1016/j.ijheh.2016.08.002>.
- Horna, D., Smale, M., Al-Hassan, R., Falck-Zepeda, J., & Timpo, S. E., 2008. Selected paper prepared for presentation at the American Agricultural Economics Association Annual Meeting, Orlando, FL. <https://ageconsearch.umn.edu> (accessed 6/9/2021).
- Ivey KL, Hodgson JM, Croft KD, Lewis JR, Prince RL. 2015. Flavonoid intake and all-cause mortality. *Am J Clin Nutr.* 1:1012–1020
- Jensen, B.H., Petersen, A., Christiansen, S., Boberg, J., Axelstad, M., Herrmann, S.S., Poulsen, M.E., Hass, U., 2013. *Food Chem. Toxicol.* 55, 113–120.
- Karanja, N. K., Njenga, M., Mutua, G. K., Lagerkvist, C. J., Kutto, E., & Okello, J. J. 2012.

- Concentrations of heavy metals and pesticide residues in leafy vegetables and implications for peri-urban farming in Nairobi, Kenya. *Journal of Agriculture, Food Systems, and Community Development*, 3(1), 255–267.
- Karembu, M., 1991. Pesticide use and misuse by small scale farmers in Kiambu. Kenyatta University. <https://ir-library.ku.ac.ke/handle/123456789/5004?show=full> (accessed 6/9/2021)
- Kariathi, V., Kassim, N., Kimanya, M., 2016. Pesticide exposure from fresh tomatoes and its relationship with pesticide application practices in Meru district. *Cogent Food & Agriculture* (2016), 2: 1196808
- Kiwango, P.A., Kassim, N., Kimanya, M.E., 2018. The risk of dietary exposure to pesticide residues and its association with pesticide application practices among vegetable farmers in Arusha, Tanzania. *Journal of Food Research*; Vol. 7, No. 2; 2018
- Knežević, Z., Serdar, M., Ahel, M., 2012. Risk assessment of the intake of pesticides in Croatian diet. *Food Control*. 23:59-65.  
<http://dx.doi.org/10.1016/j.foodcont.2011.06.011>
- Kunyanga, C. Amimo, J., Kingori L.N., Chemining'wa, G., 2018. Consumer Risk Exposure to Chemical and Microbial Hazards Through Consumption of Fruits and Vegetables in Kenya. *Food Science and Quality Management* [www.iiste.org](http://www.iiste.org). Vol.78, 2018
- Lee, K.-G., Lee, S.-K., 2012. Monitoring and risk assessment of pesticide residues in yuza fruits (*Citrus junos* Sieb. Ex Tanaka) and yuza tea samples produced in Korea. *Food Chem*. 135:2930–2933
- Li, F., Yuan, Y., Meng, P., Wu, M., Li, S., Chen, B., 2017. Probabilistic acute risk assessment of cumulative exposure to organophosphorus and carbamate pesticides from dietary vegetables and fruits in Shanghai populations, *Food Additives & Contaminants: Part A*, 34(5):819-831.
- Lozowicka, B., Kaczynski, P., Paritova, A.E., Kuzembekowa, G.B., Abzhaliyeva, A.B., Sarsembayeva, N.B., Alihan, K., 2014. Pesticide residues in grain from Kazakhstan and potential health risks associated with exposure to detected pesticides. *Food*



- Chem. Toxicol. 64, 238–248.
- Mansour, S.A., 2004. Pesticide exposure-Egyptian scene. *Toxicology* 2004; 198: 91-115
- Mtashobya, L.A., 2017. Assessment of pesticide residues in vegetables from the Western Usambara and Uruguru Mountains in Tanzania. *Environ Monit Assess* 2017; 189: 1-14.
- Mebdoua, S., Lazali, M., Ounane, S. M., & Tellah, S. (2017). Evaluation of pesticide residues in fruits and vegetables from Algeria. *Food Additives & Contaminants: Part B*, 10(2), 91-98. <http://doi.org/10.1080/19393210.2016.1278047>
- Mungai, J.K., Ouko, J., & Heiden, M., 2000. “Processing of Fruits and Vegetables in Kenya”, GTZ – Integration of tree crops into farming systems project, ICRAF House, Nairobi. [http://s3-eu-central-1.amazonaws.com/fsd-circle/wp-content/uploads/2015/08/30095816/10-07-27\\_Value\\_chain\\_study.pdf](http://s3-eu-central-1.amazonaws.com/fsd-circle/wp-content/uploads/2015/08/30095816/10-07-27_Value_chain_study.pdf) (Accessed 6/9/2021)
- Mutai, C., Inonda R. Njage E. and Ngeranwa J., 2015. Determination of Pesticide Residues in Locally Consumed Vegetables in Kenya. *African Journal of Pharmacology and Therapeutics* Vol. 4 (1) 1-6.
- Muñoz, N.C., Floriano, L., De Souza, M.P., Bandeira, N.M.G., Prestes, O.D., Zanella, R., 2017. Determination of pesticide residues in golden berry (*Physalis peruviana* L.) by modified QuEChERS method and ultra-high performance liquid chromatography tandem quadrupole mass spectrometry. *Food Anal. Methods* 10: 320–329.
- Ngatia, S.C., Kabaara, A. M., 1976. The state of the Kenya coffee industry with reference to research and extension. *Kenya Coffee* 480: 94-99
- Ngigi, M., Njenga, M., Lagerkvist, C. J, Karanja, N., & Okello, J. 2011. *Measures to reduce food safety risks in urban and peri-urban leafy vegetables value chain in Nairobi, Kenya* [Feedback Workshop Report].
- Njuguna, S.M., Makokha, V.A., Yana, X., Gituru, R.W., Wanga, Q., Wanga, J. 2019. Health risk assessment by consumption of vegetables irrigated with reclaimed waste water: A case study in Thika (Kenya). *Journal of Environmental Management* 231: 576–581
- NIP (National Implication Plan for Stockholm convention on Persistent Organic Pollutants,

- NES.),2006. Nairobi, Kenya: National Environmental Secretariat.
- Ntow, W. J., Gijzen, H. J., Kalderman, P., & Drechesel, P., 2006. Farmer perceptions and pesticides use practices in vegetable production in Ghana. *Pesticide Management Science*, 62:356–365.
- Okello, J. J., Lagerkvist, C.-J., Hess, S., Ngigi, M., & Karanja, N., 2012. Choice of fresh vegetable retail outlets by developing- country urban consumers: The case of kale consumers in Nairobi, Kenya. *European Journal of Development Research*, 24: 434–449. <http://dx.doi.org/10.1057/ejdr.2011.58>
- Okoffo, E. D., Mensah, M and Fosu-Mensah, B. Y., 2016. Pesticides exposure and the use of personal protective equipment by cocoa farmers in Ghana. *Environ Syst Res* 5:17
- Omwenga, I., Kanja, L., Nguta, J., Mbaria, J., Irungu, P., 2016. Organochlorine pesticide residues in farmed fish in Kiambu and Machakos Counties, Kenya. *Cogent Environmental Science*. <http://www.tandfonline.com/doi/full/10.1080/23311843.2016.1153215>
- Pest control products Board of Kenya, 2019. <http://www.pcpb.go.ke/list-of-registered-products/> accessed on 10/12/2019
- Picciotto, H.I., Sass J.B., Engel S., Bennett, D.H., Bradman, A., Eskenazi B., et al., 2018. Organophosphate exposures during pregnancy and child neurodevelopment: Recommendations for essential policy reforms. *PLoS Med* 15(10): e1002671. <https://doi.org/10.1371/journal.pmed.1002671>
- Pogaćnik, L., Franko, M., 2003. “Detection of organophosphate and carbamate pesticides in vegetable samples by a photothermal biosensor,” *Biosensors and Bioelectronics*, vol. 18(1): 1–9.
- Poulsen, M.E., Andersen, J.H., Petersen, A., Jensen, B.H. 2017. Results from the Danish monitoring programme for pesticide residues from the period 2004–2011. *Food Control*, 74:25-33.
- Quijano, L., Yusà, V., Font, G., Pardo, O., 2016. Chronic cumulative risk assessment of the exposure to organophosphorus, carbamate and pyrethroid and pyrethrin pesticides through fruit and vegetables consumption in the region of Valencia (Spain). *Food*

- Chem. Toxicol. 89:39–46
- Razzaghi, N., Ziarati, P., Rastegar, H., Shoeibi, S., Amirahmadi, M., Conti, G.O., Ferrante, M., Fakhri, Y., Khaneghah, A.M., 2018. The concentration and probabilistic health risk assessment of pesticide residues in commercially available olive oils in Iran. *Food Chem. Toxicol.* 120:32–40.
- Reffstrup, T.K., Larsen, J.C., Meyer, O., 2010. Risk assessment of mixtures of pesticides. Current approaches and future strategies. *Regul Toxicol Pharmacol* 56:174-192.
- Research Solutions Africa (RSA) Ltd. Report of a Study on Fresh Vegetables Market in Kenya. Desk Review; Research Solutions Africa (RSA) Ltd.: Nairobi, Kenya, 2015. [Google Scholar]
- Roberts, J., Reigart, J. Chapter 5. Organophosphates. Recognition and Management of Pesticide Poisonings. Sixth ed. Washington, D.C.: U.S. Environmental Protection Agency, Office of Pesticide Programs; 2013. Available from: <http://www2.epa.gov/pesticide-worker-safety>
- Sapozhnikova, Y., 2014. Evaluation of low-pressure gas chromatography-tandem mass spectrometry method for the analysis of >140 pesticides in fish. *J. Agric. Food Chem.* 62, 3684–3689
- Stadlinger, N., A. Mmochi and L. Kumbilad., 2013. Weak Governmental Institutions Impair the Management of Pesticide Import and Sales in Zanzibar. *Ambio* 42:72-82.
- Timchalk, C., Poet, T.S., 2008. Development of a physiologically based pharmacokinetic and pharmacodynamic model to determine dosimetry and cholinesterase inhibition for a binary mixture of chlorpyrifos and diazinon in the rat. *NeuroToxicology* 29 (2008) 428–443
- Toe, A., 2010. Final Report: Pilot Study on Agricultural Pesticide Poisoning in Burkina Faso. Secretariat of the Rotterdam Convention on the Prior Informed Consent (PIC) Procedure for Certain Hazardous Chemicals and Pesticides in International Trade. 2010.

- U.S. EPA, 2000. EPA Revised Human Health Risk Assessment on Chlorpyrifos. December 2014. Docket ID EPA-HQ-OPP-2008-0850. Available from: <http://www.epa.gov/ingredients-used-pesticide-products/revised-human-health-risk-assessment-chlorpyrifos>
- US EPA, 2006. Organophosphorus Cumulative Risk Assessment (2006) Retrieved from [www.epa.gov/pesticides/cumulative](http://www.epa.gov/pesticides/cumulative) (accessed December 2019)
- US EPA, 2007. Revised N-methyl Carbamate Cumulative Risk Assessment Retrieved from [www.epa.gov/pesticides/cumulative](http://www.epa.gov/pesticides/cumulative) (accessed December 2019)
- USEPA, 2011. Pyrethrins/pyrethroid Cumulative Risk Assessment (2011) Retrieved from [www.epa.gov/pesticides/cumulative](http://www.epa.gov/pesticides/cumulative) (accessed December 2020).
- Wesseling, C., Corriols, M., Bravo V., 2005. Acute pesticide poisoning and pesticide registration. *Toxicol Appl Pharmacol.* 2005; 207(2 Suppl): 697–705.
- World Health Organization International Programme on Chemical Safety, 2009. The WHO Recommended Classification of Pesticides by Hazard and Guidelines to Classification 2009. Geneva, Switzerland: 2009 [cited 2018 Sep 1]. Available from: [http://www.who.int/ipcs/publications/pesticides\\_hazard\\_2009.pdf?ua=1](http://www.who.int/ipcs/publications/pesticides_hazard_2009.pdf?ua=1)
- WHO, 2003. GEMS/food Regional Diets (Regional Per Capita Consumption of Raw and Semi-Processed Agricultural Commodities). Retrieved from [http://www.who.int/foodsafety/publications/chem/regional\\_diets/en/](http://www.who.int/foodsafety/publications/chem/regional_diets/en/) (accessed December 2019)
- Xu, M., Qiu, Y., Bignert, A., Zhou, Y., Zhu, Z., Zhao, J., 2015. Organochlorines in free-range hen and duck eggs from Shanghai: occurrence and risk assessment. *Environ Sci Pollut Res Int* 2015; 22: 1742-1749.
- Zhang, A., Luo, W., Sun, J., Xiao, H., Liu, W., 2015. Distribution and uptake pathways of organochlorine pesticides in greenhouse and conventional vegetables. *Sci Total Environ* 2015; 505: 1142-1147.
- Zhao, P., Huang, B., Li, Y., Han, Y., Zou, N., Gu, K., Li, X., Pan, C., 2014. Rapid multiplug filtration cleanup with multiple-walled carbon nanotubes and gas chromatography–triple–quadrupole mass spectrometry detection for 186 pesticide residues in tomato and tomato products. *J. Agric. Food Chem.* 62, 3710–3725.
- Zomer, P., & Mol, H.G.J., 2015. Simultaneous quantitative determination, identification and

qualitative screening of pesticides in fruits and vegetables using LC-Q-Orbitrap™-MS,  
Food Additives & Contaminants: Part A, 32:10,1628-1636,  
DOI:10.1080/19440049.2015.1085652

## Supplementary Material 1.

Organophosphorus pesticides and carbamates included in the suspect screening after LC-hrMS analysis of the vegetable extracts.

Compound Name	Compound Formula	Adduct used	Rt [min.]	Fragment Formula	Fragment Mass	vDIA window
Acephate	C4H10NO3PS	[M+H] <sup>+</sup>	5.72	C2H8O3PS	142.99260	150
Aldicarb	C7H14N2O2S	[M+NH4] <sup>+</sup>	8.35	C4H9S	89.04190	250
Aldicarb-sulfoxide	C7H14N2O4S	[M+Na] <sup>+</sup>	6.10	C2H6O2N	76.03930	250
Aldicarb-sulfoxide	C7H14N2O3S	[M+Na] <sup>+</sup>	5.92	C4H9S	89.04190	250
Azamethiphos	C9H10ClN2O5PS	[M+H] <sup>+</sup>	8.69	C7H4ClN2O2	182.99558	350
Azinphos-ethyl	C12H16N3O3PS2	[M+Na] <sup>+</sup>	10.97	C8H6ON	132.04439	350
Azinphos-methyl	C10H12N3O3PS2	[M+Na] <sup>+</sup>	10.10	C8H6ON	132.04439	350
Bendiocarb	C11H13NO4	[M+H] <sup>+</sup>	8.85	C6H5O2	109.02840	250
Cadusafos	C10H23O2PS2	[M+H] <sup>+</sup>	11.90	C2H8O2PS2	158.96978	250
Carbaryl	C12H11NO2	[M+H] <sup>+</sup>	9.16	C10H9O	145.06479	250
Carbetamide	C12H16N2O3	[M+H] <sup>+</sup>	8.60	C5H12NO2	118.08626	250
Carbofuran	C12H15NO3	[M+H] <sup>+</sup>	8.95	C7H7O2	123.04410	250
Carbofuran 3-hydroxy-	C12H15NO4	[M+H] <sup>+</sup>	7.40	C9H2O	121.01002	250
Carbophenothion	C11H16ClO2PS3	[M+H] <sup>+</sup>	12.78	C7H6ClS	156.98730	350
Carbosulfan	C20H32N2O3S	[M+H] <sup>+</sup>	13.70	C5H12NS	118.06850	350
Chlorfenvinphos	C12H14Cl3O4P	[M+H] <sup>+</sup>	11.52	C4H12O4P	155.04680	350
Chlorpropham	C10H12ClN2O2	[M+H] <sup>+</sup>	10.78	C7H5ONCl	154.00540	250
Chlorpyrifos	C9H11Cl3NO3PS	[M+H] <sup>+</sup>	12.61	H4O3PS	114.96133	350
Chlorpyrifos-methyl	C7H7Cl3NO2PS	[M+H] <sup>+</sup>	11.91	C6H4Cl3NO2PS	289.87610	350
Chlorthiophos	C11H15Cl2O3PS2	[M+H] <sup>+</sup>	12.84	C7H8O3Cl2PS2	304.90240	350
Coumaphos	C14H16ClO5PS	[M+H] <sup>+</sup>	11.55	C9H8O3PS	226.99263	350
Crotoxyphos	C14H19O6P	[M+NH4] <sup>+</sup>	10.41	C2H8PO4	127.01547	350
Cyanofenphos	C15H14NO2PS	[M+H] <sup>+</sup>	11.37	C6H6OPS	156.98720	350
Cythioate	C8H12NO5PS2	[M+H] <sup>+</sup>	8.08	C2H8O3PS	142.99263	350
Demeton-o	C8H19O3PS2	[M+H] <sup>+</sup>	10.29	C8H19O3PS2	258.05077	250
Demeton-s-Methyl	C6H15O3PS2	[M+Na] <sup>+</sup>	9.10	C4H9S	89.04195	250
Demeton-s-methyl-sulfone	C6H15O5PS2	[M+H] <sup>+</sup>	6.44	C4H9O2S	121.03178	250
Dialifos	C14H17ClNO4PS2	[M+H] <sup>+</sup>	11.77	C10H7O2NCl	208.01598	350
Diazinon	C12H21N2O3PS	[M+H] <sup>+</sup>	11.60	C8H13N2S	169.07940	350
Dichlorvos	C4H7Cl2O4P	[M+H] <sup>+</sup>	8.88	C2H8O4P	127.01550	250
Dicrotophos	C8H16NO5P	[M+H] <sup>+</sup>	6.77	C6H10ON	112.07569	250
Diethofencarb	C14H21NO4	[M+H] <sup>+</sup>	10.38	C11H16O4N	226.10738	250
Dimethoate	C5H12NO3PS2	[M+H] <sup>+</sup>	7.59	C2H8O3PS	142.99263	250
Disulfoton	C8H19O2PS3	[M+NH4] <sup>+</sup>	11.86	C4H9S	89.04190	250
Disulfoton-sulfone	C8H19O4PS3	[M+H] <sup>+</sup>	9.57	H4O3PS	114.96133	350
Disulfoton-sulfoxide	C8H19O3PS3	[M+H] <sup>+</sup>	9.51	C4H10O2PS2	184.98540	250
Ditalimfos	C12H14NO4PS	[M+H] <sup>+</sup>	11.01	C8H14ON	130.02874	350
Edifenphos	C14H15O2PS2	[M+H] <sup>+</sup>	11.64	C6H5S	109.01065	350
EPN	C14H14NO4PS	[M+H] <sup>+</sup>	11.83	C10H11O2	163.07536	350
Ethiofencarb	C11H15NO2S	[M+H] <sup>+</sup>	10.54	C7H7O	107.04914	250
Ethiofencarb-sulfone	C11H15NO4S	[M+H] <sup>+</sup>	6.93	C7H7O	107.04914	250
Ethiofencarb-sulfoxide	C11H15NO3S	[M+H] <sup>+</sup>	7.01	C7H7O	107.04914	250
Ethion	C9H22O4P2S4	[M+H] <sup>+</sup>	12.42	C2H4OCIS2	142.93870	350
Ethoprophos	C8H19O2PS2	[M+H] <sup>+</sup>	11.09	C3H10O2PS2	172.98540	250
Etrinfos	C10H17N2O4PS	[M+H] <sup>+</sup>	11.40	C2H8O3PS	142.99260	250
Fenamiphos	C13H22NO3PS	[M+H] <sup>+</sup>	11.17	C8H10O3PS	217.00828	250
Fenchlorphos-oxon	C8H8Cl3O4P	[M+H] <sup>+</sup>	11.17	C2H8O4P	127.01547	350
Fenitrothion	C9H12NO5PS	[M+H] <sup>+</sup>	10.39	C2H8O3PS	142.99263	250
Fenobucarb	C12H17NO2	[M+H] <sup>+</sup>	10.30	C6H7O	95.04914	250
Fensulfothion	C11H17O4PS2	[M+H] <sup>+</sup>	9.70	C7H10O4PS2	252.97526	350
Fensulfothion-oxon	C11H17O5PS	[M+H] <sup>+</sup>	7.95	C7H10O5PS	252.99302	250
Fensulfothion-oxon-sulfone	C11H17O6PS	[M+H] <sup>+</sup>	8.08	C7H10O6PS	252.99302	350

Fensulfthion-sulfone	C11H17O5PS2	[M+H] <sup>+</sup>	9.79	C11H5O4S2	265.97020	350
Fenthion	C10H15O3PS2	[M+H] <sup>+</sup>	11.44	C9H12O2PS2	247.00108	250
Fenthion-oxon	C10H15O4PS	[M+H] <sup>+</sup>	10.17	#	#	#
Fenthion-oxon-sulfone	C10H15O6PS	[M+H] <sup>+</sup>	11.21	C7H7	91.05423	250
Fenthion-oxon-sulfoxide	C10H15O5PS	[M+H] <sup>+</sup>	7.34	C8H8	104.06205	250
Fenthion-sulfone	C10H15O5PS2	[M+NH4] <sup>+</sup>	9.15	C2H8O3PS	142.99263	350
Fenthion-sulfoxide	C10H15O4PS2	[M+H] <sup>+</sup>	8.99	C6H7O2	111.04406	250
Fonofos	C10H15O5PS2	[M+H] <sup>+</sup>	11.59	C2H6OPS	108.98714	250
Formothion	C6H12NO4PS2	[M+Na] <sup>+</sup>	8.48	C3H8O2ClS	142.99280	250
Fosthiazate	C9H18NO3PS2	[M+H] <sup>+</sup>	9.66	C3H6NOS	104.01646	250
Heptenophos	C9H12ClO4P	[M+H] <sup>+</sup>	9.89	#	#	#
Iprobenfos	C13H21O3PS	[M+H] <sup>+</sup>	11.53	C7H10O3PS	205.00830	250
Isocarbophos	C11H16NO4PS	[M+Na] <sup>+</sup>	9.70	C8H8O4PS	230.98754	250
Isofenphos	C15H24NO4PS	[M+Na] <sup>+</sup>	11.72	C3H4ON	70.02874	350
Isofenphos-methyl	C14H22NO4PS	[M+Na] <sup>+</sup>	11.30	C11H14O4PS	273.03450	350
Isofenphos-oxon	C15H24NO5P	[M+H] <sup>+</sup>	10.80	C7H6O5P	200.99474	350
Isoprocab	C11H15NO2	[M+H] <sup>+</sup>	9.70	C6H7O	95.04914	150
Malaoxon	C10H19O7PS	[M+H] <sup>+</sup>	8.94	C4H3O3	99.00767	350
Malathion	C10H19O6PS2	[M+H] <sup>+</sup>	10.72	C4H3O3	99.00770	350
Methacrifos	C7H13O5PS	[M+NH4] <sup>+</sup>	10.00	C2H8O3PS	142.99263	250
Methamidophos	C2H8NO2PS	[M+H] <sup>+</sup>	5.40	CH7O3NP	112.01581	150
Methidathion	C6H11N2O4PS3	[M+H] <sup>+</sup>	10.06	C4H5O2N2S	145.00662	350
Methiocarb	C11H15NO2S	[M+H] <sup>+</sup>	10.43	C8H9O	121.06479	250
Methiocarb-sulfone	C11H15NO4S	[M+NH4] <sup>+</sup>	7.50	C8H10O	122.07262	250
Methiocarb-sulfoxide	C11H15NO3S	[M+H] <sup>+</sup>	7.14	C8H10O	122.07262	250
Methomyl	C5H10N2O2S	[M+H] <sup>+</sup>	6.54	C3H6NS	88.02150	150
Mevinphos	C7H13O6P	[M+H] <sup>+</sup>	7.90	C2H8O4P	127.01547	250
Monocrotophos	C7H14NO5P	[M+H] <sup>+</sup>	6.60	C2H8O4P	127.01547	250
Omethoate	C5H12NO4PS	[M+H] <sup>+</sup>	5.87	C4H8O4PS	182.98754	250
Oxamyl	C7H13N3O3S	[M+NH4] <sup>+</sup>	6.20	C3H6NO	72.04439	250
Oxamyl-oxime	C5H10N2O2S	[M+H] <sup>+</sup>	5.86	C3H6NO	72.04439	150
Oxydemeton-methyl	C6H15O4PS2	[M+H] <sup>+</sup>	6.36	C4H10PO3S	169.00828	250
Paraoxon	C10H14NO6P	[M+H] <sup>+</sup>	9.80	C6H7O6NP	220.00055	250
Paraoxon-methyl	C8H10NO6P	[M+H] <sup>+</sup>	8.61	C2H8O4P	127.01543	250
Parathion	C10H14NO5PS	[M+H] <sup>+</sup>	11.25	C6H7O5NPS	235.97771	350
Parathion-methyl	C8H10NO5PS	[M+H] <sup>+</sup>	9.60	#	#	#
Phenthoate	C12H17O4PS2	[M+H] <sup>+</sup>	11.27	#	#	#
Phorate	C7H17O2PS3	[M+H] <sup>+</sup>	11.75	#	#	#
Phorate-sulfone	C7H17O4PS3	[M+H] <sup>+</sup>	9.64	H4O3PS	114.96133	250
Phorate-sulfoxide	C7H17O3PS3	[M+H] <sup>+</sup>	9.54	H4O3PS	114.96133	250
Phosalone	C12H15ClNO4PS2	[M+H] <sup>+</sup>	11.68	C7H5O2ClP	186.97102	350
Phosmet	C11H12NO4PS2	[M+H] <sup>+</sup>	10.14	C8H6O2N	160.03931	350
Phosmet-oxon	C11H12NO5PS	[M+H] <sup>+</sup>	8.29	C8H6O2N	160.03931	350
Phosphamidon	C10H19ClNO5P	[M+H] <sup>+</sup>	8.60	C7H13O2NP	174.06789	250
Phoxim	C12H15N2O3PS	[M+H] <sup>+</sup>	11.56	H4O3PS	114.96133	250
Pirimicarb	C11H18N4O2	[M+H] <sup>+</sup>	9.66	C9H16N3O	182.12879	250
Pirimicarb desmethyl-	C10H16N4O2	[M+H] <sup>+</sup>	8.34	C3H6NO	72.04439	250
Pirimiphos-methyl	C11H20N3O3PS	[M+H] <sup>+</sup>	11.78	C9H14N3	164.11822	350
Profenofos	C11H15BrClO3PS	[M+H] <sup>+</sup>	12.20	C6H6[81]BrClO3PS	304.86212	350
Promecarb	C12H17NO2	[M+H] <sup>+</sup>	10.50	C7H9O	109.06479	250
Propetamphos	C10H20NO4PS	[M+H] <sup>+</sup>	10.94	C3H9ONPS	138.01372	250
Propoxur	C11H15NO3	[M+H] <sup>+</sup>	8.94	C6H7O2	111.04406	250
Prothiofos	C11H15Cl2O2PS2	[M+H] <sup>+</sup>	13.63	C10H9O2	161.05974	250
Pyrazophos	C14H20N3O5PS	[M+H] <sup>+</sup>	11.80	C9H14N3	164.11822	350
Pyridaphenthion	C14H17N2O4PS	[M+H] <sup>+</sup>	10.93	C10H9O2N2	189.06581	350
Quinalphos	C12H15N2O3PS	[M+H] <sup>+</sup>	11.40	C8H7ON2	147.05529	250
Sulprofos	C12H19O2PS3	[M+H] <sup>+</sup>	12.65	C7H8O2PS2	218.96978	350
Terbucarb	C17H27NO2	[M+H] <sup>+</sup>	11.97	C7H9O	109.06479	250
Terbufos	C9H21O2PS3	[M+H] <sup>+</sup>	12.37	C5H11S	103.05760	250

Tetrachlorvinphos	C10H9Cl4O4P	[M+H] <sup>+</sup>	11.30	C2H8O4P	127.01550	350
Thiobencarb	C12H16ClNOS	[M+H] <sup>+</sup>	11.88	C7H6Cl	125.01525	250
Thiodicarb	C10H18N4O4S3	[M+H] <sup>+</sup>	9.28	C3H6NS	88.02155	350
Tolclofos-methyl	C9H11Cl2O3PS	[M+H] <sup>+</sup>	11.67	C7H5O2Cl2	174.97120	350
Triazophos	C12H16N3O3PS	[M+H] <sup>+</sup>	10.78	C8H8ON3	162.06674	350
Trichlorfon	C4H8Cl3O4P	[M+H] <sup>+</sup>	7.59	C4H8O4Cl2P	220.95334	250
Vamidotion	C8H18NO4PS2	[M+H] <sup>+</sup>	7.34	C8H12ONS	146.06341	250

#: no fragment used in screening

## Supplementary material 2

### LC gradient

Time [min].	% A	% B
0	100	0
1	100	0
2.5	55	45
8.5	0	100
11.5	0	100
12	100	0
14	100	0

## Supplementary material 3

### Source parameters LC-MS/MS measurement

Parameter	Setting
Capillary	3 kV
Source Offset	50 V
Source Temp.	150 °C
Desolvation Temp.	590 °C
Cone Gas Flow	150 L/Hr
Desolvation Gas Flow	1000 L/Hr
Nebuliser gas flow	7 bar



**Supplementary material 4**

Compound specific parameters LC-MS/MS measurement

Name	Precursor ion	Product ion	Cone [V]	Coll. En [V]	Dwell [s]
Methamidophos Qn	142.2	94	20	13	0.05
Methamidophos Ql	142.2	125	20	13	0.05
Acephate Ql	184	125	10	20	0.1
Acephate Qn	184	143	10	17	0.1
Omethoate Ql	214	155	22	17	0.05
Qmethoate Qn	214	183	22	10	0.05
Fenthion Qn	279	169	30	18	0.01
Fenthion Ql	279	247	30	12	0.01
Pirimiphos-methyl Ql	306	108	30	25	0.01
Pirimiphos-methyl Qn	306	164	30	25	0.01
Triazophos Qn	314	119	25	35	0.01
Triazophos Ql	314	162	25	20	0.01
Azinphos-ethyl Qn	346	132	10	15	0.01
Azinphos-ethyl Ql	346	160	10	10	0.01
Chlorpyrifos Qn	350	198	20	17	0.01
Chlorpyrifos Ql	352	200	20	17	0.01
Profenofos Ql	373	97	30	33	0.01
Profenofos Qn	373	303	30	18	0.01

### Supplementary material 5

Levels of pesticides detected in vegetable samples from peri-urban Nairobi and the respective

Sample No.	Matrix	Pesticide	EU-MRL ug/kg	Level found ug/kg
22	F. beans	Metamidophos	10	22
22	F. beans	Acephate	10	41
29	F. beans	Acephate	10	60
29	F. beans	Chlorpyrifos	10	117
29	F. beans	Metamidophos	10	25
44	F. beans	Acephate	10	66
44	F. beans	Metamidophos	10	20
75	F. beans	Acephate	10	58
75	F. beans	Metamidophos	10	21
13	Kales	Acephate	10	43
13	Kales	Metamidophos	10	13
46	Kales	chlorpyrifos	10	26
65	Kales	Chlorpyrifos	10	315
21	Spinach	chlorpyrifos	10	1343
57	Spinach	Chlorpyrifos	10	24
11	Tomatoes	Acephate	10	409
11	Tomatoes	Metamidophos	10	182
11	Tomatoes	Omethoate	10	11
18	Tomatoes	Chlorpyrifos	100	78
19	Tomatoes	Profenofos	10000	64
20	Tomatoes	Chlorpyrifos	100	107
25	Tomatoes	Profenofos	10000	958
27	Tomatoes	Omethoate	10	98
27	Tomatoes	Profenofos	10000	52
28	Tomatoes	Profenofos	10000	504
41	Tomatoes	Profenofos	10000	22
68	Tomatoes	Profenofos	10000	26
69	Tomatoes	Profenofos	10000	168
70	Tomatoes	Omethoate	10	76
70	Tomatoes	Profenofos	10000	10

EU MRLs

**Supplementary material 6**

Acute reference dose and acceptable daily intake values used in this study

Pesticide	ARfD (mg/kg bw/day)	ADI (mg/kg bw/day)	Year
Chlorpyrifos	0.005	0.001	EFSA 2014
Profenofos	1	0.03	JMPR 2007
Acephate	0.1	0.03	JMPR 2005
Omethoate	0.002	0.0003	EFSA 2013
Methamidofos	0.003	0.001	EFSA Dir 06/131

**Supplementary material 7**

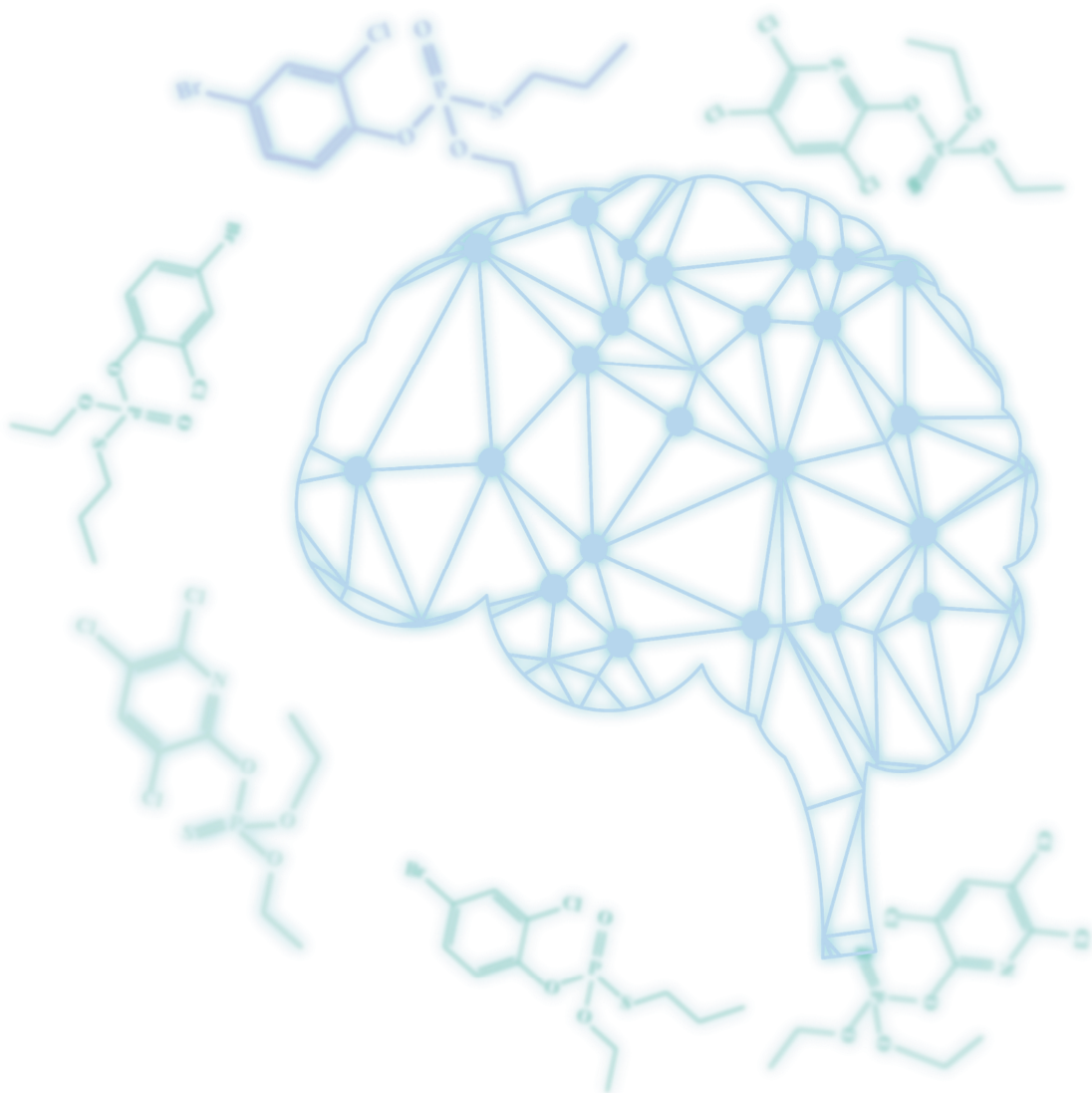
Codex MRLs for the various vegetable matrices

OP pesticide	Codex MRL (mg/kg)			
	Tomatoes	French beans	Kales	Spinach
Profenofos	10	-	-	-
Omethoate	-	-	-	-
Chlorpyrifos	-	0.01	(1) <sup>a</sup>	-
Acephate	1	5	(2) <sup>a</sup>	-
Methamidophos	-	1	-	-

<sup>a</sup>) Kales is a leafy brassica for which no codex MRLs are available. The MRL for head cabbage is listed here for information.

Acephate - Beans, except broad bean and soya bean

- MRL not available in the database



# CHAPTER 3.

Prediction of dose-dependent in vivo  
acetylcholinesterase inhibition by profenofos in rats  
and humans using physiologically based kinetic  
(PBK) modeling-facilitated reverse dosimetry

Isaac Omwenga

Shensheng Zhao

Laetitia Kanja

Hans Mol

Ivonne M.C.M. Rietjens

Jochem Louisse

*Published in: Archives of Toxicology (2021) 95: 1287–1301*

**Abstract**

Organophosphate pesticides (OPs) are known to inhibit acetylcholine esterase (AChE), a critical effect used to establish health based guidance values. This study developed a combined in vitro-in silico approach to predict AChE inhibition by the OP profenofos in rats and humans. A physiologically based kinetic (PBK) model was developed for both species. Parameter values for profenofos conversion to 4-bromo-2-chlorophenol (BCP) were derived from in vitro incubations with liver microsomes, liver cytosol, and plasma from rats (catalytic efficiencies of 1.1, 2.8, and 0.19 ml/min/mg protein, respectively) and humans (catalytic efficiencies of 0.17, 0.79, and 0.063 ml/min/mg protein, respectively), whereas other chemical-related parameter values were derived using in silico calculations. The rat PBK model was evaluated against literature data on urinary excretion of conjugated BCP. Concentration-dependent inhibition of rat and human AChE was determined in vitro and these data were translated with the PBK models to predicted dose-dependent AChE inhibition in rats and humans in vivo. Comparing predicted dose-dependent AChE inhibition in rats to literature data on profenofos-induced AChE inhibition revealed an accurate prediction of in vivo effect levels. Comparison of rat predictions (BMDL10 of predicted dose-response data of 0.45 mg/kg bw) and human predictions (BMDL10 of predicted dose-response data of 0.01 mg/kg bw) suggests that humans are more sensitive than rats, being mainly due to differences in kinetics. Altogether, the results demonstrate that in vivo AChE inhibition upon acute exposure to profenofos was closely predicted in rats, indicating the potential of this novel approach method in chemical hazard assessment.

### 3.1 Introduction

Organophosphorus or organophosphate pesticides (OPs) have been extensively used for the control of agricultural and household pests globally (Kumari and John 2019). Exposure to these pesticides has been reported for various segments of the population, including agriculture workers and their families, house hold members during home application of pesticides, people that live in proximity to farms, or the general public via residues on food (Lu et al 2000; Bradman et al 2003; Quandt et al 2004). Consequently, OPs and their metabolites have been found in human blood, serum, urine, and breast milk (Hardt and Angerer 2000; Liu et al 2014; Zhang et al 2014; Naksen et al 2016). Since various OPs have shown to cause adverse effects to the environment and to human health, many OPs are currently not registered for use as pesticides, and some OPs have even been banned (Hertz-Picciotto et al 2018).

Epidemiological studies have linked chronic OP exposure to reproductive disorders, developmental toxicity, birth defects, cancer, Parkinson's disease, Alzheimer's disease, diabetes, chronic respiratory disease, cardiovascular diseases, chronic nephropathies and amyotrophic lateral sclerosis (ALS) (Mostafalou and Abdollahi 2013). The critical effects of OPs in animal studies are related to neurotoxicity, which has been reported to be related to, amongst others, inhibition of acetylcholinesterase (AChE), neuropathy target esterase (NTE) (Costa 2018), acylpeptide hydrolase (APH) (Richards et al 2000), fatty acid amide hydrolase (FAAH) (Quistad et al 2001; Buntyn et al 2017) muscarinic M2 receptors (Costa 2006), and a variety of lipases (Quistad et al 2006). Inhibition of AChE is one of the mechanisms by which OPs cause acute neurotoxicity (Jamal et al 2002; Farahat et al 2003), characterized by decreased hydrolysis of acetylcholine in both central and peripheral cholinergic synapses, resulting initially in overstimulation of nicotinic and muscarinic receptors, followed by receptor down-regulation on post-synaptic membranes (Costa 2006). Acute or repeated exposure to OPs can lead to organophosphate ester-induced delayed polyneuropathy (OPIDP), a neurodegenerative

disorder caused by inhibition and aging of at least 70% of the activity of the neuropathy target esterase (NTE) present in nerve tissues as well as other tissues (e.g., lymphocytes, testis) (Johnson and Glynn 1995; Johnson and Glynn 2001; Costa 2018). In the hazard and risk assessment of OPs, *in vivo* animal studies on OP-induced inhibition of AChE have been used to derive a point of departure (POD) to set safe exposure levels, such as an Acute Reference Dose (ARfD). ARfDs for chlorpyrifos, acephate, methamidofos, omethoate and profenofos as reported by organizations as the European Food Safety Authority (EFSA), United States Environmental Protection Authority (EPA), and the Joint FAO/WHO Meeting on Pesticide Residues (JMPR) have been derived from data on OP-induced AChE inhibition from animal studies (EPA 2006; JMPR 2007; EPA 2011; EPA 2016; EFSA 2019). Although these *in vivo* studies do not measure complex neurotoxicity endpoints, the information on OP-induced inhibition of AChE *in vivo* is considered an important piece of information in the hazard characterization. In these *in vivo* studies, AChE activity is usually measured in blood and sometimes also brain tissue after OP exposure. In the present study we aimed to assess whether *in vivo* dose-dependent OP-induced AChE inhibition can be predicted by an animal-free approach. In order to inhibit AChE in the *in vivo* situation, the OP needs to reach its target (AChE) at sufficiently high concentrations. The *in vivo* potency of an OP to inhibit AChE is thus dependent on its intrinsic ability (potency) to inhibit AChE and the amount of OP that reaches that target. The potency of an OP to inhibit AChE can be determined using *in vitro* approaches. To estimate the amount of OP that reaches the target, so-called physiologically based kinetic (PBK) models can be used. A PBK model permits the simulation of the chemical's *in vivo* kinetics (ADME) and can relate external exposure to internal exposure at the target sites. When having PBK models for different exposure routes and/or different species, these models can be used for exposure route and/or species extrapolations. These models can also be used as a tool to estimate exposure applying reverse dosimetry of biomonitoring data (e.g.



chemical levels in blood or urine), as has been shown, for example, for chlorpyrifos in rats and humans (Timchalk et al 2002), and chlorpyrifos in children (Rigas et al 2001). Furthermore, these models can be used for reverse dosimetry of in vitro toxicity data, thereby translating in vitro effect concentrations to in vivo doses, enabling prediction of in vivo dose-dependent toxicity, as has been shown for the OP chlorpyrifos (Zhao et al 2019). Such PBK modeling-facilitated reverse dosimetry of in vitro toxicity data is considered crucial in the transition to non-animal based novel approach methods (NAMs) for the safety assessment of chemicals (Louisse et al 2017).

PBK models have been developed for various OPs including chlorpyrifos (Timchalk et al 2002; Bouchard et al 2005; Mosquin et al 2009; Lu et al 2010; Zhao et al 2019), malathion (Bouchard et al 2003; Bogen and Singhal 2017; Bouchard et al 2017), parathion (Sultatos 1990) and diazinon (Poet et al 2004). To date, no PBK model has been built for the OP profenofos, despite its widespread use in developing countries and reported cases of human accidental poisoning (Gotoh et al 2001; Eddleston et al 2009).

Profenofos (O-(4-bromo-2-chlorophenyl) O-ethyl S-propyl phosphorothioate) (Figure 1) is a thiophosphate OP pesticide ( $O=P-S-C$ ) that was developed for pest strains resistant to chlorpyrifos and other OPs (Gotoh et al 2001). Profenofos has been classified as a moderately hazardous (Toxicity Class II) pesticide by the World Health Organization (WHO) with moderate level of acute toxicity ( $LD_{50}$  of 358 to 1178 mg/kg in rat) following oral administration (Reported in JMPR (2007)). Dietary intake of profenofos is the primary exposure route for humans (Greish et al 2011) and residue levels exceeding EU MRLs have been found in various vegetables in Kenya (Karanja et al 2012). Our recent study reported profenofos as one of the most frequently encountered pesticide residues in vegetables sampled in peri-urban Nairobi, Kenya (Omwenga et al 2020).

The present study aims to develop a PBK model for profenofos in rats and humans and apply the models to predict dose-dependent in vivo AChE inhibition using PBK modeling-facilitated reverse dosimetry of in vitro data on profenofos-induced AChE inhibition, allowing interspecies comparisons and providing a proof-of-principle that OP-induced AChE inhibition can be predicted for both rats and humans without the need for in vivo studies. To that end, profenofos PBK models were developed based on in silico- and in vitro-derived input parameter values. The rat PBK model was evaluated by comparing PBK model predictions with available in vivo kinetic data in rats. Subsequently, in vitro data on profenofos-induced AChE inhibition were translated to predicted in vivo dose-dependent AChE inhibition in rats and humans, and predictions on dose-dependent AChE inhibition in rats were evaluated by comparison with available in vivo data.

## **3.2 Materials and Methods**

### **3.2.1 Materials**

Profenofos, 4-bromo-2-chlorophenol (BCP), bovine serum albumin (BSA), reduced nicotinamide adenine dinucleotide phosphate (NADPH), 5,5-dithiobis (2-nitrobenzoic acid) (DTNB) and acetylthiocholine iodide (ATC) were purchased from Sigma-Aldrich (Zwijndrecht, The Netherlands). Magnesium chloride hexahydrate ( $\text{MgCl}_2 \cdot 6\text{H}_2\text{O}$ ), trifluoroacetic acid (TFA), dimethylsulfoxide (DMSO), and calcium chloride dihydrate ( $\text{CaCl}_2 \cdot 2\text{H}_2\text{O}$ ) were purchased from VWR International (Amsterdam, The Netherlands). Acetonitrile (ACN, UPLC/MS grade) was purchased from Biosolve (Valkenswaard, The Netherlands). Human liver microsomes and cytosol (pooled from 150 human donors, mixed gender), rat liver microsomes and rat liver cytosol (pooled from 20 male Sprague Dawley rats) were purchased from Corning (Amsterdam, The Netherlands). Recombinant human acetylcholinesterase was purchased from Sigma-Aldrich (Zwijndrecht, The Netherlands). Rat

blood was purchased from BioIVT (Westbury, USA), human and rat plasma were purchased from Innovate (New York, USA).

### 3.2.2 PBK model development

#### 2.2.1 Model structure and software

The PBK model structure applied (Figure 2) is based on a generic PBK model that has been developed for humans (Jones and Rowland-Yeo 2013). Physiological parameter values (tissue volumes and blood flows) for rats and humans were taken from Jones and Rowland-Yeo (2013) (Supplementary Table 1) as collected previously by Punt et al (2020). The generic model contains separate compartments for liver, the gastrointestinal tract (GI-tract), fat, muscle, skin, bone, brain, heart, kidney, lung, spleen, venous blood, arterial blood, and a rest-of-body compartment. The uptake of profenofos from the GI-tract was described as a first order process with an absorption rate constant of  $1 \text{ hr}^{-1}$ . All absorbed profenofos was assumed to be transferred directly to the liver compartment via the portal vein. Tissue: plasma partition coefficients were estimated based on the method of Berezhkovskiy (2004) using  $\log K_{ow}$ , pKa and fraction unbound plasma (fup) as input parameters.  $\log K_{ow}$  and pKa values were estimated using chemicalize ([www.chemicalize.com](http://www.chemicalize.com)) and fup was estimated (based on LogP and pKa) using the online simcyp tool (<https://www.certara.com/software/pbpk-modeling-and-simulation/>).

The main metabolite of profenofos reported in vivo is 4-bromo-2-chlorophenol (BCP), which has been reported to be formed upon paraoxonase 1 (PON1)-mediated hydrolysis of profenofos (JMPR 2007; EPA 2016; Dadson et al 2013) (Figure 1). Profenofos hydrolysis (BCP formation) was quantified in the present study using rat and human liver microsomes, liver cytosol and plasma (section 2.2.2). Profenofos clearance was included in the blood and liver compartments of the PBK model. In in vitro studies, also CYP-mediated formation of other metabolites has

been reported (in the presence of inhibitors of hydrolysis enzymes) (Dadson et al 2013), but these are considered less relevant, since the hydrolysis reaction is more efficient than the CYP-mediated oxidations, as indicated in our in vitro metabolism studies with liver microsomes or cytosol in which practically all profenofos was converted into BCP. Because BCP was shown to not inhibit AChE (see Results section), only profenofos kinetics were considered relevant for the reverse dosimetry and included in the PBK model (Figure 2). The only in vivo data publicly available on profenofos kinetics in rats or humans, required for model evaluation, relate to the urinary excretion of conjugated BCP in rats. Therefore, to allow model evaluation, the rat PBK model was extended to include a sub-model on BCP and BCP-glucuronide formation (Supplementary Figure 1). Estimated tissue: plasma partition coefficients of BCP and BCP-glucuronide and fraction unbound plasma ( $f_{up}$ ) values used for these sub-models are presented in Supplementary Table 1.

Renal excretion is also included in the model which is described by a passive renal clearance (via glomerular filtration) of the unbound fraction in blood at the rate of  $6.7 \text{ L hr}^{-1}$  in humans and  $0.078 \text{ L hr}^{-1}$  in rats. The model equations were coded and numerically integrated in Berkeley Madonna 9.1.18 (UC Berkeley, CA, USA), using the Rosenbrock's algorithm for stiff systems. The PBK models' differential equations are provided in the Supplementary Materials.

### **3.2.3 In vitro incubations to derive kinetic parameter values for description of metabolic clearance in the PBK model**

Incubations of profenofos with rat and human liver microsomes, liver cytosol and plasma were performed to quantify in vitro rates of BCP formation. Conditions were optimized to be linear for metabolite formation with regard to incubation time and microsomal, cytosolic and plasma protein concentration (data not shown). The final incubations were carried out in 100 mM Tris HCl (pH 7.4,  $37^{\circ}\text{C}$ ) containing (final concentrations) 5 mM  $\text{MgCl}_2$ , 2 mM  $\text{CaCl}_2$  (to stimulate

PON1 activity (Carr et al 2015)), 2 mM NADPH (cofactor to also include CYP-mediated metabolism), enzyme preparation (final concentration 2 mg/ml for human liver microsomes and cytosol and 4.4 mg/ml for human plasma; 0.5 mg/ml for rat microsomes and cytosol and 1.65 mg/ml for rat plasma) and profenofos (at final concentrations ranging from 1 to 100  $\mu$ M, added from 100 times concentrated stock solutions in DMSO). Control incubations were performed in the absence of microsomes, cytosol or plasma. After 2 min pre-incubation, the reaction was initiated by adding the substrate and mixtures were incubated for 2 min in a 37 °C water bath. The total volume of the incubation mixtures was 200  $\mu$ l. The reaction was terminated by the addition of 50  $\mu$ l ice cold ACN and samples were kept on ice. The mixture was centrifuged at 14,000 g for 20 min at 4°C and the supernatant was analyzed using UPLC-UV.

### 3.2.4 UPLC-UV analysis

All samples from incubations were analyzed using a Waters Acquity UPLC H class system that consisted of a quaternary solvent manager, a sample manager, and a photodiode array (PDA) detector, equipped with a Water Acquity UPLC® BEH C18 column (1.7  $\mu$ m, 2.1  $\times$  50 mm) and Waters Xbridge UPLC® BEH C18 pre-column (2.5  $\mu$ M, 2.1 x 5 mm). The temperature of the column was kept at 40°C and the auto sampler at 10°C during the UPLC analysis. The mobile phases used for the analysis consisted of (A) 0.1% TFA in nanopure water and (B) 100% ACN. A gradient elution at a flow rate of 0.6 ml/min was applied for the analysis with the initial condition of 100% A: 0% B (v/v), changing in a linear way to 0% A: 100% B from 0 to 6 min, which was maintained for 30 s, and then changed back to the initial conditions in 30 s, which were maintained for 1 min. The injection volume for each sample was 3.5  $\mu$ l.

Under these conditions, the retention times of profenofos and BCP were 4.76 and 3.37 min, respectively. The amounts of profenofos and BCP were quantified by integrating the peak areas at 237 nm using calibration curves that were prepared using commercially available standards.

### 3.2.5 In vitro metabolism data analysis and scaling in the PBK model

Kinetic parameters including the apparent maximum velocity ( $V_{\max}$ ) and the apparent Michaelis–Menten constant ( $K_m$ ) for BCP formation were obtained by fitting the data for the substrate concentration-dependent rate of conversion (expressed in nmol/min/mg protein) using GraphPad Prism 5, version 5.04 (San Diego, California, USA) to the standard Michaelis–Menten equation:

$$V = V_{\max} * [S] / (K_m + [S])$$

in which the  $S$  represents the concentration of substrate, expressed in  $\mu\text{M}$ ,  $V$  and  $V_{\max}$  the velocity and the maximum velocity of the reaction, respectively, expressed in nmol/min/mg protein, and  $K_m$  the apparent Michaelis–Menten constant, expressed in  $\mu\text{M}$ . The kinetic parameter values for conversion of profenofos to BCP in the liver microsomes, liver cytosol and plasma were determined. To determine the catalytic efficiency,  $V_{\max}$  was divided by the  $K_m$ .

The in vitro  $V_{\max}$  values were scaled in the PBK model code (Supplementary Materials) using the following scaling factors for rats and humans: 35 mg microsomal protein/g liver, 80.7 mg cytosolic protein/g liver and 550 mg plasma/g blood (Medinsky et al 1994; Cubitt et al 2011). The apparent  $V_{\max}$  values obtained from enzymatic incubations expressed in nmol/min/mg protein were converted into  $\mu\text{mol/h/kg}$  liver and plasma in the PBK model code. The in vivo  $K_m$  values were assumed to be equal to those obtained in vitro (taking into account the differences in free fraction in vitro vs in vivo).

### 3.2.6. Model evaluation

Since the only in vivo data available on profenofos kinetics for model evaluation were on the urinary excretion of conjugated BCP in rats, the rat PBK model was extended to include a sub-

model on BCP and BCP-glucuronide (Supplementary Figure 1). Estimated partition coefficients and  $f_{up}$  values of BCP and BCP-glucuronide used for these sub-models are presented in Supplementary Table 1 and conversion of BCP to BCP-glucuronide was assumed to take place only in the liver having the same apparent  $K_m$  and  $V_{max}$  values as reported before by Strikwold et al (2013) for phenol glucuronidation. The PBK model-predicted cumulative urinary excretion of BCP-glucuronide were compared with reported in vivo data on conjugated BCP excretion in profenofos-exposed rats (Cho et al 2002).

Furthermore, a sensitivity analysis was performed to estimate the impact of the chemical-specific parameters on the model output (maximum free (unbound) blood concentrations of profenofos in this study). Normalized sensitivity coefficients (SCs) were calculated using the following equation:

$$SC = (C' - C) / (P' - P) * (P/C)$$

in which P represents the parameter value in the PBK model and P' the parameter value with a 5% increase (Evans and Andersen 2000). Likewise, C' represents the model output obtained with the 5% increase in P, while C is the model output using the initial model parameter value. The sensitivity analysis was conducted for oral exposure to predicted effect doses obtained with the reverse dosimetry analysis (BMDL<sub>10</sub> values). BMDL<sub>10</sub> values were selected since a BMDL<sub>10</sub> value from a rat study on profenofos-induced AChE inhibition was recently used to derive the POD to obtain an acute reference dose (ARfD) for profenofos by the United States Environmental Protection Agency (US EPA) (EPA 2016).

### **3.2.7 Determination of in vitro AChE inhibition by profenofos and quantitative in vitro to in vivo extrapolation using reverse dosimetry**

To perform reverse dosimetry of in vitro AChE inhibition by profenofos, first the in vitro AChE activity in the absence or presence of increasing concentrations of profenofos was determined.

For humans, commercially available recombinant AChE was used. For rats, no commercially available recombinant AChE was available, so rat AChE was obtained from rat blood as described below.

### **3.2.8 Derivation of a concentration-response curve for human recombinant AChE inhibition**

AChE inhibition was determined following the protocol of Ellman et al (1961) as modified by Chambers and Chambers (1989). The concentration of acetylthiocholine and recombinant AChE were optimized to be linear for metabolite formation (data not shown). Human recombinant AChE was dissolved in 0.1 M sodium phosphate (pH 7.4) containing 1 mg/ml BSA (which was present to stabilize human recombinant AChE (Rosenfeld and Sultatos 2006)) to reach an enzyme concentration of 200 U/ml. Subsequently, the AChE enzyme solution was further diluted with 0.1 M sodium phosphate (pH 7.4) containing 1 mg/ml BSA to a working concentration of 1 U/ml. A range of concentrated stock solutions of profenofos were prepared in ethanol and 50 times diluted by adding 5  $\mu$ l of stock solution to 245  $\mu$ l of 0.1 M sodium phosphate (pH 7.4) (containing 0.1 mg/ml BSA). For the negative control, 5  $\mu$ l of ethanol without profenofos was added to 245  $\mu$ l of 0.1 M sodium phosphate (pH 7.4) (containing 0.1 mg/ml BSA). Subsequently, 5  $\mu$ l of these working solutions were added into wells of a 96 well plate already containing 44  $\mu$ l sodium phosphate (pH 7.4) (containing 0.1 mg/ml BSA). To start the reaction (in absence or presence of a range of profenofos concentrations), 1  $\mu$ l enzyme solution was added, giving a total volume of 50  $\mu$ l per reaction with an AChE concentration of 0.02 U/ml and an ethanol concentration of 0.2%, a level that had no effect on the activity of the enzyme. After 15 minutes incubation at 37°C, the reactions were stopped by adding 150  $\mu$ l of a mixture of 5,5-dithiobis (2-nitrobenzoic acid) (DTNB) and acetylthiocholine (ATC) (final DTNB and ATC concentrations were 0.075 and 0.15 mM, respectively). Subsequently, the



time-dependent increase in absorbance due to formation of chromophore (DTNB + thiocholine) was measured at 37 °C using a wavelength of 412 nm during a period of 10 minutes, using a spectrophotometer (SpectraMax, Molecular Devices, UK).

AChE activity was expressed as enzyme activity (percent of control). The concentration of profenofos that produced a 50% decrease in AChE activity (IC<sub>50</sub>) was determined from best-fit plots of the mean (±SD) percentages of inhibition vs. the 10log logarithm of profenofos concentrations using GraphPad Prism 5, version 5.04 (San Diego, California, USA) equation;  $Y=100/(1+10^{((X-\text{LogIC}_{50}))})$

### **3.2.9 Derivation of a concentration-response curve for rat erythrocyte AChE inhibition**

#### **3.2.9.1 Blood sample processing and enzyme extraction**

Rat blood samples were processed according to a method reported by Larsen et al (2019) with a few modifications to isolate the extrinsic membrane bound AChE. Briefly, the blood sample (2 ml) was centrifuged at 3000g for 15 minutes in order to separate plasma and cells. Aliquots of 500 µl of the cells were resuspended in 4.5 ml lysis buffer (20 mM sodium phosphate; pH 7.4) and frozen at -80°C for 24 h. After that, the cell samples were thawed and centrifuged (4000 g) for 15 min at 4°C. The supernatant was poured off and the precipitate was suspended in 4.5 ml lysis buffer. This treatment was repeated another two times. The residue containing what is called erythrocyte ‘ghost’ membranes, was resuspended in 500 µl analysis buffer (100 mM sodium phosphate; pH 7.4), and stored at -80°C until analysis. Aliquots of erythrocyte ‘ghost’ membrane preparations were used for protein measurement using the Pierce™ BCA Protein Assay Kit (Thermofisher) with BSA as standard for quantification (Lowry et al 1951), and for AChE activity assessment.

#### **3.2.9.2 Rat red blood cell (RBC) AChE activity**

The effect of profenofos on rat AChE activity was assessed as described above for human recombinant AChE, with a few modifications. Briefly, a typical reaction mixture (200 µl) for

AChE activity contained 0.005 mg/ml erythrocyte 'ghost' membrane protein. The rest of the steps were as described above for measurement of human recombinant AChE activity.

### **3.2.10 Quantitative in vitro to in vivo extrapolation (QIVIVE) of AChE inhibition data with PBK modeling-facilitated reverse dosimetry**

In the present study, it was assumed that in vivo dose-dependent AChE inhibition (in blood) depends on the maximum concentration ( $C_{max}$ ) of profenofos reached in the blood. For adequate PBK modeling-facilitated reverse dosimetry, the active (unbound) concentration of a test chemical in the in vitro test system should be linked to the in vivo freely available chemical at the target site. This is important since it is assumed that it is the fraction unbound that causes the effect (AChE inhibition). In the in vitro incubations, a very low concentration of BSA (0.1 mg/mL) is present. Heilmair et al (2008) reported that with such low BSA concentrations, the free concentration of chlorpyrifos oxon is not affected. Furthermore, Rosenfeld and Sultatos (2006) found no evidence of binding of paraoxon by BSA even at a higher concentration (1 mg/ml) during incubations. Based on these observations no significant effect on the free fraction of profenofos in the in vitro AChE inhibition studies is expected, which corroborated with estimations on profenofos binding in the in vitro incubations with help of the online simcyp tool (<https://www.certara.com/software/pbpk-modeling-and-simulation/>). A description of the fraction unbound in blood is incorporated in the PBK model, hence the predicted in vivo unbound  $C_{max}$  values in blood were related to the profenofos concentrations we applied in vitro.

By calculating with the PBK model the external dose required to reach (as unbound  $C_{max}$ ) the concentrations applied in the in vitro test, each in vitro concentration was translated into an in vivo dose. In this way the concentration-response curves for rat and human AChE inhibition

were converted into in vivo dose-response curves for profenofos-induced AChE inhibition in rats and humans, respectively.

### 3.2.11 Evaluation of predicted dose-response curves for rat and human AChE inhibition

To evaluate the performance of the PBK modeling-facilitated reverse dosimetry approach to predict in vivo AChE inhibition, the predicted dose-response curve for rat AChE inhibition upon exposure to profenofos was compared with available in vivo data on AChE inhibition in rats (JMPR 2007). Furthermore, the predicted dose-response data were used for BMD modeling, using EFSA PROAST version 69.0 (<https://shiny-efsa.openanalytics.eu/app/bmd>) using the model averaging approach in order to allow evaluation of the prediction by comparison of BMDL<sub>10</sub> values obtained from the predicted dose-response data to points of departure derived by regulatory bodies (JMPR 2007; EPA 2016; EFSA 2019). To that end, the obtained BMDL<sub>10</sub> values were compared with a reported BMDL<sub>10</sub> value from a rat study on profenofos-induced RBC AChE inhibition, which was recently used to obtain an ARfD by the US EPA (EPA 2016), and a reported NOAEL value on profenofos-induced rat brain acetylcholinesterase inhibition, which has been used to obtain an ARfD by JMPR (2007).

## 3.3 Results

### 3.3.1 In vitro conversion of profenofos to BCP

The conversion of profenofos to BCP was measured in incubations with both rat and human liver microsomes, cytosol and plasma. UPLC analysis revealed that only one peak (BCP) appeared when analyzing the samples obtained from these incubations. In control incubations, small amounts (max 0.04% of the amount of profenofos added) of BCP were detected, indicating some spontaneous hydrolysis of profenofos in the aqueous environment, which has also been observed in previous studies (Aly and Badawy 1982). The BCP formation data for

microsomes, cytosol and plasma were therefore corrected for BCP levels detected in control incubations.

The concentration-dependent velocity of BCP formation following incubation of profenofos with both human and rat liver microsomes, liver cytosol and plasma is depicted in Figure 3A-3C. The kinetic parameters derived from these data ( $K_m$  and  $V_{max}$ ) as well as the catalytic efficiencies, calculated as  $V_{max}/K_m$ , are presented in Table 1.

The results indicate differences in the catalytic efficiencies for conversion of profenofos to BCP by rats and humans (Table 1). The catalytic efficiency for microsomal biotransformation of profenofos to BCP was 6.5-fold lower in incubations with human liver microsomes than with rat liver microsomes, due to a 7.7-fold lower  $V_{max}$  and a 1.2-fold lower  $K_m$  (Table 1). Likewise, the catalytic efficiency for cytosolic biotransformation of profenofos to BCP was 3.8-fold lower for human liver cytosol, with a 1.1-fold higher  $V_{max}$ , and a 4.1-fold higher  $K_m$  for human liver cytosol as compared to rat liver cytosol. Largest differences were observed for plasma, indicated by the 32-fold lower catalytic efficiency of biotransformation of profenofos to BCP for human plasma than for rat plasma, due to a 1.5-fold higher  $V_{max}$  and 44-fold higher  $K_m$  for human plasma as compared to rat plasma.

**Table 1.** Kinetic parameter values ( $K_m$ ,  $V_{max}$ ) and catalytic efficiencies ( $V_{max}/K_m$ ) for in vitro conversion of profenofos to BCP.

	Human	Rat
<b>Liver microsomes</b>		
$K_m$ ( $\mu M$ )	6.9	8.1
$V_{max}$ (nmol/min/mg microsomal protein)	1.2	8.9
Catalytic efficiency (ml/min/mg protein)	0.17	1.1
<b>Liver cytosol</b>		
$K_m$ ( $\mu M$ )	1.4	0.34
$V_{max}$ (nmol/min/mg cytosolic protein)	1.1	0.95
Catalytic efficiency (ml/min/mg protein)	0.79	2.8
<b>Plasma</b>		
$K_m$ ( $\mu M$ )	158	3.6
$V_{max}$ (nmol/min/mg plasma protein)	0.99	0.68
Catalytic efficiency (ml/min/mg protein)	0.0063	0.19

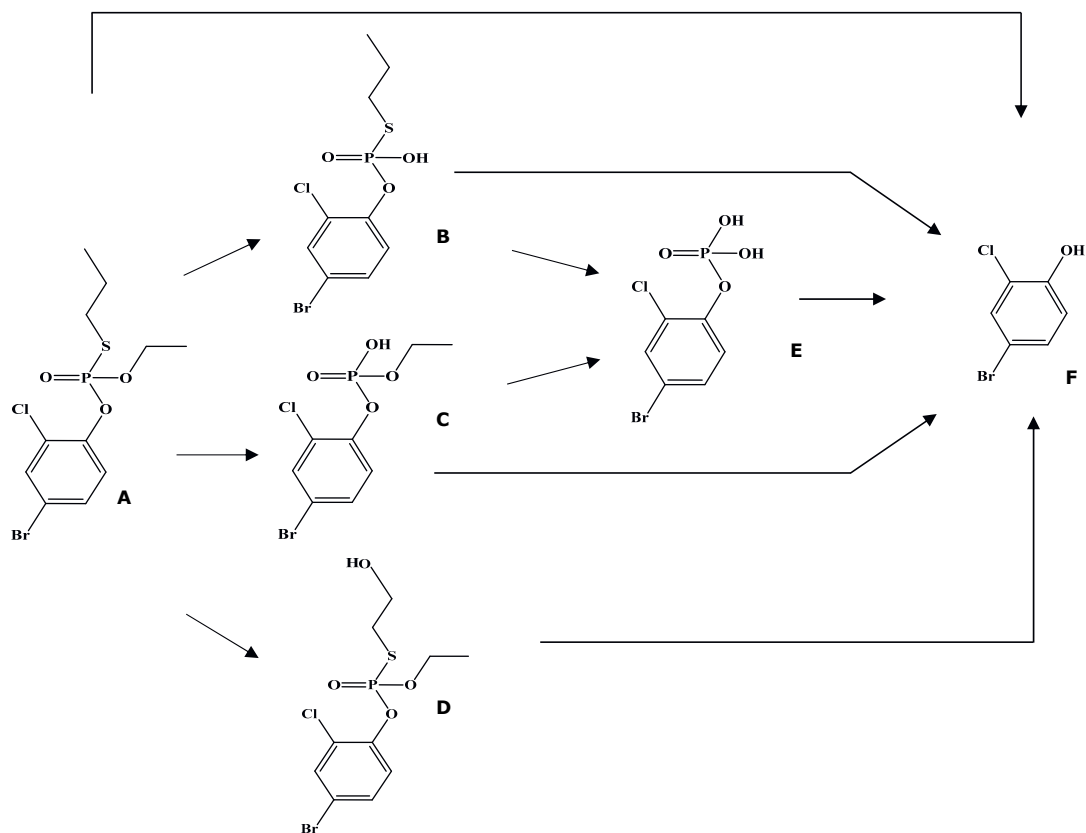


Figure 1. Metabolic pathways for metabolism of profenofos (A) based on data reported in previous studies (Gotoh et al 2001; Dadson et al 2013). Metabolites include desethylated profenofos (B), desthiopropylprofenofos / des-S-propylated profenofos (C), hydroxypropyl profenofos (D), 4-bromo-2-chlorophenyl dihydrogen phosphate (E), and 4-bromo-2-chlorophenyl (BCP) (F).

### 3.3.2 PBK model development and evaluation

Using the kinetic parameters thus defined and the input parameters obtained with *in silico* methods summarized in Supplementary Table 1, PBK models for profenofos in rat and human were made. Figure 4 presents the rat PBK model-based prediction of the urinary BCP excretion. In a subsequent step first the developed rat profenofos PBK model was evaluated against *in vivo* data on urinary excretion of conjugated BCP in rats from a study by Cho et al (2002). These results indicate that the predictions made by the newly developed PBK model for rat match the reported *in vivo* data well. Due to a lack of *in vivo* kinetic data for humans, evaluation of the performance of the PBK model for profenofos in humans could not be performed. However, the human model was considered to be adequate, since it is based on the same conceptual model and *in vitro*- and *in silico*-derived input parameters were defined in the same way as those for the rat model.

Further evaluation of the PBK models included a local sensitivity analysis in which the impact of each chemical-specific parameter on the predicted free (unbound)  $C_{max}$  of profenofos in the rat and human PBK model was determined upon exposure to predicted effect doses ( $BMDL_{10}$  values derived from predicted dose-response data (see section 3.2.6)). Figure 5 presents the parameters for which the SCs are higher than 0.1 (absolute value). For both rat and human models, the prediction of the  $C_{max}$  of profenofos appeared to be mainly affected by the kinetic parameters for conversion of profenofos to BCP by enzymes from especially plasma and liver cytosol, in addition to the absorption rate constant ( $k_a$ ) and the gut to plasma partition coefficient.

The obtained PBK models reveal differences in kinetics in rats and humans (Figure 6). Figure 7 shows the PBK model-predicted dose-dependent  $C_{max}$  values (free concentration) in rats and humans, indicating that humans are expected to reach around twenty-fold higher blood

concentrations than rats at equal oral exposure levels, mainly due to the lower catalytic efficiency for metabolic clearance of profenofos in humans.

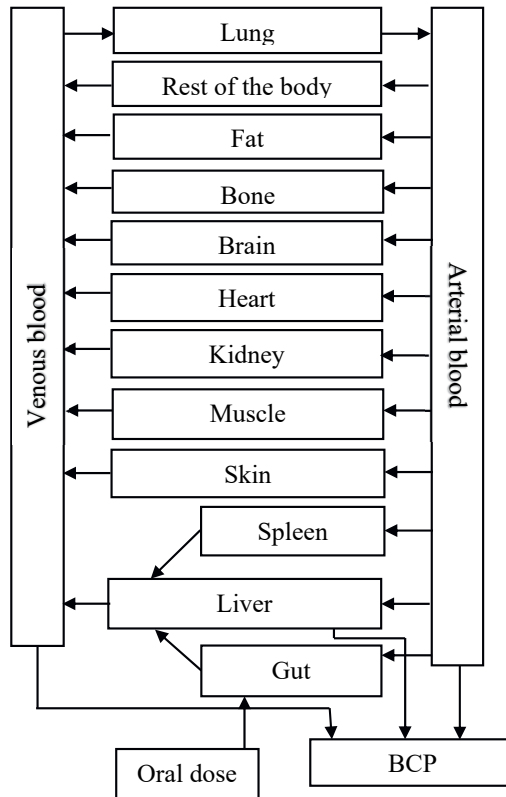


Figure 2. Schematic diagram of the PBK model for profenofos for rats and humans.



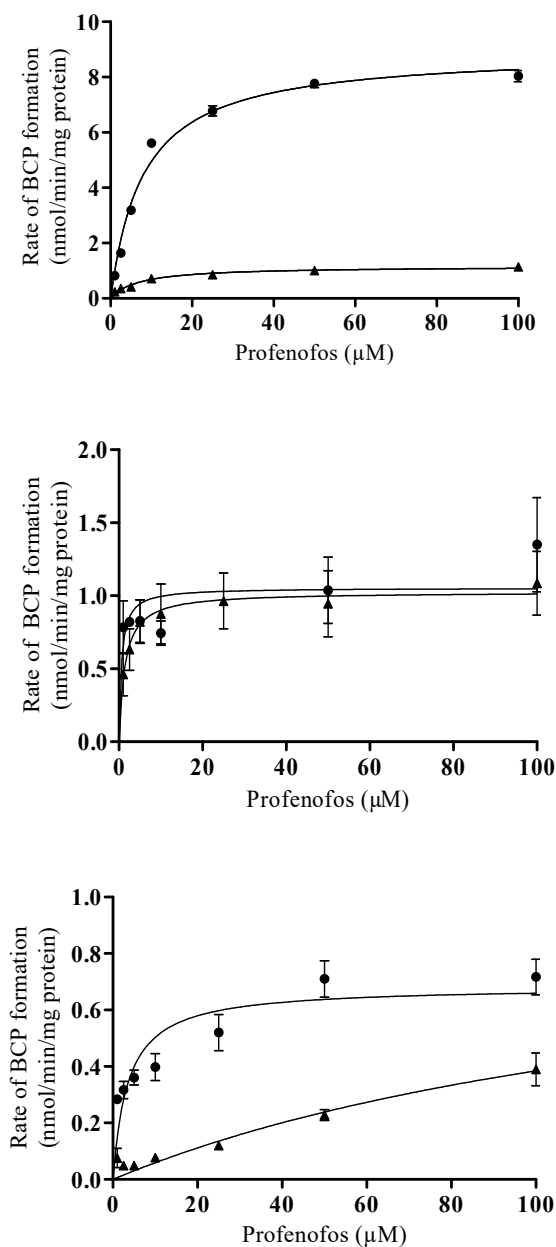


Figure 3. Concentration-dependent rate of profenofos conversion to BCP in incubations with human (triangles) and rat (dots) (A) liver microsomal proteins, (B) liver cytosolic proteins, and (C) plasma proteins. Results represent data from 3 independent experiments and are presented as mean  $\pm$  SEM.

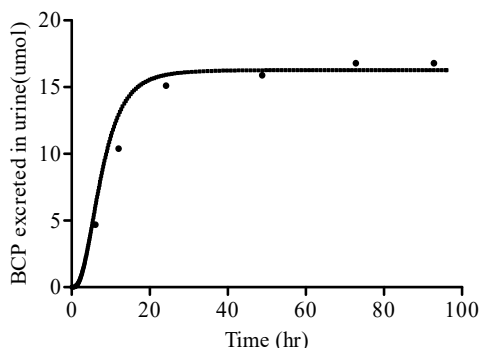


Figure 4. Comparison of PBK model-predicted (continuous line) and experimentally determined (symbols, Cho et al 2002) time-dependent cumulative urinary excretion of BCP-glucuronide in rats upon oral administration of 35.8 mg profenofos/kg bw.

### 3.3.3 Prediction of in vivo dose-dependent AChE inhibition by PBK modeling-facilitated reverse dosimetry of in vitro data and comparison with reported in vivo effect data

Concentration-dependent inhibition of rat RBC AChE (obtained from rat blood) and human (recombinant) AChE by profenofos were obtained in vitro (Figure 7). Profenofos inhibited human AChE with an IC<sub>50</sub> value of 302 nM, which is very close to the IC<sub>50</sub> value of 350 nM reported by Das and Kamil (2006) using freshly obtained human erythrocytes. Profenofos inhibited rat AChE with an IC<sub>50</sub> of 312 nM, suggesting no species difference in profenofos-induced AChE inhibition, based on effect concentrations related to 50% AChE inhibition.

The concentration-dependent AChE inhibition curves obtained in this study were converted into in vivo dose-dependent AChE inhibition curves in rats and humans (Figure 8) using the PBK modeling-facilitated reverse dosimetry approach as described in the materials and methods section. Figure 8 also presents in vivo data for male and female rat profenofos-induced AChE inhibition in RBCs and in the brain available from literature (JMPR 2007). The results reveal that predicted in vivo dose-response curves for rat AChE inhibition are close to the

reported in vivo data for male and female rat AChE inhibition in RBCs and in the brain (JMPR 2007), indicating that with this combined in vitro-in silico approach, good predictions for rats were obtained. Predictions for humans indicate that humans are expected to be more sensitive than rats regarding profenofos-induced AChE inhibition (Figure 8), which is mainly due to the slower metabolic clearance of profenofos, resulting in higher C<sub>max</sub> values at the same dose levels (Figure 7). Toxicity data for humans for further evaluation of the predicted dose-response curves are not available.

BMD analysis was performed on predicted dose-response data for rats and human. Results of these analyses are presented in Supplementary Tables 2 and 3 and Supplementary Figures 2 and 3. BMDL<sub>10</sub> values obtained for rats and humans upon model averaging were 0.45 and 0.01 mg/kg bw, respectively, predicting humans to be more sensitive than rats. In theory, BMD values obtained from predicted dose-response data may serve as PODs for setting safe exposure levels, i.e. an ARfD, and these BMD values were therefore compared with PODs that have been used by the US EPA, JMPR and EFSA in their assessments.

The US EPA considered erythrocyte (RBC) AChE inhibition to be more suitable to derive a POD for human safety assessments, since it is more sensitive than brain AChE inhibition in case of profenofos exposure (EPA 2016). A 10% RBC inhibition of AChE has been adopted by the US EPA to obtain a POD to define the ARfD for profenofos (EPA 2016). The US EPA reported a BMDL<sub>10</sub> of 1.99 mg/kg bw for profenofos-induced RBC AChE inhibition in adult rats upon a single exposure to profenofos, being 4 times higher than the BMDL<sub>10</sub> obtained from the predicted dose-response data for rats in our study (0.45 mg/kg bw).

JMPR used a NOAEL value of 100 mg/kg bw to derive an ARfD, based on a dataset on profenofos-induced inhibition of brain AChE in rats (upon a single exposure to profenofos). This NOAEL value is 50-fold higher than the BMDL<sub>10</sub> value reported by the US EPA and 200-

fold higher than the BMDL<sub>10</sub> value obtained from our predicted dose-response data in rats (0.45 mg/kg bw), suggesting the NOAEL to result in a POD that may be too high.

In a recent report from EFSA (EFSA 2019), an ARfD for profenofos of 0.005 mg/kg bw was reported, based on a German evaluation in 2001 that defined an ARfD based on a NOAEL in a dog study using inhibition of brain cholinesterase activity as critical effect. Unfortunately, no further information (e.g. NOAEL) on that particular dog study is publicly available. If a safety factor of 100 was used to derive this ARfD, the NOAEL derived from the dog study would be close to the BMDL<sub>10</sub> value obtained from our predicted dose-response data in rats (0.45 mg/kg bw (~ 100-fold higher than the ARfD)).

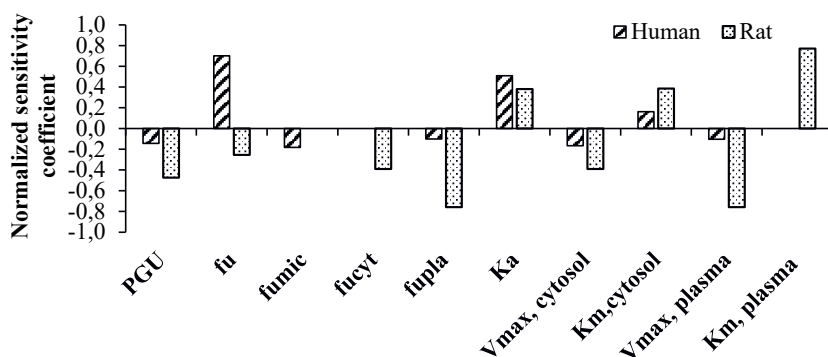


Figure 5. Sensitivity analysis representing the influence of model parameters on the predicted blood C<sub>max</sub> of profenofos in humans and rats at predicted BMDL<sub>10</sub> values of 0.01 and 0.45 mg/kg bw, respectively. PGU= gut:plasma partition coefficient; fu= fraction unbound in plasma; fmic= fraction unbound in microsomal incubation; fucyt= fraction unbound in cytosolic incubation; fupla= fraction unbound in incubation with plasma; ka= absorption constant; V<sub>max</sub>, cytosol= maximum rate of conversion of profenofos to BCP by liver cytosol; K<sub>m</sub>, cytosol= Michaelis-Menten constant for conversion of profenofos to BCP by liver cytosol; V<sub>max</sub>, plasma= maximum rate of conversion of profenofos to BCP by plasma; K<sub>m</sub>, plasma= Michaelis-Menten constant for conversion of profenofos to BCP by plasma.

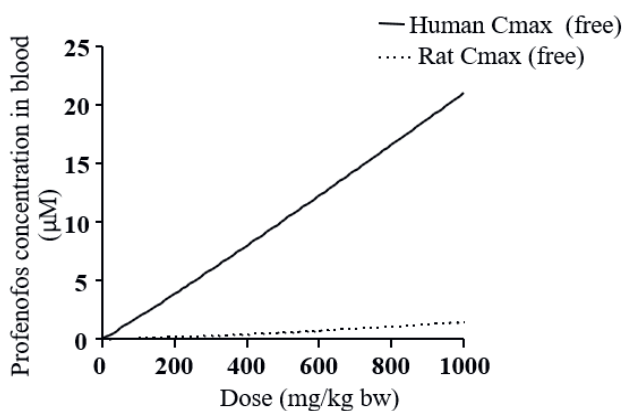


Figure 6. PBK model-predicted dose-dependent C<sub>max</sub> (free) in blood upon oral profenofos exposure in rats (dotted line) and humans (continuous line).

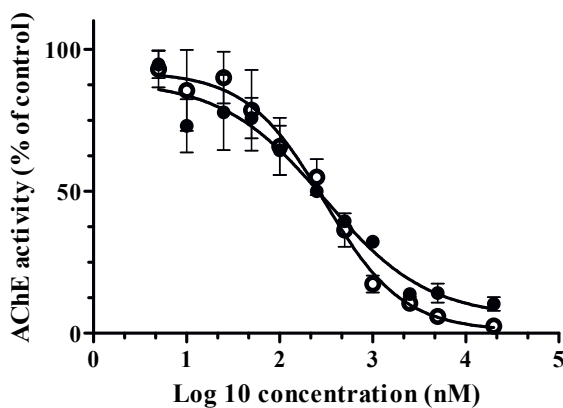


Figure 7. Acetylcholinesterase (AChE) activity in RBCs of Sprague-Dawley rats (closed symbols) and of human recombinant AChE (open symbols) with increasing concentrations of profenofos. AChE activity in the solvent control is set at 100%. Results represent data from 3 independent experiments and are presented as mean  $\pm$  SEM.

### 3.4 Discussion

The aim of the current study was to develop a physiologically based kinetic (PBK) model in rats and humans solely based on *in vitro* and *in silico* input parameters to be applied for the prediction of *in vivo* AChE inhibition by the OP pesticide profenofos by reverse dosimetry of *in vitro* AChE inhibition data. To this end, profenofos PBK models were developed for rats and humans and used to predict dose-dependent internal profenofos concentrations, which were applied for reverse dosimetry to translate *in vitro* concentration-dependent data on profenofos-induced inhibition of AChE to *in vivo* dose-response curves for profenofos-induced inhibition of AChE in blood. The results indicate that profenofos-induced AChE inhibition in rats was closely predicted and that humans are predicted to be more sensitive to profenofos-induced AChE inhibition than rats upon acute exposure.

This study has shown marked interspecies differences in toxicokinetics of profenofos with predicted blood C<sub>max</sub> values for profenofos in humans being around 20-fold higher than in rats at equal levels of exposure (Figure 6). This is mainly due to higher catalytic efficiencies for microsomal, cytosolic and plasma biotransformation of profenofos to BCP in rats as compared to humans as observed in this study (Table 1). Profenofos, being an oxon, is mainly detoxified through hydrolysis by hepatic and plasma PON1 and CYP450-mediated detoxification, resulting in the production of BCP (JMPR 2007; EPA 2016; Dadson et al 2013). Interspecies differences in activities between human and rat PON1 have been reported, with human PON1 having lower catalytic activity as compared to rat PON1 (Kaliste-Korhonen et al 1996). Another possible reason for the differences in profenofos detoxification may be related to quantitative differences in B-esterases in rats and humans, which may affect the metabolism and disposition of ester compounds including OPs (Ecobichon and Comeau 1973; Maxwell et al 1987). B-esterases, such as carboxylesterase (CaE), butyrylcholinesterase (BuChE) and acetylcholinesterase (AChE), detoxify oxons, but these enzymes are inhibited by the oxons as

a consequence (Chanda et al 1997). It has been reported that rat plasma contains almost all types of esterases including CaE, PON1, BChE, and AChE (Sato and Hosokawa 2006; Bahar et al 2012), whereas humans are deficient of plasma CaE (Li et al 2005; Berry et al 2009; Williams et al 2011) and plasma AChE (Ecobichon and Comeau 1973). The relevance of CaE in OP detoxification is indicated by a study that demonstrated that in vivo inhibition of CaEs by cresylbenzodioxaphosphorin oxide (CBDP) caused an increase in the toxicity of many OPs in rats, mice, rabbits and guinea pigs (Ecobichon and Comeau 1973; Maxwell et al 1987). In the same study, the interspecies differences observed in the toxicity of OPs were lost in the group treated with the in vivo CaE inhibitor (CBDP) (Maxwell et al 1987). The absence of CaE in human plasma in addition to low PON1 activity may therefore be responsible for lower profenofos clearance resulting in higher sensitivity of humans to profenofos as compared to rodents (Kaliste-Korhonen et al 1996). In this way, B-esterases may play a protective role in rats but not humans.

Data on RBC AChE inhibition can be considered as an appropriate surrogate measure of potential organophosphate effects on the peripheral and central nervous systems in absence of brain AChE inhibition data (Das and Kamil 2006; Chen et al 1999).

To predict profenofos dose levels that result in AChE inhibition in rats and humans, profenofos in vitro concentration-response curves for RBC AChE inhibition (Figure 7) were translated to in vivo dose-response curves for RBC AChE inhibition for both rats and humans (Figure 8). The predicted data thus obtained for the rat matched with the available in vivo rat data as reported by JMPR (2007) (Figure 8), and the BMDL<sub>10</sub> obtained from the predicted dose-response data differed only 4-fold from the BMDL<sub>10</sub> obtained from data from an in vivo rat study on profenofos-induced blood AChE inhibition used by the US EPA for determination of an ARfD for profenofos. This indicates that in vivo dose-dependent AChE inhibition was closely predicted based on our approach, giving confidence in the human predictions, which

could not be further evaluated because of the lack of human *in vivo* data on this endpoint. Our predictions suggest that humans are more sensitive than rats towards profenofos-induced AChE inhibition. The interspecies differences (45-fold difference in BMDL<sub>10</sub>) were predicted to be mainly due to interspecies differences in toxicokinetics, as discussed above, and these would not be covered by the standard uncertainty factor of 10 to account for interspecies differences. Currently we work on the assessment of human interindividual differences in profenofos metabolic clearance (using plasma and liver fractions of different donors) to be incorporated in PBK models, providing insight into whether a combined uncertainty factor of 100 (10 for interspecies differences and 10 for intraspecies differences) applied to the rat AChE inhibition data is expected to be sufficiently protective for sensitive human individuals.

In the present study, the BMDL<sub>10</sub> calculated based on predicted rat data was 4 times lower than the BMDL<sub>10</sub> value used by EPA and 200-fold lower than the NOAEL used by JMPR to obtain an ARfD, implying that our prediction is more conservative as compared to the rat data used by the two agencies. In a possible future risk assessment paradigm that would be independent of animal data, BMDL<sub>10</sub> values obtained from the predicted human dose-response data may be applied. In the present study, we determined a BMDL<sub>10</sub> value for ‘an average human’ (0.01 mg/kg bw), not quantifying possible interindividual differences. To take interindividual differences into account an uncertainty factor may be applied, but it would be scientifically more sound to quantify interindividual differences in the human population in profenofos detoxification. This is especially of interest given the reported genetic polymorphisms of human PON1 (and BuChE) with related phenotypes of low and high activities (Geldmacher et al 1989; Schwarz et al 1995), which may play a role in the interindividual differences in PON1 activity (Darney et al 2020), suggesting possible large human interindividual differences in profenofos detoxification. As indicated above, we currently work on the determination of such



interindividual differences in profenofos detoxification in humans and integrate these data in the human PBK modeling-based predictions of profenofos toxicity.

Although the current models quantitatively predicted profenofos tissue dosimetry and the resulting AChE inhibition, possible limitations of the approach should be considered. In the current PBK model, gut absorption of profenofos was estimated to be 100% using a first order process with an absorption rate constant of  $1 \text{ hr}^{-1}$ . Although this resulted in the adequate prediction of time-dependent BCP-glucuronide in rat urine, it must be noted that that specific model output is not so sensitive to the  $k_a$  (data not shown), whereas the (unbound)  $C_{max}$  is (Figure 6). It is noteworthy that the extent of absorption varies depending on the dosing method, dose formulation (solution) and variations in species, strain and gender (Kararli 1995). Furthermore, profenofos absorption as present in the food matrix may be different.

We used a static approach to determine the AChE inhibitory effect concentrations, using a single preincubation time point (15 minutes). When including more time points, information on the time-dependent inhibition kinetics can be obtained. However, a previous study with chlorpyrifos oxon showed that human recombinant acetylcholinesterase active sites were 100% inhibited after a pre-incubation period of 11 minutes (Kaushik et al 2007). One would expect that effect concentrations would decrease with longer incubation times until 100% of the binding sites is inhibited, as shown before by Aurbek et al (2006) and Krstić et al (2008). With a relatively long pre-incubation time of 15 minutes as we have used in the present study, similar to incubation times previously applied by other research groups (e.g. Aurbek et al 2006; Kasteel et al 2020), we aimed to obtain a relevant and conservative estimation of the effect concentrations, as also indicated by the small difference between the  $BMDL_{10}$  value obtained with our predicted rat dose-response data and the  $BMDL_{10}$  value from a reported *in vivo* study in rats.

It must also be noted that the approach used in this study may be suitable to estimate AChE inhibition upon a single exposure, while not predicting effects upon repeated exposure, since upon longer exposures, one must take the time-dependent de novo AChE production into account to adequately estimate the AChE activity upon a second and further exposure. In that regard a phenomenon referred to as steady state AChE inhibition is of interest, which is the situation when the degree of AChE inhibition reaches equilibrium with the production of new enzyme at which AChE inhibition remains constant at a specified dose over the exposure period (EPA 2016). Adequate prediction of these processes based on only in vitro data, as applied in the present study, seems at this stage not possible. Furthermore, one must consider that OPs inhibit detoxifying enzymes, such as CaE and BuChE, which may result in a decrease in metabolic clearance, and related higher internal concentrations and increased sensitivity upon repeated dosing.

Another limitation of the approach is that the prediction of OP toxicity was only based on AChE inhibition as the endpoint. It should, however, be noted that OPs may affect a number of additional targets (such as Neuropathy target esterase (NTE) (Costa 2018), muscarinic M2 receptors (Costa 2006), acylpeptide hydrolase (APH) (Richards et al 2000), fatty acid amide hydrolase (FAAH) (Quistad et al 2001; Buntyn et al 2017) and a variety of lipases (Quistad et al 2006)) that lead to OP toxicity, including neuroinflammation, autoimmunity and axonal transport deficits (Naughton and Terry 2018). On the other hand, AChE inhibition has been used as an endpoint to set a POD for the risk assessment (EPA 2016; EFSA 2019), indicating its relevance. The QIVIVE approach could be extended in the future to also predict dose-dependent effects related to other OP targets, allowing a more extensive hazard assessment based on NAMs.

In conclusion, the predicted dose-dependent profenofos-induced AChE inhibition in rats are close to reported data on dose-dependent in vivo AChE inhibition in rats upon single dosing,

providing also confidence in the predictions obtained for humans. Results from this study suggest that humans may be more sensitive to AChE inhibition upon profenofos exposure than rats, which is mainly due to differences in profenofos detoxification. Altogether, the results demonstrate the ability to predict *in vivo* AChE inhibition by profenofos, providing another proof-of-principle that with NAMs *in vivo* effects of chemicals can be predicted without the use of *in vivo* studies.

### **Acknowledgements**

This work is supported by the Netherlands Universities Foundation for International Cooperation (Nuffic) (scholarship granted to Isaac Omwenga (PhD.17/0019)), the China Scholarship Council (scholarship (No. 201707720063) granted to Shensheng Zhao), and the Dutch Ministry of Agriculture, Nature and Food Quality (project KB-23-002-021).

### **Conflict of interest statement**

The authors declare that they have no conflicts of interest.

**References**

- Aly OA, Badawy MI (1982) Hydrolysis of organophosphate insecticides in aqueous media. *Environ Int* 7:373-377.
- Aurbek N, Thiermann H, Szinicz L, Eyer P, Worek F (2006) Analysis of inhibition, reactivation and aging kinetics of highly toxic organophosphorus compounds with human and pig acetylcholinesterase. *Toxicology* 224:91–99.
- Bahar FG, Ohura K, Ogiwara T, Imai T (2012) Species difference of esterase expression and hydrolase activity in plasma. *J Pharm Sci* 101:3979-3988.
- Berezhkovskiy LM (2004) Volume of distribution at steady state for a linear pharmacokinetic system with peripheral elimination. *J Pharm Sci* 93:1628-1640.
- Berry LM, Wollenberg L, Zhao Z (2009) Esterase activities in the blood, liver and intestine of several preclinical species and humans. *Drug Metab Lett* 3:70–77.
- Bradman A, Barr DB, Claus-Henn BG, Drumheller T, Curry C, Eskenazi B (2003) Measurement of pesticides and other toxicants in amniotic fluid as a potential biomarker of prenatal exposure: a validation study. *Environ Health Perspect* 111:1779-1182.
- Bogen KT, Singhal A (2017) Malathion dermal permeability in relation to dermal load: Assessment by physiologically based pharmacokinetic modeling of in vivo human data. *J Environ Sci Health B* 52:138-146.
- Bouchard M, Gosselin NH, Brunet RC, Samuel O, Dumoulin MJ, Carrier G (2003) A toxicokinetic model of malathion and its metabolites as a tool to assess human exposure and risk through measurements of urinary biomarkers. *Toxicol Sci* 73:182-194.
- Bouchard M, Carrier G, Brunet RC, Bonvalot Y, Gosselin NH (2005) Determination of biological reference values for chlorpyrifos metabolites in human urine using a toxicokinetic approach. *J Occup Environ Hyg* 2:155-168.
- Bouchard M, Gosselin NH, Brunet RC, Samuel O, Dumoulin M, Carrier G (2017) A toxicokinetic model of malathion and its metabolites as a tool to assess human exposure and risk through measurements of urinary biomarkers. *Toxicol Sci* 73:182-194.
- Buntyn RW, Alugubelly N, Hybart RL, Mohammed AN, Nail CA, Parker GC, Ross MK, Carr RL (2017) Inhibition of endocannabinoid-metabolizing enzymes in peripheral tissues following developmental chlorpyrifos exposure in rats. *Int J Toxicol* 36:395-402.
- Chambers JE, Chambers JW (1989) Oxidative desulfuration of chlorpyrifos, chlorpyrifos-methyl and leptophos by rat brain and liver. *J Biochem Toxicol* 4:201-203.
- Chanda SM, Mortensen SR, Moser VC, Padilla S (1997) Tissue-specific effects of

- chlorpyrifos on carboxylesterase and cholinesterase activity in adult rats: an in vitro and in vivo comparison. *Fundam Appl Toxicol* 38:148-157.
- Carr RL, Dail MB, Chambers HW, Chambers JE (2015) Species differences in paraoxonase mediated hydrolysis of several organophosphorus insecticide metabolites. *J Toxicol* 470189.
- Chen WL, Sheets JJ, Nolan RJ, Mattsson JL (1999) Human red blood cell acetylcholinesterase inhibition as the appropriate and conservative surrogate endpoint for establishing chlorpyrifos reference dose. *Regul Toxicol Pharmacol* 29:15-22.
- Cho Y, Min K, Lee I, Cha C (2002) Determination of urinary metabolite of profenofos after oral administration and dermal application to rats. *J Fd Hyg Safety* 17:20–25.
- Costa LG (2006) Current issues in organophosphate toxicology. *Clin Chim Acta* 366:1-13.
- Costa LG (2018) Organophosphorus Compounds at 80: Some Old and New Issues. *Toxicol Sci* 162:24-35.
- Cubitt HE, Houston JB, Galetin A (2011) Prediction of human drug clearance by multiple metabolic pathways: integration of hepatic and intestinal microsomal and cytosolic data. *Drug Metab Dispos* 39:864-873.
- Dadson OA, Ellison CA, Singleton ST, Chi L, McGarrigle BP, Pamela J, Lein JP, Farahat FM, Farahat T, Olson JR (2013) Metabolism of profenofos to 4-bromo-2-chlorophenol, a specific and sensitive exposure biomarker. *Toxicology* 306:35-39.
- Darney K, Kasteel EEJ, Buratti FM, Turco L, Vichi S, Béchaux C, Roudot AC, Kramer NI, Testai E, Dorne JLCM, Di Consiglio E, Lautz LS (2020) Bayesian meta-analysis of inter-phenotypic differences in human serum paraoxonase-1 activity for chemical risk assessment. *Environ Int* 138:105609.
- Das GP, Jamil K (2006) Effect of Four Organophosphorus Compounds on Human Blood Acetylcholinesterase: In Vitro Studies. *Toxicol Mech Methods* 16:455-459.
- Ecobichon DJ, Comeau AM (1973) Pseudocholinesterases of mammalian plasma: Physicochemical properties and organophosphate inhibition in eleven species. *Toxicol Appl Pharmacol* 24:92-100.
- Eddleston M, Worek F, Eyer P, Thiermann H, Von Meyer L, Jeganathan K, Sheriff MHR, Dawson AH, Buckley NA (2009) Poisoning with the S-Alkyl organophosphorus insecticides profenofos and prothiofos. *QJM: Int J Med.* 102:785-792.
- Ellman GL, Courtney KD, Andres V, Featherstone RM (1961) A new rapid colorimetric determination of acetylcholinesterase activity. *Biochemical Pharmacology* 7:88–95.
- EFSA (European Food Safety Authority) (2019). Scientific Report on scientific support for

- preparing an EU position in the 51st Session of the Codex Committee on Pesticide Residues (CCPR). EFSA Journal 17:5797.
- EPA (1999) Data evaluation record study type: special non-guideline assessment for RBC Cholinesterase in humans. Retrieved from <https://archive.epa.gov/scipoly/sap/meetings/web/pdf/kisickider.pdf> [Accessed January 2019]
- EPA (2006) Reregistration Eligibility Decision for Dimethoate. Retrieved from [https://archive.epa.gov/pesticides/reregistration/web/pdf/dimethoate\\_red.pdf](https://archive.epa.gov/pesticides/reregistration/web/pdf/dimethoate_red.pdf) [Accessed December 2020]
- EPA (2011) Chlorpyrifos Preliminary Human Health Risk Assessment DP No. D388070 Retrieved from <https://www.regulations.gov/contentStreamer?documentId=EPA-HQ-OPP-2008-0850-0025&contentType=pdf> [Accessed December 2020]
- EPA (2016) Profenofos: Human health draft risk assessment (DRA) for registration review. [https://www3.epa.gov/pesticides/chem\\_search/cleared\\_reviews/csr\\_PC-111401\\_19-Oct-16.pdf](https://www3.epa.gov/pesticides/chem_search/cleared_reviews/csr_PC-111401_19-Oct-16.pdf). [Accessed March 2020]
- Evans MV, Andersen ME (2000) Sensitivity analysis of a physiological model for 2, 3, 7, 8-tetrachlorodibenzo-p-dioxin (TCDD): assessing the impact of specific model parameters on sequestration in liver and fat in the rat. *Toxicol Sci* 54:71-80.
- Farahat TM, Abdelrasoul GM, Amr MM, Shebl MM, Farahat FM, Anger WK (2003) Neurobehavioral effects among workers occupationally exposed to organophosphorous pesticides. *Occup Environ Med* 60:279-286.
- Geldmacher-v M, Diepgen TL (1989) Human serum paraoxonase polymorphism, specificity, classification. In: Reiner E, Aldridge WN and Hoskin FCG (eds.) *Enzymes hydrolyzing organophosphorus compounds* Ellis Horwood Limited, West Sussex, England pp. 15-29.
- Gotoh M, Sakata M, Endo T, Hayashi H, Seno H, Suzuki O (2001) Profenofos metabolites in human poisoning. *Forensic Sci Int* 116: 221-226.
- Greish S, Ismail SM, Mosleh Y, Loutfy N, Dessouki AA, Ahmed MT (2011) Human risk assessment of profenofos: A case study in Ismailia, Egypt. *Polycyclic Aromat Compd* 31:28-47.
- Heilmair R, Eyer F, Eyer P (2008) Enzyme-based assay for quantification of chlorpyrifos oxon in human plasma. *Toxicol Lett* 181:19-24.
- Hertz-Picciotto I, Sass JB, Engel S, Bennett DH, Bradman A, Eskenazi B, Lanphear B, Whyatt

- B (2018) Organophosphate exposures during pregnancy and child neurodevelopment: Recommendations for essential policy reforms. *PLoS Med* 15(10): e1002671.
- Hardt J, Angerer J (2000) Determination of dialkyl phosphates in human urine using gas chromatography-mass spectrometry. *J Anal Toxicol* 24:678-684.
- Johnson MK, Glynn P, (1995) Neuropathy target esterase (NTE) and 675 organophosphorus induced delayed polyneuropathy (OPIDP): recent 676 advances. *Toxicol Lett* 82-83: 459-463.
- Johnson MK, Glynn P (2001) Neuropathy target esterase In *Handbook of Pesticide Toxicology*, (Krieger R., Ed.), 953–965. Academic Press, San Diego.
- Larsen KE, Lifschitz AL, Lanusse CE, Virkel GL (2019) In vitro and in vivo effects of chlorpyrifos and cypermethrin on blood cholinesterases in sheep. *J Vet Pharmacol Therap* 42:548-555.
- Jamal GA, Hansen S, Julu POO (2002) Low level exposures to organophosphorus esters may cause neurotoxicity. *Toxicology* 181-182: 23-33.
- Joint FAO/WHO Meeting on Pesticide Residues (JMPR) (2007) Pesticide residues in food 2007. <http://www.inchem.org/documents/jmpr/jmpmono/v2007pr01.pdf> [Accessed August 2020]
- Jones HM, Rowland-Yeo K (2013) Basic concepts in physiologically based pharmacokinetic modeling in drug discovery and development. *CPT Pharmacometrics Syst Pharmacol* 2:e63.
- Kaliste-Korhonen E, Tuovinen K, Hänninen O (1996) In vitro interspecies differences in enzymes reacting with organophosphates and their inhibition by paraoxon. *Hum Exp Toxicol* 15:972.
- Kararli TT (1995) Comparison of the gastrointestinal anatomy, physiology and biochemistry of humans and commonly used laboratory animals. *Biopharm Drug Dispos* 16:351-380.
- Karanja NK, Njenga M, Mutua GK, Lagerkvist CJ, Kutto E, Okello JJ (2012) Concentrations of heavy metals and pesticide residues in leafy vegetables and implications for peri-urban farming in Nairobi, Kenya. *Journal of Agriculture, Food Systems, and Community Development* 3:255-267.
- Kasteel EEJ, Nijmeijer SM, Darney K, Lautz LS, Dorne JLCM, Kramer NI, Westerink RHS (2020) Acetylcholinesterase inhibition in electric eel and human donor blood: an in vitro approach to investigate interspecies differences and human variability in toxicodynamics. *Arch Toxicol* 94: 4055-4065.

- Kaushik R, Rosenfeld CA, Sultatos LG (2007) Concentration-dependent interactions of the organophosphates chlorpyrifos oxon and methyl paraoxon with human recombinant acetylcholinesterase. *Toxicol Appl Pharmacol* 221:243-250.
- Krstić DZ, Colović M, Kralj MB, Franko M, Krinulović K, Trebse P, Vasić V (2008) Inhibition of AChE by malathion and some structurally similar compounds. *J Enzyme Inhib Med Chem* 23:562-73.
- Kumari D, John S (2019) Health risk assessment of pesticide residues in fruits and vegetables from farms and markets of Western Indian Himalayan Region, *Chemosphere* 224:162-167.
- Li B, Sedlacek M, Manoharan I, Boopathy R, Duysen EG, Masson P, and Lockridge O (2005) Butyrylcholinesterase, paraoxonase, and albumin esterase, but not carboxylesterase, are present in human plasma. *Biochem Pharmacol* 70:1673-1684.
- Liu P, Wu CH, Chang XL, Qi XJ, Zheng ML, Zhou ZJ (2014) Assessment of chlorpyrifos exposure and absorbed daily doses among infants living in an agricultural area of the Province of Jiangsu, China. *Int Arch Occup Environ Health* 87:753-762.
- Louis J, Beekmann K, Rietjens IMCM (2017) Use of physiologically based kinetic modeling-based reverse dosimetry to predict in vivo toxicity from in vitro data. *Chem Res Toxicol* 30:114–125.
- Lowry O, Rosebrough N, Farr A, Randall R (1951) Protein measurement with the folin phenol reagent. *J Biol Chem* 193:265–275.
- Lu C, Fenske RA, Simcox NJ, Kalman D (2000) Pesticide exposure of children in agricultural community: evidence of household proximity to farmland and take home exposure pathways. *Environ Res Sect A* 84:290-302.
- Lu C, Holbrook CM, Andres LM (2010) The implications of using a physiologically based pharmacokinetic (PBPK) model for pesticide risk assessment. *Environ Health Perspect* 118:125-130.
- Medinsky MA, Leavens TL, Csanady GA, Gargas ML, Bond JA (1994) In vivo metabolism of butadiene by mice and rats: a comparison of physiological model predictions and experimental data. *Carcinogenesis* 15:1329-1340.
- Maxwell DM, Lenz DE, Groff WA, Kaminskis A, Froehlich HL (1987) The effects of blood flow and detoxification on in vivo cholinesterase inhibition by soman in rats. *Toxicol Appl Pharmacol* 88: 66-76.
- Mosquin PL, Licata AC, Liu B, Sumner SC, Okino MS (2009) Reconstructing exposures from



- small samples using physiologically based pharmacokinetic models and multiple biomarkers. *J Expo Sci Environ Epidemiol* 19:284-297.
- Mostafalou S, Abdollahi M (2013) Pesticides and human chronic diseases: evidences, mechanisms, and perspectives. *Toxicol Appl Pharmacol* 268:157-177.
- Naksen W, Prapamontol T, Mangklabruks A, Chantara S, Thavornnyutikarn P, Robson MG, Panuwet P (2016) A single method for detecting 11 organophosphate pesticides in human plasma and breastmilk using GC-FPD. *J Chromatogr B Analyt Technol Biomed Life Sci* 1025:92-104.
- Naughton SX, Terry AV Jr (2018) Neurotoxicity in acute and repeated organophosphate exposure. *Toxicology* 408:101-112.
- Omwenga I, Kanja L, Zomer P, Louisse J, Rietjens IMCM, Mol H (2021) Organophosphate and carbamate pesticide residues and accompanying risks in commonly consumed vegetables in Kenya. *Food Addit Contam Part B Surveill*. 14(1):48-58.
- Poet TS, Kousba AA, Dennison SL, Timchalk C (2004) Physiologically based pharmacokinetic/pharmacodynamic model for the organophosphorus pesticide diazinon. *Neurotoxicology* 25:1013-1030.
- Punt A, Pinckaers N, Peijnenburg A, Louisse J (2020) Development of a web-based toolbox to support quantitative in vitro-to-in vivo extrapolations (QIVIVE) within non-animal testing strategies. Accepted for publication in *Chem Res Toxicol*.
- Quandt SA, Arcury TA, Rao P, Snively BM, Camann DE, Doran AM, Yau AY, Hoppin JA, Jackson DS (2004) Agricultural and residential pesticides in wipe samples from farmworker family residences in North Carolina and Virginia. *Environ Health Perspect* 112:382-387.
- Quistad GB, Sparks SE, Casida JE (2001) Fatty acid amide hydrolase inhibition by neurotoxic organophosphorus pesticides. *Toxicol Appl Pharmacol* 173: 48-55.
- Quistad GB, Liang SN, Fisher KJ, Nomura DK, Casida JE (2006) Each lipase has a unique sensitivity profile for organophosphorus inhibitors. *Toxicol Sci* 91:166-172.
- Richards PG, Johnson MK, Ray DE (2000) Identification of acylpeptide hydrolase as a sensitive site for reaction with organophosphorus compounds and a potential target for cognitive enhancing drugs. *Mol Pharmacol* 58:577-583.
- Rigas ML, Okino MS, Quackenboss JJ (2001) Use of a pharmacokinetic model to assess chlorpyrifos exposure and dose in children, based on urinary biomarker measurements. *Toxicol Sci* 61:374-381.
- Rosenfeld CA, Sultatos LG (2006) Concentration-dependent kinetics of acetylcholinesterase

- inhibition by the organophosphate paraoxon. *Toxicol Sci* 90:460–469.
- Satoh T, Hosokawa M (2006) Structure, function and regulation of carboxylesterases. *Chem Biol Interact* 162:195-211.
- Schwarz M, Loewenstein-Lichtenstein Y, Glick D, Liao J, Norgaard-Pedersen B, Soreq H (1995) Successive organophosphate inhibition and oxime reactivation reveals distinct responses of recombinant human cholinesterase variants. *Brain Res Mol Brain Res* 31:101-110.
- Strikwold M, Spenkelink B, Woutersen R, Rietjens IMCM, Punt A (2013) Combining in vitro embryotoxicity data with physiologically based kinetic (PBK) modelling to define in vivo dose response curves for developmental toxicity of phenol in rat and human. *Arch Toxicol* 87:1709-1723.
- Sultatos LG (1990) A physiologically based pharmacokinetic model of parathion based on chemical-specific parameters determined in vitro. *J Amer Coll Toxicol* 9:611-619.
- Timchalk C, Nolan RJ, Mendrala AL, Dittenber DA, Brzak KA, Mattsson JL (2002) A physiologically based pharmacokinetic and pharmacodynamic (PBPK/PD) model for the organophosphate insecticide chlorpyrifos in rats and humans. *Toxicol Sci* 66:34-53.
- Williams ET, Bacon JA, Bender DM, Lowinger JJ, Guo WK, Ehsani ME, Wang X, Wang H, Qian YW, Ruterbories KJ, Wrighton SA, Perkins EJ (2011) Characterization of the expression and activity of carboxylesterases 1 and 2 from the beagle dog, cynomolgus monkey, and human. *Drug Metab Dispos* 39:2305-2313.
- Zhang Y, Han S, Liang D, Shi X, Wang F, Liu W, Zhang L, Chen L, Gu Y, Tian Y (2014) Prenatal exposure to organophosphate pesticides and neurobehavioral development of neonates: a birth cohort study in Shenyang, China. *PloS one*, 9:88491.
- Zhao S, Kamelia L, Boonpawa R, Wesseling S, Spenkelink B, Rietjens IMCM (2019) Physiologically based kinetic modelling-facilitated reverse dosimetry to predict in vivo red blood cell acetylcholinesterase inhibition following exposure to chlorpyrifos in the Caucasian and Chinese population. *Toxicol Sci* 171: 69–83.

**Supplementary Table 1.** Physiological and chemical-specific parameters used for the PBK models.

<b>Model parameter</b>	<b>Human</b>	<b>Rat</b>
<b>Physiological parameters</b>		
Body weight	70	0.20
<u>Fractional tissue volumes</u>		
Fat	0.213	0.07
Bone	0.0856	0.0659
Brain	0.02	0.0052
Gut	0.0171	0.026
Heart	0.0057	0.0044
Kidney	0.0044	0.0092
Liver	0.021	0.036
Lung	0.0076	0.0052
Muscle	0.4	0.488
Skin	0.0371	0.1656
Spleen	0.0026	0.0024
Venous blood	0.0514	0.0429
Arterial blood	0.0257	0.0215
Rest of body	0.1098	0.0577
Cardiac output (mL/s)	108.33	1.33
<u>Fractional tissue blood flows</u>		
Fat	0.05	0.059
Bone	0.05	0.10
Brain	0.12	0.014

Gut	0.1465	0.0101
Heart	0.04	0.04
Kidney	0.19	0.145
Liver (Venous side)	0.2154	0.242
Lung	1	1
Muscle	0.17	0.237
Skin	0.05	0.051
Spleen	0.0172	0.011
Rest of body	0.02119	0.112
Renal clearance (L/hr)	6.7	0.078

**Chemical specific parameters profenofos**

Molecular weight	373.63
LogP	4.88
pKa	NA
LogD*(olive oil: water)	4.09

Binding data

Fu blood	0.034
----------	-------

Fraction unbound microsomes	0.07 <sup>a</sup>	0.232 <sup>b</sup>
Fraction unbound cytosol	0.07 <sup>c</sup>	0.232 <sup>d</sup>
Fraction unbound plasma (in vitro incubations)	0.83 <sup>e</sup>	0.93 <sup>f</sup>

Tissue to plasma partition coefficients

Fat	96.3	147
Bone	15.4	11.9

Brain	14.1	23.3
Gut	11.1	14.1
Heart	3.47	7.47
Kidney	5.35	8.84
Liver	8.82	9.70
Lung	1.24	11.1
Muscle	5.43	5.44
Skin	6.62	12.4
Spleen	5.45	5.05
Rest of body	1	1
Absorption Ka (/hr)	1	1
Fraction absorbed	1	1

**Chemical specific parameters: BCP**

LogP	-	3.04
pKa	-	7.54
LogD*(olive oil: water)	-	1.80

Tissue plasma partition coefficients

Fat	-	5.62
Bone	-	2.90
Brain	-	5.65
Gut	-	3.54
Heart	-	2.05
Kidney	-	2.36
Liver	-	2.52
Lung	-	2.87
Muscle	-	1.58
Skin	-	3.11
Spleen	-	1.49
Rest of body	-	1

Binding data

Fu blood	-	0.113
Fraction unbound microsomes	-	0.761 <sup>g</sup>

**Chemical specific parameters: BCP glucuronide**

LogP	-	1.06
pKa	-	2.72

LogD* (olive oil: water)	-	4.85
--------------------------	---	------

Tissue to plasma partition coefficients

Fat	-	0.13
Bone	-	0.79
Brain	-	1.49
Gut	-	1.16
Heart	-	1.00
Kidney	-	1.05
Liver	-	1.01
Lung	-	1.12
Muscle	-	0.93
Skin	-	1.05
Spleen	-	1.02
Rest of body	-	1

Binding data

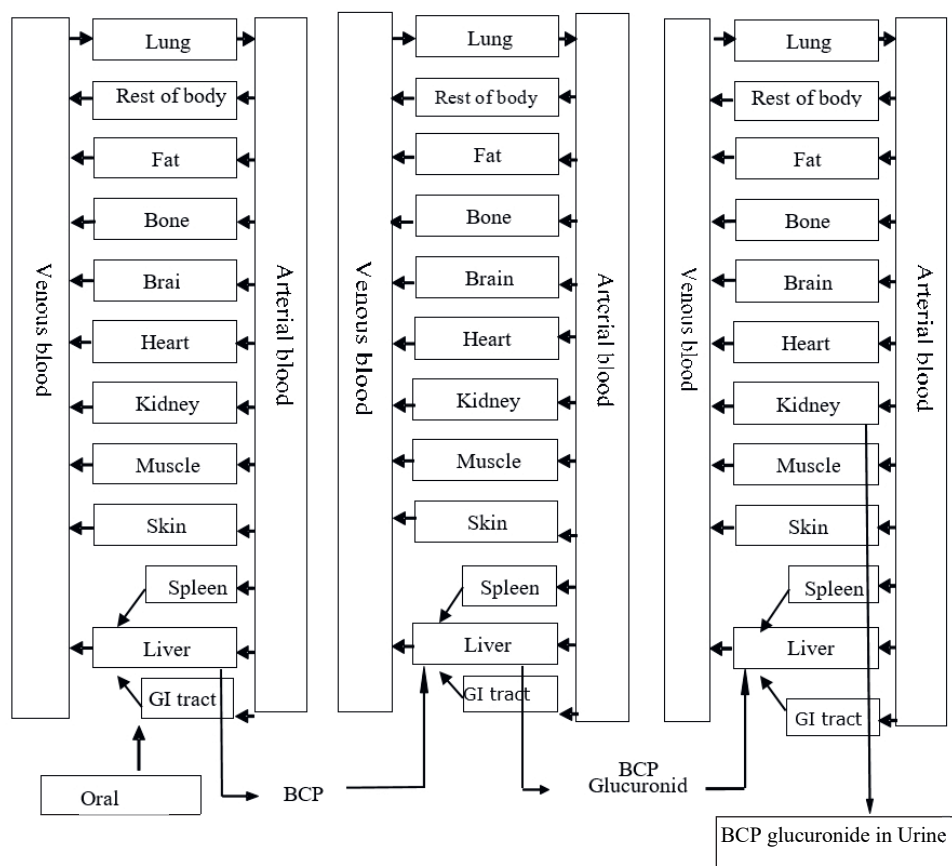
Fu blood	-	0.226
----------	---	-------

**Scaling factors**

Microsomal protein (mg) per g liver	32	35
Cytosolic protein (mg) per g liver	80.7	80.7
Plasma (mg) per g blood	550	550

- <sup>a</sup> fraction unbound profenofos in human microsome incubation (with 2 mg/mL)
- <sup>b</sup> fraction unbound profenofos in rat microsome incubation (with 0.5 mg/mL)
- <sup>c</sup> fraction unbound profenofos in human cytosol incubation (with 2 mg/mL)
- <sup>d</sup> fraction unbound profenofos in rat cytosol incubation (with 0.5 mg/mL)
- <sup>e</sup> fraction unbound profenofos in human plasma incubation (estimated with help of simcyp (via  $K_d$ : 13  $\mu$ M); 4.4 mg plasma/mL (0.20 g albumin/L))
- <sup>f</sup> fraction unbound profenofos in rat plasma incubation (estimated with help of simcyp (via  $K_d$ : 13  $\mu$ M); 1.65 mg plasma/mL (0.074 g albumin/L))
- <sup>g</sup> fraction unbound BCP in rat microsome incubation (with 1 mg/mL)





of the PBK model for profenofos for rat  
 · profenofos (left), 4-bromo-2-chlorophenol  
 (BCP) (center) and for BCP glucuronide (right). BCP formation is also described in the blood  
 compartments in the PBK model, but for the sake of clarity of the figure, this is not depicted in  
 the schematic diagram.

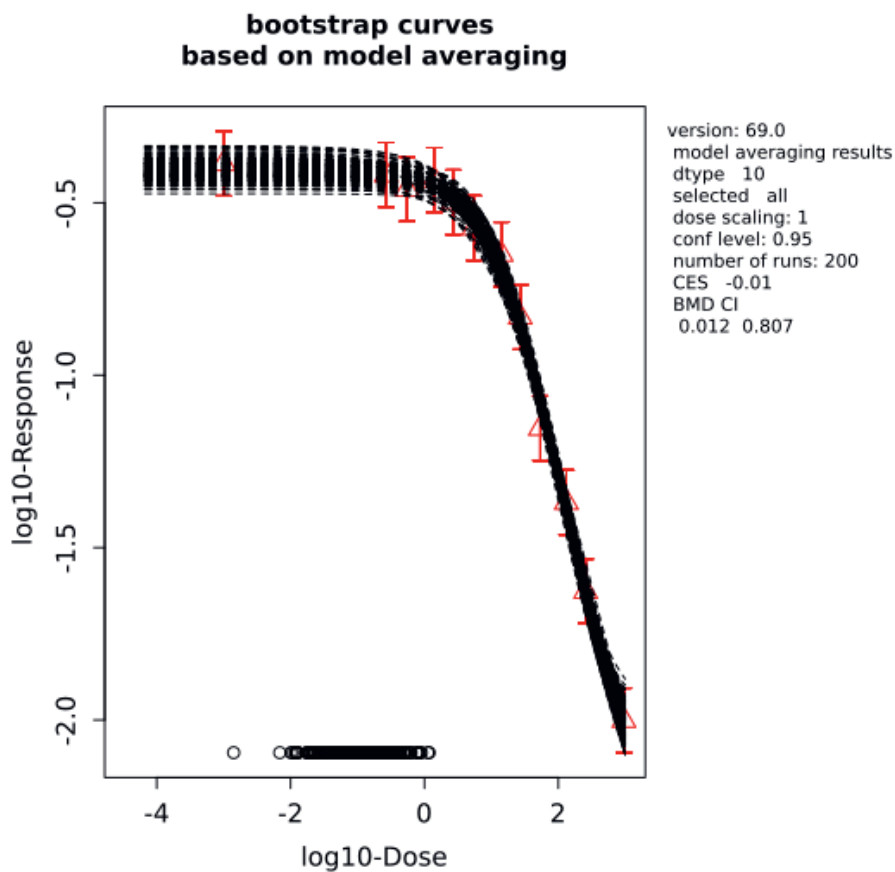
Abbreviation: GI tract: gastrointestinal tract.

**Supplementary Table 2.** Results of BMD modelling of predicted human dose-response data, applying model averaging

## Fitted Models

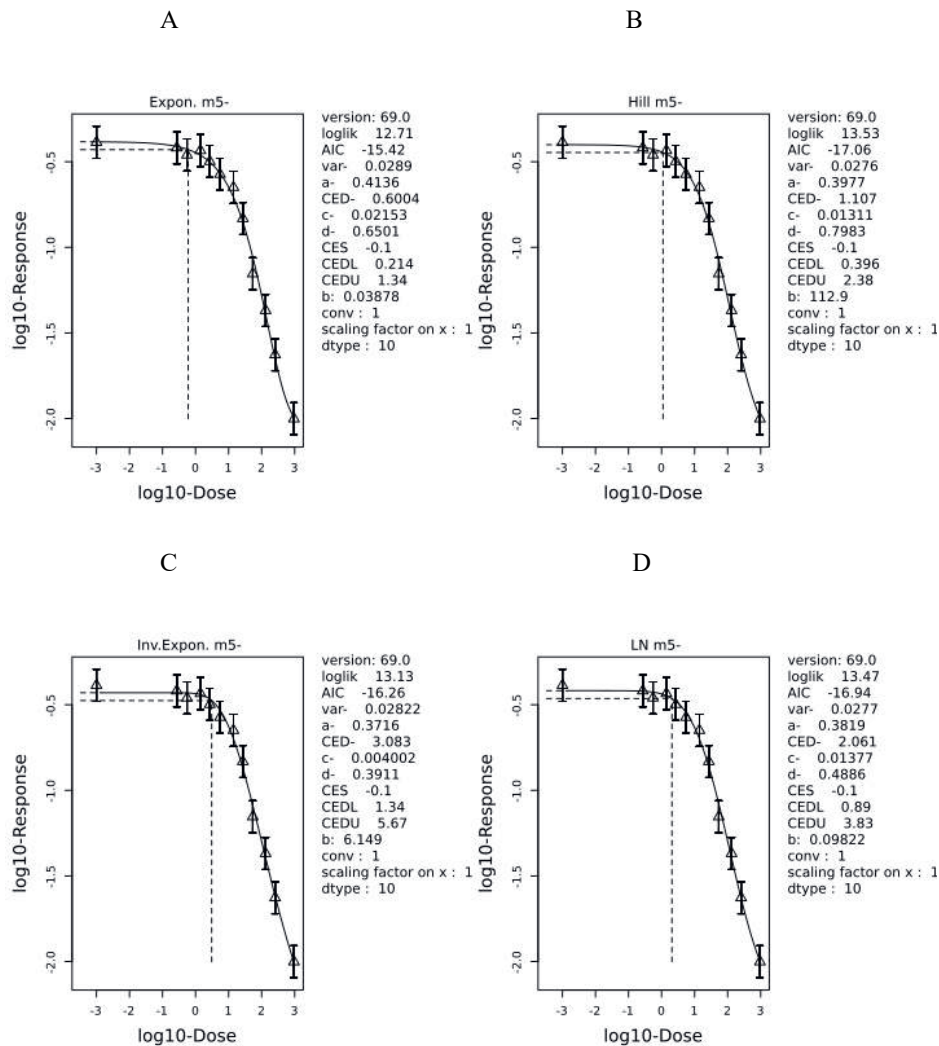
model	converged	loglik	npar	AIC
full model	Yes	17.79	13	-9.58
null model	Yes	-57.88	2	119.76
Expon. m3-	Yes	-1.13	4	10.26
Expon. m5-	Yes	12.71	5	-15.42
Hill m3-	Yes	-0.61	4	9.22
Hill m5-	Yes	13.53	5	-17.06
Inv.Expon. m3-	Yes	4.78	4	-1.56
Inv.Expon. m5-	Yes	13.13	5	-16.26
LN m3-	Yes	2.16	4	3.68
LN m5-	Yes	13.47	5	-16.94
Weights for Model Averaging				
EXP	HILL	INVEXP	LOGN	EXP
0.14	0.33	0.22	0.31	0.14
Final BMD Values				
endpoint	subgroup	BMDL	BMDU	
Response	All	0.01	0.81	

Supplementary Figure 2



Bootstrap curves based on model averaging for predicted human AChE inhibition.

Supplementary Figure 3



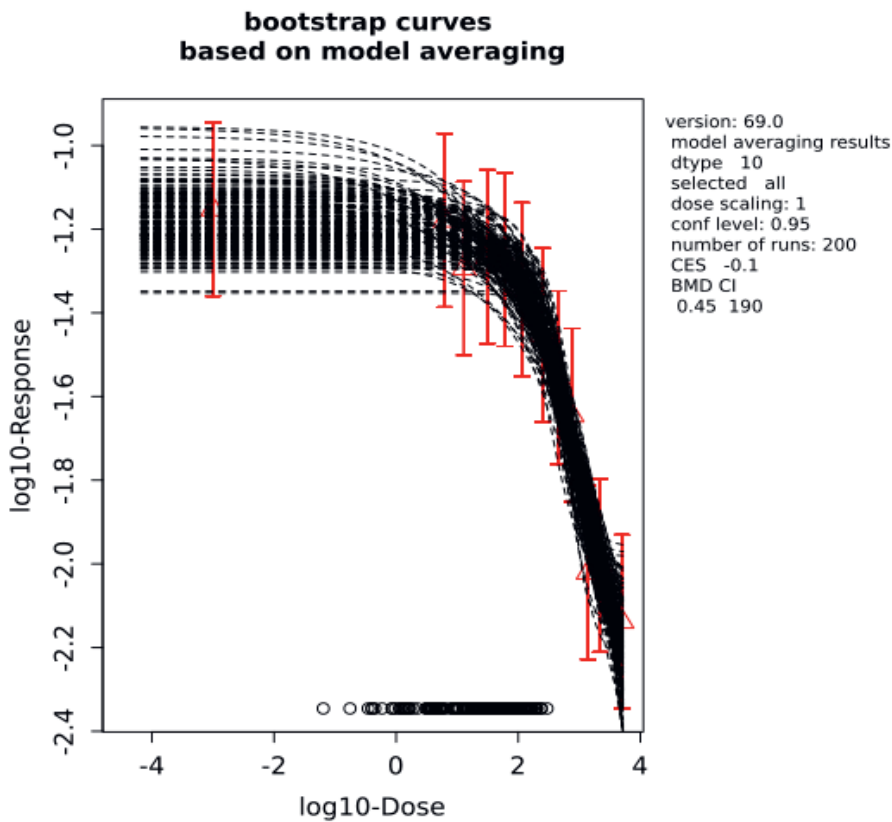
BMD modelling results for individual models for predicted human AChE inhibition. A: Exponential model 5, B: Hill model 5, C:Inv. Exponential model 5, D: Log-Normal Family model 5.

**Supplementary Table 3.** Results of BMD modelling of predicted rat dose-response data, applying model averaging.

## Fitted Models

model	converged	loglik	npar	AIC
full model	yes	-10.87	13	47.74
null model	yes	-44.71	2	93.42
Expon. m3-	yes	-15.31	4	38.62
Expon. m5-	yes	-12.87	5	35.74
Hill m3-	yes	-15.25	4	38.50
Hill m5-	yes	-13.15	5	36.30
Inv.Expon. m3-	yes	-14.61	4	37.22
Inv.Expon. m5-	yes	-13.70	5	37.40
LN m3-	yes	-14.87	4	37.74
LN m5-	yes	-13.38	5	36.76
Weights for Model Averaging				
EXP	HILL	INVEXP	LOGN	EXP
0.35	0.27	0.17	0.21	0.35
Final BMD Values				
endpoint	subgroup	BMDL	BMDU	
Response	all	0.45	190	

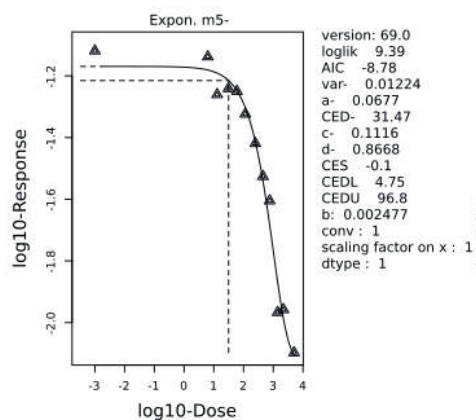
Supplementary Figure 4



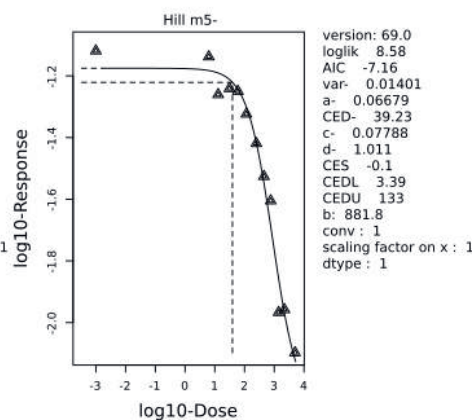
Bootstrap curves based on model averaging for predicted rat AChE inhibition.

## Supplementary Figure 5

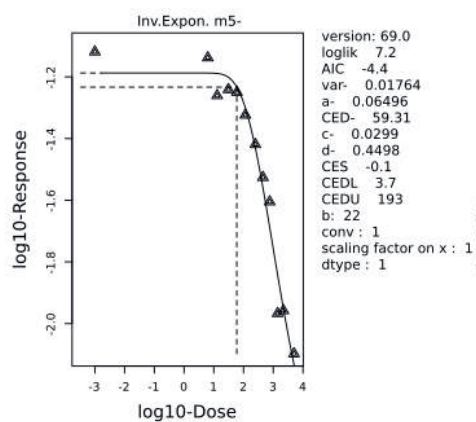
A



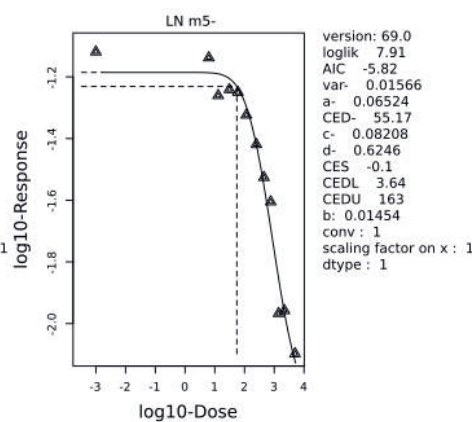
B



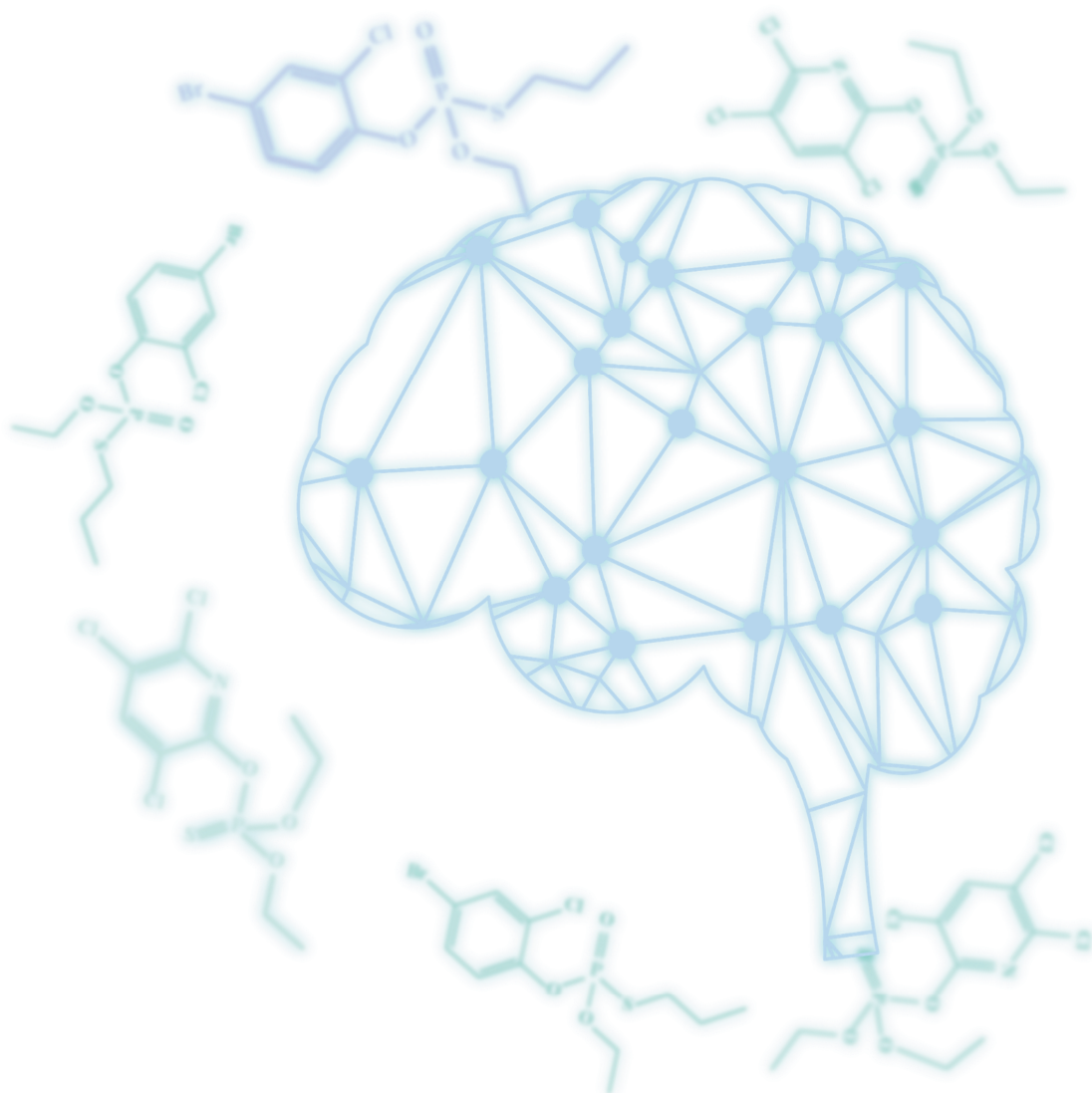
C



D



BMD modelling results for individual models for predicted rat AChE inhibition. A: Exponential model 5, B: Hill model 5, C: Inv. Exponential model 5, D: Log-Normal Family model 5.





# CHAPTER 4.

Prediction of in vivo acetylcholinesterase inhibition  
upon acute combined exposure to profenofos and  
chlorpyrifos by using a combined in vitro and in silico  
approach

Isaac Omwenga  
Shensheng Zhao  
Hans Mol  
Ivonne M.C.M. Rietjens  
Jochem Louisse

*In Preparation*

**Abstract**

Residues of organophosphates (OPs) such as profenofos (PFF) and chlorpyrifos (CPF) have been detected together in various fruits and vegetables. Consequently, consumers can be concurrently exposed to these OPs and knowledge on adverse effects upon combined exposure is desirable. The present study aims to provide insight into the combination effects of two selected OPs (PFF and CPF), by studying the combined effects of PFF and CPF's toxic metabolite CPF oxon (CPO) on acetylcholinesterase (AChE) inhibition *in vitro*, as well as the effects of CPF and CPO on PFF biotransformation (detoxification) by human liver microsomes, cytosol, and human plasma. AChE inhibition was shown to be 199-fold more potent by CPO than by PFF, and combined exposure to CPO and PFF resulted in effects that are in line with the principles of dose addition. CPF and CPO appeared to affect PFF detoxification to its main metabolite (BCP) in a non-competitive manner at high concentrations, with  $K_i$  values of 120, 256 and 473  $\mu\text{M}$  for CPF, and 80, 63 and 326  $\mu\text{M}$  for CPO, for liver microsomes, liver cytosol and plasma, respectively, concentrations far higher than considered relevant *in vivo*. Using the parameters thus defined, our recently published physiologically based kinetic (PBK) model of PFF was extended to include the description of CPF kinetics, using also *in vitro* kinetic data from the literature and *in silico* calculations. PFF concentrations in the model were expressed as CPO-equivalents allowing prediction of total internal CPO-equivalents upon combined exposure to PFF and CPF. By comparing PBK model-predicted internal CPO-equivalents to *in vitro* data on CPO-induced AChE inhibition, combined exposure to PFF and CPF at their ARfD (0.005 mg/kg bw) was predicted to not affect AChE activity. Altogether, this study reveals that AChE inhibition upon combined exposure to these OPs follows the concept of dose addition, and that at estimated exposure levels, no toxicokinetic interactions of CPF on PFF detoxification are expected.

## 4.1 Introduction

Organophosphate pesticides (OPs) are among the most widely used pesticides in agriculture. OP usage has been on the rise in the field of agriculture from the 1960's to such an extent that at present the majority of all the pesticides used in the world belong to this category (Thunga et al., 2010; Kaushal et al., 2021). In developing countries, where the economy depends on the agricultural produce, OPs have become an indispensable part of the agricultural process where they are necessary for pest control (Omwenga et al., 2016; Omwenga et al., 2021a; Kaushal et al., 2021). In contrast, the use of OPs is on the decline in western countries such as the USA and the EU member countries (U.S. EPA, 2002, 2004; Sudakin and Power, 2007). Human exposure to these pesticides has been reported through inhalation, dermal absorption or ingestion via residues on food (Bradman et al., 2003; Suratman et al., 2015; EFSA, 2019a). Since a variety of pesticides is being used, environmental, occupational and dietary exposures are primarily to pesticide mixtures. Consequently, there is lifelong combined exposure to various pesticides from, for example, one food item containing multiple compounds or combinations of food items, each containing different residues (Boobis et al., 2008). If these pesticides have a similar mechanism of action and toxic end point, assessing the dietary risk of exposure for each pesticide separately may lead to underestimation of the health risk (Boon et al., 2008). Therefore, current approaches in pesticide risk assessment include cumulative and probabilistic approaches in order to include the amount and variety of pesticide residues likely to be present in the vegetable sample (Jensen et al., 2015; Boon et al., 2015; Elgueta et al., 2019; Omwenga et al., 2021a). The first step in assessing effects on combined exposure to pesticide mixtures is to identify substances with a similar mechanism of toxicity (Gallagher et al., 2015; EFSA, 2019b). For example, acetylcholinesterase (AChE) inhibitors, such as OPs and carbamates have been assigned to the same cumulative assessment group (CAG) by the United States Environmental Protection Agency (US EPA) as well as by the European Food Safety

Authority (EFSA) (USEPA, 2007, 2011; EFSA, 2019b). AChE inhibition occurs through phosphorylation of the serine residue at the active site of the AChE enzyme, leading to diminished ability to hydrolyse the neurotransmitter, acetylcholine. For chemicals in the same CAG, the current scientific and regulatory recommendations for the risk assessment of mixtures follows a test strategy based on a component-based assessment, a concept with dose addition as the default model (Kortenkamp et al., 2009; EFSA, 2014a; Bopp et al., 2015; EFSA, 2019c).

We recently reported profenofos (PFF) and chlorpyrifos (CPF) (Figure 1) as the most frequently detected pesticide residues in commonly consumed vegetables in Kenya (Omwenga et al., 2021a). In the same study, co-occurrence of PFF and CPF was reported in some of these vegetables including tomatoes (Omwenga et al., 2021a). PFF and CPF are both OP pesticides assigned to the CAG related to brain and/or erythrocyte AChE inhibition (EFSA, 2019b). Therefore, risks of combined exposure to these (and other) OPs is suggested to be based on a component-based assessment with dose addition as the default model. Although dose addition is plausible, it would be of help to have experimental data supporting the concept of dose addition for these chemicals. Approaches that combine *in vitro* studies and *in silico* modelling are promising tools to obtain such insights. One must consider combination effects at both the toxicodynamic and toxicokinetic level. At the dynamic level, combined effects may show concentration addition, but possibly also less than addition or more than additive effects. At the kinetic level, chemicals may affect (increase in case of enzyme induction, or inhibit) each other's biotransformation. In case of enzyme induction they may increase (in case of bioactivation) or decrease (in case of detoxification) each other's toxicity. In contrast, in case of enzyme inhibition they may increase (in case of detoxification) or decrease (in case of bioactivation) each other's toxicity. With *in vitro* studies, combined effects related to the toxicodynamics (AChE inhibition) and possible toxicokinetics can be studied in isolation and

integrated in physiologically based kinetic/dynamic (PBK/D) models to predict responses upon combined exposure scenarios.

In the present study, we assessed the combination effects of PFF and CPO, the toxic metabolite of CPF, on human recombinant AChE activity *in vitro*. To that end, PFF and CPO were tested alone and in an equipotent mixture. The data were assessed using PROAST software, using an approach as developed in the Euromix project to assess whether combination effects follow the concept of dose addition (Fischer et al., 2020). Regarding toxicokinetic interactions, we assessed whether CPF and/or CPO affect the detoxification of PFF. Possible inhibition of PFF detoxification may result in increased internal exposure of PFF upon combined exposure, possibly causing a potentiation of PFF toxicity by CPF. We used our recently developed human PBK model for PFF, which was developed to predict dose-dependent AChE inhibition in humans upon acute (single) oral exposure (Omwenga et al., 2021b) and extended it to also include a description of the kinetics of CPF and CPO, as well as possible kinetic interactions of CPF and/or CPO with the kinetics of PFF, allowing prediction of AChE inhibition by both PFF and CPO upon combined oral exposure to these pesticides.

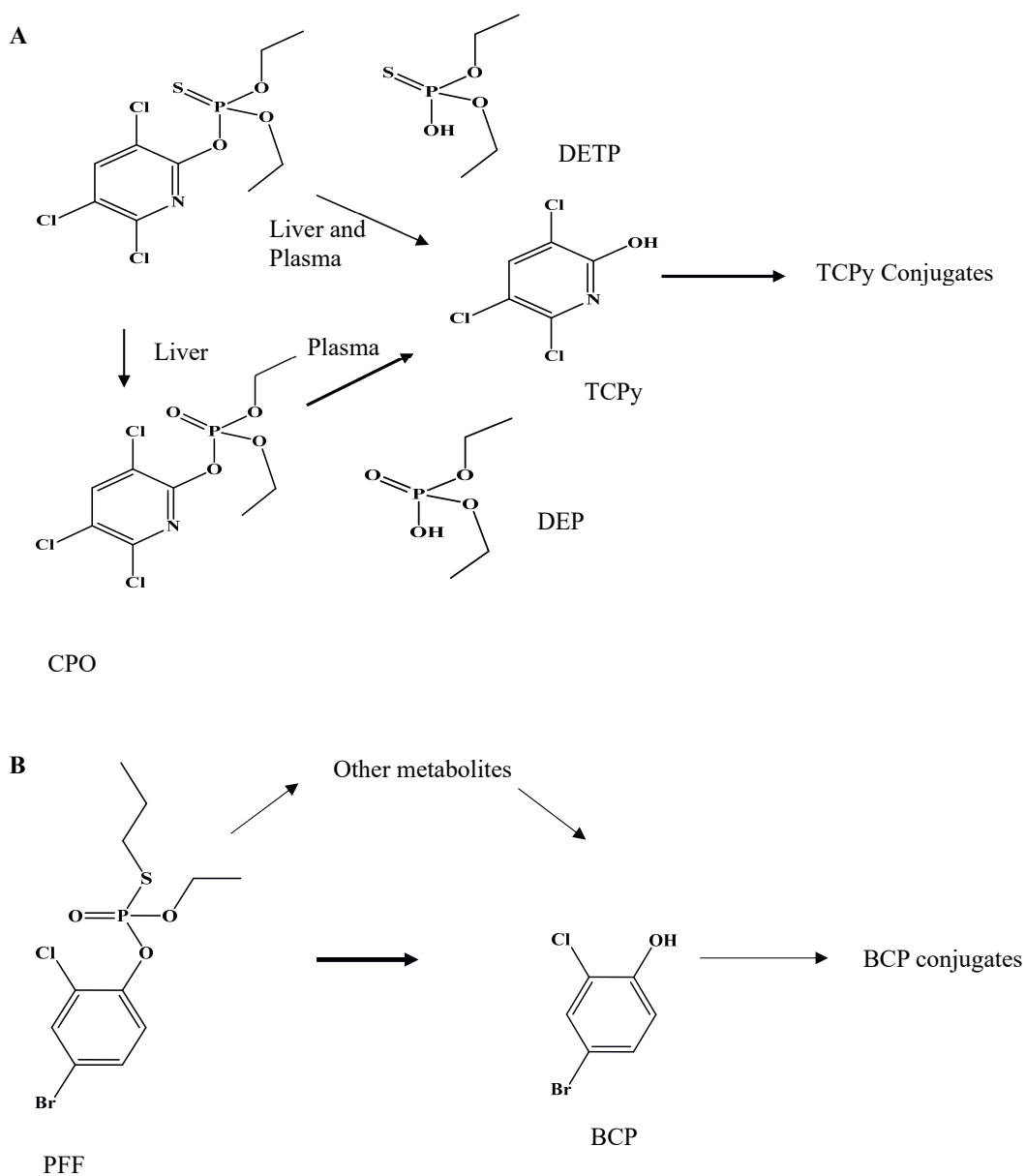


Figure 1. A) Metabolic pathways for CPF and its metabolites CPO, DETP, DEP and TCPy based on data reported in previous studies (Timchalk et al., 2008). B) Metabolic pathway for profenofos (PFF) as described in the PBK model (conversion of PFF to BCP).

## 4.2. Materials and methods

### 4.2.1 Materials and chemicals

Profenofos (PFF), 4-bromo-2-chlorophenol (BCP), chlorpyrifos (CPF), recombinant human acetylcholinesterase (AChE) enzyme, bovine serum albumin (BSA), and reduced nicotinamide adenine dinucleotide phosphate (NADPH) were purchased from Sigma-Aldrich (Zwijndrecht, The Netherlands). Chlorpyrifos-oxon (CPO) was purchased from TRC-Canada (Toronto, Ontario, Canada). Magnesium chloride hexahydrate ( $\text{MgCl}_2 \cdot 6\text{H}_2\text{O}$ ), dimethylsulfoxide (DMSO), trifluoroacetic acid (TFA) and calcium chloride dihydrate ( $\text{CaCl}_2 \cdot 2\text{H}_2\text{O}$ ) were purchased from VWR International (Amsterdam, The Netherlands). Acetonitrile (ACN, UPLC/MS grade) was purchased from Biosolve (Valkenswaard, The Netherlands). Human liver microsomes (pooled from 150 human donors, mixed gender Lot No.38271) were purchased from Corning (Amsterdam, The Netherlands). Pooled human plasma was from Innovative research inc (Novi, USA). For the human plasma further information on number of individuals used to create the samples or on gender was not provided by the company. Pooled mixed-gender human liver cytosol (pool of 10) was purchased from Xenotech (Kansas City, USA).

### 4.2.2 Human recombinant AChE inhibition by PFF, CPO and PFF/CPO mixtures

AChE inhibition by single compounds and mixtures was determined following the protocol of Ellman et al. (1961) as modified by Chambers and Chambers (1989). A range of concentrated stock solutions of PFF, CPO and an equipotent mixture prepared in this study based on their estimated relative potencies, were prepared in ethanol and 50 times diluted by adding 5  $\mu\text{l}$  of stock solution to 245  $\mu\text{l}$  of 0.1 M sodium phosphate (pH 7.4) containing 0.1 mg/ml BSA, which was present to stabilize the human recombinant AChE. For the negative control, 5  $\mu\text{l}$  of ethanol without the test compounds was added to 245  $\mu\text{l}$  of 0.1 M sodium phosphate (pH 7.4)

(containing 0.1 mg/ml BSA). Subsequently, 5  $\mu$ l of these working solutions were added into wells of a 96 well plate already containing 44  $\mu$ l sodium phosphate (pH 7.4) (containing 0.1 mg/ml BSA). To start the reaction, 1  $\mu$ l enzyme solution containing 1 U/ml AChE and 1 mg/ml BSA (present to stabilize human recombinant AChE (Rosenfeld and Saltatos, 2006)) were added, giving a total volume of 50  $\mu$ l per reaction with an AChE concentration of 0.02 U/ml and an ethanol concentration of 0.2%, a level that has no effect on the activity of the enzyme. After 15 minutes incubation at 37°C, 150  $\mu$ l of a mixture of 5,5-dithiobis (2-nitrobenzoic acid) (DTNB) and acetylthiocholine (ATC) were added (final DTNB and ATC concentrations were 0.075 and 0.15 mM, respectively). Subsequently, the time-dependent increase in absorbance due to formation of chromophore (DTNB + thiocholine) was measured at 37°C using a wavelength of 412 nm during a period of 10 minutes, using a spectrophotometer (SpectraMax, Molecular Devices, UK). AChE activity was expressed as percentage enzyme activity compared to the solvent control.

#### **4.2.2.1 Analysis of mixture effects and relative potencies**

To obtain insight into relative potencies between PFF and CPO, AChE inhibition studies for PFF and CPO were first conducted separately. The BMD approach was then applied to determine the BMC50 for AChE inhibition and these values were used to estimate potency differences of CPO and PFF. BMD analysis was performed using PROAST (version 70.1, <https://proastweb.rivm.nl>, RIVM, Bilthoven, The Netherlands) as described by previous studies and in the PROAST manual instructions (Slob, 2002; Kienhuis et al., 2015; EFSA., 2017; Lichtenstein et al., 2020). Data expressed as percentage of the solvent control were loaded to PROAST as continuous, summary data in tab-delimited text files containing mean AChE activity (as percentage of control), standard deviation and sample size. Concentration-response data are analyzed by fitting the following 4-parameter exponential and hill models;



Exponential model:  $y = a [c - (c - 1) \exp(-bx^d)]$

Hill model:  $y = a[1 + (c-1)x^d / bd-x^d]$

Previously, these models have been reported to adequately describe a wide range of toxicological dose-response data (Slob and Setzer, 2014).

Based on the obtained information on relative potencies of PFF and CPO, equipotent mixtures were prepared for the mixture studies. To obtain a relative potency factor (RPF) and to assess whether combination effects follow the concept of concentration addition, the approach as described by Lichtenstein et al. (2020) was used. To that end AChE inhibition were performed for PFF, CPO and the equipotent mixture of PFF and CPO. As described by Lichtenstein et al. (2020), first data are analysed of the single compounds and initial RPF values were derived. RPFs were calculated for a benchmark response of 50% (BMC50, as well as with confidence limits BMCL-BMCU), including the corresponding two-sided 90% RPF confidence interval given by the RPFL (lower bound of the RPF confidence interval) and the RPFU (upper bound of the RPF confidence interval). Then BMD analysis was performed including in the analysis besides the data of the individual OPs also the data for the equipotent mixture. In that analysis, RPF values are calculated by PROAST taking into account the data of the single chemicals as well as the mixture data in such a way that all three datasets are best described by the fitted concentration-response curve. As explained in the study of Lichtenstein et al. (2020), the RPFs from both analyses (with and without inclusion of mixture data) were compared by calculating a ratio of overlap of the confidence intervals of the RPF values obtained by both analyses. Thereby, the highest RPFL is divided by the other RPFU and the obtained ratio(s) of overlap can be used to conclude whether dose addition applies. Ratios above 1 indicate a high degree of deviation of dose addition (i.e. dose addition does not apply) as the RPF derived when including data of the mixture experiment significantly differs from the RPF in the single compound analysis. Ratios below 1 indicate that dose addition can be assumed. Thus, the ratio

of overlap in principle describes numerically what one can already see graphically in the PROAST plots: in case of dose addition, dose-response curves of single compounds and their related mixture, all expressed in reference compound equivalents, appear close together and can be adequately described by one concentration-response curve. We considered the RPF value obtained from the analysis including the mixture data the most relevant, since it is based on both the data on the single chemicals as well as the mixture data.

#### **4.2.3 In vitro incubations to assess kinetic interactions of CPF and CPO on PFF detoxification**

Human liver microsomal, cytosolic and plasma incubations were conducted as described before by Omwenga et al. (2021b). Briefly, the incubations of PFF with human liver microsomes, liver cytosol and plasma were conducted to quantify in vitro rates of detoxication of PFF to BCP. The final incubations were carried out in 100 mM Tris HCl (pH 7.4, 37°C) containing (final concentrations) 5 mM MgCl<sub>2</sub>, 2 mM CaCl<sub>2</sub> (to stimulate PON1 activity (Carr et al., 2015)), 2 mM NADPH (cofactor to also include CYP-mediated metabolism), enzyme preparation (final concentration 2 mg/ml for liver microsomes and cytosol and 4.4 mg/ml for plasma) at final concentrations ranging from 5 to 100 µM, added from 200 times concentrated stock solutions in DMSO. Control incubations were performed in the absence of microsomes, cytosol or plasma. After 2 min pre-incubation, the reaction was initiated by adding the substrate and mixtures were incubated for 2 min in a 37 °C water bath. The total volume of the incubation mixtures was 200 µl. The reaction was terminated by the addition of 50 µl ice cold ACN and samples were kept on ice. The mixture was centrifuged at 14,000 g for 20 min at 4°C and the supernatant was analyzed using UPLC-UV.

For the interaction studies, incubations were performed with PFF in the presence of CPF or CPO. First, a concentration range-finding study was performed to choose an inhibitor concentration inhibiting PFF conversion by around 50% using a PFF substrate concentration of

100  $\mu\text{M}$  (providing a velocity of PFF conversion close to  $V_{\text{max}}$ ). From these studies (data not shown) a concentration of 100  $\mu\text{M}$  was chosen for both CPF and CPO for all incubations (microsomes, cytosol, plasma) and used in inhibition studies in which PFF conversion to BCP was determined at different PFF concentrations (5, 10, 25, 50, 100  $\mu\text{M}$ , added from 200 times concentrated stock solutions in DMSO).

#### 4.2.3.1 UPLC-UV analysis

Following incubation, the samples were analyzed using a Waters Acquity UPLC H class system with a sample manager, a quaternary solvent manager and a photodiode array (PDA) detector, equipped with a Water Acquity UPLC® BEH C18 column (1.7  $\mu\text{m}$ , 2.1  $\times$  50 mm) and Waters Xbridge UPLC® BEH C18 pre-column (2.5  $\mu\text{m}$ , 2.1  $\times$  5 mm). The column temperature was kept at 40°C and the auto sampler at 10°C during the UPLC analysis. The mobile phases used for the analysis consisted of 0.1% TFA in nanopure water (A) and 100% ACN (B). A gradient elution at a flow rate of 0.6 ml/min was applied for the analysis with the starting condition of 100% A: 0% B (v/v), changing linearly to 0% A: 100% B from 0 to 6 min, which was maintained for 30 s, and then changed back to the initial starting conditions in 30 s, which were maintained for 1 min. The injection volume for each sample was 3.5  $\mu\text{l}$ .

Under these conditions, the retention times of PFF and BCP were 4.76 and 3.37 min, respectively. The amount of BCP was quantified by integrating the peak areas at 237 nm using calibration curves that were prepared using the commercially available standards.

#### 4.2.3.2 Kinetic data analysis

Kinetic parameters, including the apparent maximum velocity ( $V_{\text{max}}$ ) and the apparent Michaelis–Menten constant ( $K_{\text{m}}$ ) for BCP formation were obtained by fitting the data for the substrate concentration-dependent rate of conversion (expressed in nmol/min/mg protein) using

GraphPad Prism 5, version 5.04 (San Diego, California, USA) to the standard Michaelis–Menten equation:

$$V=V_{\max}*[S]/(K_m+[S])$$

in which the S represents the concentration of substrate, expressed in  $\mu\text{M}$ , V and  $V_{\max}$  the velocity and the maximum velocity of the reaction, respectively, expressed in  $\text{nmol/min/mg}$  protein, and  $K_m$  the apparent Michaelis–Menten constant, expressed in  $\mu\text{M}$ . The kinetic parameter values for conversion of PFF to BCP in the incubations with liver microsomes, liver cytosol or plasma were determined in the present study and are summarised in Table 1 and discussed in some more detail in the Results section. To determine the catalytic efficiency,  $V_{\max}$  was divided by the  $K_m$ .

$K_m$  and  $V_{\max}$  values obtained with the PFF biotransformation data in the presence of  $100\ \mu\text{M}$  CPF or  $100\ \mu\text{M}$  CPO were compared to  $K_m$  and  $V_{\max}$  values obtained with the PFF biotransformation data in the absence of CPF or CPO, in order to get insight into the type of inhibition. In case of a decrease in the apparent  $V_{\max}$  but no change in the  $K_m$  value as compared to the values of the uninhibited reaction (without CPF and CPO), a non-competitive type of inhibition is assumed (Delaune and Alsayouri, 2020). In this type of inhibition, the inhibitor binds at the allosteric site which is independent of substrate binding, modulating the enzyme activity in the process. The inhibitor shares the same affinity for both enzyme and enzyme-substrate complex in this type of inhibition (Delaune and Alsayouri, 2020). There is a relative decrease in the apparent  $V_{\max}$  but not  $K_m$  and thus the  $K_i$  value can be calculated by fitting the kinetic parameters to the related equation, e.g. using GraphPad Prism (GraphPad Prism 5, version 5.04 (San Diego, California, USA)):

$$(V'_{\max}/inh=V_{\max}/(1+([I]/K_i)))$$

in which the  $V'_{\max}/h$  represents the maximum velocity of the inhibited reaction,  $[I]$  represents the concentration of the inhibitor (CPF or CPO), expressed in  $\mu\text{M}$ , and  $V_{\max}$  the maximum velocity of the uninhibited reaction (in the absence of CPF or CPO).

#### 4.2.4 Human PBK model describing kinetics of PFF, CPF and CPO (and other CPF metabolites)

Our human PFF PBK model previously developed (Omwenga et al., 2021b) was extended to include a description of the kinetics of CPF and CPF metabolites (CPO, TCPy, DEP, DETP and TCPy-conjugates) (Figure 1). The model includes separate compartments for the gastrointestinal tract (GI-tract), the liver, fat, skin, muscle, bone, brain, lung, heart, kidney, spleen, venous blood, arterial blood, and a rest-of-body compartment. Intestinal uptake rate constants for PFF and CPF were estimated based on the approach described in Punt et al. (2020) based on the topological surface areas, which were obtained from Pubchem. Fraction binding to plasma, tissue: plasma partition coefficients and binding to tissue fractions were estimated based on the LogP and pKa of the chemicals and metabolites (which were estimated with Chemicalize) using the method of Lobell and Sivarajah (2003), and Berezhkovskiy (2004), respectively. Data on PFF conversion obtained in the present study were included in the model and scaled as described in Omwenga et al. (2021b). Data on the metabolism of CPF were obtained from the literature (CPF to CPO and CPF to TCPy in liver from Zhao et al. (2019), and CPF to TCPy and CPO to TCPy in blood from Furlong et al. (1989) and Ned Smith et al. (2011)). TCPy conjugation was also described in the model, and the kinetic parameters for this conjugation were fitted in order to best describe plasma concentrations and total urine levels of TCPy as reported from human studies in the literature. Model predictions for CPF were evaluated against human in vivo data as reported in the literature (Drevenkar et al., 1993; Brzak, 2000; Timchalk et al., 2002).

PFF and CPF share a similar mechanism of toxicity, hence belong to the same CAG related to brain and/or erythrocyte AChE inhibition (EFSA, 2019b). Therefore, to determine the combined effect of PFF and CPF at the target site, the free effective blood maximum concentration of PFF and the active metabolite of CPF (CPO) was expressed in CPO equivalents using a relative potency factor (RPF) (see Eq. below):

$$\text{Total free CPO equivalents} = [\text{PFF}] \times \text{fuPFF in vivo} \times \text{RPF}_{\text{PFF}} + [\text{CPO}] \times \text{fuCPO in vivo} \times \text{RPF}_{\text{CPO}},$$

in which the ‘Total free CPO equivalents’ represents the free blood concentration of CPO and PFF expressed in CPO equivalents, [PFF] and [CPO] represent the blood concentrations of PFF and CPO, fuPFF in vivo and fuCPO in vivo represent the unbound fraction in blood in vivo, and RPF<sub>PFF</sub> and RPF<sub>CPO</sub> represent the RPF values for PFF and CPO (the RPF for the latter set at 1). The RPF was calculated from the BMD analysis as described in section 2.2.1.

The PBK model code was numerically integrated in Berkeley Madonna 9.1.18 (UC Berkeley, CA, USA), using the Rosenbrock’s algorithm for stiff systems. The PBK models’ differential equations are provided in the Supplementary Materials.

### 4.3. Results

#### 4.3.1 Human AChE inhibition by PFF, CPO and the equipotent mixture

A first study was performed to estimate the potency differences of CPO and PFF based on the BMC50 values for AChE inhibition obtained using BMD analysis (data not shown). Based on these results, an equivalent mixture was prepared, which was applied in the mixture experiment, in which also full concentration-response curves of CPO and PFF as single compounds were included. We assessed the data thus obtained for dose-addition applying the approach described previously by Lichtenstein et al., (2020). Data on concentration-dependent inhibition of human

(recombinant) AChE by PFF, CPO and the binary mixture are presented in Figure 2, expressed in PFF equivalents. The data were analysed using RIVM PROAST software as described in the materials and methods section, analysing first the data of PFF and CPO separately, obtaining a BMC50 of 783  $\mu\text{M}$  for PFF (with confidence limits BMCL-BMCU of 733-836) and an RPF of 155 for CPO (with RPFL-RPFU of 143-175) (Figure 2A). In the second analysis, data were analysed again using the PROAST software, also including the data on the combined exposure. From that analysis, the RPF of CPO was estimated to amount to 199 (with RPFL-RPFU of 163-242) and the BMC50 for PFF was 724  $\mu\text{M}$  (with confidence limits BMCL-BMCU of 615-852). These analyses indicate that the confidence intervals of the estimated RPF in both analyses overlap (highest RPFL (163) divided by the other RPFU (175) amounts to 0.93), from which can be concluded that in vitro AChE inhibition by combined exposure to PFF and CPO follow dose addition principles (Lichtenstein et al., 2020). Figure 2B shows the visual plot of the second BMD analysis, indicating that the mixture data (red asterisks) are scattered around the curve fit with no deviation from the overall concentration-response fit, also corroborating that dose addition can be assumed (Figure 2B) (Slob, 2002; Slob et al., 2014; Kienhuis et al., 2015; Lichtenstein et al., 2020). We used the RPF of 199 for further analyses, as this value is considered most relevant, since obtained from analysing both data on single and combined exposures.

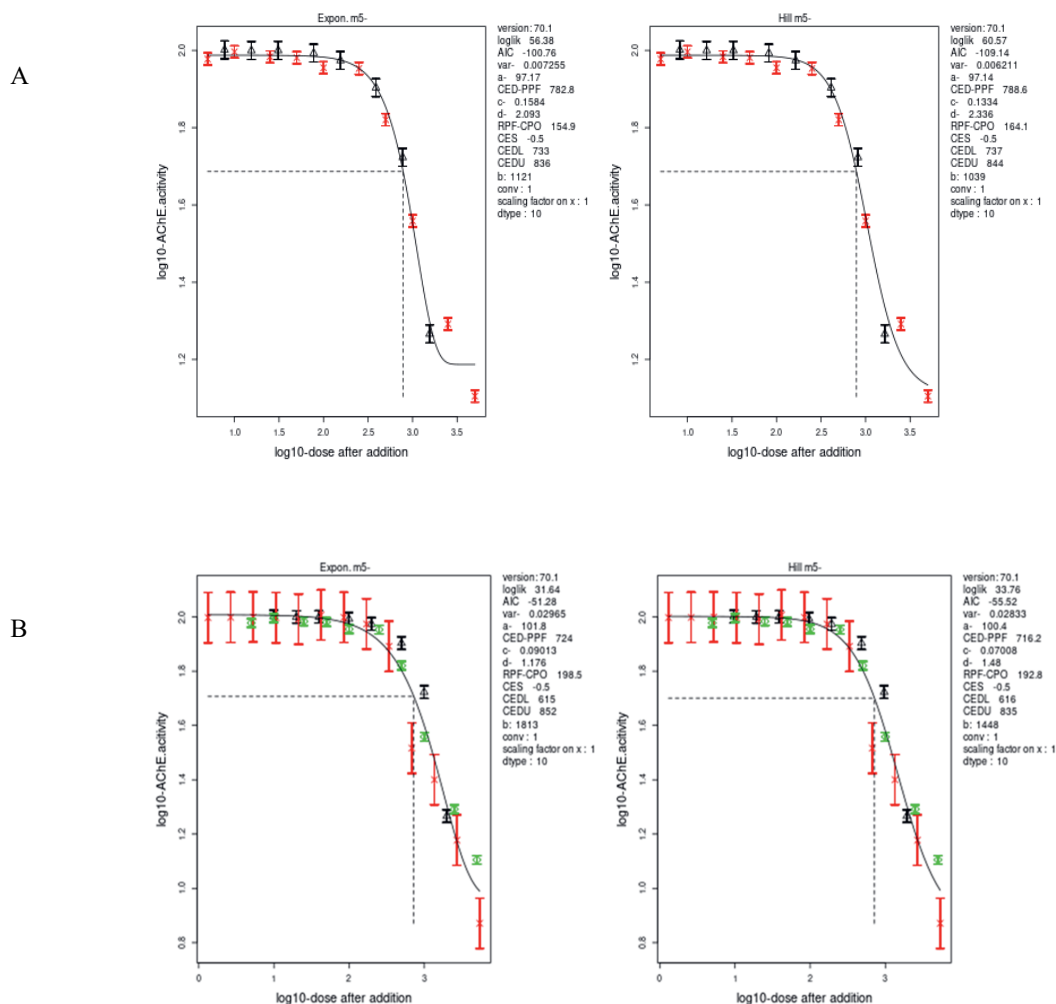


Figure 2. PROAST-based concentration-response modeling of AChE inhibition data of PFF (red asterixes in Fig A; green diamonds in Fig B), CPO (black triangles) and binary mixture (PFF and CPO, red asterixis in Fig B) of the datasets without inclusion of the mixture data (A) and with inclusion of the mixture data (B). Concentrations are all expressed in PFF equivalents (nM). The curves represent the four-parameter exponential and hill models.



#### 4.3.2 In vitro inhibition of PFF metabolism by CPF and CPO

The kinetics of PFF conversion to BCP in the absence and presence of CPF or CPO were investigated for human liver microsomes, cytosol and plasma. Incubations were conducted in the absence and presence of 100  $\mu\text{M}$  CPF or CPO with human liver microsomes, cytosol and plasma. The PFF concentration-dependent BCP formation in presence and absence of CPF or CPO in incubations with liver microsomes, cytosol and plasma is depicted in Figure 3. The related kinetic parameters (apparent  $V_{\text{max}}$  and  $K_{\text{m}}$  values) for the detoxication of PFF to BCP in the presence and absence of CPF and CPO are shown in Table 1. Generally, there was a decrease in the apparent  $K_{\text{m}}$  and  $V_{\text{max}}$  values of the reactions in the presence of CPF or CPO as compared to those of the uninhibited reaction (without CPF or CPO). However, confidence intervals of apparent  $K_{\text{m}}$  and  $V_{\text{max}}$  values overlap for the apparent  $K_{\text{m}}$  values (Table 1). For most conditions, apparent  $V_{\text{max}}$  values were significantly lowered by the inhibitors, especially by CPO, as indicated by the non-overlapping confidence intervals. The inhibition was therefore considered to be a non-competitive type of inhibition (Delaune and Alsayouri, 2020), and  $K_{\text{i}}$  values were estimated by fitting the data to the formula for non-competitive inhibition (GraphPad Prism 5, version 5.04 (San Diego, California, USA)).

Unlike non-competitive inhibition, competitive inhibition is characterised by an increase in  $K_{\text{m}}$  while  $V_{\text{max}}$  remains unchanged. On the other hand, uncompetitive inhibition is characterised by a decrease in  $K_{\text{m}}$  because of increased binding efficiency and decrease in  $V_{\text{max}}$  due to interference with substrate binding, resulting from hampered catalysis in the enzyme substrate complex. As indicated above, results obtained indicate that both CPF and CPO inhibited PFF metabolism to its main metabolite (BCP) in a non-competitive manner, with estimated  $K_{\text{i}}$  values amounting to 119 (90% confidence intervals of 69-169), 251 (90% confidence intervals of 126-375) and 456 (90% confidence intervals of 73-839)  $\mu\text{M}$ , respectively, for CPF, and 80 (90% confidence intervals of 52-107), 62 (90% confidence intervals of 38-84) and 314 (90%

confidence intervals of 111-516)  $\mu\text{M}$ , respectively, for CPO (Table 1). Based on the in vitro results of this study, effects of CPF or CPO on the detoxification of PFF are expected to take place only at high internal CPF and CPO concentrations given these high  $K_i$  values, indicating that occurrence of interaction effects are considered to be unlikely (see for further information next section).

Table 1: Kinetic parameters for formation of BCP by pooled human liver microsomes, cytosol and plasma in the absence or presence of 100  $\mu\text{M}$  CPO or CPF. Data represent estimated  $V_{\text{max}}$ ,  $K_m$  and  $K_i$  values including 95% confidence intervals between brackets.  $K_i$  values were obtained by fitting the data to the equations as present in GraphPad Prism 5 on noncompetitive inhibition.

		$V_{\text{max}}$ (nmol/min/mg protein)	$K_m$ ( $\mu\text{M}$ )	$K_i$ ( $\mu\text{M}$ )
Microsomes	No inhibitor	1.4 (1.1-1.8)	21 (7.2-35)	NA
	With CPF	0.80 (0.50-1.1)	23 (0-46)	119 (69-169)
	With CPO	0.57 (0.44-0.69)	14 (4.1-24)	80 (52-107)
Cytosol	No inhibitor	1.1 (0.87-1.3)	23 (11-35)	NA
	With CPF	0.69 (0.52-0.87)	16 (3.6-29)	251 (126-375)
	With CPO	0.34 (0.20-0.49)	12 (0-29)	62 (38-84)
Plasma	No inhibitor	0.44 (0.34-0.53)	17 (6.0-29)	NA
	With CPF	0.31 (0.25-0.37)	9.5 (2.7-16)	456 (73-839)
	With CPO	0.26 (0.22-0.31)	6.5 (1.8-11)	314 (111-516)

NA: not applicable

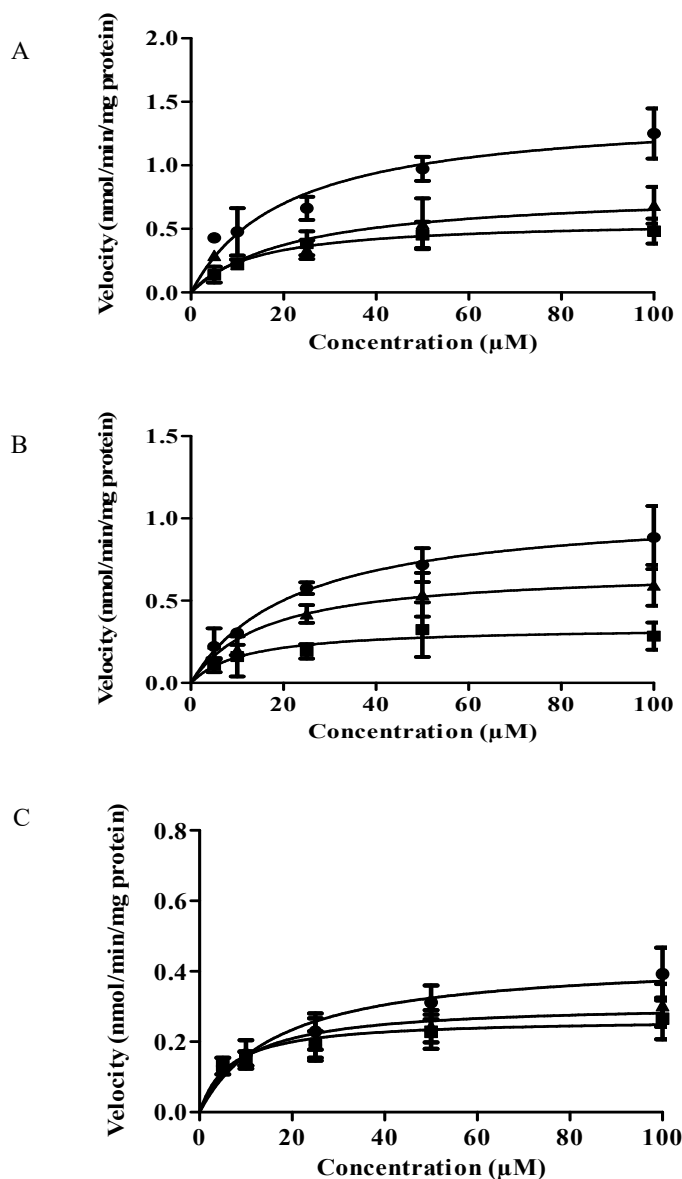
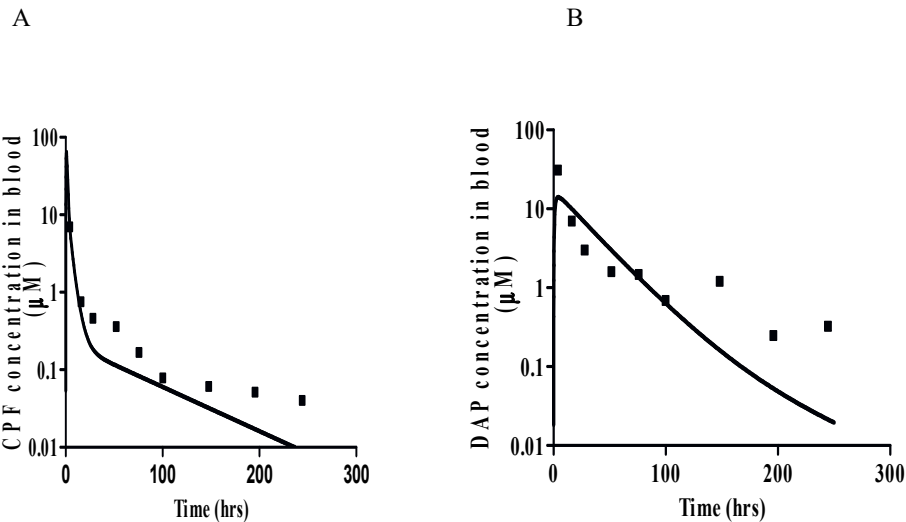


Figure 3. Concentration-dependent rate of PFF conversion to BCP in absence of CPF and CPO (dots) and in the presence of 100 μM CPF (triangles) or 100 μM CPO (squares) in incubations with (A) human liver microsomal proteins, (B) human liver cytosolic proteins, or (C) human plasma proteins. Results represent data from 3 independent experiments and are presented as mean ± SEM.

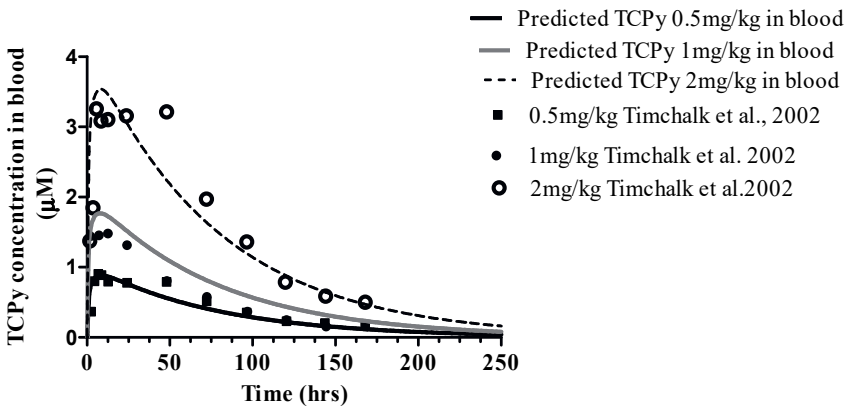
### 4.3.3 PBK model development and evaluation

Our previously published PBK model for PFF (Omwenga et al., 2021b) was extended to include CPF kinetics, based on *in silico* estimations of parameters related to uptake, plasma protein binding, plasma: tissue partitioning and *in vitro* data on kinetic conversions from the literature. The model was developed to describe the dose-dependent internal concentrations of PFF and CPO, and to describe the combined internal concentrations of the two expressed in CPO-equivalents, applying the RPF of 0.005 for PFF (=1/199). The model also describes the kinetics of CPO and other CPF metabolites being DETP, DEP and TCPy, used for model evaluation. In addition, the model describes the blood concentrations of the dialkyl phosphate (DAP) metabolites in a similar manner as reported for *in vivo* studies in the literature, being the sum of DEP and DETP.

The CPF sub model included in the developed PBK model was evaluated against *in vivo* data on CPF and DAP in blood in a hospitalized person with CPF poisoning (Figure 4A and 4B (Drevenkar et al., 1993)) and TCPy concentrations in blood as well as TCPy in urine from human volunteers (Figure 4C and 4D (Timchalk et al., 2002)). These results indicate that the predictions made by the newly developed binary PBK model match the reported *in vivo* data quite well. The obtained  $K_i$  values related to CPF- and CPO-induced inhibition of PFF conversion were in the high  $\mu\text{M}$  range and the PBK model predicts that these concentrations of CPF and CPO cannot be reached *in vivo*, due to rapid conversion of both CPF and CPO (Figure 5).



C



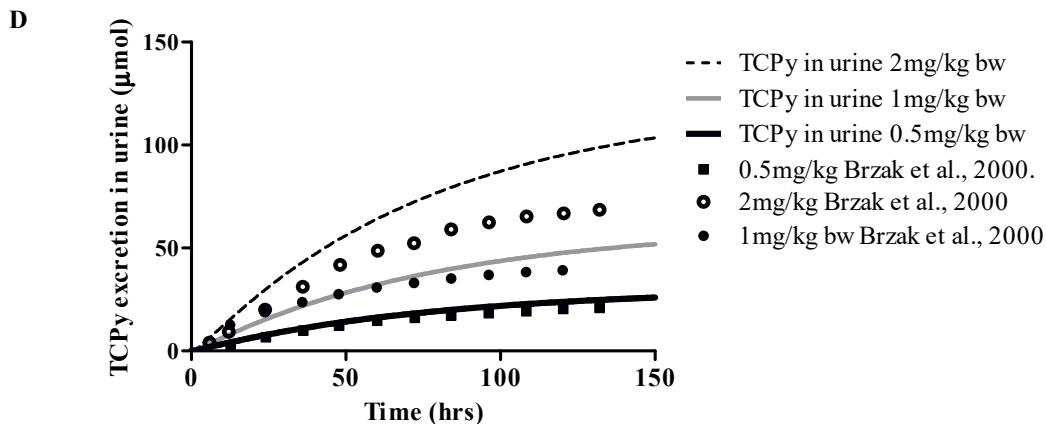


**Figure 4.** A) Comparison of PBK model-based predicted CPF concentrations in blood (continuous line) and reported CPF blood concentrations of a hospitalized person with CPF poisoning (~150 mg/kg) (Drevenkar et al., 1993); B) Comparison of PBK model-based predicted DAP concentrations in blood (continuous line) and reported DAP blood concentrations of a hospitalized person with CPF poisoning (~150 mg/kg) (Drevenkar et al., 1993); C) Comparison of PBK model-based predicted TCPy concentrations in blood (lines) and reported blood concentrations in human volunteers upon exposure to 0.5, 1 or 2 mg/kg bw CPF (Timchalk et al., 2002); and D) Comparison of PBK model-predicted and experimentally determined time-dependent cumulative urinary excretion of TCPy (lines) and reported urinary excretion in human volunteers upon exposure to 0.5, 1 or 2 mg/kg CPF (Brzak, 2000).

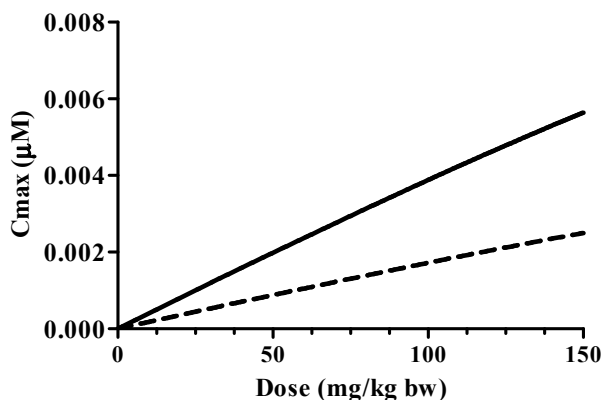


Figure 5. Predicted CPF (solid continuous line) and CPO (dashed line) maximum blood concentrations upon oral exposure to CPF up to a dose of 150 mg/kg bw. Considering the high  $K_i$  values obtained in the *in vitro* kinetic studies (high  $\mu\text{M}$  range), the dose dependent  $C_{\text{max}}$  values predicted reveal that occurrence of interaction effects are considered to be unlikely in the *in vivo* situation.

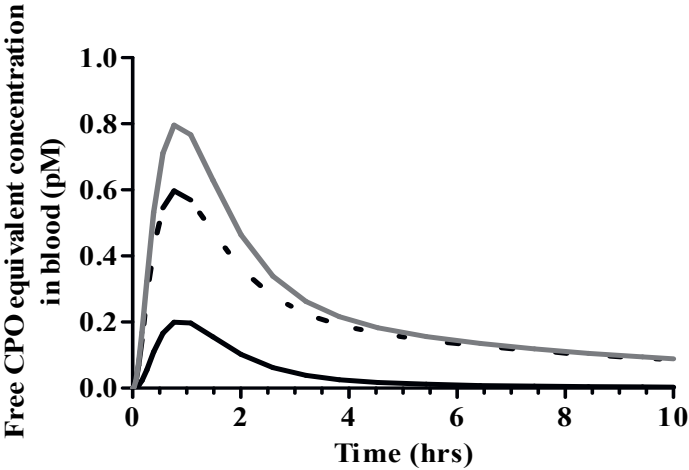
#### 4.3.4 PBK model-based predictions of AChE inhibition upon single and combined acute exposure to PFF and CPF

After PBK model evaluation, the model was used to describe the dose-dependent internal (in blood) maximal free CPO and PFF concentrations, expressed in CPO-equivalents at two combined exposure scenarios (Figure 6A and 6B). Figure 6A shows the dose-dependent maximal blood concentrations in CPO-equivalents upon exposure to 0.005 mg/kg bw CPF (ARfD CPF, (EFSA, 2014b) black continuous curve) or 0.005 mg/kg bw PFF (ARfD PFF reported by a German evaluation as reported by EFSA (2019d), black dotted curve), indicating

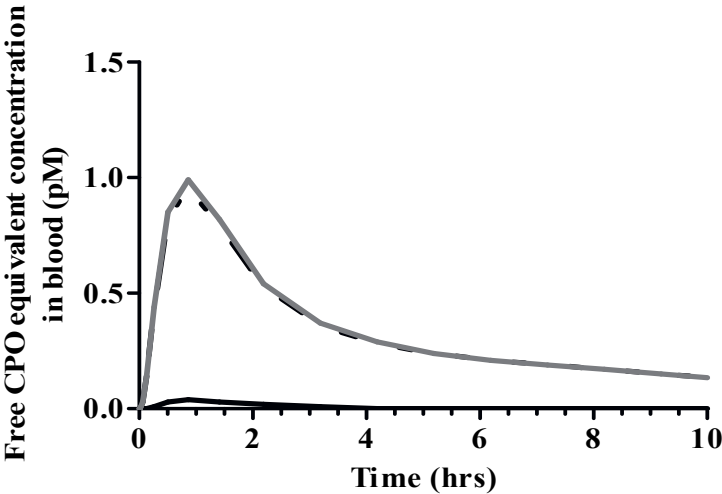
that upon equal oral exposure levels, PFF is expected to be a bit more potent in AChE inhibition than CPF. The prediction of in vivo AChE inhibition was evaluated using the data for the hospitalized patient (Drevenker et al., 1993), from which the in vivo kinetic data were also used for PBK model evaluation (Figure 4 A and B). At the reported dose of 150 mg/kg bw the C<sub>max</sub> of free CPO in blood was predicted to amount to 57 nM. When interpolating this concentration into the concentration-response curve of CPO-induced AChE inhibition (Figure 6C) an inhibition of 60% would be predicted. AChE inhibition for the hospitalized patient was reported to amount to 50%, indicating that quite an accurate prediction was obtained. The model was then used to estimate internal CPO-equivalents at defined exposure scenarios, including combined exposure to the ARfD of PFF and CPF (0.005 mg/kg bw each) (EFSA, 2014b; EFSA, 2019d) as well as the estimated acute exposure upon intake of tomatoes contaminated with PFF and CPF residues as we measured before (Omwenga et al., 2021a), using a maximum daily consumption rate of 560 g/day for tomatoes and a residue concentration of 958 and 107 µg/kg for PFF and CPF respectively, amounting to an estimated intake of 0.0077 and 0.00086 mg/kg bw, respectively, using a bw of 70 kg. Obtained internal free maximal CPO-equivalent concentrations in blood were then compared to the in vitro concentration-response data on AChE inhibition by CPO (Figure 6C) to estimate whether AChE inhibition is expected with these exposure scenarios. The predicted C<sub>max</sub> values expressed in free CPO-equivalents in these exposure scenarios amount to 0.8 pM (combined exposure ARfDs) and 1 pM (consumption of tomatoes with both residues), being 1500 and 1200-fold lower than the BMC<sub>10</sub> of CPO-induced human AChE inhibition of 1270 pM suggesting that at these exposure scenarios no effects on AChE activity are expected.



A



B



C

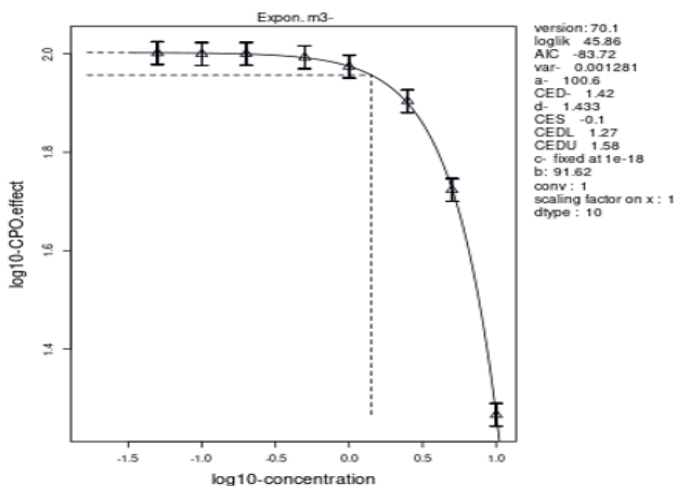


Figure 6. PBK model predicted CPO-equivalents in blood (free concentration) upon A) oral exposure to an equal acute reference dose of PFF and/or CPF (0.005 mg/kg bw) and B) acute exposure to estimated intake of tomatoes contaminated with PFF and CPF residues (Omwenga et al., 2021a), upon a maximum daily consumption rate of 560 g/day of tomatoes, resulting in an estimated intake of 0.008 mg/kg bw and 0.0009 mg/kg bw, respectively. Straight grey line: CPO-equivalents from combined CPF and PFF exposure. Straight black line: CPO-equivalents from CPF exposure; dotted line: CPO-equivalents from PFF exposure; and C) PROAST-based concentration-response modeling of AChE inhibition data of CPO (black triangles), resulting in a BMDL10 of 1.27nM.

#### 4.4. Discussion

The present study was conducted to develop a combined in vitro-in silico approach to predict the effects of combined exposure to CPF and PFF on AChE activity in humans. To that end, our previously published PBK model of PFF was extended to also include the description of CPF kinetics, allowing to describe internal concentrations of PFF and CPO as chemical entities

responsible for AChE inhibition at defined exposure scenarios based on CPO equivalents. In vitro combination studies showed that combined exposure to PFF and CPO follows the concept of concentration addition, with PFF shown to be 199-fold less potent than CPO. PFF concentrations in the PBK model were therefore expressed as CPO-equivalents, allowing the description of total AChE inhibiting entities in CPO-equivalents at combined exposure to both pesticides. In vitro kinetic studies on possible interaction effects showed that inhibition of PFF detoxification (BCP formation) by CPF or CPO takes place only at very high concentrations that are not reached at relevant exposure scenarios and even not at high CPF exposures that have been reported to be encountered in CPF poisoning cases (Figure 5). Therefore, interaction effects of CPF on PFF are considered unlikely at the kinetic (biotransformation) level, and the data from the present study support the assumption of dose addition related to AChE inhibition upon combined exposure to these pesticides.

Although PFF and CPO share a common detoxification pathway and a common mode of toxicological action, they quantitatively differ in their potential for AChE inhibition as shown in the in vitro AChE inhibition studies (Figure 2). Combining the in vitro toxicity data with PBK modelling shows that, in spite of the 199-fold lower AChE inhibitory potency of PFF than CPO, the internal maximal concentrations expressed in CPO-equivalents are estimated to be higher for PFF than for CPF at similar oral dose levels (Figure 6A). This is due to the fact that PFF exposure occurs from a the parent compound while CPO has to be formed from CPF as a metabolite. Furthermore, it should be noted that the toxic potency of OPs is dependent upon a balance between bioactivation versus detoxification of OP dose delivered to the target site (Calabrese, 1991; Poet et al., 2003), hence the significance of PFF during combined exposure given the toxicity in its original form as well as slower clearance. By enabling description of C<sub>max</sub> values in terms of CPO equivalents the PBK model appears able to provide a way to quantitatively integrate data on individual compounds to obtain insight in the consequences of

combined exposures. This indicates the clear added value of the application of PBK modelling for the translation of *in vitro* toxicity data to the *in vivo* situation.

This study shows that *in vitro* toxicodynamic effects on AChE activity upon combined exposure to PFF and CPO follow the concept of dose addition. Furthermore, comparison of the PBK model-based predictions of plasma levels of CPF and CPO to the kinetic parameters for inhibitory interactions at the level of biotransformation enzymes, suggests that at realistic dose levels no toxicokinetic interactions for binary exposure are expected, suggesting that the overall *in vivo* effect on AChE activity upon combined exposure is expected to also follow the concept of dose addition. Dose additivity for OPs has also been reported by Richardson et al. (2001) who observed that *in vitro* combined effects of CPO and azinophosmethyl-oxon on brain AChE activity were best characterized using a dose-additive model. Another study by Timchalk and Poet (2008) evaluated AChE effects upon combined exposure to CPF and diazinon in rats using *in vitro* methods and a binary PBK model. Their results suggested that AChE inhibition by a binary mixture of CPF and diazinon was also best described by a dose additive model. These findings therefore support the current scientific and regulatory recommendation that promote the application of the dose addition model as a default model for risk assessment of OP pesticides within the same CAG.

The model simulations performed in this study were consistent with the published *in vivo* data on CPF and DAP concentrations in blood in a hospitalized person with CPF poisoning (Figure 4A and 4B (Drevenkar et al., 1993)) and TCPy concentrations in blood as well as TCPy excretion in urine from human volunteer studies in the Caucasian population (Figure 4C and 4D (Brzak et al., 2000; Timchalk et al., 2002)). These results indicate that the predictions made by the newly developed binary PBK model match the reported *in vivo* kinetic data well. Furthermore, combining the PBK model-predicted free C<sub>max</sub> of CPO with the *in vitro* concentration-response curve of CPO-induced AChE inhibition, shows that AChE inhibition of

a person exposed to 150 mg/kg bw CPF was estimated to amount to 50% inhibition, being close to the reported AChE inhibition of 60% reported for a hospitalized patient that was exposed to this high dose of CPF. This finding further re-enforces the concept that PBK modeling together with focused in vitro experimentation can be utilized to estimate in vivo oral equivalent doses of related in vitro bioactivity data that can be used in the hazard assessment of chemicals. For chemicals that follow the concept of concentration addition in vitro, the RPF approach as used in the current study for CPO and PFF in the PBK model could be extended in the future to also include other OPs and carbamates, allowing a more extensive assessment of the combined exposure to OPs and carbamates based on novel approach methods (NAMs) as applied in the present study. Such an approach to include data for more than one chemical has recently been used by our group to predict in vivo human and rat RBC (AChE) inhibition upon acute exposure to diazinon and its active metabolite, diazinon oxon (Zhao et al., 2021).

Although the current NAM-based approach combining in vitro toxicity data and PBK modelling is promising in evaluating combined effects of chemicals that follow the principles of dose addition, it cannot be applied as such when combined effects of chemicals do not follow the concept of dose addition, like when other combination effects, such as synergism or antagonism apply. Possible synergistic or antagonist effects can be identified using in vitro studies (Cedergreen 2014). However, extrapolating such findings for specific applied exposure conditions to other (non-tested) combination exposures is more difficult than when combination effects follow the concept of dose addition. Consequently, predicting effects of mixtures would be more complex in case of less than dose addition or more than dose addition. It should, however, be noted that deviations from predicted additivity are considered to be rare (Kortenkamp et al., 2009; Cedergreen, 2014).

In conclusion, this study showed that effects of CPF or CPO on the detoxification of PFF are expected to take place only at unrealistic high concentrations, indicating that interaction effects

are considered to be unlikely, and that the OP-induced AChE inhibition upon combined exposure to PFF and CPF follows the concept of dose addition, supporting the use of a relative potency factor (RPF)-coded PBK model approach for assessing effects on AChE activity upon combined exposure to these OPs.

### **Acknowledgements**

This work is supported by the Netherlands Universities Foundation for International Cooperation (Nuffic) (scholarship granted to Isaac Omwenga (PhD.17/0019)), and the Dutch Ministry of Agriculture, Nature and Food Quality (project KB-23-002-021).

### **Conflict of interest statement**

The authors declare that they have no conflicts of interest.

## References

- Abass, K., Reponen, P., Jalonen, J. & Pelkonen, O. 2007. In vitro metabolism and interaction of profenofos by human, mouse and rat liver preparations. *Pesticide Biochemistry and Physiology*, 87, 238-247.
- Alhusainy, W., Paini, A., Punt, A., Louisse, J., Spenkelink, A., Vervoort, J., Delatour, T., Scholz, G., Schilter, B., Adams, T., Van Bladeren, P. J. & Rietjens, I. M. 2010. Identification of nevadensin as an important herb-based constituent inhibiting estragole bioactivation and physiology-based biokinetic modeling of its possible in vivo effect. *Toxicol Appl Pharmacol*, 245, 179-90.
- Belden, J.B., Gilliom, R.J., Lydy, J., Journal, M.A.I., 2007. How well can we predict the toxicity of pesticide mixtures to aquatic life. 3, 364–372.
- Berezhkovskiy, L.M. 2004. Volume of distribution at steady state for a linear pharmacokinetic system with peripheral elimination. *J Pharm Sci* 93:1628-1640.
- Bradman, A., Barr, D. B., Claus Henn, B. G., Drumheller, T., Curry, C. & Eskenazi, B. 2003. Measurement of pesticides and other toxicants in amniotic fluid as a potential biomarker of prenatal exposure: a validation study. *Environmental health perspectives*, 111, 1779-1782.
- Brzak, K.A. 2000. A Rising Dose Toxicology Study to Determine the No- Observable-Effect-Levels (NOEL) for Erythrocyte Acetylcholinesterase (AChE) Inhibition and Cholinergic Signs and Symptoms of Chlorpyrifos at Three Dose Levels–Part B (Report No. 981176). Midland, Mich.: Toxicology & Environmental Research and Consulting, Dow Chemical Company, 2000.
- Boobis AR, Ossendorp BC, Banasiak U, Hamey PY, Sebestyen I, Moretto A. 2008. Cumulative risk assessment of pesticide residues in food. *Toxicol Lett*. 180:137–150.
- Boon PE, Van der Voet H, Van Raaij MT, Van Klaveren JD. 2008. Cumulative risk assessment of the exposure to organophosphorus and carbamate insecticides in the dutch diet. *Food Chem Toxicol*. 46:3090–3098.
- Boon P.E., van Donkersgoed G., Christodoulou D., Crépet A., D'Addezio L., Desvignes V., Ericsson B.G., Galimberti F., Ioannou-Kakouri E., Jensen B.H., et al. 2015. Cumulative dietary exposure to a selected group of pesticides of the triazole group in different European countries according to the EFSA guidance on probabilistic modelling. *Food Chem Toxicol*. 79:13–31.
- Bopp, S., Berggren, E., Kienzler, A., Van der Linden, S., Worth, A., 2015. Scientific

- methodologies for the assessment of combined effects of chemicals - a survey and literature review. EUR 27471 EN 1–64. <https://doi.org/10.2788/093511>. Scientific methodologies for the assessment of combined effects of chemicals - a survey and literature review. EUR 27471 EN 1–64. <https://doi.org/10.2788/093511>.
- Bouchard, M., Carrier, G., Brunet, R. C., Bonvalot, Y., and Gosselin, N. H. 2005. Determination of biological reference values for chlorpyrifos metabolites in human urine using a toxicokinetic approach. *J. Occup. Environ. Hygiene* 2, 155–168
- Buntyn, R. W., Alugubelly, N., Hybart, R. L., Mohammed, A. N., Nail, C. A., Parker, G. C., Ross, M. K. & Carr, R. L. 2017. Inhibition of Endocannabinoid-Metabolizing Enzymes in Peripheral Tissues Following Developmental Chlorpyrifos Exposure in Rats. *Int J Toxicol*, 36, 395-402.
- Calabrese, E. J. (Ed.) (1991). Comparative metabolism: The principal cause of differential susceptibility to toxic and carcinogenic agents. In *Principles of Animal Extrapolation* (E. J. Calabrese, Ed.), pp. 203–276. Lewis Publishers, Chelsea, MI.
- Carr, R. L., Dail, M. B., Chambers, H. W. & Chambers, J. E. 2015. Species differences in paraoxonase mediated hydrolysis of several organophosphorus insecticide metabolites. *J Toxicol*, 2015, 470189.
- Cedergreen, N., 2014. Quantifying Synergy: a Systematic Review of Mixture Toxicity Studies within Environmental Toxicology, vol. 9 e96580
- Chambers, J. E. & Chambers, H. W. 1989. Oxidative desulfuration of chlorpyrifos, chlorpyrifos-methyl, and leptophos by rat brain and liver. *J Biochem Toxicol*, 4, 201-3.
- Chanda, S. M., Mortensen, S. R., Moser, V. C. & Padilla, S. 1997. Tissue-Specific Effects of Chlorpyrifos on Carboxylesterase and Cholinesterase Activity in Adult Rats: An in Vitro and in Vivo Comparison. *Toxicological Sciences*, 38, 148-157.
- Clement, J. G. 1984. Role of aliesterase in organophosphate poisoning. *Fundam Appl Toxicol*, 4, S96-105.
- Croom, E.L., Wallace, A.D., Hodgson, E. 2010. Human variation in CYP-specific chlorpyrifos metabolism. *Toxicology*. 276(3), 184-91.
- Costa, L. G. 2006. Current issues in organophosphate toxicology. *Clinica Chimica Acta*, 366, 1-13.
- Costa, L. G. 2017. Organophosphorus Compounds at 80: Some Old and New Issues. *Toxicological Sciences*, 162, 24-35.



- Dadson, O. A., Ellison, C. A., Singleton, S. T., Chi, L. H., McGarrigle, B. P., Lein, P. J., Farahat, F. M., Farahat, T. & Olson, J. R. 2013. Metabolism of profenofos to 4-bromo-2-chlorophenol, a specific and sensitive exposure biomarker. *Toxicology*, 306, 35-9.
- Delaune, K.P., Alsayouri, K. 2020. Physiology, Noncompetitive Inhibitor. In: StatPearls [Internet]. Treasure Island (FL): StatPearls Publishing; 2021 Jan-.  
<https://www.ncbi.nlm.nih.gov/books/NBK545242/>
- Drevenkar, V., Vasilčić, Z., Stengl, B., Fröbe, Z., Rumenjak, V. 1993. Chlorpyrifos metabolites in serum and urine of poisoned persons. *Chem Biol Interact.* 87(1-3):315-22.
- EFSA (European Food Safety Authority) Panel on Plant Protection Products and their Residues (PPR), 2014a. Scientific Opinion on the identification of pesticides to be included in cumulative assessment groups on the basis of their toxicological profile (2014 update). *EFSA Journal* 2013;11(7):3293, 131 pp. doi:10.2903/j.efsa.2013.3293
- EFSA (European Food Safety Authority), 2014b. Conclusion on the peer review of the pesticide human health risk assessment of the active substance chlorpyrifos. *EFSA J.* 12, 3640.
- EFSA (European Food Safety Authority), Scientific Committee, Hardy, A., Benford, D., Halldorsson, T., Jeger, M.J., Knutsen, K.H., More, S., Mortensen, A., Naegeli, H., Noteborn, H., Ockleford, C., Ricci, A., Rychen, G., Silano, V., Solecki, R., Turck, D., Aerts, M., Bodin, L., Davis, A., Edler, L., Gundert-Remy, U., Sand, S., Slob, W., Bottex, B., Abrahantes, J.C., Marques, D.C., Kass, G., Schlatter, J.R., 2017. Update: Guidance on the use of the benchmark dose approach in risk assessment. *EFSA Journal* 2017;15(1):4658, 41 pp. doi:10.2903/j.efsa.2017.4658
- EFSA (European Food Safety Authority), 2019a. Scientific report on the 2017 European Union report on pesticide residues in food. *EFSA Journal* 2019;17(6):5743, 152 pp.  
<https://doi.org/10.2903/j.efsa.2019.5743>
- EFSA (European Food Safety Authority), Crivellente, F., Hart, A., Hernandez-Jerez, A.F., Hougaard Bennekou, S., Pedersen, R., Terron, A., Wolterink, G., Mohimont, L.,

- 2019b. Scientific report on the establishment of cumulative assessment groups of pesticides for their effects on the nervous system. EFSA Journal 2019;17(9):5800, 115 pp. <https://doi.org/10.2903/j.efsa.2019.5800>
- EFSA (European Food Safety Authority), 2019c. Scientific Report on scientific support for preparing an EU position in the 51st Session of the Codex Committee on Pesticide Residues (CCPR). EFSA Journal 2019;17(7):5797, 243 pp.
- EFSA Scientific Committee, More, S.J., Bampidis, V., Benford, D., Bennekou, S.H., Bragard, C., Halldorsson, T.I., Hernandez-Jerez, A.F., Koutsoumanis, K., Naegeli, H., Schlatter, J.R., Silano, V., Nielsen, S.S., Schrenk, D., Turck, D., Younes, M., Benfenati, E., Castle, L., Cedergreen, N., Hardy, A., Laskowski, R., Leblanc, J.C., Kortenkamp, A., Ragas, A., Posthuma, L., Svendsen, C., Solecki, R., Testai, E., Dujardin, B., Kass, G.E.N., Manini, P., Jeddi, M.Z., Dorne, J-L.C.M., Hogstrand, C., 2019c. Guidance on harmonised methodologies for human health, animal health and ecological risk assessment of combined exposure to multiple chemicals. EFSA Journal 2019;17(3):5634, 77
- U.S. EPA. 2000. Supplementary Guidance for Conducting Health Risk Assessment of Chemical Mixtures. Office of Research and Development, Washington, DC. EPA/630/R-00/002. Available in PDF format at: [www.epa.gov/NCEA/raf/chem\\_mix.htm](http://www.epa.gov/NCEA/raf/chem_mix.htm)
- U.S. EPA. 2001. Preliminary Cumulative Risk Assessment for the Organophosphorus Pesticides. Office of Pesticide Programs, Washington, DC.
- U.S. EPA. 2002. US EPA: US EPA: Guidance on Cumulative Risk Assessment of Pesticide Chemicals That Have a Common Mechanism of Toxicity. [https://www.epa.gov/sites/production/files/2015-07/documents/guidance\\_on\\_common\\_mechanism.pdf](https://www.epa.gov/sites/production/files/2015-07/documents/guidance_on_common_mechanism.pdf)
- U.S. EPA. 2003. Developing Relative Potency Factors For Pesticide Mixtures: Biostatistical Analyses Of Joint Dose-Response. U.S. Environmental Protection Agency, Washington, DC, EPA/600/R-32/052, 2003.
- U.S. EPA. 2006. Organophosphorus Cumulative Risk Assessment 2006 Update

- <http://www.epa.gov/pesticides/cumulative/rra-op/>.
- El-Masri, H. A., Mumtaz, M. M. & Yushak, M. L. 2004. Application of physiologically-based pharmacokinetic modeling to investigate the toxicological interaction between chlorpyrifos and parathion in the rat. *Environ Toxicol Pharmacol*, 16, 57-71.
- Ellman, G. L., Courtney, K. D., Andres, V. & Featherstone, R. M. 1961. A new and rapid colorimetric determination of acetylcholinesterase activity. *Biochemical Pharmacology*, 7, 88-95.
- Elgueta S, Fuentes M, Valenzuela M, Zhao G, Liu S, Lu H, Correa A. 2019. Pesticide residues in ready-to-eat leafy vegetables from markets of Santiago, Chile and consumer's risk. *Food Addit Contam Part B*. 12:259–267.
- El-Masri, H.A., Reardon, K.F., Yang, R.S. 1997. Integrated approaches for the analysis of toxicologic interactions of chemical mixtures. *Crit Rev Toxicol* 1997;27(2): 175–97.
- Fischer, B.C., Rotter, S., Schubert, J., Marx-Stoelting, P., Solecki, R. 2020. Recommendations for international harmonisation, implementation and further development of suitable scientific approaches regarding the assessment of mixture effects. *Food Chem Toxicol*. 141:111388.
- Furlong, C.E., Richter, R.J., Seidel, S.L., Costa, L.G., Motulsky, A.G. 1989. Spectrophotometric assays for the enzymatic hydrolysis of the active metabolites of chlorpyrifos and parathion by plasma paraoxonase/arylesterase. *Anal Biochem*. 180(2):242-7.
- Halpert, J., Hammond, D. & Neal, R. A. 1980. Inactivation of purified rat liver cytochrome P-450 during the metabolism of parathion (diethyl p-nitrophenyl phosphorothionate). *J Biol Chem*, 255, 1080-9.
- Hodgson, E., Rose, R.L. 2006. Organophosphorus chemicals: potent inhibitors of the human metabolism of steroid hormones and xenobiotics. *Drug Metab Rev* 2006;38(1–2):149–62.
- Junghans, M., Backhaus, T., Faust, M., Scholze, M., Grimme, L.H., 2006. Application and validation of approaches for the predictive hazard assessment of realistic pesticide mixtures. *Aquat. Toxicol*. 76, 93–110.
- Joo, H., Choi, K., Rose, R.L., Hodgson, E. 2007. Inhibition of fipronil and nonane metabolism in human liver microsomes and human cytochrome P450 isoforms by chlorpyrifos. *J Biochem Mol Toxicol* 2007;21(2):76–80.
- Kortenkamp, A., Backhaus, T., Faust, M.J.C., 2009. State of the Art Report on Mixture Toxicity, vol. 70307. pp. 94–103.

- Heilmair R, Eyer F, Eyer P (2008) Enzyme-based assay for quantification of chlorpyrifos oxon in human plasma .*Toxicol Lett* 181:19-24.
- Karanth, S., Liu, J., Olivier, K., Jr. & Pope, C. 2004. Interactive toxicity of the organophosphorus insecticides chlorpyrifos and methyl parathion in adult rats. *Toxicol Appl Pharmacol*, 196, 183-90.
- Karanth, S., Olivier, K., Jr., Liu, J. & Pope, C. 2001. In vivo interaction between chlorpyrifos and parathion in adult rats: sequence of administration can markedly influence toxic outcome. *Toxicol Appl Pharmacol*, 177, 247-55.
- Kaushal J, Khatri M, Arya SK. 2021. A treatise on Organophosphate pesticide pollution: Current strategies and advancements in their environmental degradation and elimination. *Ecotoxicol Environ Saf.* 207:111483.
- Kaur, G., Jain, A.K. & Singh, S. 2017. CYP/PON genetic variations as determinant of organophosphate pesticides toxicity. *J Genet* 96, 187–201
- Kienhuis, A. S., Slob, W., Gremmer, E. R., Vermeulen, J. P. & Ezendam, J. 2015. A Dose-Response Modeling Approach Shows That Effects From Mixture Exposure to the Skin Sensitizers Isoeugenol and Cinnamal Are in Line With Dose Addition and Not With Synergism. *Toxicol Sci*, 147, 68-74.
- Kousba, A. A., Sultatos, L. G., Poet, T. S. & Timchalk, C. 2004. Comparison of Chlorpyrifos-Oxon and Paraoxon Acetylcholinesterase Inhibition Dynamics: Potential Role of a Peripheral Binding Site. *Toxicological Sciences*, 80, 239-248.
- Krishnan, K., Haddad, S., Béliveau, M. & Tardif, R. 2002. Physiological modeling and extrapolation of pharmacokinetic interactions from binary to more complex chemical mixtures. *Environ Health Perspect*, 110 Suppl 6, 989-94.
- Lavy, T. L., Mattice, J. D., Massey, J. H. & Skulman, B. W. 1993. Measurements of year-long exposure to tree nursery workers using multiple pesticides. *Arch Environ Contam Toxicol*, 24, 123-44.
- Lichtenstein, D., Luckert, C., Alarcán, J., De Sousa, G., Gioutlakis, M., Katsanou, E. S., Konstantinidou, P., Machera, K., Milani, E. S., Peijnenburg, A., Rahmani, R., Rijkers, D., Spyropoulou, A., Stamou, M., Stoopen, G., Sturla, S. J., Wollscheid, B., Zucchini-Pascal, N., Braeuning, A. & Lampen, A. 2020. An adverse outcome pathway-based approach to assess steatotic mixture effects of hepatotoxic pesticides in vitro. *Food and Chemical Toxicology*, 139, 111283.

- Lobell, M., Sivarajah, V. 2003. In silico prediction of aqueous solubility, human plasma protein binding and volume of distribution of compounds from calculated pKa and AlogP98 values. *Mol Divers.* 7(1), 69-87.
- Ma, T. & Chambers, J. E. 1994. Kinetic parameters of desulfuration and dearylation of parathion and chlorpyrifos by rat liver microsomes. *Food and chemical toxicology : an international journal published for the British Industrial Biological Research Association*, 32 8, 763-7.
- Marinovich, M., Ghilardi, F. & Galli, C. L. 1996. Effect of pesticide mixtures on in vitro nervous cells: comparison with single pesticides. *Toxicology*, 108, 201-6.
- Mileson, B. E., Chambers, J. E., Chen, W. L., Dettbarn, W., Ehrich, M., Eldefrawi, A. T., Gaylor, D. W., Hamernik, K., Hodgson, E., Karczmar, A. G., Padilla, S., Pope, C. N., Richardson, R. J., Saunders, D. R., Sheets, L. P., Sultatos, L. G. & Wallace, K. B. 1998. Common Mechanism of Toxicity: A Case Study of Organophosphorus Pesticides. *Toxicological Sciences*, 41, 8-20.
- Moser, V. C., Casey, M., Hamm, A., Carter, W. H., Jr., Simmons, J. E. & Gennings, C. 2005. Neurotoxicological and statistical analyses of a mixture of five organophosphorus pesticides using a ray design. *Toxicol Sci*, 86, 101-15.
- Moser, V. C., Simmons, J. E. & Gennings, C. 2006. Neurotoxicological Interactions of a Five-Pesticide Mixture in Preweanling Rats. *Toxicological Sciences*, 92, 235-245.
- Omwenga I, Kanja L, Nguta J, Mbaria J, Irungu P. 2016. Organochlorine pesticide residues in farmed fish in Kiambu and Machakos Counties, Kenya. *Cogent Environ Sci.* 2:1. d
- Omwenga, I., Kanja, L., Zomer, P., Louisse, J., Rietjens, I.M.C.M., Mol, H. 2021. Organophosphate and carbamate pesticide residues and accompanying risks in commonly consumed vegetables in Kenya. *Food Addit Contam Part B Surveill.* 2021 Mar;14(1):48-58.
- Omwenga, I., Zhao, S., Kanja, L., Mol, H., Rietjens, I.M.C.M., Louisse, J. 2021. Prediction of dose-dependent in vivo acetylcholinesterase inhibition by profenofos in rats and humans using physiologically based kinetic (PBK) modeling-facilitated reverse dosimetry. *Archives of Toxicology* (in press)
- Poet, T. S., Wu, H., Kousba, A. A. & Timchalk, C. 2003. In vitro rat hepatic and intestinal metabolism of the organophosphate pesticides chlorpyrifos and diazinon. *Toxicol Sci*, 72, 193-200.
- Quistad, G. B., Sparks, S. E. & Casida, J. E. 2001. Fatty acid amide hydrolase inhibition by neurotoxic organophosphorus pesticides. *Toxicol Appl Pharmacol*, 173, 48-55.

- Reffstrup, T. K., Larsen, J. C. & Meyer, O. 2010. Risk assessment of mixtures of pesticides. Current approaches and future strategies. *Regul Toxicol Pharmacol*, 56, 174-92.
- Richards, P. G., Johnson, M. K. & Ray, D. E. 2000. Identification of acylpeptide hydrolase as a sensitive site for reaction with organophosphorus compounds and a potential target for cognitive enhancing drugs. *Mol Pharmacol*, 58, 577-83.
- Richardson, J. R., Chambers, H. W. & Chambers, J. E. 2001. Analysis of the additivity of in vitro inhibition of cholinesterase by mixtures of chlorpyrifos-oxon and azinphos-methyl-oxon. *Toxicol Appl Pharmacol*, 172, 128-39.
- Rosenfeld, C. A. & Sultatos, L. G. 2006. Concentration-dependent kinetics of acetylcholinesterase inhibition by the organophosphate paraoxon. *Toxicol Sci*, 90, 460-9.
- Sams, C., Mason, H. J. & Rawbone, R. 2000. Evidence for the activation of organophosphate pesticides by cytochromes P450 3A4 and 2D6 in human liver microsomes. *Toxicol Lett*, 116, 217-21.
- Slob, W., Setzer, R.W., 2014. Shape and steepness of toxicological dose–response relationships of continuous endpoints. *Crit. Rev. Toxicol.* 44, 270–297.
- Smith, J.N., Timchalk, C., Bartels, M.J., Poet, T.S. 2011. In vitro age-dependent enzymatic metabolism of chlorpyrifos and chlorpyrifos-oxon in human hepatic microsomes and chlorpyrifos-oxon in plasma. *Drug Metab Dispos.* 39(8):1353-62.
- Sudakin D.L., Power L.E. 2007. Organophosphate exposures in the United States: a longitudinal analysis of incidents reported to poison centers. *J Toxicol Environ Health A*. 2007 Jan 15;70(2):141-7.
- Sultatos, L. G. & Murphy, S. D. 1983. Kinetic analyses of the microsomal biotransformation of the phosphorothioate insecticides chlorpyrifos and parathion. *Fundamental and Applied Toxicology*, 3, 16-21.
- Suratman, S., Edwards, J. W. & Babina, K. 2015. Organophosphate pesticides exposure among farmworkers: pathways and risk of adverse health effects. *Rev Environ Health*, 30, 65-79.
- Tang, J., Cao, Y., Rose, R. L., Brimfield, A. A., Dai, D., Goldstein, J. A. and Hodgson, E. 2001. Metabolism of chlorpyrifos by human cytochrome P450 isoforms and human, mouse, and rat liver microsomes. *Drug Metab Dispos.* 29, 1201-4.
- Tang, J., Cao, Y., Rose, R.L., Hodgson, E. 2002. In vitro metabolism of carbaryl by human cytochrome P450 and its inhibition by chlorpyrifos. *Chem Biol Interact.* 20;141(3):229-41.

- Timchalk, C., Nolan, R. J., Mendrala, A. L., Dittenber, D. A., Brzak, K. A., and Mattsson, J. L. (2002). A physiologically based pharmacokinetic and pharmacodynamic (PBPK/PD) model for the organophosphate insecticide chlorpyrifos in rats and humans. *Toxicol. Sci.* 66, 34–53.
- Timchalk, C. and Poet, T. S. 2008. Development of a physiologically based pharmacokinetic and pharmacodynamic model to determine dosimetry and cholinesterase inhibition for a binary mixture of chlorpyrifos and diazinon in the rat. *Neurotoxicology*, 29, 428-43.
- Timchalk, C., Poet, T. S., Hinman, M. N., Busby, A. L. and Kousba, A. A. 2005. Pharmacokinetic and pharmacodynamic interaction for a binary mixture of chlorpyrifos and diazinon in the rat. *Toxicol Appl Pharmacol*, 205, 31-42.
- Thunga, Girish, Sam, Kishore Ganna, Khera, Kanav, Pandey, Sureshwar, Vidya Sagar, Sudha, 2010. Evaluation of incidence, clinical characteristics and management in organophosphorus poisoning patients in a tertiary care hospital. *J. Toxicol. Environ. Health Sci.* Vol. 2 (5):73–76.
- Wu, H., Poet, T.S., Timchalk, C., 2004. Inhibition of diazinon metabolism by chlorpyrifos in rat liver microsomes. *Toxicol. Sci.* 78 (1-S), 425.
- Zhao, S., Kamelia, L., Boonpawa, R., Wesseling, S., Spenkelink, B., Rietjens, I.M.C.M., 2019. Physiologically based kinetic modelling-facilitated reverse dosimetry to predict in vivo red blood cell acetylcholinesterase inhibition following exposure to chlorpyrifos in the Caucasian and Chinese population. *Toxicol Sci.* 2019 Jun 19;171(1):69–83.
- Zhao, S., Wesseling, S., Spenkelink, B., Rietjens, I.M.C.M., 2021. Physiologically based kinetic modelling based prediction of in vivo rat and human acetylcholinesterase (AChE) inhibition upon exposure to diazinon. *Arch Toxicol.* 2021 May;95(5):1573-1593.

**Supplementary material 1**

Data format for single compound analysis

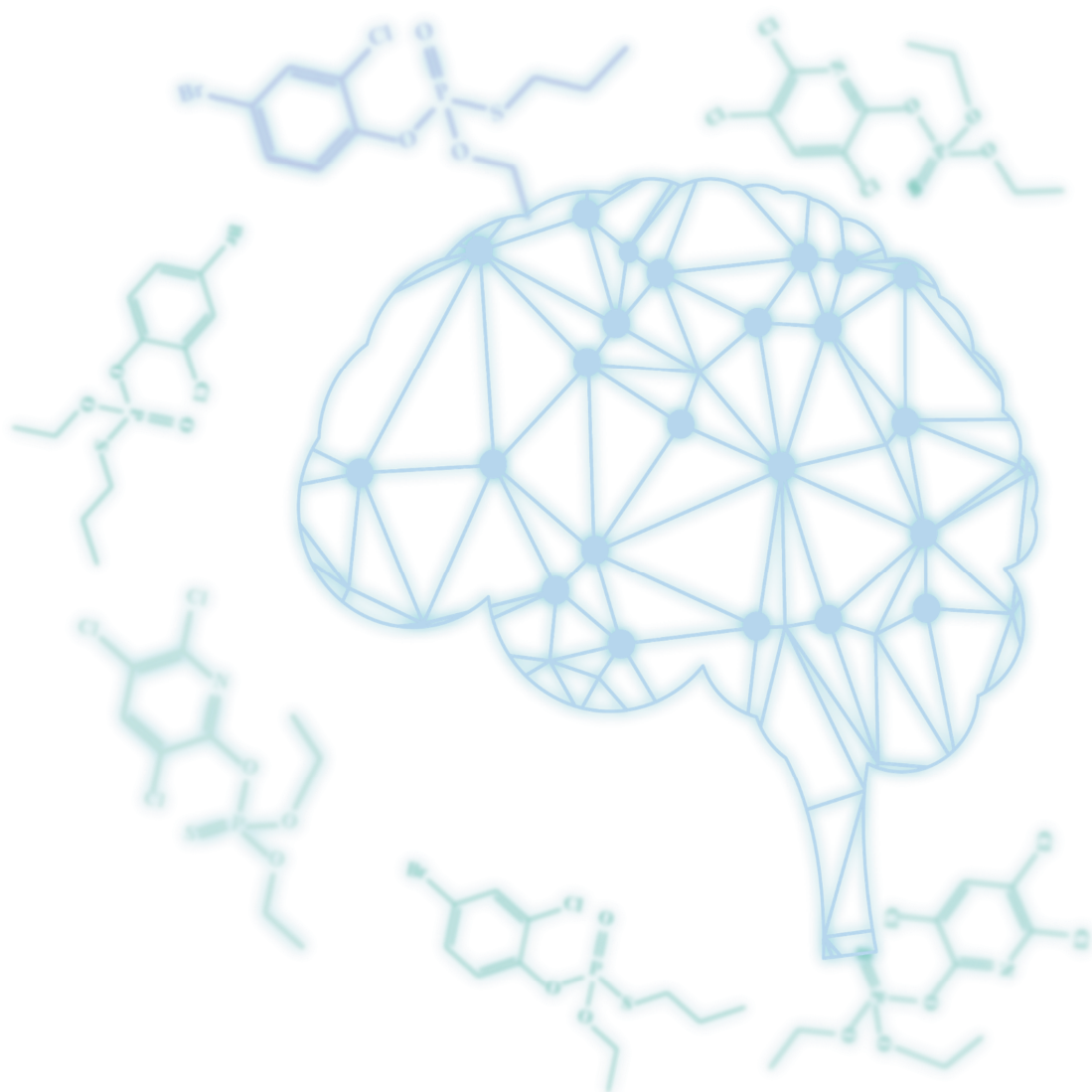
PPF	CPO	Admin.comp	AChE	SD	N
			activity		
5	0	PPF	94.99953	1.533608	3
10	0	PPF	99.23282	3.662433	3
25	0	PPF	96.30271	1.85084	3
50	0	PPF	95.75581	1.48049	3
100	0	PPF	90.17884	0.222605	3
250	0	PPF	89.79521	0.928884	3
500	0	PPF	66.17205	1.921244	3
1000	0	PPF	36.21096	1.504951	3
2500	0	PPF	19.59966	0.936861	3
5000	0	PPF	12.75182	0.540977	3
0	0.05	CPO	100.3569	0.432987	3
0	0.1	CPO	99.96475	1.241101	3
0	0.2	CPO	100.0426	1.658234	3
0	0.5	CPO	98.41019	2.49912	3
0	1	CPO	94.20221	1.860128	3
0	2.5	CPO	80.16323	3.552664	3
0	5	CPO	52.92886	2.181251	3
0	10	CPO	18.55614	1.861837	3



**Supplementary material 2**

Data format for mixture analysis

PF	CPO	Admin.comp	AChE activity	SD	N
5	0	PPF	94.99953	1.533608	3
10	0	PPF	99.23282	3.662433	3
25	0	PPF	96.30271	1.85084	3
50	0	PPF	95.75581	1.48049	3
100	0	PPF	90.17884	0.222605	3
250	0	PPF	89.79521	0.928884	3
500	0	PPF	66.17205	1.921244	3
1000	0	PPF	36.21096	1.504951	3
2500	0	PPF	19.59966	0.936861	3
5000	0	PPF	12.75182	0.540977	3
0	0.05	CPO	100.3569	0.432987	3
0	0.1	CPO	99.96475	1.241101	3
0	0.2	CPO	100.0426	1.658234	3
0	0.5	CPO	98.41019	2.49912	3
0	1	CPO	94.20221	1.860128	3
0	2.5	CPO	80.16323	3.552664	3
0	5	CPO	52.92886	2.181251	3
0	10	CPO	18.55614	1.861837	3
0.603042	0.003655	ZZ-tern	99.48359	4.175577	3
1.206084	0.00731	ZZ-tern	99.66572	3.631524	3
2.412168	0.014619	ZZ-tern	99.95854	1.201876	3
4.824336	0.029238	ZZ-tern	99.47792	4.965794	3
9.648671	0.058477	ZZ-tern	98.21343	5.179981	3



# CHAPTER 5.

Predicting interindividual differences in profenofos  
detoxification based on in vitro kinetic data and a  
physiologically based kinetic (PBK) and Monte Carlo  
modelling approach

Isaac Omwenga

Hans Mol

Ivonne M.C.M. Rietjens

Jochem Louisse

*In Preparation*

**Abstract**

The aim of the present study was to predict human interindividual differences in profenofos (PFF) detoxification based on a combined in vitro-in silico approach. To that end, PFF conversion to 4-bromo-2-chlorophenol (BCP) was studied in in vitro incubations with liver S9 fractions of 25 different Caucasian donors and plasma samples of 25 different Caucasian donors. The obtained information on the variation in the in vitro kinetic constants  $V_{max}$  and  $K_m$  was applied in our previously published physiologically based kinetic (PBK) model using a Monte Carlo simulation modelling approach. Analysis of the predicted internal maximum concentrations of the simulated population indicated a 1.4- and 1.5-fold difference between the geometric mean (GM) and the 90<sup>th</sup> and 99<sup>th</sup> percentile, respectively, of the simulated population, being smaller than the default uncertainty factor accounting for human variability in toxicokinetics of 3.16. Concentration-response curves for inhibition of human AChE determined in vitro were translated with the PBK model to predicted dose-dependent AChE inhibition in humans in vivo. In line with the differences in  $C_{max}$  values, the 99<sup>th</sup> percentile of the population was predicted to be 1.5-fold more sensitive to PFF-induced AChE inhibition than the GM of the population based on the BMDL10 values derived from predicted dose-response data for the virtual population. This predicted BMDL10 of 0.0057 mg/kg bw (99<sup>th</sup> percentile of population) is comparable to the ARfD adopted by EFSA (0.005 mg/kg bw) and EPA (0.002 mg/kg bw), but much lower than the ARfD adopted by JMPR (1 mg/kg bw). Altogether, the results obtained demonstrate that integrating PBK modelling with Monte Carlo simulations using human in vitro data provides a powerful strategy to quantify human interindividual variation in kinetics, which can be used to refine the hazard characterization of organophosphate pesticides.

## 5.1 Introduction

Organophosphates (OPs) are chemicals extensively used for the control of agricultural and household pests (van der Veen and de Boer, 2012). The OPs have played a key role in controlling pests and increasing agricultural production since the 1970s (Zhao and Yu, 2013). Despite their role in pest control, about three million OP pesticide poisoning cases are annually reported on the global scale, with an estimated 220,000–250,000 deaths, of which up to 99% have occurred in low-income or developing countries (Robb and Baker, 2000; Roberts and Aaron, 2007; Chiari et al., 2017). Consequently, some countries have taken measures to reduce the use of OPs, with many OPs currently deregistered for use as pesticides, while some have been banned (Hertz-Picciotto et al 2018; Pesticide Action Network International, 2020).

Unlike many other OPs, PFF is a direct acting phosphorothioate OP pesticide with the capability of inhibiting  $\beta$ -esterases such as butyrylcholinesterase, acetylcholinesterase, and carboxylesterase without requiring activation (Dadson et al., 2013). It has been reported to be mainly detoxified through paraoxonase 1 (PON1)-mediated hydrolysis in the liver and plasma as well as CYP450-mediated detoxification, resulting in the production of 4-bromo-2-chlorophenol (BCP) (FAO, 2012; Dadson et al., 2013; EPA, 2016) (Figure 1).

Recently, we developed a physiologically based kinetic (PBK) model for PFF detoxification in rats and humans based on in vitro and in silico input data (Omwenga et al., 2021). We used this model to predict in vivo AChE inhibition, translating in vitro concentration-response data on PFF-induced AChE inhibition to in vivo dose-response data using a reverse dosimetry approach. We showed that with this approach in vivo AChE inhibition in rats was adequately predicted, and that humans were predicted to be 45-fold more sensitive than rats, due to a less efficient PON1- and CYP-mediated PFF detoxification by humans than by rats as well as interspecies differences in B-esterases, with rat plasma containing almost all types of esterases including CaE, PON1, BChE, and AChE (Sato and Hosokawa, 2006; Bahar et al., 2012),

whereas humans are deficient of plasma CaE (Berry et al., 2009; Li et al., 2005; Williams et al., 2011) and plasma AChE (Ecobichon and Comeau, 1973). We used the predicted dose-response data to derive points-of-departure (BMDL10 values) for AChE inhibition, which can be used as a starting point in the hazard assessment (Omwenga et al., 2021). Since we used pooled human liver fractions and plasma for the in vitro kinetic studies we were able to make predictions for ‘an average human’, but we could not take interindividual differences into account, which may occur as a result of differences in kinetic processes between individuals. In general, a default uncertainty factor of 3.16 is applied to account for human variation in toxicokinetics (IPCS 2005). However, having more detailed insights in possible interindividual variation might provide risk assessors a more science-based approach to derive factors accounting for intraspecies and interspecies differences in toxicokinetics, which may be applied to define chemical specific adjustment factors (CSAFs) for chemicals.

In the present study we aimed to predict interindividual differences in PFF detoxification by determining PFF detoxification in in vitro incubations with liver S9 fractions of 25 different Caucasian donors and with plasma samples of 25 different Caucasian donors. The obtained information on the variation in the in vitro kinetic constants  $V_{max}$  and  $K_m$  was applied in our previously published PBK model using a Monte Carlo simulation modelling approach, providing insights into human interindividual differences in PFF detoxification in a simulated adult human population, allowing estimation of expected differences between internal exposure for the geometric mean (GM) of the population compared to that of sensitive individuals (90-99<sup>th</sup> percentile).

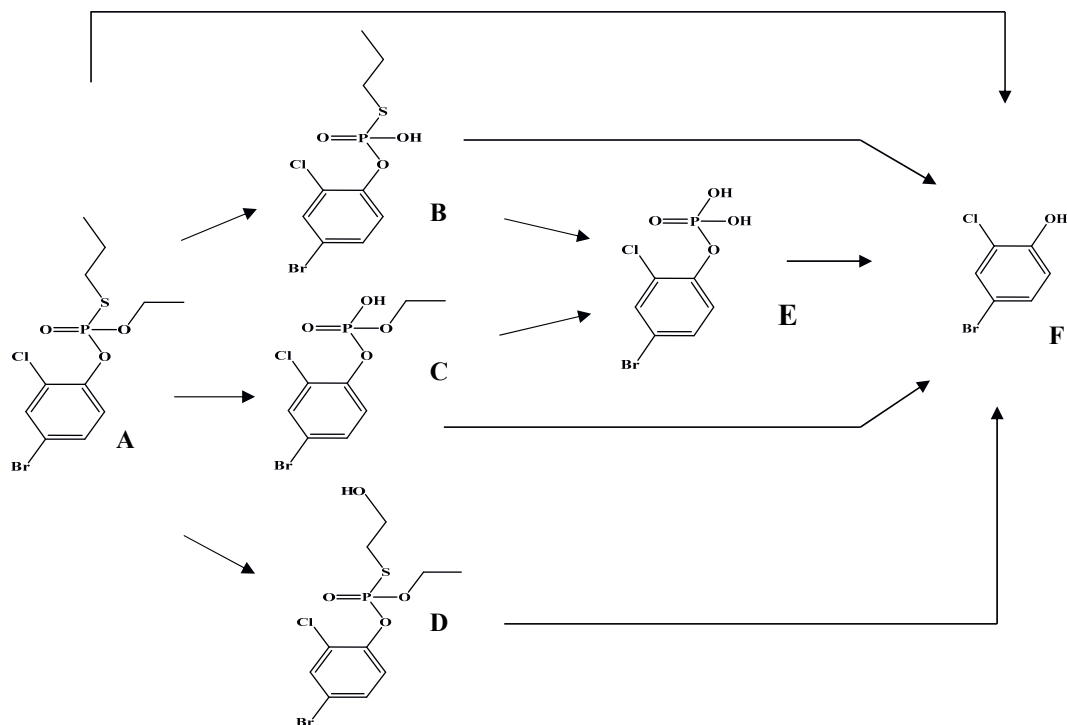


Figure 1. Metabolic pathways for metabolism of profenofos (A) based on data reported in previous studies (Gotoh et al., 2001; Dadson et al., 2013). Metabolites include desethyated profenofos (B), desthiopropylprofenofos / des-S-propylated profenofos (C), hydroxypropyl profenofos (D), 4-bromo-2-chlorophenyl dihydrogen phosphate (E), and 4-bromo-2-chlorophenyl (BCP) (F).

## **5.2. Materials and Methods**

### **5.2.1 Materials**

PFF, 4-bromo-2-chlorophenol (BCP), bovine serum albumin (BSA), reduced nicotinamide adenine dinucleotide phosphate (NADPH), 5,5-dithiobis (2-nitrobenzoic acid) (DTNB) and acetylthiocholine iodide (ATC) were purchased from Sigma-Aldrich (Zwijndrecht, The Netherlands). Magnesium chloride hexahydrate ( $\text{MgCl}_2 \cdot 6\text{H}_2\text{O}$ ), trifluoroacetic acid (TFA), dimethylsulfoxide (DMSO), and calcium chloride dihydrate ( $\text{CaCl}_2 \cdot 2\text{H}_2\text{O}$ ) were purchased from VWR International (Amsterdam, The Netherlands). Acetonitrile (ACN, UPLC/MS grade) was purchased from Biosolve (Valkenswaard, The Netherlands). S9 liver fractions of 25 different Caucasian donors and plasma samples of 25 different Caucasian donors were obtained from SEKISUI XenoTech (Kansas City, USA) and BIOIVT (West Sussex, UK), respectively.

#### **5.2.2.1 General outline of PBK modelling approach with Monte Carlo simulation to study interindividual differences in PFF detoxification**

To predict and simulate human interindividual differences in the detoxification of PFF, the present study follows the steps as described below.

1) The conversion of PFF to BCP in the liver was studied using liver S9 fractions of 25 Caucasian individuals and the conversion of PFF to BCP in plasma was studied using plasma samples of 25 Caucasian individuals. From these studies, kinetic parameters ( $K_m$ ,  $V_{max}$  and  $k_{cat}$ ) were derived.

2) The in vitro kinetic data were applied in the PBK model using two approaches. In the first approach 625 PBK models were prepared combining each S9 dataset to each plasma dataset ( $25 \times 25$ ). For the second approach the interindividual variation in the Caucasian population in the kinetic constants  $V_{max}$  and  $K_m$  of PFF conversion to BCP were included in the PBK model in connection with Monte Carlo simulations to predict interindividual variation of PFF



clearance by the liver and in the plasma. For results obtained with both approaches, differences between the C<sub>max</sub> values for the geometric mean (GM) of the simulated population compared to the C<sub>max</sub> values for the 90<sup>th</sup>, 95<sup>th</sup> and 99<sup>th</sup> percentile in the population were determined and were compared with the default uncertainty factor applied for interindividual variation in toxicokinetics (3.16; IPCS, 2005).

3) Finally, we performed reverse dosimetry of *in vitro* data on PFF-induced AChE inhibition from our previous study (Omwenga et al., 2021) to estimate BMDL10 values for PFF-induced AChE inhibition in humans for the GM of the simulated human population as well as for the more sensitive individuals with slower PFF clearance. We used these data to estimate whether at different reported ARfD values for PFF, effects on AChE activity are to be expected in the simulated human population based on our predictions.

#### **5.2.2.2 Step 1: *In vitro* incubations to derive individual human liver S9 and plasma kinetic parameter values for description of metabolic clearance of PFF in the PBK model**

Incubations of PFF with human individual liver S9 and plasma to quantify *in vitro* rates of BCP formation were performed as described before by Omwenga et al. (2021) for incubations with pooled samples. Briefly, the final incubations were carried out in 100 mM Tris HCl (pH 7.4, 37°C) containing (final concentrations) 5 mM MgCl<sub>2</sub>, 2 mM CaCl<sub>2</sub> (to stimulate PON1 activity (Carr et al., 2015)), 2 mM NADPH (cofactor to also include CYP-mediated metabolism), enzyme preparation (final concentration 2 mg S9 protein/ml for human liver S9 and 7.7 mg plasma protein/ml for individual human plasma) and PFF (at final concentrations ranging from 1 to 100 µM, added from 200 times concentrated stock solutions in DMSO). Control incubations were performed in the absence of individual human liver S9 or plasma. After 2 min pre-incubation, the reaction was initiated by adding the substrate and mixtures were incubated for 2 min in a 37 °C water bath. The total volume of the incubation mixtures was 200 µl. The

reaction was terminated by the addition of 50 µl ice cold ACN and samples were kept on ice. The mixture was centrifuged at 14,000 g for 20 min at 4°C and the supernatant was analyzed using UPLC-UV.

#### **5.2.2.2.1 UPLC-UV analysis**

All samples from incubations were analyzed using a Waters Acquity UPLC H class system that consisted of a quaternary solvent manager, a sample manager, and a photodiode array (PDA) detector, equipped with a Water Acquity UPLC® BEH C18 column (1.7 µm, 2.1 × 50 mm) and Waters Xbridge UPLC® BEH C18 pre-column (2.5 µm, 2.1 x 5 mm). The temperature of the column was kept at 40°C and the auto sampler at 10°C during the UPLC analysis. The mobile phases used for the analysis consisted of (A) 0.1% TFA in nanopure water and (B) 100% ACN. A gradient elution at a flow rate of 0.6 ml/min was applied for the analysis with the initial condition of 100% A: 0% B (v/v), changing in a linear way to 0% A: 100% B from 0 to 6 min, which was maintained for 30 s, and then changed back to the initial conditions in 30 s, which were maintained for 1 min. The injection volume for each sample was 3.5 µl. Under these conditions, the retention times of PFF and BCP were 4.76 and 3.37 min, respectively. The amounts of PFF and BCP were quantified by integrating the peak areas at 237 nm using calibration curves that were prepared using commercially available standards.

#### **5.2.2.3 Step 2: Inclusion of interindividual variation in the kinetic constants of PFF detoxification in the PBK model in connection with Monte Carlo simulations to predict interindividual variation in internal PFF exposure**

##### **5.2.2.3.1 In vitro metabolism data analysis and scaling in the PBK model**

Kinetic parameters including the apparent maximum velocity ( $V_{max}$ ) and the apparent Michaelis–Menten constant ( $K_m$ ) for BCP formation were obtained by fitting the data for the

substrate concentration-dependent rate of conversion (expressed in nmol/min/mg protein) using GraphPad Prism 5, version 5.04 (San Diego, California, USA) to the standard Michaelis–Menten equation:

$$V = V_{\max} * [S] / (K_m + [S])$$

in which [S] represents the concentration of substrate, expressed in  $\mu\text{M}$ , V and  $V_{\max}$  the velocity and the maximum velocity of the reaction, respectively, expressed in nmol/min/mg protein, and  $K_m$  the apparent Michaelis–Menten constant, expressed in  $\mu\text{M}$ . The kinetic parameter values for conversion of PFF to BCP by the individual human liver S9 and plasma samples were determined. To determine the catalytic efficiency,  $V_{\max}$  was divided by the  $K_m$ .

The in vitro  $V_{\max}$  values were scaled in the PBK model code (Supplementary Materials) using the following scaling factors for humans: 121 mg S9 protein/g liver and 550 mg plasma protein/g blood (Houston and Galetin, 2008; Nishimuta et al., 2014; Cubitt et al., 2011). The apparent  $V_{\max}$  values obtained from enzymatic incubations expressed in nmol/min/mg protein were converted into  $\mu\text{mol/h/kg}$  liver and plasma in the PBK model code. The in vivo  $K_m$  values were assumed to be equal to those obtained in vitro (taking into account the differences in free fraction in vitro vs in vivo).

#### 5.2.2.3.2 PBK model structure and software

The PBK model previously developed for PFF in adult Caucasians was used in the present study to evaluate the human interindividual variation in PFF detoxification and related PFF-induced AChE inhibition resulting from differences in the detoxification of PFF in the liver and plasma. Our human PFF PBK model previously developed was modified to include equations for Monte Carlo simulations (Omwenga et al., 2021).

The main metabolite of PFF reported in vivo is BCP, which has been reported to be formed upon PON1-mediated hydrolysis of PFF (JMPR 2007; EPA 2016; Dadson et al 2013). CYP-

mediated formation of other metabolites has been reported (Dadson et al., 2013), but these are considered less relevant, since the hydrolysis reaction is more efficient than the CYP-mediated oxidations, as indicated in our in vitro metabolism studies with liver microsomes or cytosol in which practically all PFF was converted into BCP. PFF hydrolysis (BCP formation) was quantified in the present study using human liver S9 and plasma and was included in the blood and liver compartments of the PBK model.

The model equations were coded and numerically integrated in Berkeley Madonna 9.1.18 (UC Berkeley, CA, USA), using the Rosenbrock's algorithm for stiff systems. The PBK models' differential equations are provided in the Supplementary Materials.

#### **5.2.2.3.3 Integration of in vitro kinetic data of individual samples in PBK modelling approach**

In the present study, we were able to derive in vitro data on interindividual differences in PFF detoxification in the liver and in plasma. These data were applied in the PBK model to obtain insight into internal PFF concentrations in humans using two different approaches. In the first approach, 625 different PBK models were made based on the scaled datasets for metabolism, combining each human liver S9 dataset with each plasma dataset, resulting in  $25 \times 25 = 625$  combinations. At 0.01 mg/kg bw internal exposures ( $C_{\max}$  unbound PFF concentration) were determined with each PBK model and from these data the GM, the 90<sup>th</sup>, 95<sup>th</sup> and 99<sup>th</sup> percentile of this 'population' was determined. For the second approach obtained information on the variation in biotransformation kinetics was applied in our PFF PBK model using Monte Carlo simulations, using a similar approach as applied by Punt et al. (2016), Strikwold et al. (2017) and Ning et al. (2019). For the Monte Carlo analysis, a total of 10,000 simulations were performed, where in each simulation, the  $V_{\max}$  and  $K_m$  of PFF detoxification in the liver and of PFF detoxification in plasma were randomly taken from a log-normal distribution. The

distributions were truncated at  $\pm 3SD$  by excluding individuals with kinetic constants that were three times higher or lower than the GM values from the Monte Carlo simulation (Punt et al., 2016; Strikwold et al., 2017, Ning et al., 2019). The kinetic constants for the PFF detoxification in the liver and plasma were assumed to vary independently. The mean ( $\mu_w$ ) and standard deviation ( $\sigma_w$ ) describing the log-normal distribution of  $V_{max}$  and  $K_m$  values were derived using the following equation (Zhang et al. 2007):

$$\mu_w = \ln\left(\frac{\mu_x}{\sqrt{1 + CV_x^2}}\right) \text{ and } \sigma_w = \ln(1 + CV_x^2)$$

where  $\mu_x$  is the mean of  $V_{max}$  or  $K_m$  and  $CV_x$  is the coefficient of variation for each parameter. Monte Carlo simulations were performed to obtain insight into the variation in human PFF  $C_{max}$  values in blood (unbound) upon exposure to 0.01 mg/kg bw per day, being the predicted BMDL10 for PFF-induced AChE inhibition in humans from our earlier study (Omwenga et al., 2021).

The output of the Monte Carlo simulations was further analyzed with GraphPad (GraphPad Prism software version 5.04, San Diego California USA) to obtain the different percentiles, i.e. GM, 90<sup>th</sup>, 95<sup>th</sup> and 99<sup>th</sup> percentile of the PFF  $C_{max}$  in blood (unbound) in the simulated population. The difference between the GM and the 90<sup>th</sup>, 95<sup>th</sup> and 99<sup>th</sup> percentile were obtained by dividing the 90<sup>th</sup>, 95<sup>th</sup> or 99<sup>th</sup> percentile of BCP formation by the GM (IPCS, 2005).

#### 5.2.2.4 Step 3: Reverse dosimetry of in vitro AChE inhibition data

In our previous study (Omwenga et al., 2021), the in vitro concentration-response data for PFF-induced inhibition of human (recombinant) AChE were translated to in vivo dose-response data using PBK modelling-based reverse dosimetry. This quantitative in vitro to in vivo extrapolation (QIVIVE) was performed based on the  $C_{max}$  (the unbound maximum concentration in blood). For the QIVIVE, each concentration of PFF in the in vitro studies, was

set equal to the free C<sub>max</sub> of PFF in blood in the PBK model to calculate the oral dose that results in this concentration (Omwenga et al., 2021). In the present study, a similar approach was applied to define the dose-response curve for the average population (GM), while the dose-response curves of the sensitive individuals (90<sup>th</sup>, 95<sup>th</sup> and 99<sup>th</sup> percentile) in the human population, were derived by applying the obtained values on the differences between these high percentiles and the GM of the population (see section 5.2.2.3). BMD modelling was applied on these dose-response datasets using PROAST software as described before in Omwenga et al. (2021) to obtain a BMDL10 for the average human (Caucasian), as well as for the more sensitive individuals. The obtained predicted dose-response data were applied to estimate whether at defined PFF exposure scenarios (different PFF ARfD values reported (0.005 mg/kg (EFSA, 2014), 0.002 mg/kg (EPA, 2016) and 1 mg/kg (JMPR, 2007)) effects of PFF in the simulated human population is to be expected.

### **5.3. Results**

#### **5.3.1 In vitro conversion of PFF to BCP by liver S9 and plasma of different human donors**

Tables 1, 2 and 3 show the kinetic constants V<sub>max</sub> and K<sub>m</sub>, and the catalytic efficiencies for conversion of PFF to BCP by 25 Caucasian individuals, derived from experiments with liver S9 and plasma incubations, respectively. It also presents for these kinetic constants the mean ( $\mu_w$ ), the standard deviation ( $\sigma_w$ ) and the % coefficient of variation (%CV). The difference between the highest and the lowest catalytic efficiencies for Caucasian liver S9 amounted to 5.8-fold with a mean ( $\mu_w$ ) of 143  $\mu\text{l}/\text{min}/\text{mg}$  and a CV of 41%. This relatively high CV is mainly caused by individuals 098H0533 and 098H0447 which have relatively high V<sub>max</sub> and low K<sub>m</sub> values resulting in catalytic efficiencies that are 1.8- and 1.6-fold higher respectively than the mean ( $\mu_w$ ) catalytic efficiency (Table 2). The difference between the highest and the lowest catalytic efficiencies for Caucasian plasma was 6.4-fold with a mean ( $\mu_w$ ) of 15

$\mu\text{l}/\text{min}/\text{mg}$  and a CV of 62%. Individuals HMN431414 and HMN431432 have relatively high  $V_{\text{max}}$  and low  $K_{\text{m}}$  values resulting in catalytic efficiencies that are both 2.7-fold higher than the mean ( $\mu_{\text{w}}$ ) catalytic efficiency of human plasma (Table 3).

Table 1. In vitro kinetic constants  $V_{\text{max}}$  and  $K_{\text{m}}$  and catalytic efficiencies for the conversion of PFF to BCP by 25 Caucasian individual liver S9 fractions.

Code	$V_{\text{max}}^{\text{a}}$	$K_{\text{m}}$ ( $\mu\text{M}$ )	Catalytic efficiency <sup>b</sup>
098H0025	1.7	9.1	190
098H0026	1.4	19	74
098H0033	1	9.3	108
098H0041	0.96	12	78
098H0057	1.4	11	127
098H0062	1.6	34	46
098H0068	1.7	20	87
098H0164	1.8	9.2	193
098H0177	0.89	3.9	230
098H0208	1.3	6.3	204
098H0217	2.1	19	113
098H0220	1.4	5.9	232
098H0236	1.5	7.7	200
098H0246	0.97	8.6	111
098H0291	2.1	19	111
098H0311	1.9	14	137
098H0397	1.8	12	151
098H0420	1.5	18	84
098H0428	1.6	12	136
098H0430	1.5	12	124
098H0447	1.7	7.4	233
098H0463	1.8	29	64
098H0487	2.4	17	141
098H0533	2.1	8	261
098H0751	1.8	12	152
Mean <sup>c</sup> ( $\mu_{\text{x}}$ )	1.6	13	143
SD <sup>d</sup>	0.38	6.9	58.5
CV <sub>x</sub> % <sup>e</sup>	23.7	52.2	40.9
$\mu_{\text{w}}$ <sup>f</sup>	-2.7	-1.36	-2
$\Sigma w$ <sup>g</sup>	2.5	2.81	3.15
3-fold SD high=EXP( $\mu_{\text{w}}+\sigma_{\text{w}}*3$ )	0.73	3.76	31.5
3-fold SD low=EXP( $\mu_{\text{w}}-\sigma_{\text{w}}*3$ )	0.006	0.018	1.95052E-07

<sup>a</sup> nmol/min/mg liver S9 and plasma protein for PFF conversion to BCP

<sup>b</sup>  $\mu\text{l/min/mg}$  liver S9 and plasma protein for PFF conversion to BCP

<sup>c</sup> Mean of kinetic constants  $V_{\text{max}}$  and  $K_m$ , and catalytic efficiency for PFF conversion to BCP for 25 Caucasian individuals

<sup>d</sup> Standard deviation of kinetic constants  $V_{\text{max}}$  and  $K_m$ , and catalytic efficiency for PFF conversion to BCP for the 25 Caucasian individuals

<sup>e</sup> Coefficient variation % =  $\text{SD/mean } (\mu x) \times 100\%$

<sup>f</sup> The mean for describing the log-normal distribution  $\mu_w = \ln \left[ \frac{\mu x}{\text{sqrt}(1 + CV x^2)} \right]$

<sup>g</sup> The standard deviation for describing the log-normal distribution ( $\sigma_w = \ln(1 + CV x^2)$ )



Table 2. In vitro kinetic constants Vmax and Km and catalytic efficiencies for the conversion of PFF to BCP by 25 Caucasian individual plasma fractions.

Code	Vmax <sup>a</sup>	Km ( $\mu$ M)	Catalytic efficiency <sup>b</sup>
HMN431413	0.7036	38.91	18.08
HMN431414	0.9395	22.77	41.26
HMN431415	1.076	81.1	13.27
HMN431416	1.446	125.2	11.55
HMN431417	0.8388	27.85	30.12
HMN431418	0.8348	62.77	13.3
HMN431419	1.488	157.8	9.43
HMN431420	1.693	101.4	16.7
HMN431421	2.412	277.9	8.68
HMN431422	1.177	93.25	12.62
HMN431423	2.061	165.1	12.48
HMN431424	0.3436	49.28	6.97
HMN431425	0.7404	74.27	9.97
HMN431426	0.8455	56.5	14.96
HMN431427	0.6893	25.57	26.96
HMN431428	1.399	217.7	6.43
HMN431429	3.131	347.5	9.01
HMN431430	1.088	130.4	8.34
HMN431431	1.655	195	8.49
HMN431432	2.969	72.51	40.95
HMN431433	2.594	253.2	10.24
HMN431434	4.014	314.7	12.76
HMN431435	1.783	116.5	15.3
HMN431436	2.21	199.2	11.09
HMN431437	1.869	190.6	9.81
Mean <sup>c</sup>	1.6	135.88	15.15
SD <sup>d</sup>	0.88	91.38	9.39
CV <sub>x</sub> % <sup>e</sup>	54.9	67.2	61.98
$\mu$ w <sup>f</sup>	-3.54	0.7	-1.41
$\sigma$ w <sup>g</sup>	2.83	2.9	2.87
3-fold SD high=EXP( $\mu$ w+ $\sigma$ w*3)	0.43	32.19	1339.43
3-fold SD low=EXP( $\mu$ w- $\sigma$ w*3)	0.002	0.13	4.4501E-05

<sup>a</sup> nmol/min/mg liver S9 and plasma protein for PFF conversion to BCP<sup>b</sup>  $\mu$ l/min/mg liver S9 and plasma protein for PFF conversion to BCP<sup>c</sup> Mean of kinetic constants Vmax and Km, and catalytic efficiency for PFF conversion to BCP for 25 Caucasian individuals

<sup>d</sup> Standard deviation of kinetic constants Vmax and Km, and catalytic efficiency for PFF conversion to BCP for the 25 Caucasian individuals

<sup>e</sup> Coefficient variation % =  $SD/mean (\mu x) \times 100\%$

<sup>f</sup> The mean for describing the log-normal distribution  $\mu w = \ln \left[ \frac{\mu x}{\sqrt{1+CVx^2}} \right]$

<sup>g</sup> The standard deviation for describing the log-normal distribution ( $\sigma w = \ln(1 + CVx^2)$ )

Table 3. Geometric mean (GM), CV (%) and the fold difference between the minimum and maximum Cmax of PFF upon exposure to an oral dose of 0.01 mg PFF/kg bw predicted by 625 individual PBK models and by PBK modelling linked to Monte Carlo (MC) simulation.

	Cmax of PFF of 625 individual PBK models	Cmax of PFF of PBK model with MC simulation
GM (pM)	0.1827	0.1572
CV (%)	11.1%	27.1%
Fold-difference min-max	0.69 <sup>a</sup>	9.3 <sup>b</sup>

<sup>a</sup> Fold-difference between the predicted minimum and maximum Cmax of PFF by individual PBK models

<sup>b</sup> Fold-difference between the predicted minimum and maximum Cmax of PFF by PBK models coupled with Monte Carlo simulation

### 5.3.2 Individual PBK models and Monte Carlo simulation

The impact of the interindividual differences in PFF metabolism in liver and plasma on the C<sub>max</sub> in plasma (free concentration) were evaluated by two methods. Firstly, the variation in C<sub>max</sub> of PFF was determined using the kinetic data derived from in vitro incubations of PFF using one set of 25 Caucasian liver S9 fractions and one set of 25 individual plasma samples (Tables 1 and 2). The individual kinetic parameters, i.e. V<sub>max</sub> and K<sub>m</sub>, present in these data sets were combined to result in 625 individual PBK models. Figure 2 shows the box and whisker plot for the predicted C<sub>max</sub> of PFF obtained with these 625 individual PBK models at an oral dose equivalent to a BMDL10 of 0.01mg/kg bw derived from the predicted dose-response data on PFF-induced AChE inhibition from our previous study (Omwenga et al., 2021). Table 3 presents the GM, CV (%) and fold-variation between the minimum and maximum of the predictions thus obtained.

In the second approach, a Monte Carlo simulation was performed at an oral predicted BMDL10 of 0.01 mg/kg bw (Omwenga et al., 2021) and the highest reported ARfD of PFF of 1 mg/kg bw (JMPR, 2007) to evaluate the interindividual variation in PFF metabolism that could occur in a larger population. The Monte Carlo simulation was performed in order to take the combination of the variability in liver S9 and plasma kinetics into account. In the Monte Carlo simulation 10,000 individuals were considered. The box and whisker plot for the predicted PFF C<sub>max</sub> obtained from the Monte Carlo simulations is also shown in Figure 2. The frequency distributions for the predicted C<sub>max</sub> obtained from the simulated population for both doses are presented in Figures 3A and 3B. The GM, CV (%) and the fold variations of the simulated population are presented in Table 3. The GM for the C<sub>max</sub> of PFF obtained from the Monte Carlo simulation (at a dose level of 0.01 mg/kg bw) appeared to be comparable (1.2-fold higher) to the GM obtained from the 625 individual PBK models.

Figure 4 shows the PBK model-based predictions for the time-dependent blood concentration of PFF at an oral dose of 0.01 mg/kg bw for the average, and the most and least active of the 625 Caucasian individuals. The difference between the predicted C<sub>max</sub> of PFF in blood for the individual with the highest and the lowest efficiency in PFF depletion is 1.7-fold fold for the 625 individuals.

Applying a Monte Carlo simulation, the difference between the GM and the 90<sup>th</sup>, 95<sup>th</sup> and the 99<sup>th</sup> percentile values was 1.4, 1.4 and 1.5 for the 90<sup>th</sup>, 95<sup>th</sup> and the 99<sup>th</sup> percentiles at 0.01 mg/kg bw. At an ARfD of 1 mg/kg bw as reported by JMPR, (2007), the difference between the GM and the 90<sup>th</sup>, 95<sup>th</sup> and the 99<sup>th</sup> percentile values were the same.

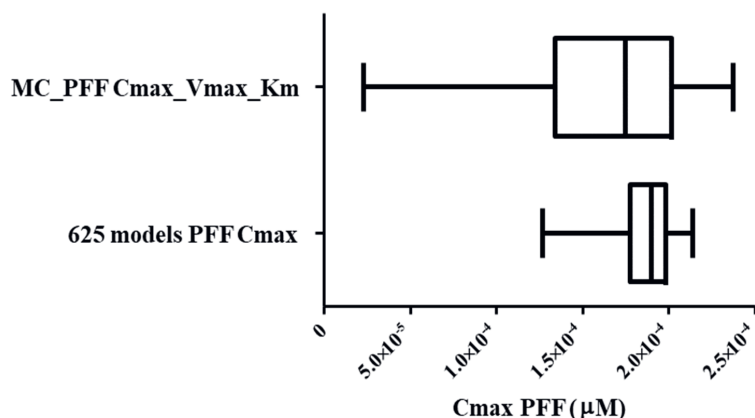


Figure 2. Box and whisker plot representing the distribution of the PFF maximum blood concentration (C<sub>max</sub>, unbound) at an oral dose of 0.01 mg/kg bw, referring to the predicted BMDL<sub>10</sub> of PFF from our previous study (Omwenga et al., 2021), predicted with the 625 individual PBK models from a combination of kinetic data obtained with 25 individual human liver S9 fractions and 25 individual human plasma samples (lower part figure). Also, the distribution in C<sub>max</sub> predicted with the PBK model linked with a Monte Carlo (MC) simulation for 10,000 individuals including the variation in V<sub>max</sub> and K<sub>m</sub> for PFF detoxification in the liver and human plasma metabolism is presented (upper part figure). The whiskers represent the 1<sup>st</sup> and 99<sup>th</sup> percentile of the C<sub>max</sub> of the virtual populations. The vertical lines of the box represent the 25<sup>th</sup> percentile, GM and the 75<sup>th</sup> percentile.

### 5.3.3 Predicted dose–response curve for the PFF-induced AChE inhibition

Figure 5 shows the predicted in vivo dose–response curves for AChE inhibition by PFF for the average and the most sensitive individuals of the simulated Caucasian population (GM, 95<sup>th</sup> and 99<sup>th</sup> percentile of the population). The dose-response curves of the sensitive individuals (95<sup>th</sup> and 99<sup>th</sup> percentile, were derived by applying the obtained values on the differences between these high percentiles and the GM of the population. Considering that a factor of 1.4 and 1.5 were used to derive the dose response curves for the 95<sup>th</sup> and the 99<sup>th</sup> percentile population, it was expected that the obtained BMDL10 related to PFF-induced AChE inhibition will be 1.4- and 1.5- fold lower in individuals within the 95<sup>th</sup> and 99<sup>th</sup> percentile in the virtual population than ‘an average Caucasian’. Indeed, the obtained BMDL10 values were 0.0085 mg/kg bw for the GM of the population (close to the BMDL10 of 0.010 mg/kg bw we predicted before for ‘an average Caucasian’ (Omwenga et al., 2021)), and 0.0060 mg/kg bw and 0.0057 mg/kg bw for the 95<sup>th</sup> and 99<sup>th</sup> percentiles respectively.

Comparing the predicted BMDL10 of 0.0057mg/kg bw for the 99<sup>th</sup> percentile with that of the regulatory bodies reveals a close similarity to the ARfD adopted by EFSA (2019) of 0.005 mg/kg bw (based on a German evaluation in 2001 that defined an ARfD based on a NOAEL in a dog study using inhibition of brain cholinesterase activity as critical effect) and is slightly higher than that of EPA (2016) of 0.002 mg/kg bw (based on RBC AChE inhibition with a BMDL10 of 1.99mg/kg/day, (EPA, 2016)). It is however 200-fold lower than the ARfD of 1mg/kg bw adopted by JMPR (2007) (based on RBC AChE inhibition, with a NOAEL of 100mg/kg/day (JMPR, 2007)).

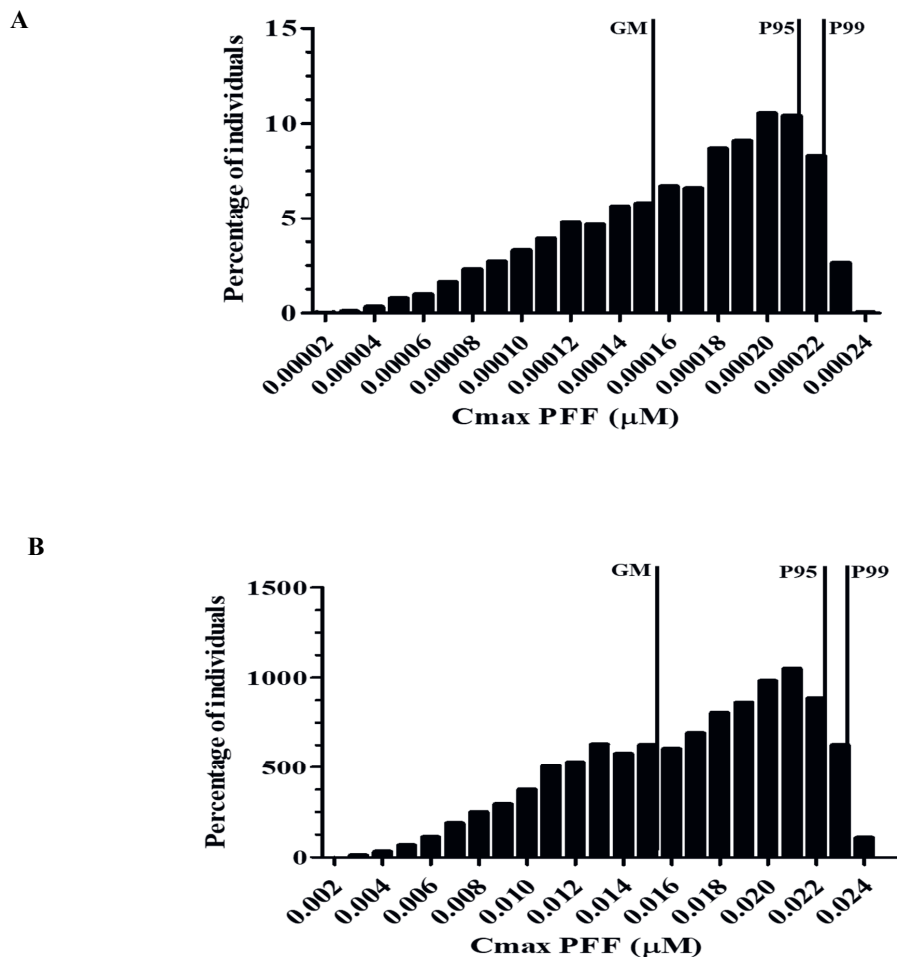


Figure 3. Frequency distribution for the maximum predicted unbound plasma concentration ( $C_{\text{max}}$ ) of PFF in 10000 individuals after Monte Carlo simulation including variation in  $V_{\text{max}}$  and  $K_m$  in PFF metabolism as measured with human liver S9 and plasma integrated in the PFF PBK model at A) our previously predicted BMDL10 of AChE inhibition of 0.01 mg/kg bw upon single exposure (Omwenga et al., 2021) and B) the ARfD of 1 mg/kg bw reported by JMPR (2007). The GM, P95, and P99 represent the geometric mean, the 95th and the 99th percentile of the distribution corresponding to 0.216, 0.2215, and 0.2283 pM for a dose of 0.01 mg/kg bw and 0.02207, 0.02275 and 0.0235  $\mu\text{M}$  for a dose of 1 mg/kg bw.

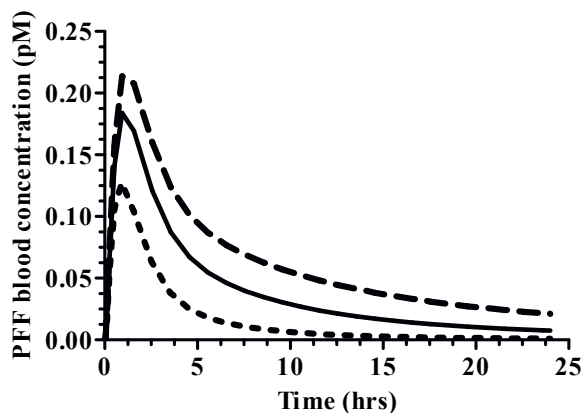


Figure 4. PBK model-predicted time-dependent unbound blood concentration of PFF at an oral PFF dose of 0.01 mg/kg bw in the virtual Caucasian population. The dashed line represents individuals in the population within the 99<sup>th</sup> percentile (lowest efficiencies in PFF detoxification) while the dotted line represents individuals in the 1<sup>st</sup> percentile (highest efficiencies in PFF detoxification). The average population is represented by the solid line (average detoxification).

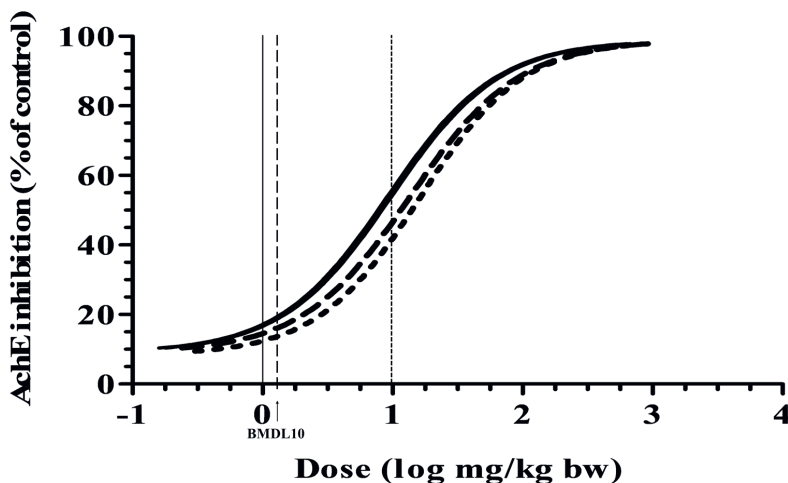


Figure 5. Predicted dose-response curves for PFF-induced decrease of AChE activity for the GM of the virtual human population (dashed line) and the sensitive individuals of that population (99<sup>th</sup> percentile population; continuous line). The dotted line represents the dose-response curve for PFF-induced AChE inhibition for the average human previously reported by our group (Omwenga et al., 2021). Acute reference doses (ARfDs) of 0.005mg/kg bw (EFSA, 2014), 0.002mg/kg bw (EPA, 2016) and 1mg/kg bw (JMPR, 2007) are included (vertical line, dashed line and dotted line respectively). The predicted BMDL10 of the 99<sup>th</sup> percentile (0.0057 mg/kg bw) is indicated by an arrow, being close to EFSA's ARfD.

#### 5.4. Discussion

This study was conducted to investigate the effect of the inter-individual human kinetic variation in PFF detoxification in a virtual Caucasian population by integrating in vitro kinetic data with PBK modelling and Monte Carlo simulations. The obtained differences in PFF C<sub>max</sub> values between the GM and the 90<sup>th</sup>, 95<sup>th</sup> and 99<sup>th</sup> percentile of this virtual population amounted



to 1.4-, 1.4- and 1.5-fold, respectively, indicating that expected differences between adult individuals are minor and well covered by the default uncertainty factor for human interindividual differences in kinetics (3.16). Translation of in vitro concentration-response data on PFF-induced AChE inhibition provided a BMDL10 value of 0.0085 and 0.0057 mg/kg bw for the GM and the 99<sup>th</sup> percentile of this virtual population, the former being close to the BMDL10 of 0.010 mg/kg bw obtained in our previous study for ‘an average Caucasian’ (Omwenga et al., 2021).

PFF, being an oxon, is mainly detoxified through hydrolysis by hepatic and plasma PON1 and CYP450-mediated detoxification, resulting in the production of BCP (FAO, 2012; EPA, 2016; Dadson et al., 2013). In addition, previous studies have reported the involvement of CYP in the formation of other PFF metabolites (Dadson et al., 2013), that are eventually also converted to BCP. In our previous study we assessed the liver biotransformation kinetics by assessing conversion by both microsomes and cytosol. Since both liver fractions showed conversion, we used liver S9 fractions in the present study, consisting of both microsomal and cytosolic proteins. Paraoxonase-1 (PON1) is an esterase synthesized by the liver and found in the plasma associated with high-density lipoproteins (Camps et al., 2009; Pyati et al., 2015). The enzyme (PON1) causes hydroxylation of oxygen analogues of OPs, aromatic esters and carbamate insecticides (Costa et al., 2005), and has been regarded as a good predictor of individual susceptibility to OP toxicity (Costa et al., 2013; Alejo-González et al., 2018; Dardiotis et al., 2019). Unlike CYP-mediated metabolism that occurs predominantly in the liver, PON1-mediated detoxification occurs to an important extent in the plasma due to PON-1 excretion from liver to blood (Pyati et al. 2015). Up to 200 single-nucleotide polymorphisms (SNPs) have been identified in PON1 in different regions (Harel et al. 2004; Darney et al., 2020) and polymorphisms in the PON1 gene have been reported to influence the expression levels and enzyme activity of PON1 (Jarvik et al., 2000; Li et al., 2000). Although the current study

indicates minor differences in PFF conversion in the different human samples, it must be taken into account that individuals may exist that show more distinct differences in PFF conversion, due to SNPs in PON1 that may result in different catalytic efficiencies.

The SNPs of the coding region at positions 192 (glutamine (Q) / arginine (R) substitution at codon 192) have been reported to result in different hydrolytic activities towards various substrates, including OPs such as PFF (Humbert et al., 1993). Moreover, the arginine (Arg, R) /glutamine (Gln, Q) substitution has been reported to affect PON1 substrate specificity (10-fold decrease in paraoxon hydrolyzing activity), a phenomenon hypothetically attributed to differences in docking sites on the enzyme (Darney et al., 2020). On the other hand, the leucine (Leu, L)/methionine (Met, M) substitution of the L55M SNP has been reported to affect the stability and enzymatic activity of PON1. Furthermore, variant alleles have been found to have a lower frequency than the wild-type allele for the Caucasian population (Ginsberg, 2013). For example, the 192R allele is present in 20–30% of subjects in the Caucasian population, and in similar percentages in the Turkish, Asian Indian, and Canadian Inuit populations (Ginsberg, 2013). Moreover, the \*55M allele has been found to have a lower frequency than \*55L in all populations for which there are data, with the allele frequency ranging from 3–9% in Asians to 26–38% in Caucasians (Ginsberg, 2013). In addition, the variability in the metabolic activity of PON1 may also be introduced by age and lifestyle in addition to polymorphisms (Ginsberg et al., 2009; Nalcakan et al., 2016). For example, previous studies showed that PON 1 activity is 24% lower in pre-term babies as compared to babies at term (Ecobichon and Stephens, 1973) and that the activity increases steadily until it reaches a plateau phase at about 6 months to a few years post-partum (Huen et al., 2010; Smith et al., 2011).

Comparing the differences obtained between the GM and the 99th percentile for the conversion of PFF to BCP obtained from the Monte Carlo simulations to the default uncertainty factor of 3.16 for inter-individual kinetic variation reveals that the default uncertainty factor may be

adequately protective for PFF-induced AChE inhibition in the adult Caucasian population now studied. However, it should be noted that it remains to be established whether this holds equally well for specific potentially sensitive groups of the population such as children or pregnant women. Such studies should also consider inclusion of other endpoints potentially relevant for specific sensitive subgroups, such as neurodevelopmental effects in the unborn child upon exposure of pregnant women, for which more complex and sensitive *in vitro* assays for reverse dosimetry may be required.

Our previous findings reported humans to be 40-fold more sensitive to PFF-induced AChE inhibition as compared to rats, mainly due to differences in kinetics. Recently, we demonstrated limited interspecies differences (rats vs humans) in PFF-induced AChE inhibition *in vitro* (Omwenga et al., 2021). Furthermore, Kasteel et al. (2020) reported limited interindividual differences in OP-induced AChE inhibition (Kasteel et al., 2020). Combining our previously determined interspecies factor of 40, to account for differences between rats and ‘an average human’, with the factor of 1.5 determined in the present study, accounting for differences between ‘an average human’ and sensitive adult individuals’, results in a factor of 60. Although this may suggest that applying the default uncertainty factor of 100 for differences between the experimental animal and sensitive human individuals to be protective when setting a point of departure from a rat study on PFF-induced AChE inhibition, it should be noted that sensitive populations including infants, children, youths, and women of childbearing age have not yet been considered. As indicated before, one should take into account that more sensitive individuals could exist than modelled in the present studies, when having SNPs in PON1 leading to decrease in function, which may lead to limited biotransformation and detoxification of PFF, resulting in relatively high internal exposure. Furthermore, it should be noted that in the current approach, only toxicokinetic variability in PFF detoxification was considered. Other kinetic factors may play a role in interindividual susceptibility to OP toxicity such as differences

in oral uptake rate, plasma protein binding and/or plasma: tissue partitioning. Also, one must take into account that for specific endpoints in sensitive subgroups, such as neurodevelopmental toxicity in the unborn child upon exposure of pregnant women, more complex and sensitive in vitro assays are required to adequately predict toxicity dose levels based on reverse dosimetry. In conclusion, the present study shows that linking Monte Carlo simulations with PBK modelling can be used to predict the effect of inter-individual human kinetic variation in PFF-induced AChE inhibition. Such information may be applied in the risk evaluation of chemicals, e.g. to provide supporting data for the derivation of CSAF values. Comparing the predicted BMDL10 of 0.0057 mg/kg bw for the 99th percentile with established health based guidance values reveals a close similarity to the ARfD adopted by EFSA (2019) of 0.005 mg/kg bw and by EPA (2016) of 0.002 mg/kg bw. Overall, the present study shows that integrating PBK modelling with Monte Carlo simulations is a powerful strategy to quantify interindividual variation in kinetics, which can be used to refine human risk assessment of OPs based on only human in vitro and in silico data.

### **Acknowledgements**

This work is supported by the Netherlands Universities Foundation for International Cooperation (Nuffic) (scholarship granted to Isaac Omwenga (PhD.17/0019)) and the Dutch Ministry of Agriculture, Nature and Food Quality (project KB-23-002-021).

### **Conflict of interest statement**

The authors declare that they have no conflicts of interest.

## REFERENCES

- Abass, K., Turpeinen M., Rautio A., Hakkola J. and Pelkonen O., 2012. Metabolism of pesticides by human cytochrome p450 enzymes in vitro—a survey. In *Insecticides—advances in integrated pest management*, pp. 165–194. InTech Open Access Publisher, New York, USA
- Alejo-González, K., Hanson-Viana, E., Vazquez-Duhalt, R., 2018. Enzymatic detoxification of organophosphorus pesticides and related toxicants. *J. Pestic. Sci.* 43, 1–9. <https://doi.org/10.1584/jpestics.D17-078>.
- Bahar, F.G., Ohura, K., Ogihara, T., Imai, T. 2012. Species difference of esterase expression and hydrolase activity in plasma. *J Pharm Sci* 101:3979-3988.
- Berry, L.M., Wollenberg, L., Zhao, Z., 2009. Esterase activities in the blood, liver and intestine of several preclinical species and humans. *Drug Metab Lett* 3:70–77.
- Carr, R.L, Dail M.B., Chambers, H.W., Chambers, J.E., 2015. Species differences in paraoxonase mediated hydrolysis of several organophosphorus insecticide metabolites. *J. Toxicol.* doi: 10.1155/2015/470189
- Camps, J., Marsillach, J., Joven, J., 2009. Measurement of serum paraoxonase-1 activity in the evaluation of liver function. *World J Gastroenterol.* 15(16):1929-33. doi: 10.3748/wjg.15.1929.
- Costa, L.G. 2006. Current issues in organophosphate toxicology. *Clin. Chim. Acta* 366:1–13.
- Costa, L. G., Vitalone, A., Cole T. B. and Furlong C. E., 2005. Modulation of paraoxonase (PON1) activity. *Biochem. Pharmacol.* 69, 541–550
- Costa, L.G., Giordano, G., Cole, T.B., Marsillach, J., Furlong, C.E., 2013. Paraoxonase 1 (PON1) as a genetic determinant of susceptibility to organophosphate toxicity. *Toxicology* 307, 115–122. <https://doi.org/10.1016/j.tox.2012.07.011>.
- Dadson, O.A., Ellison, C.A., Singleton, S.T., Chi, L., McGarrigle, B.P., Pamela, J., Lein, J.P., Farahat, F.M., Farahat, T., Olson, J.R., 2013. Metabolism of profenofos to 4-bromo-2-chlorophenol, a specific and sensitive exposure biomarker. *Toxicology* 306:35– 39
- Dardiotis, E., Aloizou, A.-M., Siokas, V., Tsouris, Z., Rikos, D., Marogianni, C., Aschner, M.,

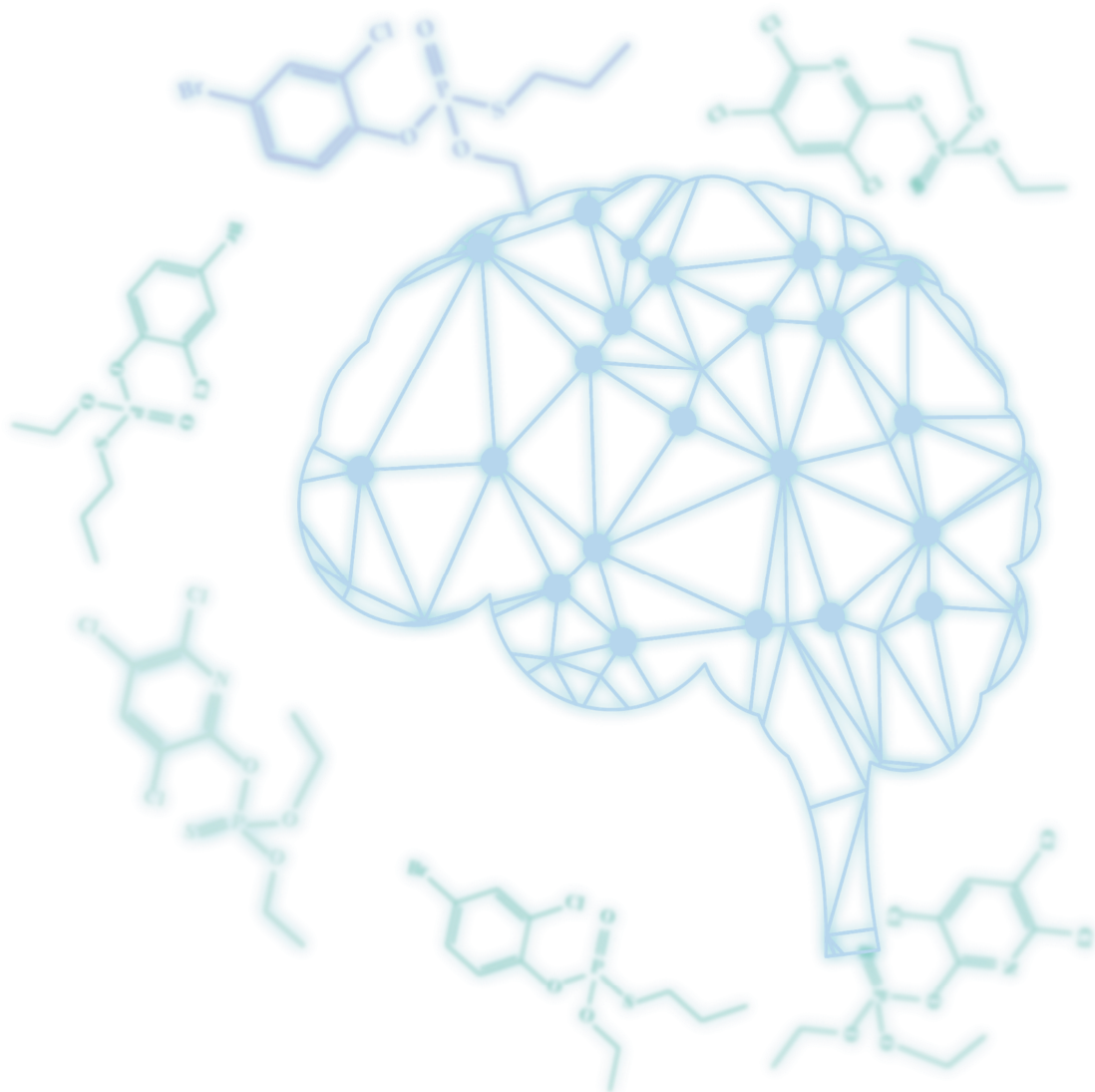
- Kovatsi, L., Bogdanos, D.P., Tsatsakis, A., 2019. Paraoxonase-1 genetic polymorphisms in organophosphate metabolism. *Toxicology* 411, 24–31. <https://doi.org/10.1016/j.tox.2018.10.012>.
- Darney, K., Kasteel, E.E.J., Buratti, F.M., Turco, L., Vichi, S., Béchaux, C., Roudot, A.C., Kramer, N.I., Testai, E., Dorne, J.L.C.M., Di Consiglio, E., Lautz, L.S., 2020. Bayesian meta-analysis of inter-phenotypic differences in human serum paraoxonase-1 activity for chemical risk assessment. *Environ Int.* 2020
- Ecobichon, D.J., Stephens, D.S., 1973. Perinatal development of human blood esterases. *Clin. Pharmacol. Ther.* 14, 41–47. <https://doi.org/10.1002/cpt197314141>.
- Ecobichon, D.J., Comeau, A.M., 1973. Pseudocholinesterases of mammalian plasma: Physicochemical properties and organophosphate inhibition in eleven species. *Toxicol Appl Pharmacol* 24:92-100.
- Edwards, T. M. and Myers, J. P., 2008. Environmental exposures and gene regulation in disease etiology. *Cien Saude Colet.* 13,269–281.
- EPA, 2016. Profenofos: Human health draft risk assessment(DRA) for registration review. [https://www3.epa.gov/pesticides/chem\\_search/cleared\\_reviews/csr\\_PC-111401\\_19-Oct-16.pdf](https://www3.epa.gov/pesticides/chem_search/cleared_reviews/csr_PC-111401_19-Oct-16.pdf). (accessed on 12/3/2020).
- FAO, 2012. Food and Agriculture Organization of the United Nations (2012) [http://www.fao.org/fileadmin/templates/agphome/documents/Pests\\_Pesticides/JMPR/Evaluation08/Profenofos.pdf](http://www.fao.org/fileadmin/templates/agphome/documents/Pests_Pesticides/JMPR/Evaluation08/Profenofos.pdf). Accessed 2012/08.
- Fire, A., Kostas, S., Montgomery, M., Timmons, L., Xu, S., Tabara, H. *et al.*, 2013. Genetic inhibition by double-stranded RNA. US Patent No. 20,130,029,425.
- Ginsberg, G., Neafsey, P., Hattis, D., Guyton, K.Z., Johns, D.O., Sonawane, B., 2009. Genetic polymorphism in paraoxonase 1 (PON1): Population distribution of PON1 activity. *J. Toxicol. Environ. Health B Crit. Rev.* 12, 473–507. <https://doi.org/10.1080/10937400903158409>.
- Guengerich, F. P., 1993 Cytochrome p450 enzymes. *Am. Sci.* 81,440–447.
- Hertz-Picciotto, I., Sass, J.B., Engel, S., Bennett, D.H., Bradman, A., Eskenazi, B., Lanphear, B., Whyatt, B., 2018. Organophosphate exposures during pregnancy and child neurodevelopment: Recommendations for essential policy reforms. *PLoS Med* 15(10): e1002671. <https://doi.org/10.1371/journal.pmed.1002671>
- Hodgson, E., 2012 Biotransformation of individual pesticides: some examples. In *Pesticide biotransformation and disposition*, Chap. 9, 3rd edition, pp. 195–207, Academic Press, Elsevier Oxford, UK.

- Huen, K., Harley, K., Bradman, A., Eskenazi, B., Holland, N., 2010. Longitudinal changes in PON1 enzymatic activities in Mexican-American mothers and children with different genotypes and haplotypes. *Toxicol. Appl. Pharmacol.* 244, 181–189. <https://doi.org/10.1016/j.taap.2009.12.031>.
- Humbert, R., Adler D. A., Disteché C. M., Hassett C., Omiecinski C. J. and Furlong C. E., 1993 The molecular basis of the human serum paraoxonase activity polymorphism. *Nat. Genet.* 3, 73–76.
- Kasteel, E.E.J., Nijmeijer, S.M., Darney, K., Lautz, L.S., Dorne, J.L.C.M., Kramer, N.I., Westerink, R.H.S., 2020. Acetylcholinesterase inhibition in electric eel and human donor blood: an in vitro approach to investigate interspecies differences and human variability in toxicodynamics. *Arch Toxicol.* 2020 Dec;94(12):4055-4065.
- Koda, Y., Tachida, H., Soejima, M., Takenaka, O., Kimura, H., 2004. Population differences in DNA sequence variation and linkage disequilibrium at the PON1 gene. *Ann. Hum. Genet.* 68, 110–119. <https://doi.org/10.1046/j.1529-8817.2003.00077.x>.
- International Programme on Chemical Safety (IPCS), 2005. Chemical- specific adjustment factors for interspecies differences and human variability: guidance document for use of data in dose/ concentration-response assessment. WHO, Geneva
- Jarvik, G. P., Rozek L. S., Brophy V. H., Hatsukami T. S., Richter R. J., Schellenberg G. D. et al. 2000. Paraoxonase (PON1) phenotype is a better predictor of vascular disease than is PON1192 or PON155 genotype. *Arterioscler. Thromb. Vasc. Biol.* 20, 2441–2447.
- Kaur, G, Jain AK, Singh, S., 2017. CYP/PON genetic variations as determinant of organophosphate pesticides toxicity. *J Genet.* 96(1):187-201.
- Lionetto, M.G., Caricato, R., Calisi, A., Giordano, M.E., Schettino, T., 2013. Acetylcholinesterase as a biomarker in environmental and occupational medicine: new insights and future perspectives. *Biomed Res. Int.* 2013, 321213. <https://doi.org/10.1155/2013/321213>.
- Liu, C., Bednarska A. J., Sibly R. M., Murfitt R. C., Edwards P. and Thorbek P. 2013

- Incorporating toxicokinetics into an individual based model for more realistic pesticide exposure estimates: a case study of the wood mouse. *Ecol. Model.* 280:30–39.
- Li, W. F., Costa L. G., Richter R. J., Hagen T., Shih D. M., Tward A. et al. 2000 Catalytic efficiency determines the in vivo efficacy of PON1 for detoxifying organophosphates. *Pharmacogenetics* 10, 1–13.
- Li, B., Sedlacek, M., Manoharan, I., Boopathy, R., Duysen, E.G., Masson, P., Lockridge, O., 2005. Butyrylcholinesterase, paraoxonase, and albumin esterase, but not carboxylesterase, are present in human plasma. *Biochem Pharmacol* 70:1673-1684.
- Mohamed, A., S., Chia, S.E., 2008. Interethnic variability of plasma paraoxonase (PON1) activity towards organophosphates and PON1 polymorphisms among Asian populations—a short review. *Ind. Health* 46:309–317.
- Nalcakan, G.R., Varol, S.R., Turgay, F., Nalcakan, M., Ozkol, M.Z., Karamizrak, S.O., 2016. Effects of aerobic training on serum paraoxonase activity and its relationship with PON1-192 phenotypes in women. *J. Sport Health Sci.* 5 (4):462–468.
- Ning, J., Rietjens, I.M.C.M., Strikwold, M., 2019. Integrating physiologically based kinetic (PBK) and Monte Carlo modelling to predict inter-individual and inter-ethnic variation in bioactivation and liver toxicity of lasiocarpine. *Arch Toxicol.* 2019 Oct;93(10):2943-2960
- Pesticide Action Network (2017) International Consolidated List of Banned Pesticides 2017 [Accessed November 9, 2019]. Available from: <http://pan-international.org/pan-international-consolidated-list-of-bannedpesticides/>
- Punt, A., Jeurissen, S.M., Boersma, M.G., Delatour, T., Scholz, G., Schilter, B., van Bladeren, P.J., Rietjens, I.M., 2010. Evaluation of human interindividual variation in bioactivation of estragole using physiologically based biokinetic modelling. *Toxicol Sci.* 2010 Feb;113(2):337-48.
- Pyati, A.K., Halappa, C.K., Pyati, S.A. 2015. Serum basal paraoxonase 1 activity as an additional liver function test for the evaluation of patients with chronic hepatitis. *J Clin Diagn Res JCDR* 9:BC12
- Rahmioglu, N., Heaton, J., Clement, G., Gill, R., Surdulescu, G., Zlobecka, K., Hodgkiss, D.,



- Ma, Y., Hider, R.C., Smith, N.W., Ahmadi, K.R. 2011. Genetic epidemiology of induced CYP3A4 activity. *Pharmacogenetic Genom* 21:642–651
- Robb EL, Baker MB. Organophosphate Toxicity. [Updated 2020 Jul 27]. In: StatPearls [Internet]. Treasure Island (FL): StatPearls Publishing; 2021 Jan-. Available from: <https://www.ncbi.nlm.nih.gov/books/NBK470430/>
- Satoh, T., Hosokawa, M., 2006. Structure, function and regulation of carboxylesterases. *Chem Biol Interact* 162:195-211.
- Smith, J.N., Timchalk, C., Bartels, M.J., Poet, T.S., 2011. In vitro age-dependent enzymatic metabolism of chlorpyrifos and chlorpyrifos-oxon in human hepatic microsomes and chlorpyrifos-oxon in plasma. *Drug Metab. Dispos.* 39:1353–1362. <https://doi.org/10.1124/dmd.111.038745>.
- Sözmen B., Peker S., Kaya Ü., Erkan M. and Sözmen E. Y. 2007 Markers of long-term exposure to organophosphorus pesticides in farmers who work in viniculture and tobacco production in turkey. *Toxicol. Mech. Meth.* 17:379–384.
- Strikwold M, Spenkeliink B, Woutersen RA, Rietjens IMCM, Punt A. Development of a Combined In Vitro Physiologically Based Kinetic (PBK) and Monte Carlo Modelling Approach to Predict Interindividual Human Variation in Phenol-Induced Developmental Toxicity. *Toxicol Sci.* 2017 Jun 1;157(2):365-376.
- van der Veen I, de Boer J. Phosphorus flame retardants: properties, production, environmental occurrence, toxicity and analysis. *Chemosphere.* 2012 Aug;88(10):1119-53.
- Williams, E.T., Bacon, J.A., Bender, D.M., Lowinger, J.J., Guo, W.K., Ehsani, M.E., Wang, X., Wang, H., Qian, Y.W., Ruterbories, K.J., Wrighton, S.A., Perkins, E.J., 2011. Characterization of the expression and activity of carboxylesterases 1 and 2 from the beagle dog, cynomolgus monkey, and human. *Drug Metab Dispos* 39:2305-2313
- Zhang, X., Tsang, A.M., Okino, M.S., Power, F.W., Knaak, J.B., Harrison, L.S., Dary, C.C. 2007. A physiologically based pharmacokinetic/ pharmacodynamic model for carbofuran in Sprague–Dawley rats using the exposure-related dose estimating model. *Toxicol Sci* 100:345–359



# CHAPTER 6.

General Discussion and Future Perspectives

## GENERAL DISCUSSION AND FUTURE PERSPECTIVES

### 6.1 Overview and discussion of the results

Pesticides are chemical substances that are primarily used to prevent, kill or control the growth of pests including insects, rodents and certain kind of animals that can damage crops as well as unwanted plant growth and fungi that can eventually damage the crops (Kaushal et al., 2021). The present thesis focussed on organophosphate pesticides (OPs). Epidemiological studies have linked chronic OP exposure to reproductive disorders, developmental toxicity, birth defects, cancer, Parkinson's disease, Alzheimer's disease, diabetes, chronic respiratory disease, cardiovascular diseases, chronic nephropathies and amyotrophic lateral sclerosis (ALS) (Mostafalou & Abdollahi, 2013). Due to the extensive use for agricultural produce, OPs have found their way in the ground water and rivers through run off agricultural water and run off from the surface of the plants that have been sprayed with these pesticides. Human exposure to OPs is mainly through diet (González-Alzaga et al., 2014; Costa, 2018). To date, the acute reference dose (ARfD) values of OPs have mainly been derived from data obtained for the inhibition of red blood cell (RBC) AChE activity as the surrogate for brain AChE activity, and are based on points of departure (PODs) like a benchmark dose (BMD), its lower confidence limit (BMDL) or a no observed adverse effect level (NOAEL) for this adverse effect. RBC AChE is more sensitive and easier to sample compared with AChE in other target organs like the spinal cord, brain and the peripheral nervous system (EPA, 2011). The current thesis aimed at developing non-animal approaches in OP risk assessment and application of these novel methods to predict the potential of the OPs to inhibit AChE in vivo upon acute exposure, also taking combined exposure into account. Furthermore, this thesis aimed to obtain data on the occurrence of OPs on commonly consumed vegetables in Kenya, as such data, and related estimations of human exposure, are lacking.

The use of chemical pesticides is indispensable in Kenya due to the hot and humid tropical environmental conditions that are conducive to the development of pests, weeds, and disease vectors (Omwenga et al., 2016). Chemical use is on the rise, especially use of fertilizers, veterinary chemicals and pesticides, in an attempt to increase agricultural produce to feed the rapidly increasing population, provide raw materials for the food related industries as well as earn foreign exchange (NIP, 2006). Vegetables provide vitamins, minerals and active compounds known to reduce the effect of cardiovascular diseases (Ivey et al., 2015). According to the WHO, vegetables and fruits constitute on average 30% of food consumption (WHO, 2003). In Kenya, it is estimated that fresh fruits and vegetables constitute 25% and >80% of the diets in the urban and the rural areas, respectively (Mungai et al., 2000; Kunyanga et al., 2018). Among them, kales (*Brassica oleraceae var acephala*), spinach (*Spinacia oleracea*), tomatoes (*Solanum lycopersicum*) and to a lesser extent French beans (*Phaseolus vulgaris*) are the most common vegetables used in various dishes (Karanja et al., 2012; Okello et al., 2012; Mutai et al., 2015; RSA, 2015; Njuguna et al., 2019). Like most countries, vegetable production in Kenya relies on extensive use of pesticides to control insect pests. Monitoring pesticide residues in vegetables is therefore key in determining and mitigating possible risks to human health from daily dietary pesticide exposure of consumers (Curl et al., 2003). Developed countries such as the USA, Canada and the EU have implemented pesticide monitoring programs. However, little effort has been focused on monitoring of pesticides exposure of the agricultural workers and local consumers in developing countries, leading to paucity of data on pesticide residue levels and the resulting adverse effects (Ecobichon, 2001). Many studies have reported on the levels of pesticide residues in various food products, including milk products (Golge et al., 2018), poultry and sheep fat (EFSA, 2019a), cereal (Lozowicka et al., 2014; EFSA, 2019a), olive oils (Razzaghi et al., 2018), fish (Sapozhnikova, 2014), and fruit and vegetables from various countries including Korea (Lee and Lee, 2012), Chile (Elgueta et al., 2019), Indonesia

(Bhandari et al., 2019), China (Wang et al., 2019; Jiang et al., 2021), EU countries (EFSA 2019a), Turkey (Hepsağ and Kizildeniz, 2021), Canada (Wang et al., 2019) and the USA (Baker et al., 2002; Hu et al., 2016; Chiu et al., 2018). However, few data are available on the presence and levels of pesticide residues in vegetables consumed in Kenya (Ngatia and Kabaara, 1976; Karembu, 1991; Karanja et al., 2012; Mutai et al., 2015; Kunyanga et al., 2018). This thesis therefore assessed OP and carbamate pesticide residues in tomatoes, kales, spinach and French beans and the associated dietary exposure and potential health risks to children and adults in Kenya upon acute and chronic exposure (**Chapter 2**). A total of 90 samples, collected in peri-urban Nairobi, Kenya, were analysed by liquid chromatography/high resolution tandem mass spectrometry. Residues of acephate, chlorpyrifos (CPF), methamidophos, omethoate and profenofos (PFF) were found in 22% of the samples, at levels ranging from 10 to 1343 µg/kg. The EU MRL for these OPs was exceeded in 21%, 10%, 8% and 22% of the samples of French beans, kales, spinach, and tomatoes, respectively. CPF in spinach had an acute Health Quotient (HQ) of 3.3 and 2.2 for children and adults, respectively, implying that potential health risks with respect to acute dietary exposure cannot be excluded. For chronic dietary exposure, all chronic HQs were below 1. The Health Index (HI) for the pesticides, i.e. the sum of the chronic HQs, was 0.54 and 0.34 for children and adults, respectively. The risk assessments corroborate the need to continue routine monitoring of OPs and carbamates in vegetables to minimize consumer's health risks, considering the high vegetable consumption among the Kenyan population and the fact that pesticide use is indispensable in Kenya due to the hot and humid tropical environmental conditions that are conducive to the development of pests, weeds, and disease vectors (Omwenga et al., 2016).

In the hazard and risk assessment of OPs, *in vivo* animal studies on OP-induced inhibition of AChE have been used to derive a point of departure (POD) to set safe exposure levels, such as an Acute Reference Dose (ARfD). ARfDs for CPF, acephate, methamidofos, omethoate and

PFF as reported by organizations as EFSA, EPA and the JMPR have been derived from data on OP-induced AChE inhibition from animal studies (JMPR, 2007; EPA, 2006; EPA 2011; EPA, 2016; EFSA, 2019b). However, the reliance on approaches based on animal experimentation has its drawbacks in terms of economical, ethical and scientific limitations. Therefore, an important aim of the present thesis was to assess whether *in vivo* dose-dependent OP-induced AChE inhibition can be predicted by an animal-free approach (**Chapter 3, 4 and 5**). In order to inhibit AChE in the *in vivo* situation, the OP needs to reach its target (AChE) at sufficiently high concentrations. The *in vivo* potency of an OP to inhibit AChE is thus dependent on its intrinsic ability (potency) to inhibit AChE and the amount of OP that reaches that target. To estimate the amount of OP that reaches the target, so-called physiologically based kinetic (PBK) models can be used. PBK modelling-based reverse dosimetry can support the prediction of toxic dose levels based on *in vitro* toxicity data by enabling quantitative *in vitro in vivo* extrapolation (QIVIVE) (Louisse et al., 2017; Paini et al., 2019).

PBK models have been developed for various OPs including CPF (Timchalk et al., 2002; Bouchard et al., 2005; Mosquin et al., 2009; Lu et al., 2010; Zhao et al., 2019), malathion (Bouchard et al., 2003; Bogen and Singhal, 2017; Bouchard et al., 2017), parathion (Sultatos, 1990) and diazinon (Poet et al., 2004). At the start of this thesis work, no PBK model had been built for the OP PFF, despite its widespread use in developing countries and reported cases of human accidental poisoning (Gotoh et al., 2001; Eddleston et al., 2009). In addition, PFF was the most frequently encountered pesticide residue in vegetables sampled in peri-urban Nairobi, Kenya at the initial stages of this study (**Chapter 2**). Therefore, in the present thesis a PBK model was developed for PFF in rat and human (**Chapter 3**). The rat PBK model was evaluated against literature data on urinary excretion of conjugated 4-bromo-2-chlorophenyl (BCP) (Cho et al., 2002). To facilitate PBK model based quantitative *in vitro* to *in vivo* extrapolation (QIVIVE), concentration-dependent inhibition of rat and human AChE was determined *in vitro*

and these data were translated with the PBK models to predicted dose-dependent AChE inhibition curves in rats and humans *in vivo*. When the predicted dose-response curve for PFF-induced AChE inhibition in rats was compared to literature data, the prediction of the *in vivo* effect levels appeared accurate. Comparison of rat predictions (the BMDL10 of the predicted dose-response curve being 0.45 mg/kg bw) and human predictions (the BMDL10 of the predicted dose-response curve being 0.01 mg/kg bw) suggested humans to be more sensitive than rats. The PBK models revealed that this difference appeared to be mainly due to higher catalytic efficiencies for microsomal, cytosolic and plasma biotransformation of PFF to BCP in rats as compared to humans. PFF, being an oxon, is mainly detoxified through hydrolysis by hepatic and plasma paraoxonase 1 (PON1) and cytochrome P450 (CYP450)-mediated detoxification, resulting in the production of BCP (JMPR, 2007; EPA, 2016; Dadson et al., 2013). Interspecies differences in activities between human and rat PON1 have indeed been reported, with human PON1 having lower catalytic activity as compared to rat PON1 (Kaliste-Korhonen et al., 1996). Another possible reason for the differences in PFF detoxification may be related to quantitative differences in B-esterases in rats and humans, which may affect the metabolism and disposition of ester compounds including OPs (Ecobichon and Comeau, 1973; Maxwell et al., 1987). B-esterases, such as carboxylesterase (CaE), butyrylcholinesterase (BuChE) and acetylcholinesterase (AChE), detoxify oxons, but these enzymes are inhibited by the oxons as a consequence (Chanda et al., 1997). In this way, B-esterases may play a protective role in rats but not humans. It has been reported that rat plasma contains almost all types of esterases including CaE, PON1, BChE, and AChE (Bahar et al., 2012; Satoh and Hosokawa, 2006), whereas humans are deficient of plasma CaE (Williams et al., 2011; Berry et al., 2009; Li et al., 2005) and plasma AChE (Ecobichon and Comeau, 1973). The absence of CaE in human plasma in addition to low PON1 activity may therefore be responsible for lower PFF



clearance resulting in higher sensitivity of humans to PFF as compared to rodents (Kaliste-Korhonen et al., 1996).

As earlier indicated, human exposure to OPs originates mainly from ingestion via residues on food (Bradman et al., 2003; Suratman et al., 2015; EFSA, 2019a). Since a variety of pesticides is being used, environmental, occupational and dietary exposures are primarily to pesticide mixtures. Consequently, there is lifelong combined exposure to various pesticides from, for example, one food item containing multiple compounds or combinations of food items, each containing different residues (Boobis et al., 2008). If these pesticides have a similar mechanism of action and toxic endpoint, assessing the dietary risk of exposure for each pesticide separately may lead to underestimation of the health risk (Boon et al., 2008). Therefore, current approaches in pesticide risk assessment include cumulative and probabilistic approaches in order to include the amount and variety of pesticide residues likely to be present in the vegetable sample (Jensen et al., 2013; Boon et al., 2015; Elgueta et al., 2019). The first step in assessing effects of combined exposure to pesticide mixtures is to identify substances with a similar mechanism underlying their toxicity (Gallagher et al., 2015; EFSA, 2019a). For chemicals in the same cumulative assessment group (CAG), the current scientific and regulatory recommendations for the risk assessment of mixtures follows a test strategy based on a component-based assessment, a concept with dose addition as the default model (EFSA, 2019; Bopp et al., 2015; EFSA, 2013; Kortenkamp et al., 2009). As reported in Chapter 2 of this thesis, PFF and CPF were the most frequently detected pesticide residues in commonly consumed vegetables in Kenya (Omwenga et al., 2021a). In the same study, co-occurrence of PFF and CPF was reported in some of these vegetables including tomatoes (Omwenga et al., 2021a). PFF and CPF are both OPs assigned to the CAG related to brain and/or red blood cell (RBC) AChE inhibition (EFSA et al., 2019). Consequently, consumers can be concurrently exposed to these OPs and knowledge on adverse effects upon combined exposure is desirable. In **Chapter 4**, combination effects of PFF and

CPF were determined, by studying the combined effects of PFF and CPF's toxic metabolite CPF oxon (CPO) on AChE inhibition *in vitro*, as well as the effects of CPF and CPO on PFF biotransformation (detoxification) by human liver microsomes, cytosol, and human plasma. AChE inhibition was shown to be 199-fold more potent by CPO than by PFF, and combined exposure to CPO and PFF resulted in effects that are in line with the principles of dose addition. CPF and CPO appeared to affect PFF detoxification to its main metabolite (BCP) in a non-competitive manner at high concentrations, with  $K_i$  values of 120, 256 and 473  $\mu\text{M}$  for CPF, and 80, 63 and 326  $\mu\text{M}$  for CPO, for liver microsomes, liver cytosol and plasma, respectively, concentrations far higher than *in vivo* relevant concentrations. The PBK model of PFF (Chapter 3) was extended to include the description of CPF kinetics, using *in vitro* kinetic data from the literature and *in silico* calculations. PFF concentrations in the model were expressed in CPO-equivalents allowing prediction of total internal CPO-equivalents upon combined exposure to PFF and CPF. The model adequately predicted the AChE inhibition in a hospitalized person with CPF poisoning as reported in the literature (Drevenkar et al., 1993). Combined exposure to PFF and CPF at their ARfD (0.005 mg/kg bw ; NB: the latest reported ARfD of PFF (EFSA, 2019b) was used in this study, being lower than the ARfD applied in chapter 2) was predicted to not affect AChE activity.

In developing the PBK models, pooled human liver fractions and plasma were used to derive the *in vitro* kinetic data for the detoxification of PFF, hence the resulting predictions were for 'an average human'. Therefore, we could not take interindividual differences into account, which may occur as a result of differences in kinetic processes between individuals. In general, a default uncertainty factor of 3.16 is applied to account for human variation in toxicokinetics (IPCS, 2005). However, having more detailed insights in possible interindividual variation might provide risk assessors a more science-based approach to derive factors accounting for intraspecies and interspecies differences in toxicokinetics, which may be applied to define

chemical specific adjustment factors (CSAFs) for chemicals. The final experimental chapter (**Chapter 5**) of this thesis therefore aimed to predict interindividual differences in PFF detoxification. To that end, PFF conversion to BCP was studied in *in vitro* incubations with liver S9 fractions of 25 different Caucasian donors and with plasma samples of 25 different Caucasian donors. The obtained information on the variation in the *in vitro* kinetic constants  $V_{max}$  and  $K_m$  was combined with the PBK model developed in Chapter 3 using a Monte Carlo simulation modelling approach. Analysis of the predicted internal maximum concentrations of PFF in the simulated population indicated a 1.4-, 1.4- and 1.5-fold difference between the geometric mean (GM) and the 90th, 95th and 99th percentile, respectively, of the simulated population. These factors are below the default uncertainty factor accounting for human variability in toxicokinetics of 3.16. Concentration-response curves for inhibition of human AChE determined *in vitro* were translated with the PBK models to predicted dose-dependent AChE inhibition in humans *in vivo*. In line with the differences in  $C_{max}$  values, the 99th percentile of the population was predicted to be 1.5-fold more sensitive to PFF-induced AChE inhibition than the GM of the population based on the BMDL10 values of predicted dose-response data for the virtual populations. Comparing the predicted BMDL10 of 0.0057 mg/kg bw for the 99th percentile with health based guidance values proposed by the regulatory bodies reveals a close similarity to the ARfD reported by EFSA, (2019) of 0.005 mg/kg bw, based on a German evaluation, and being slightly higher than the ARfD adopted by EPA, (2016) of 0.002 mg/kg bw. It is, however, 200-fold lower than the ARfD of 1 mg/kg bw adopted by JMPR, (2007). Interestingly, EFSA (2019 b) mentioned that “Due to the limited details available in the JMPR Report and the German evaluation, a final conclusion on the acceptability of the toxicological reference values derived by the two bodies cannot be made”. The results from this thesis would support the use of the ARfD of 0.005 mg/kg bw rather than the ARfD of 1 mg/kg bw, as at 1 mg/kg bw clear PFF-induced AChE inhibition was predicted in humans. Altogether,

the results obtained demonstrate that integrating PBK modelling with Monte Carlo simulations using human in vitro data provides a powerful strategy to quantify human interindividual variation in kinetics, which can be used to refine the hazard characterization of OPs.

Given the results of the present thesis, several topics are discussed to a further extent in the next sections, including:

- Pesticide residue levels and their health concerns following exposure via vegetables from urban areas of Kenya
- Use of alternative testing strategies and how they can be used to develop PODs to set health based guidance values for OPs
- Use of PBK modelling coupled to Monte Carlo analysis to study inter-individual human kinetic differences in metabolism and toxicity of OPs
- Risk assessment of combined exposure to OPs and to OPs together with other types of pesticides
- OPs and long term effects considering neurodegenerative diseases including Parkinsonism
- Future perspectives

## **6.2 Pesticide residue levels in vegetables from urban areas of Kenya and their health concerns following exposure**

Studies worldwide reveal that infants, adults, and the elderly are exposed to pesticide residues as a consequence of their presence in food (Smegal, 2000; Risher and Navarro, 1997). The OPs and carbamates produce their effects by inhibiting acetylcholinesterase (AChE), the enzyme that terminates the action of the neurotransmitter acetylcholine (ACh) within neuromuscular junctions and nerve tissue, leading to overstimulation of the post-synaptic membrane (Timchalk

and poet, 2008). Reported effects related to exposure to OPs vary from mild short-term impacts such as nausea and headaches to chronic effects such as infertility, birth defects, blood disorders, nerve disorders, endocrine disruption and reproductive effects (Mansour, 2004; Alavanja et al., 2013).

Due to their health effects, OP residues in crops, food, and food by-products especially residues exceeding the Maximum Residue Levels (MRL) can be a threat to health and international trade (Zhang et al., 2008). Consequently, pesticide monitoring programmes have been implemented in various countries of the world. However, this is not in place in Kenya, and as a result few data are available on the presence and levels of pesticide residues in vegetables consumed in Kenya (Ngatia and Kabaara, 1976; Karembu, 1991; Karanja et al., 2012; Mutai et al., 2015; Kunyanga et al., 2018).

In chapter 2, this thesis reports OP residues in tomatoes, kales, spinach and French beans and the associated dietary exposure and potential health risks to children and adults upon acute and chronic exposure. PFF and CPF were among the most frequently encountered OPs among the screened vegetables. These findings corroborate those of previous studies involving pesticide screening in vegetables in peri urban Nairobi that reported PFF (Karanja et al., 2012) and CPF (Kunyanga et al., 2018) as the most frequently detected pesticides among others. Kunyanga et al., (2012) reported PPF levels of 4100 µg/kg in kales. These levels are four fold higher compared to those reported in tomatoes in our study (960 µg/kg) collected from peri-urban Nairobi. However, no PFF was detected in kales in this study. Furthermore, Kunyanga et al., (2012) reported CPF levels of 30 µg/kg in amaranth leafy vegetable, levels lower as compared to those from our study in the range of 78 to 107 µg/kg in tomatoes (11 % of samples), 26 to 315 µg/kg in kales (7% of samples), and 24-1,343 µg/kg in spinach (8% of samples), respectively. Another study by Karanja et al., (2012) reported levels of PFF, diazinon,

cypermethrin and bitertanol above EU permissible limits in kales in peri-urban Nairobi. Routine monitoring of OPs in vegetables is recommended to minimize consumer's potential health risks. In order to characterize health risks associated with consumption of the vegetables in children and adults, chapter 2 determined the hazard quotients (HQs) for the detected pesticides. CPF was found to have an acute HQ of 3.3 and 2.2 for children and adults, respectively, implying that potential health risks with respect to acute dietary exposure cannot be excluded (Chapter 2). When using the JMPR ARfD of 1 mg/kg for determination of the HQ of PFF in tomatoes, all HQs were below 1, implying no risk to consumers. However, when the recent EFSA-reported ARfD of 0.005mg/kg was used, the HQs were 2.33 and 1.53 for children and adults respectively, again calling for urgent monitoring of pesticide residues in Kenyan vegetables. This therefore indicates the variability in risk assessment when different human health based guidance values from different regulatory authorities are used. In future, for a more harmonized risk assessment, the PODs should be harmonized. EFSA (2019b) mentions that "a final conclusion on the acceptability of the toxicological reference values derived by the two bodies cannot be made". The present study supports the use of the ARfD of 0.005 mg/kg bw, showing the added value of this NAM-based approach for the hazard characterization. When risk assessment of PFF in kales was conducted in this thesis based on reported PFF levels in the study of Kunyanga et al. (2012) was conducted, HQ values of 9.98 and 6.56 were obtained for children and adults, a finding that urgently calls for monitoring of the pesticide levels since kales are among the commonly consumed vegetables in Kenya. In addition, training of farmers on better use of PFF should be conducted in order to reduce PFF residues levels in kales. Pesticide residues need to comply with MRLs which are based on Good Agricultural Practice (GAP). Since GAP may differ in different countries, also MRLs can differ. Exceedance of local MRLs are an indication that local GAP is not well followed. There are no national MRLs in Kenya, and this could lead to inadequate monitoring of pesticide residues in vegetables. Failure

to follow GAP may lead to exposure of consumers to higher than maximum allowable limits, which may lead to adverse health effects (Zhang et al., 2008). In addition, MRL exceedances may impede trade leading to reduced export of the vegetable produce to the EU and other trade partner countries (Ngolo et al., 2019). For example, Kenya is one of 14 countries listed in the 2017 European Food Safety Agency report (2019) in which Maximum Residue Limits (MRLs) were exceeded in more than 10 % of samples tested. In that report, high residues above the European MRLs were detected in kales, tomatoes and water (Ngolo et al., 2019).

The MRL exceedances reported in chapter 2 could be due to failure to adhere to the withdrawal intervals, which may lead to increased human pesticide exposure (Ntow et al., 2006; Darko & Akoto, 2008; Akoto et al., 2015; Bujwa and Sandhu, 2014). Failure to adhere to pre-harvest intervals and other indiscreet agricultural practices like pesticide use above recommended doses may be linked to high illiteracy amongst the farming communities in Kenya. A recent report indicated that vegetable farming in Kenya is mostly conducted by woman, and that Kenyan women tend to have lower levels of education than men, making it impossible for them to read labels and instruction manuals (Horna et al., 2008; Policy Department for External Relations, 2021). Ngigi et al., (2011) made a similar observation in Kenya among 85 percent of peri-urban farmers. High literacy skills in pesticide regulation and application is more adequate in the large-scale commercial export farms. It should however be noted that in Kenya, smallholders constitute up to 80 % of horticultural products, half of which are for export markets (Ridolfi et al., 2018). Moreover, it has been a challenge to create awareness for pesticide residue issues among this largely dispersed population by government agencies. Similar observations have been reported in other African countries such as Ghana where farmers were involved in indiscreet practices such as application of higher than recommended doses of pesticides on crops and failure to implement the pre-harvest time frame after application (Akoto et al., 2015;

FAO, 2014). Therefore capacity building and training of small holder farmers on GAP should be prioritized to minimize risks of OP residues in the food chain.

Although the Kenyan pesticide regulation regime has been considered as one of the most rigorous on the African continent and closest to global benchmarks, a few challenges still exist (Talk Africa, 2019). Currently, Kenyan pesticide industry is regulated by Chapter 346 of the Pest Control Products Act (PCPA) issued in 1985. In this regulation, new products by companies must first go through the trial conducted by the Pest Control Products Board (PCPB), followed by application for a certificate that is valid for three years (Kenya Law Reports, 2012). It should, however be noted that during the registration, only the purity and efficacy of the product are tested, and there is no mention of the potential threats to the environment, human health, or biodiversity by the PCPA. This is a serious pitfall as human risk assessment remains unaddressed, considering that OPs of environmental and human health concern that have been banned in developed countries such as EU, USA and Canada are still used in Kenya and other developing countries (Hertz-Picciotto et al., 2018). Indeed, a recent report by the directorate-general for external policies of the EU parliament mentioned Kenya as a major destination for pesticides that have been banned for use within the EU (Policy Department for External Relations, 2021). In chapter 2, the pesticides detected in vegetables such as chlorpyrifos, profenofos, acephate, metamidophos, dimethoate and omethoate are all banned in Europe while they still remain in use in other countries including Kenya (PCPB, 2019).

Comparing the MRLs set by various regulatory authorities, MRLs set by the EU are in general lower than those in North America. For example, MRLs of cypermethrin on strawberries was set twice lower by the EU as compared to Canada, while in the USA, carbaryl MRLs on apples are 1200 times higher than those in EU, partly because the MRLs in the EU is set to a default 0.01 mg/kg given that they are no longer registered for use. Also, MRLs for malathion and diazinon are 25 to 400 times higher in North America than in Europe (Nguyen et al., 2020).



However, in some cases, MRLs from the EU and US are comparable, such as those for permethrin in potato or DDT and glyphosate in tomato. Rarely, lower MRLs are imposed in the US than in Europe, an example being glyphosate in strawberry and potato, deltamethrin in potato and cypermethrin in tomato (Nguyen et al., 2020). This variation in MRLs between countries may lead to challenges in case there is a need for universal enforcement to promote international trade. Therefore, it is recommended, where possible, that harmonized MRLs are set that are universally accepted and enforced jointly for promotion of public health and international trade.

A bottleneck in a common approach in enforcement of MRLs is the selective use of some pesticides in some countries while they remain banned in others. For example, sometimes pesticides that are banned in Canada or the US, are still permitted in Europe or Africa and vice versa.

Due to extensive use of OPs to control pests in vegetable farming, one expects consumer exposure to insecticide mixtures. Indeed, a number of biomonitoring studies have reported the presence of several dialkyl phosphate metabolites resulting from OP metabolism in urine and inhibition of AChE in plasma of agricultural workers (Nishihama, et al., 2021). Therefore, many studies begin to characterize the toxicological effects of exposures to concurrent or sequential OP mixtures (Timchalk & Poet, 2008; Refstrup et al., 2010). In Chapter 2 of the thesis it was also shown that some vegetables contained more than one type of pesticide residue. The presence of multiple residues could be a result of plant uptake of persistent pesticides (Zhang et al., 2015), spray drift (Coronado et al., 2011) and poor agricultural practices that involve mixing of more than one kind of pesticide during application based on the conception that as a mixture they will be more potent, as has been observed among Nepalese farmers (Bhandari et al., 2018). Indeed, the practice of using pesticide cocktails that sometimes include unapproved or banned pesticides is worrying but in practice among some farmers in Africa. Exposure to

two or more pesticides may result in additive and/or interactive effects (Saha and Zaman, 2012; Reffstrup et al., 2010).

### **6.3 Use of alternative testing strategies and how they can be used to derive PODs to set health based guidance values for OPs**

In chapter 3 of this thesis PBK models for PFF were developed for rats and humans and successfully applied to predict dose-dependent in vivo AChE inhibition using PBK modeling-facilitated reverse dosimetry of in vitro data on PFF-induced AChE inhibition,. This allowed interspecies comparisons and provided a proof-of-principle that OP-induced AChE inhibition can be predicted for both rats and humans without the need for in vivo studies. Furthermore, chapter 4 assessed the combination effects of PPF and CPO, the toxic metabolite of CPF, on human recombinant AChE activity in vitro also translating these effects upon combined exposure to the in vivo situation, while Chapter 5 predicted human interindividual differences in PPF detoxification based on a combined in vitro-in silico approach. These studies add to previous work that reported the suitability of PBK models to predict OP dose-dependent in vivo AChE inhibition using PBK modeling-facilitated reverse dosimetry of in vitro data, for example for malathion CPF (Zhao et al., 2019) and diazinon (Zhao et al., 2021). In order to allow risk assessors to implement this alternative testing strategy, more proofs-of-principle using this approach with more OPs would be of use and provide a topic for future work in which the approach may prove to be of general use for OP risk assessment.

In this thesis, a chemical-specific PBK model was developed in order to predict the levels of PFF in various compartments. However, to allow chemical assessors to implement this alternative strategy in a broader way, there is need to develop generic OP PBK models for increased efficiency. In most cases the generic PBK models are built on IT platforms (Madden et al., 2019), allowing computing several chemicals with the same type of input data and similar assumptions and limitations. Furthermore the simulation of more than one chemical can be

carried out at the same time when generic PBK models are used. Such generic models hence simplify the task of carrying out a mixture risk assessment provided they also enable modelling of kinetic interactions as done in Chapter 4 of this thesis (Desalegn et al., 2018; Pletz et al., 2020). Moreover, the application of generic PBK models provides a more homogenous way of comparing various chemicals thereby eliminating biases. In this thesis, the PFF PBK model was developed based on a generic PBK model structure first developed by Jones and Rowland-Yeo, (2013). The developed PFF model was then extended to include CPF since all chemical-specific input data were already available (Chapter 3). This model can form the basis for PBK models of other OPs.

For quantifying relevant toxicodynamic effects of PFF, *in vitro* experiments using recombinant AChE for humans and red blood cell (RBC) AChE from rats were conducted to define the concentration-response curves. The obtained curves were translated into *in vivo* dose-dependent AChE inhibition curves in rats and humans using the PBK modelling-facilitated reverse dosimetry approach, after which the predictions for rats could be compared to *in vivo* data for PFF-induced AChE inhibition in RBCs and in the brain of rats (JMPR, 2007). In **chapter 2**, the derived BMDL10 was compared to the US EPA reported BMDL10 of 1.99 mg/kg bw for PFF-induced RBC AChE inhibition in adult rats upon a single exposure to PFF, with this EPA value being 4 times higher than the BMDL10 obtained from the predicted dose-response data for rats in our study (0.45 mg/kg bw). Furthermore, comparison to the JMPR NOAEL value of 100 mg/kg revealed a 200-fold difference for the point of departure based on AChE inhibition as compared to the BMDL10 value obtained from our predicted dose-response data in rats (0.45 mg/kg bw). This indicates that the NOAEL may represent a POD that may be too high and may not be protective to all segments of the population including the sensitive group. Indeed, when studying the interindividual differences in profenofos induced AChE inhibition based on *in vitro* kinetic data and a PBK modelling approach coupled to a Monte

Carlo simulations (**Chapter 5**), it became evident that exposure to the JMPR ARfD of 1 mg/kg bw PFF may lead to significant levels of AChE inhibition in the virtual human population, whereas the predicted AChE inhibition is minimal when exposed to 0.005 mg/kg the EU reported ARfD (EFSA, 2019)). The predicted BMDL10 in humans for the sensitive part of the population amounted to 0.0057 mg/kg bw. Therefore, this thesis supports the use of the ARfD of 0.005 mg/kg bw rather than the one of 1 mg/kg bw in future PFF risk assessment studies. This is an example where a NAM-based assessment can aid in selection of the most appropriate POD when more than one option is presented.

The use of RBC AChE as a surrogate for brain AChE inhibition is based on the fact that RBC AChE is biochemically similar to the AChE present in the neuromuscular junction and the central nervous system, and this has been supported by various regulatory bodies (EPA, 2016, Carlock et al., 1999; EPA, 2008, 2012). The US EPA considered RBC AChE inhibition to be more suitable to derive a POD for human safety assessments, since it is more sensitive than brain AChE inhibition in case of PFF exposure (EPA, 2016). In addition, RBC AChE is easier to sample compared with AChE in other target organs like the spinal cord, brain and the peripheral nervous system (EPA, 2011). Indeed, the points of departure (POD) in risk assessment of OPs such as a benchmark dose (BMD), its lower confidence limit (BMDL) or a no observed adverse effect level (NOAEL) have been derived from data obtained from the inhibition of RBC AChE activity as the surrogate for brain AChE activity. Human cholinergic effect data or RBC AChE inhibition should, when available, take precedence over animal data for determination of PODs (Carlock et al., 1999). Since there are no adverse effects associated with a limited (10 or 20%) inhibition of RBC AChE, the use of a 10-fold uncertainty factor from the POD based on RBC AChE inhibition is considered adequate when RBC AChE inhibition data from either animal or human studies are used to assess human risk (Clegg et al., 1999; Carlock et al., 1999). Moreover, a default uncertainty factor of 100 is considered adequate

when the POD is derived from animal studies for brain AChE inhibition and cholinergic effects, with a possibility for lower uncertainty factors on a case-by-case basis (Clegg et al., 1999; Carlock et al., 1999). In addition, a POD based on cholinergic effects derived from human studies may only require an uncertainty factor of 10 for interindividual variability, since an interspecies extrapolation factor from animals to humans is not necessary (Clegg et al., 1999; Carlock et al., 1999). However, recent epidemiological studies have consistently identified associations between OP exposure and neurodevelopmental outcomes in human, for example attention problems, autism spectrum disorder in early childhood, delays in mental development in infants (24-36 months) as well as intelligence decrements in school age children. Consequently, there is a need for protection of children from OP exposures that could cause these effects. The mode of action of OPs related neurodevelopmental effects is thought to be associated with AChE inhibition. Indeed, a study by Suarez-Lopez et al. (2013) reported associations between decreased AChE activity and lower overall neurodevelopment, inhibitory control, attention, and memory. In that study, the associations were reported to be gender specific, with correlations present in boys but not in girls. It should also be noted that neurodevelopmental effects have been reported to occur at OP dose levels below levels that cause overt AChE inhibition (US EPA, 2014; Abreu-Villaca and Levin, 2017). Given that the current derivation of HBGVs is based on animal data using 10% AChE inhibition as the critical effect, this implies that HBGVs derived from PODs based on animal models may not be sensitive enough and provide for full protection against adverse effects of OPs, when using a default uncertainty factor of 100. Currently, the extra Food Quality Safety Act (FQPA) safety factor of 10 for interindividual variability has been retained for some OPs including CPF and PFF for the population subgroups consisting of infants, children, women of childbearing age and youth for all exposure scenarios. Novel approach methods (NAMs) may play a future role

in defining interindividual differences in sensitivity towards OPs including also sensitive subpopulations.

In the *in vitro* AChE inhibition study used in this thesis, a static approach was used to determine the AChE inhibitory effect concentrations, using a single preincubation time point (15 minutes). When including more time points, information on the time-dependent inhibition kinetics can be obtained. However, a previous study with CPF oxon showed that human recombinant AChE active sites were 100% inhibited after a pre-incubation period of 11 minutes (Kaushik et al., 2007). One would expect that effect concentrations would decrease with longer incubation times until 100% of the binding sites is inhibited, as shown before by Aurbek et al., (2006) and Krstić et al., (2008). With a relatively long pre-incubation time of 15 minutes as used in the present study and also in other studies (e.g. Aurbek et al., 2006; Kasteel et al., 2020), it is expected that a relevant and conservative estimation of the effect concentrations will be obtained, as also indicated by the small difference between the BMDL10 value obtained with the predicted rat dose-response data and the BMDL10 value from a reported *in vivo* study in rats (Chapter 3).

This thesis mainly addressed risk associated with AChE inhibition upon a single exposure. However, chronic poisoning may occur in agricultural workers with daily exposure to OP compounds as well as consumers upon daily consumption of OP-contaminated food. Some OPs have the capacity to induce organophosphate-induced delayed neuropathy (OPIDN), a symmetrical sensorimotor axonopathy, with severe effects reported in long axons, and encountered 7 to 14 days following acute high dose exposure or repeated low dose exposure. OPIDN is initiated by phosphorylation and subsequent aging of >70% of the functional neuropathy target esterase (NTE) in peripheral nerves or depletion of ornithine decarboxylase in spinal cord (Balali-Mood and Saber, 2012). In risk assessment for longer exposures, one must also take the time-dependent *de novo* AChE production into account to adequately

estimate the AChE activity upon a second and further exposure. In that regard a phenomenon referred to as steady state AChE inhibition is of interest, which is the situation when the degree of AChE inhibition reaches equilibrium with the production of new enzyme at which AChE inhibition remains constant at a specified dose over the exposure period (EPA, 2016). Adequate prediction of these processes based on only *in vitro* data, as applied in the present study, is an interesting challenge for future studies. Furthermore, one must consider that OPs inhibit detoxifying enzymes, such as CaE and BuChE, which may result in a decrease in metabolic clearance, and related higher internal concentrations and increased sensitivity upon repeated dosing.

#### **6.4 Use of PBK modelling coupled to Monte Carlo analysis to study inter-individual human kinetic differences in metabolism and toxicity of OPs**

In chapter 5, the effect of inter-individual human kinetic variation in PFF-induced AChE inhibition was predicted by linking Monte Carlo simulations with PBK modelling. Careful literature review indicates that the studies on inter-individual human kinetic differences described in the present thesis are the first attempt to use PBK modelling to identify inter-individual kinetic differences in detoxification of OPs, especially PFF and thus sensitivity towards AChE inhibiting OPs and carbamates. The Monte Carlo sampling approach for generating a ‘virtual population’ was applied in order to characterize the response for a representative population. In this thesis, a total of 10,000 simulations was performed, where in each simulation, the  $V_{max}$  and  $K_m$  of PFF detoxification in the liver and of PFF detoxification in plasma were randomly taken from a log-normal distribution. In previous studies on simulations considering the general population, Monte Carlo simulations with a sample size of 10,000 is often used (Slob, 2006; Sprandel et al., 2006; Goutelle et al., 2009; Punt et al., 2016, Ning et al., 2019). Another study on the number of replications required in Monte Carlo simulations considering a total of 22 studies concluded that the minimum recommended number

of replications (also considered as the sample size) is less than 10,000 (Mundform et al., 2011). In general, about 7500 to 8000 replications can produce robust results, while in some instances a total number 5000 replications may be enough (Mundform et al., 2011).

The developed PBK model for PFF in humans was based on parameters gathered for the Caucasian population (Chapter 5). In risk assessment, inter-individual differences including interethnic differences are taken into account by applying an uncertainty factor of 10 for human variability in kinetics (factor of 3.16) and in dynamics (factor of 3.16) (IPCS, 2005). However, having more detailed insights in possible interindividual variation might provide risk assessors a more science-based approach to derive factors accounting for intraspecies and interspecies differences in toxicokinetics, which may be applied to define chemical specific adjustment factors (CSAFs). In the future applications of this approach, variability in other parameters such as for example body weight, age and gender can be included. Moreover, previous studies have demonstrated the capability of PBK modelling to address age-related changes in physiology and their resulting influence on pharmacokinetics, mainly to predict age related variation between adults and children or to simulate life-time chemical exposures (e.g. Haddad et al., 2001; Price et al., 2003; Pelekis et al., 2003; Clewell et al., 2004; Beaudouin et al., 2010; Bosgra et al., 2012). In most approaches, a mathematical description of the changes of average organ sizes and other parameters with age are included in the PBK model in order to reflect the expected variation by using Gompertz growth curves, polynomial or biexponential functions (Bosgra et al., 2012).

In this thesis, exposure assessment conducted in chapter 2 focused on the situation in Kenya. However, in chapters 3, 4 and 5, the human liver subcellular fractions and plasma used to derive the kinetic parameters for the PBK models were from the Caucasian population. Previous studies have, however, reported interethnic differences between the Caucasian and African population in expression of kinetic enzymes such as PON1 (Davis et al., 2009). Indeed,



knowledge of PON1 enzymatic activities as related to phenotype, genotype, sex, race, and age within a population may provide a useful explanation for some of the disparities in OP metabolism among the various demographic groups (Davis et al., 2009). In the absence of the African kinetic data due to the lack of commercial availability of plasma and liver samples, the African American population data may be applied to compare the interethnic differences in metabolism, since they share a common ancestry. For example, it has been reported that PON1R192 hydrolyses CPO faster than PON1Q192 (Mohammed Ali and Chia, 2008; Eyer et al., 2009; Mutch et al., 2007). Various studies have found that African Americans have a weighted PON1Q192 allele frequency of 0.37 and a weighted PON1R192 allele frequency of 0.63, while the Caucasians have a weighted PON1Q192 allele frequency of 0.73 and a weighted PON1R192 allele frequency of 0.27 (Chen et al., 2003; Scacchi et al., 2003). A higher efficiency of CPO hydrolysis in the Caucasian population could be due to a relatively higher frequency of the RR genotype in the Caucasian population as compared to the African population. In future studies, it is recommended that *in vitro* kinetic studies should be conducted using human liver and plasma subcellular fractions from the Kenyan African population in order to derive HBVGs specific to the study population, and/or to evaluate whether the default uncertainty factor for interindividual differences in kinetics adequately covers the differences between these ethnic groups.

A risk assessment approach that employs Monte Carlo simulation taking inter-individual variability (caused by inherent genetic variability as well as random variability as a result of external factors) into consideration is key to a better understanding of the risks of pesticide exposure which could cause unexpected dose response outcomes that might happen with rare frequency among the sensitive segment of the population. This is particularly evident in individuals with a low PON1 status leading to an increased susceptibility to OP toxicity in humans (Costa, 2013). In future risk assessment using PBK models, *in vitro* input data based

on recombinant enzymes that represent the sensitive segment of the population should be included.

Considering all these, one must be prudent during interpretation of the simulation outcomes because of the uncertainties related to other sources of variability. Generally when performing model-based risk assessment, some assumptions are necessary because not all of the information pertaining all parameters of the compound under consideration is available. In future, it would be of use to build mathematical models and run various simulations under several assumptions with uncertainties and to identify the key components that play key roles by sensitivity analyses. In so doing, the toxicity of various compounds can be well studied as this approach provides quantitative answers to fundamental questions regarding the worst-case scenario based on current knowledge and helps to prioritize the uncertainties and assumptions that should be solved.

### **6.5 Risk assessment of combined exposure to OPs and to OPs and other types of pesticides**

Assessment of exposures to pesticide mixtures is important in the assessment of the aggregate risk (Hernandez et al., 2017), hence the initiative to conduct studies to examine the effects of combinations of OPs. **Chapter 4** provides insights into the combination effects of two selected OPs (PFF and CPF), by studying the combined effects of PFF and CPF's toxic metabolite CPF oxon (CPO) on AChE inhibition *in vitro*, as well as the effects of CPF and CPO on PFF biotransformation (detoxification) by human liver microsomes, cytosol, and human plasma using *in vitro* and *in silico* methods. In addition, *in vivo* AChE inhibition as a result of the combined exposure was determined using PBK modelling-facilitated reverse dosimetry of the *in vitro* data. The results reveal that AChE inhibition upon combined exposure to these OPs follows the concept of dose addition, and that at reported exposure levels, no toxicokinetic interactions of CPF on PPF detoxification are expected. These findings resonate with those

reported by Timchalk et al., (2008) where binary exposure to CPF and diazinon was found to follow dose addition in cholinesterase inhibition, using a physiologically based pharmacokinetic and pharmacodynamic model. Again, this provides another proof-of-principle that approaches that combine in vitro studies and PBK modelling-facilitated reverse dosimetry are promising tools for risk assessment upon combined exposure to pesticide mixtures. Indeed, since a variety of pesticides is being used, environmental, occupational and dietary exposures to pesticide mixtures are likely to occur. Consequently, there is lifelong combined exposure to various pesticides from, for example, one food item containing multiple compounds or combinations of food items, each containing different residues (Boobis et al., 2008; Hernández et al., 2017). These findings therefore support the current scientific and regulatory recommendations for the risk assessment of mixtures that recommend a test strategy based on a component-based assessment, and dose addition as the default model for chemicals in the same cumulative assessment group (EFSA, 2019; Bopp et al., 2015; EFSA, 2013; Kortenkamp et al., 2009).

For pesticides with different modes of action, however, the various mixture effects can be evaluated by determining chemical interactions at both kinetic and dynamic level as well as the cellular or molecular targets of individual pesticides (Hernández et al., 2017). In addition, the complexity of toxicological interactions can lead to unpredictable effects of pesticide mixtures. In general, the interactions on metabolic pathways affecting the biotransformation of pesticides is by far the most common mechanism of synergism. For example, in a study to evaluate the combined effect of a binary mixture of CPF and diazinon, the metabolic interactions between CPF and DZN at the level of their CYP450 mediated conversion were evaluated in vitro, showing that each insecticide was found to inhibit the other's in vitro metabolism in a concentration-dependent manner (Timchalk et al., 2008). However, that synergism is rare at dietary exposure levels, and is likely to occur at experimentally unrealistic high dose levels and

concentrations (Timchalk et al., 2008; Larsen et al., 2019). A similar observation was made in chapter 4, where interactions between PFF and CPF and its metabolite, CPF-oxon were predicted to occur only at relatively high dose levels, largely exceeding expected daily intakes (EDIs). Obviously PBK modeling provides an adequate way to evaluate the consequences of such interactions at realistic low dose levels.

Although PBK modelling is promising in evaluating combined effects of chemicals that follow the principles of dose addition, it cannot be applied as such when combined effects of chemicals do not follow the concept of dose addition, but when other combination effects, such as synergism or antagonism apply. Most synergistic interactions are thought to result from interactions at the level of metabolic processes (Cedergreen, 2014), making it possible to potentially screen synergists using either in vitro assays on for example CYP P450 enzyme activity or esterase inhibition potential, or determination of kinetics in in vivo studies using representative test species. However, the in vivo studies would be labour intensive (Cedergreen, 2014), and may be difficult to extrapolate to the human situation and especially to low dose exposure regimens. In another study, several specific binary combinations of AZM-oxon and CPF-oxon caused a synergistic effect on the ChE inhibition in *P. corneus* homogenates. The degree of synergism tended to increase as the ratio of AZM-oxon to CPF-oxon decreased. These results suggest that synergism is likely to occur in *P. corneus* snails exposed in vivo to binary mixtures of the OPs AZM and CPF (Cacciatore et al., 2012). Consequently, predicting effects of mixtures would be more complex in case of less than dose addition or more than dose addition. It should, however, be noted that deviations from predicted additivity are considered to be rare (Kortenkamp et al., 2009; Cedergreen et al., 2014).

## 6.6 OPs and long term effects considering neurodegenerative diseases including Parkinsonism

Neurodegenerative diseases are diseases linked with a wide variety of pathological and clinical conditions associated with aging. Examples include diseases such as Parkinson's disease (PD), amyotrophic lateral sclerosis (ALS) or Alzheimer's disease (AD) (Costa, 2018). Although the etiology of these diseases is unknown, it is believed that both genetic and environmental factors may play a role. Several genes implicated as monogenic causes of parkinsonism are only responsible for approximately 10% of cases (Ball et al., 2019), while the remaining 90% of the cases are idiopathic, with different environmental exposures being implicated as either risk factors (pesticides exposure and heavy metals) or protective factors (such as caffeine intake and tobacco smoking) (Schneider Medeiros et al., 2020). OPs constitute the largest group of insecticides currently used in farming despite being responsible for about 3 million cases of poisonings and about 300,000 deaths annually worldwide, according to Robb and Baker, (2020) and others (Buckley et al., 2004; Terry, 2012; Costa, 2006). Furthermore, some human subjects that survive acute OP poisoning have been found to develop signs of parkinsonism, suggesting that OPs may have a negative effect on the striatal dopaminergic system (Bhatt et al., 1999; Hashim et al., 2011). These lesions are similar to the main pathological lesions in PD, where there is a slow and progressive degeneration of dopaminergic neurons in the substantia nigra of the brain, with clinical signs such as resting tremor, gait disturbances and bradykinesia appearing with the degeneration of about 80% of dopaminergic neurons. Pathologically it has been reported that neuroinflammatory processes and oxidative stress are prominent in most neurodegenerative diseases such as PD (Costa, 2018; Wani et al., 2017), and some OPs have indeed been reported to cause these (Naughton and Terry, 2018; Pope, 1999; Wani et al., 2017). Moreover, previous studies have linked acute exposure to OPs with causation of Parkinsonism (Muller-Vahl et al., 1999; Baldi et al., 2003). Chuang et al. (2017) recently reported an increased

risk of PD following OP and carbamate poisoning. Indeed, a positive association between chronic exposure to OPs and PD has been reported (Wang et al., 2014), especially in individuals with particular paraoxonase-1 (PON1) genotypes that affect proper PON-1 functioning (Paul et al., 2017). With all these associations being reported, the Board for the Authorisation of Plant Protection Products and Biocides (Ctgb) and EFSA have expressed interest in conducting research to establish the link (if any) between exposure to plant protection products including OPs and the development of Parkinsonism (<https://www.ctgb.nl/documenten/brieven/2021/03/23/efas-reply-on-possible-relation-ppp-and-parkinson>). On their part, EFSA has undertaken activities by the PPR Panel culminating in the development of adverse outcome pathways (AOP) for Parkinsonian disorders. The measurable key events (KEs) included in the AOP could be used to test and identify chemicals with potential to contribute to the disease via the identified pathway. An AOP approach is key in the study of mechanisms of toxicity required in linking those mechanisms through epidemiological studies to neurological disorders such as parkinsonism. The mechanistic understanding enables the development of tools necessary for a predictive toxicology approach, which is essential for regulatory decisions.

Other pesticides such as organochlorine insecticides, maneb, paraquat and rotenone may have neurotoxic actions that potentially play a role in the development of PD, with previous epidemiological studies showing a relation between these pesticides and PD (Dick, 2006; Brown et al., 2006; Wright et al., 2005). Since these pesticides have been linked to PD, and considering that they have different modes of action, there is need to also better characterize and understand the consequences of such combined exposures.

## 6.7 Future perspectives

The present thesis provided proofs-of-principle that PBK modelling-based reverse dosimetry of *in vitro* data is able to predict *in vivo* acute OP-induced AChE inhibition (PFF and CPF) in a quantitative way. In order to increase the applicability and impact of this novel approach, one may consider to provide proofs-of-principle for endpoints other than OP-induced AChE inhibition, including especially examples on compounds with different target organs and different AOPs also including in addition to effects of acute exposure effects of chronic low dose exposure. For example, it would be interesting to study the sub-chronic to chronic adverse effect of OPs, resulting from long-term repeated exposure to low concentrations using recombinant AChE with an *in vitro* system capable of mimicking the *de novo* synthesis of the enzyme as well as metabolic enzyme activities in order to predict AChE inhibition and other endpoints of OPs upon daily low dose exposure. Besides the AChE inhibition in the brain and RBC, other toxic endpoints and target tissues should be investigated. For example, results following inhibition of enzymes like neuropathy target esterase (NTE) (Costa, 2018), acylpeptide hydrolase (APH) (Richards et al., 2000), fatty acid amide hydrolase (FAAH) (Quistad et al., 2001; Buntyn et al., 2017) muscarinic M2 receptors (Costa, 2006), and a variety of lipases (Quistad et al 2006) have not been analysed for their *in vivo* relevance. Already, SH-SY5Y human neuroblastoma cells have shown promise in development as *in vitro* assay to measure OP effects on NTE activities (Sogorb et al., 2010). Some studies have reported the endocrine disrupting effect of OPs (Yang et al., 2019; Ortiz-Delgado et al., 2019), which may play a role in the mode of action responsible for neurodevelopmental effects. Consequently, *in vitro* assays employing novel human stem cell models have been developed for testing developmental neurotoxicity (Bal-Price et al., 2018; López-Tobón et al., 2018; Lupu et al., 2020). For example, human induced pluripotent stem cells derived neuro-progenitor cells (Human iPSC-derived NPC) from different brain regions have been used to develop *in vitro*

assays with capability to measure the relevant neurodevelopmental effects including neurite, differentiation, network formation and activity as well as migration during early embryonic development (Bal-Price et al., 2018; López-Tobón et al., 2018; Lupu et al., 2020). In addition, in order to understand the molecular mechanisms of OP-induced neurobehavioral deficits such as observed in PD (see section 6.6), various models have been developed to study the molecular effects of OPs in relevant cell types. For example, some studies have investigated molecular responses following *in vivo* exposures, and attempted to correlate these findings with behavioral outcomes without inducing overt toxicity related to AChE inhibition activity in isolated tissue or cell culture systems. Furthermore, it has been demonstrated that OPs induce neuronal damage or death at levels that do not ablate AChE activity (Voorhees et al., 2017). Another example of an *in vitro* system is that of a cortical culture system where hippocampal slice cultures were treated with CPO at levels that reduced hippocampal AChE activity by 50% after 3 and 7 days of exposure, showing also neuronal injury that was both concentration- and time-dependent (Zimmer et al., 2000). Development of *in vitro* models to measure OP effects on APH, FAAH, muscarinic M2 receptors and lipases are yet to be developed.

Once these *in vitro* systems are developed, PBK model based reverse dosimetry could be applied to translate the *in vitro* data to the *in vivo* situation and allow their use in hazard characterization and risk assessment.

The present thesis studied the inter-individual variations in kinetics of OP metabolism, whereas the effect of inter-individual dynamic differences remains to be elucidated in future studies. A recent *in vitro* study suggested limited interindividual differences in OP-induced AChE inhibition (Kasteel et al., 2020). Studies in this thesis also reported similar AChE inhibition patterns in both human and rat AChE, concluding that the differences between rats and humans in PFF-induced AChE inhibition are mainly driven by differences in kinetics. Therefore, the current PBK models could be extended to physiologically based dynamic (PBD) models, in



which for example AChE inhibition could be integrated. Combining the current PBK model with an equation describing the concentration-dependent AChE inhibition of OPs and carbamates in different human individual RBC samples, as well as an extension of the PBK models coupled to Monte Carlo simulation to also predict toxicodynamics, could provide a way forward to fully predict the interindividual differences in *in vivo* dose-response curves for OP- and carbamate-induced AChE inhibition and resulting toxicity in humans.

Another important point that can be considered in the future when using PBK modelling-based reverse dosimetry of *in vitro* data for risk assessment is the uncertainty factor to be used when a POD for risk assessment is defined by a QIVIVE approach. This requires insight in the uncertainties inherent to the approach and the model applied. Uncertainty comes, for example, from the level of inaccuracy in the various model parameters. In the present thesis, a sensitivity analysis was performed to evaluate the impact of model parameters on the model output so that the effect of small changes in parameter values on the model outcome can be evaluated. Furthermore, the PODs derived in the present thesis were based on a human PBK model and human recombinant AChE derived *in vitro* data, hence human specific physiology, metabolism and inhibitory effects were taken into account. Consequently, the UF of 10 for inter-species differences would no longer be required. Then an extra UF of 10 could be applied because the POD was derived by an alternative *in vitro-in vivo* testing strategy. This would still result in an uncertainty factor of 100 to be applied when a POD is derived using the combined human based *in vitro-in silico* NAM approach, to account for the uncertainties brought about by the *in vitro-in silico* QIVIVE approach (factor 10) and the interindividual differences (factor 10). For the OPs studied in the present thesis, differences in predicted toxicity values of PFF and those values derived from rat *in vivo* toxicity studies were within 4-fold (EPA, 2016) while for average humans the predicted BMDL10 value was 2-fold higher than EFSA's ARfD value (EFSA, 2019) (chapter 3), indicating that an extra uncertainty factor of for example 10 would

be by far sufficient to cover for the uncertainties related to use of the QIVIVE approach. Earlier studies have shown that the PODs for developmental toxicity predicted with the in vitro PBK approach were within 0.2 to 10-fold difference compared to the corresponding values derived from in vivo data (Louisse et al., 2015; Louisse et al., 2010; Strikwold et al., 2017; Strikwold et al., 2013). Thus, based on the available data one would conclude that an uncertainty factor of 10 may be used when a POD is derived with the combined in vitro PBK modelling approach to predict developmental toxicity. To further substantiate the uncertainty factor to be used when using PBK modelling based reverse dosimetry to perform QIVIVE and predict in vivo dose response curves to define PODs for risk assessment, more examples and proofs-of principles for other chemicals and other endpoints would be required to make this proposed UF more robust. In such assessments predictions made for experimental animals can be compared to animal toxicity data for evaluation of the approach and predictions in humans can be compared to currently available health based guidance values, to provide better insight into what uncertainty factor is considered adequate to apply when defining HBGVs using PBK modelling-based QIVIVE of in vitro toxicity data to provide similar protective HBGVs for humans as those currently derived based on animal toxicity data.

Taking it all together it can be concluded on the basis of the currently available data that when the combined in vitro PBK modelling approach would be based on an adequate human in vitro model and a human PBK model describing respectively the dynamics and kinetics directly for humans, it might be advocated to replace the default uncertainty factor 10 for inter-species differences by the uncertainty factor required when a POD for risk assessment is defined by a QIVIVE approach. Assuming that a factor of 10 would be sufficiently protective to cover the uncertainties of the QIVIVE approach the overall default uncertainty factor could then still be 100. However, the default factor of 10 is used if no data on interindividual differences are

available and may be replaced by a possible chemical specific adjustment factor (CSAF) when data on interindividual differences are available (IPCS, 2005).

## 6.8 Conclusion

In conclusion, the present thesis showed novel insights into hazards and risks following exposure to OPs via residues present in vegetables in Kenya. The assessment of the levels of OPs in vegetables in Kenya revealed that PFF and CPF were the most frequently encountered pesticide residues, and that CPF and PPF (when applying EFSA's latest ARfD) had for some situations an acute HQ higher than 1, implying that potential health risks with respect to acute dietary exposure cannot be excluded. Therefore, routine monitoring of OPs and carbamates in vegetables is recommended to minimize consumers' health risks.

Upon development of a PBK model for PFF, adequate predictions were obtained for dose levels leading to in vivo AChE inhibition upon acute exposure in rats providing another proof-of-principle that with this new approach methodology (NAM) in vivo effects of chemicals can be predicted without the use of in vivo studies. Moreover, the combined exposure to PPF and CPF at their ARfD was predicted to not affect AChE activity, and the AChE inhibition upon combined exposure to these OPs follows the concept of dose addition. Furthermore, at reported exposure levels, no toxicokinetic interactions of CPF on PPF detoxification are expected. Moreover prediction of interindividual differences in PFF detoxification using PBK modelling linked to Monte Carlo simulation followed by PBK modelling based reverse dosimetry revealed a close similarity between the predicted BMDL10 of the sensitive segment of the population and the latest ARfD reported by EFSA (2019) based on German evaluation, and that adopted by EPA (2016). The predicted BMDL10 was however 200-fold lower than the ARfD derived by JMPR (2007), which appeared to be non-protective as it was predicted to lead to AChE inhibition in humans.

Finally, the present thesis has provided further proofs-of-principle that the PBK model-facilitated reverse dosimetry solely based on in vitro assays and in silico data, together with a relative potency factor methodology or Monte Carlo simulation, can be adequately used to derive PODs and provide data that may be used to derive a chemical specific adjustment factor (CSAF) value for defining inter-species and inter-individual differences in OP-induced RBC AChE inhibition resulting from the variability in toxicokinetics following acute oral exposure to an OP. The current and next generation human health risk assessors for OPs may utilize data generated in the present thesis on directly predicted PODs for the human situation based on the combined in vitro and in silico approach without the need for in vivo animal studies. Altogether, the current work supports the implementation of the 3Rs principle, the application of NAMs in next generation OP-human risk assessment and regulatory decision making.

## REFERENCES

- Abreu-Villaca, Y., Levin, E.D., 2017. Developmental neurotoxicity of succeeding generations of insecticides. *Environ Int.* 99:55–77.
- Akoto, o., Gavor, s., Appah, M.K., Apau, K., 2015. Estimation of human health risk associated with the consumption of pesticide-contaminated vegetables from Kumasi, Ghana, *Environ Monit Assess* 187:244
- Alavanja, M.C.R., Ross, M.K., Bonner, M.R., 2013. Increased cancer burden among pesticide applicators and others due to pesticide exposure. *Cancer J. Clin.* 63, 120–142
- Aurbek, N., Thiermann, H., Szinicz, L., Eyer, P., Worek, F., 2006. Analysis of inhibition, reactivation and aging kinetics of highly toxic organophosphorus compounds with human and pig acetylcholinesterase. *Toxicology* 224:91–99
- Bahar, F.G., Ohura, K., Ogihara, T., Imai, T. 2012. Species difference of esterase expression and hydrolase activity in plasma. *J Pharm Sci* 101:3979-3988.
- Baker, B.P., Benbrook, C.M., Groth, E. Lutz Benbrook, K., 2002. Pesticide residues in conventional, integrated pest management (IPM)-grown and organic foods: insights from three US data sets. *Food Addit Contam.* 19(5):427-46.
- Bal-Price, A., Pistollato, F., Sachana, M., Bopp, S.K., Munn, S., Worth, A., 2018. Strategies to improve the regulatory assessment of developmental neurotoxicity (DNT) using in vitro methods. *Toxicol Appl Pharmacol.* 1;354:7-18.
- Balali-Mood, M., Saber, H., 2012. Recent advances in the treatment of organophosphorous poisonings. *Iran J Med Sci.* 37(2):74-91. PMID: 23115436; PMCID: PMC3470074.
- Baldi, I., Cantagrel, A., Lebailly, P., Tison, F., Dubroca, B., Chrysostome, V., Dartigues, J.F., Brochard, P., 2003. Association between Parkinson's disease and exposure to pesticides in southwestern France. *Neuroepidemiology.* 22(5):305-10. doi: 10.1159/000071194. PMID: 12902626.

- Bujwa, U., Sandhu KS. Effect of handling and processing on pesticide residues in food- A review. *Journal of Food Science and Technology*. 2014;51(2):201–220.
- Ball, N., Teo, W.P., Chandra, S., Chapman, J., 2019. Parkinson's disease and the environment. *Front Neurol*. 10:218.
- Beaudouin, R., Micallef, S., Brochot, C., 2010. A stochastic whole-body physiologically based pharmacokinetic model to assess the impact of inter-individual variability on tissue dosimetry over the human lifespan. *Regul Toxicol Pharmacol* 57:103–116.
- Bhandari, G., Atreya, K., Yang, X., Fan, L., Geissen, V., 2018. Factors affecting pesticide safety behaviour: The perceptions of Nepalese farmers and retailers. *Science of The Total Environment* 2018; 631-632: 1560-1571.
- Bhatt, M.H., Elias, M.A., Mankodi, A.K., 1999. Acute and reversible parkinsonism due to organophosphate pesticide intoxication: five cases. *Neurology*. Apr 22; 1999 52(7):1467–71.
- Bogen, K.T., Singhal, A. 2017. Malathion dermal permeability in relation to dermal load: Assessment by physiologically based pharmacokinetic modeling of in vivo human data. *J Environ Sci Health B* 52:138-146.
- Bosgra, S., van Eijkeren, J., Bos, P., Zeilmaker, M., Slob, W., 2012. An improved model to predict physiologically based model parameters and their inter-individual variability from anthropometry. *Crit Rev Toxicol*. 42(9):751-67.
- Boon, P.E., Van der Voet, H., Van Raaij, M.T., Van Klaveren, J.D., 2008. Cumulative risk assessment of the exposure to organophosphorus and carbamate insecticides in the dutch diet. *Food Chem Toxicol*. 46:3090–3098.
- Bouchard, M., Carrier, G., Brunet, R.C., Bonvalot, Y., Gosselin, N.H. 2005. Determination of

- biological reference values for chlorpyrifos metabolites in human urine using a toxicokinetic approach. *J Occup Environ Hyg* 2:155-168.
- Bouchard, M., Gosselin, N.H., Brunet, R.C., Samuel, O., Dumoulin, M.J., Carrier, G. 2003. A toxicokinetic model of malathion and its metabolites as a tool to assess human exposure and risk through measurements of urinary biomarkers. *Toxicol Sci* 73:182-194.
- Bouchard, M., Gosselin, N.H., Brunet, R.C., Samuel, O., Dumoulin, M., Carrier, G., 2017. A toxicokinetic model of malathion and its metabolites as a tool to assess human exposure and risk through measurements of urinary biomarkers. *Toxicol Sci* 73:182-194.
- Berry, L.M., Wollenberg, L., Zhao, Z., 2009. Esterase activities in the blood, liver and intestine of several preclinical species and humans. *Drug Metab Lett* 3:70–77.
- Bradman, A., Quiros-Alcala, L., Castorina, R., et al., 2003. Effect of organic diet intervention on pesticide exposures in young children living in low-income urban and agricultural communities. *Environ. Health Perspect.* 123, 1086–1093. <https://doi.org/10.1289/ehp.1408660>.
- Brown, T.P., Rumsby, P.C., Capleton, A.C., Rushton, L., Levy, L.S., 2006. Pesticides and Parkinson's disease--is there a link? *Environ Health Perspect.* 2006 Feb;114(2):156-64. doi: 10.1289/ehp.8095. PMID: 16451848; PMCID: PMC1367825
- Boobis, A.R., Ossendorp, B.C., Banasiak, U., Hamey, P.Y., Sebestyen, I., Moretto, A., (2008). Cumulative risk assessment of pesticide residues in food. *Toxicol Lett* 180:137–150
- Bopp, S., Berggren, E., Kienzler, A., Van der Linden, S., Worth, A., 2015. Scientific methodologies for the assessment of combined effects of chemicals - a survey and literature review. *EUR 27471 EN* 1–64. <https://doi.org/10.2788/093511>. Scientific methodologies for the assessment of combined effects of chemicals - a survey and literature review. *EUR 27471 EN* 1–64.

- Buckley, N.A., Roberts, D., Eddleston, M., 2004. Overcoming apathy in research on organophosphate poisoning. *BMJ.* 329(7476):1231–3. [PubMed: 15550429]
- Buntyn, R.W., Alugubelly, N., Hybart, R.L., Mohammed, A.N., Nail, C.A., Parker, G.C., Ross, M.K., Carr, R.L., 2017. Inhibition of endocannabinoid-metabolizing enzymes in peripheral tissues following developmental chlorpyrifos exposure in rats. *Int J Toxicol* 36:395-402.
- Carlock, L.L., Chen, W.L., Gordon, E.B., Killeen, J.C., Manley, A., Meyer, L.S., Mullin, L.S., Pendino, K.J., Percy, A., Sargent, D.E., Seaman, L.R., Svanborg, N.K., Stanton, R.H., Tellone, C.I., Van Goethem, D.L., 1999. Regulating and assessing risks of cholinesterase-inhibiting pesticides: divergent approaches and interpretations. *J Toxicol Environ Health B Crit Rev.* 2(2):105-60.
- Cedergreen, N., 2014. Quantifying synergy: a systematic review of mixture toxicity studies within environmental toxicology. *PLoS One.* 2;9(5):e96580.
- Chanda, S.M., Mortensen, S.R., Moser, V.C., Padilla, S. 1997. Tissue-specific effects of chlorpyrifos on carboxylesterase and cholinesterase activity in adult rats: an in vitro and in vivo comparison. *Fundam Appl Toxicol* 38:148-157.
- Chen, J., Kumar, M., Chan, W., Berkowitz, G., Wetmur, J.W., 2003. Increased influence of genetic variation on PON1 activity in neonates. *Environ Health Perspect* 111:1403–1409
- Chiu, W.A., Barton, H.A., DeWoskin, R.S., Schlosser, P., Thompson, C.M., Sonawane, B., Lipscomb, J.C., and Krishnan, K., 2007. Evaluation of physiologically based pharmacokinetic models for use in risk assessment. *J. Appl. Toxicol.*, 27, 218-237.
- Chiu, Y.H., Williams, P.L., Gillman, M.W., Hauser, R., Rifas-Shiman, S.L., Bellavia, A.,



- Fleisch, A.F., Oken, E., Chavarro, J.E., 2018. Maternal intake of pesticide residues from fruits and vegetables in relation to fetal growth. *Environ Int.* 2018 Oct;119:421-428. doi: 10.1016/j.envint.2018.07.014.
- Cho, Y., Min, K., Lee, I., Cha, C., 2002. Determination of urinary metabolite of profenofos after oral administration and dermal application to rats. *J. Fd Hyg. Safety* 17(1): 20–25
- Chuang, C. S., Su, H. L., Lin, C. L., and Kao, C. H., (2017) Risk of Parkinson disease after organophosphate or carbamate poisoning. *Acta Neurol. Scand.* 136, 129–137.
- Clegg, D.J., van Gemert, M., 1999. Determination of the reference dose for chlorpyrifos: proceedings of an expert panel. *J Toxicol Environ Health B Crit Rev.* 1999 Jul-Sep;2(3):211-55.
- Clewell, R.A., and Clewell, H.J., 2008. Development and specification of physiologically based pharmacokinetic models for use in risk assessment. *Regul. Toxicol. Pharmacol.*, 50, 129-143.
- Clewell, H.J., Gentry, P.R., Covington, T.R., Sarangapani, R., Teeguarden, J.G., 2004. Evaluation of the potential impact of age- and gender specific pharmacokinetic differences on tissue dosimetry. *Toxicol Sci* 79:381–393.
- Costa, L.G., 2006. Current issues in organophosphate toxicology. *Clin Chim Acta* 366:1-13.
- Costa, L. G., Giordano, G., Cole, T. B., Marsillach, J., & Furlong, C. E. 2013. Paraoxonase 1 (PON1) as a genetic determinant of susceptibility to organophosphate toxicity. *Toxicology*, 307, 115–122. <https://doi.org/10.1016/j.tox.2012.07.011>
- Costa, L.G., 2018. Organophosphorus Compounds at 80: Some Old and New Issues. *Toxicol Sci* 162:24-35.
- Curl, C. L., Fenske, R.A., Elgethum, K., 2003. “Organophosphorus pesticide exposure of urban and suburban preschool children with organic and conventional diets,” *Environmental Health Perspectives*, vol. 111, no. 3, pp. 377–382, 2003.

- Coronado, G.D., Holte, S., Vigoren, E., Griffith, W.C., Barr, D.B., Faustman, E., Thompson, B., 2011. Organophosphate pesticide exposure and residential proximity to nearby fields: evidence for the drift pathway. *J Occup Environ Med* 2011; 53: 884-891.
- Dadson, O.A., Ellison, C.A., Singleton, S.T., Chi, L., McGarrigle, B.P., Pamela, J., Lein, J.P., Farahat, F.M., Farahat, T., Olson, J.R. 2013. Metabolism of profenofos to 4-bromo-2-chlorophenol, a specific and sensitive exposure biomarker. *Toxicology* 306:35-39.
- Darko, G., Akoto, O., 2008. Dietary intake of organophosphorus pesticide residues through vegetables from Kumasi, Ghana. *Food Chem Toxicol* 2008; 46: 3703-3706.
- Davis, K.A., Crow, J.A., Chambers, H.W., Meek, E.C., Chambers, J.E., 2009. Racial differences in paraoxonase-1 (PON1): a factor in the health of southerners? *Environ Health Perspect.* 2009 Aug;117(8):1226-31. doi: 10.1289/ehp.0900569. Epub 2009 Mar 12. PMID: 19672401; PMCID: PMC2721865.
- Desalegn, A., et al., 2018. 'Role of physiologically based kinetic modelling in addressing environmental chemical mixtures – A review'. *Comput. Toxicol. Elsevier* 10, 158–168. <https://doi.org/10.1016/j.comtox.2018.09.001>.
- Dick, F.D., 2006. Parkinson's disease and pesticide exposures. *Br Med Bull.* 2006;79-80:219-31. doi: 10.1093/bmb/ldl018. Epub 2007 Jan 22. PMID: 17242039.
- Drevenkar, V., Vasilić, Z., Stengl, B., Fröbe, Z., Rumenjak, V. 1993. Chlorpyrifos metabolites in serum and urine of poisoned persons. *Chem Biol Interact.* 87(1-3):315-22.
- Ecobichon, D.J., Comeau, A.M., 1973. Pseudocholinesterases of mammalian plasma: Physicochemical properties and organophosphate inhibition in eleven species. *Toxicol Appl Pharmacol* 24:92-100.

Ecobichon, D.J. (2001) Pesticide Use in Developing Countries. *Toxicology*, 160, 27-33.

[http://dx.doi.org/10.1016/S0300-483X\(00\)00452-2](http://dx.doi.org/10.1016/S0300-483X(00)00452-2)

Eddleston, M., Worek, F., Eyer, P., Thiermann, H., Von Meyer, L., Jeganathan, K., Sheriff, M.H.R., Dawson, A.H., Buckley, N.A. 2009. Poisoning with the S-Alkyl organophosphorus insecticides profenofos and prothiofos. *QJM: Int J Med.* 102:785-792.

European Food Safety Authority (EFSA) 2008 Annual Report on Pesticide Residues according to Article 32 of Regulation (EC) No 396/2005; EFSA: Parma, Italy, 2010; Volume 8.

European Food Safety Authority (EFSA) (EFSA) Panel on Plant Protection Products and their Residues (PPR), 2014. Scientific Opinion on the identification of pesticides to be included in cumulative assessment groups on the basis of their toxicological profile (2014 update). *EFSA Journal* 2013;11(7):3293, 131 pp. doi:10.2903/j.efsa.2013.3293

Elgueta, S., Fuentes, M., Valenzuela, M., Zhao, G., Liu, S., Lu, H., Correa, A., 2019.

Pesticide residues in ready-to-eat leafy vegetables from markets of Santiago, Chile, and consumer's risk, *Food Additives & Contaminants: Part B*, DOI: 10.1080/19393210.2019.1625975

European Food Safety Authority (EFSA)., 2014. Panel on Plant Protection Products and their Residues (PPR). Scientific Opinion on the identification of pesticides to be included in cumulative assessment groups on the basis of their toxicological profile (2014 update). *EFSA Journal* 2013;11(7):3293, 131 pp. doi:10.2903/j.efsa.2013.3293 o

European Food Safety Authority (EFSA), 2019a. Scientific report on the 2017 European Union report on pesticide residues in food. *Efsa J.* 17(6):5743.

European Food Safety Authority (EFSA) 2019b. Scientific Report on scientific support for

preparing an EU position in the 51st Session of the Codex Committee on Pesticide Residues(CCPR). EFSA Journal 2019;17(7):5797, 243 pp.

<https://doi.org/10.2903/j.efsa.2019.5797>

European Food Safety Authority, (EFSA), 2014. Conclusion on the peer review of the pesticide human health risk assessment of the active substance chlorpyrifos. EFSA J. 12, 3640.

European Food Safety Authority (EFSA), 2014. Scientific Opinion on good modelling practice in the context of mechanistic effect models for risk assessment of plant protection products EFSA Journal 12:3589

EPA., 2016. Profenofos: Human health draft risk assessment(DRA) for registration review. [https://www3.epa.gov/pesticides/chem\\_search/cleared\\_reviews/csr\\_PC-111401\\_19-Oct-16.pdf](https://www3.epa.gov/pesticides/chem_search/cleared_reviews/csr_PC-111401_19-Oct-16.pdf). (accessed on 12/3/2020).

Eyer F, Roberts DM, Buckley NA, Eddleston M, Thiermann H, Worek F, Eyer P. Extreme variability in the formation of chlorpyrifos oxon (CPO) in patients poisoned by chlorpyrifos (CPF). *Biochem Pharmacol.* 2009 Sep 1;78(5):531-7. doi: 10.1016/j.bcp.2009.05.004. Epub 2009 May 9. PMID: 19433070; PMCID: PMC2714474.

EPA., 2016. Chlorpyrifos: Revised Human Health Risk Assessment for Registration Review. Available at: [https:// www.regulations.gov/document? D=EPA-HQ-OPP-2015-0653-0454](https://www.regulations.gov/document?D=EPA-HQ-OPP-2015-0653-0454). file ID: EPA-HQ-OPP-2015-0653-0454. Accessed July 23, 2021.

EPA (U.S. Environmental Protection Agency) 2008. A Set of Scientific Issues Being Considered by the Environmental Protection Agency Regarding: The Agency's Evaluation of the Toxicity Profile of Chlorpyrifos: Minutes of the FIFRA Science Advisory Panel Meeting held on September 16–18, 2008. FIFRA Scientific Advisory

Panel (SAP) Minutes No. 2008-04. Available at  
[http://www.epa.gov/scipoly/sap/meetings/2008/091608\\_mtg.htm](http://www.epa.gov/scipoly/sap/meetings/2008/091608_mtg.htm).

EPA (U.S. Environmental Protection Agency) Meeting of the FIFRA Scientific Advisory

Panel. Draft Issue Paper: Scientific Issues Concerning Health Effects of Chlorpyrifos  
 Office of Chemical Safety and Pollution Prevention. Washington, DC: 2012. [Google  
 Scholar]

EPA, 2006. Reregistration Eligibility Decision for Dimethoate. Retrieved from

[https://archive.epa.gov/pesticides/reregistration/web/pdf/dimethoate\\_red.pdf](https://archive.epa.gov/pesticides/reregistration/web/pdf/dimethoate_red.pdf)

[Accessed December 2020]

EPA, 2011. Chlorpyrifos Preliminary Human Health Risk Assessment DP No. D388070

Retrieved from <https://www.regulations.gov/contentStreamer?documentId=EPA-HQ-OPP-2008-0850-0025&contentType=pdf> [Accessed December 2020]

EPA, 2016. Protenofos: Human health draft risk assessment (DRA) for registration

review. [https://www3.epa.gov/pesticides/chem\\_search/cleared\\_reviews/csr\\_PC-111401\\_19-Oct-16.pdf](https://www3.epa.gov/pesticides/chem_search/cleared_reviews/csr_PC-111401_19-Oct-16.pdf). [Accessed March 2020]

USEPA, 2014. EPA Revised Human Health Risk Assessment on Chlorpyrifos. Docket ID

EPA-HQ-OPP-2008-0850. Available from: <http://www.epa.gov/ingredients-used-pesticide-products/revised-human-health-risk-assessment-chlorpyrifos>.

EPA, 2011. Chlorpyrifos Preliminary Human Health Risk Assessment DP No. D388070

Retrieved from <https://www.regulations.gov/contentStreamer?documentId=EPA-HQ-OPP-2008-0850-0025&contentType=pdf> [Accessed December 2020]

FAO. (2014). Annotated list of Guidelines for the implementation of the International Code of  
 Conduct on Pesticide Management. In (Vol. 2018).

FIFRA, Scientific Advisory Panel. (2012). Transmittal of the Meeting Minutes from the FIFRA

- Scientific Advisory Panel Meeting of April 10-12, 2012. FIFRA Scientific Advisory Panel, Office of Science Coordination and Policy, Office of Prevention, Pesticides and Toxic Substances, U.S. Environmental Protection Agency. Washington, DC. Available: <http://www.epa.gov/scipoly/sap/meetings/2012/041012meeting.html>
- Gallagher, S.S., Rice, G.E., Scarano, L.J., Teuschler, L.K., Bolleweg, G., Martin, L. 2015. Cumulative risk assessment lessons learned: a review of case studies and issue papers *Chemosphere*, 120 (2015), pp. 697-705
- Golge, O., Koluman, A., Kabak, B., 2018. Validation of a modified QuEChERS method for the determination of 167 pesticides in milk and milk products by LC-MS/MS. *Food Anal. Methods* 11, 1122–1148
- González-Alzaga, B., Lacasaña, M., Aguilar-Garduño, C., Rodríguez-Barranco, M., Ballester, F., Rebagliato, M., Hernández, A.F., 2014. A systematic review of neurodevelopmental effects of prenatal and postnatal organophosphate pesticide exposure. *Toxicol Lett.* 2014 Oct 15;230(2):104-21. doi: 10.1016/j.toxlet.2013.11.019. Epub 2013 Nov 26. PMID: 24291036.
- Gotoh, M., Sakata, M., Endo, T., Hayashi, H., Seno, H., Suzuki, O., 2001. Profenofos metabolites in human poisoning. *Forensic Sci Int* 116: 221-226.
- Goutelle, S., Bourguignon, L., Maire, P.H., Van Guilder, M., Conte, J.E. Jr, Jelliffe, R.W., 2009. Population modeling and Monte Carlo simulation study of the pharmacokinetics and antituberculosis pharmacodynamics of rifampin in lungs. *Antimicrob Agents Chemother.* 2009 Jul;53(7):2974-81.
- Haddad, S., Restieri, C., Krishnan, K., 2001. Characterization of age-related changes in body weight and organ weights from birth to adolescence in humans. *J Toxicol Environ Health Part A* 64:453–464.
- Hashim, H.Z., Wan Musa, W.R., Ngiu, C.S., Wan Yahya, W.N., Tan, H.J., Ibrahim, N., 2011

- Parkinsonism complicating acute organophosphate insecticide poisoning. *Ann Acad Med Singapore*. Mar; 2011 40(3):150–1.
- Hepsağ, F., Kizildeniz, T., 2021. Pesticide residues and health risk appraisal of tomato cultivated in greenhouse from the Mediterranean region of Turkey. *Environ Sci Pollut Res Int*. 2021 May;28(18):22551–22562. doi: 10.1007/s11356-020-12232-7.
- Hernandez, A. F., Gil, F., and Lacasana, M. (2017). Toxicological ~ interactions of pesticide mixtures: An update. *Arch. Toxicol*.91, 3211–3223.
- Hertz-Picciotto, I., Sass, J.B., Engel, S., Bennett, D.H., Bradman, A., Eskenazi, B., Lanphear, B., Whyatt, B., 2018. Organophosphate exposures during pregnancy and child neurodevelopment: Recommendations for essential policy reforms.
- Horna, D., Smale, M., Al-Hassan, R., Falck-Zepeda, J., & Timpo, S. E., 2008. Selected paper prepared for presentation at the American Agricultural Economics Association Annual Meeting, Orlando, FL.
- Hu, Y., Chiu, Y.H., Hauser, R., Chavarro, J., Sun, Q., 2016. Overall and class-specific scores of pesticide residues from fruits and vegetables as a tool to rank intake of pesticide residues in United States: A validation study. *Environ Int*. 92-93:294-300. doi: 10.1016/j.envint.2016.04.028.
- International Programme on Chemical Safety (IPCS) (2005) Chemical- specific adjustment factors for interspecies differences and human variability: guidance document for use of data in dose/ concentration-response assessment. WHO, Geneva
- Ivey, K.L., Hodgson, J.M., Croft, K.D., Lewis, J.R., Prince, R.L., 2015. Flavonoid intake and all-cause mortality. *Am J Clin Nutr*. 1:1012–1020
- Jensen, B.H., Petersen, A., Christiansen, S., Boberg, J., Axelstad, M., Herrmann, S.S., Poulsen, M.E., Hass, U., 2013. *Food Chem. Toxicol*. 55, 113–120.
- Jiang, M., Gao, H., Liu, X., Wang, Y.U., Lan, J., Li, Y., Lv, S., Zhu, K., Gong, P., 2021.

- Detection of Pesticide Residues in Vegetables Sold in Changchun City, China. *J Food Prot* 84(3):481-489.
- Joint FAO/WHO Meeting on Pesticide Residues, (JMPR) 2007. Pesticide residues in food 2007. <http://www.inchem.org/documents/jmpr/jmpmono/v2007pr01.pdf> [Accessed August 2020]
- Jones, H.M., Rowland-Yeo, K. 2013. Basic concepts in physiologically based pharmacokinetic modeling in drug discovery and development. *CPT Pharmacometrics Syst Pharmacol* 2:e63.
- Kaliste-Korhonen, E., Tuovinen, K., Hänninen, O., 1996. In vitro interspecies differences in enzymes reacting with organophosphates and their inhibition by paraoxon. *Hum Exp Toxicol* 15:972.
- Karanja, N. K., Njenga, M., Mutua, G. K., Lagerkvist, C. J., Kutto, E., & Okello, J. J. 2012. Concentrations of heavy metals and pesticide residues in leafy vegetables and implications for peri-urban farming in Nairobi, Kenya. *Journal of Agriculture, Food Systems, and Community Development*, 3(1), 255–267.
- Kasteel, E.E.J., Nijmeijer, S.M., Darney, K., Lautz, L.S., Dorne, J.L.C.M., Kramer, N.I., Westerink, R.H.S., 2020. Acetylcholinesterase inhibition in electric eel and human donor blood: an in vitro approach to investigate interspecies differences and human variability in toxicodynamics. *Arch Toxicol* 94: 4055-4065.
- Karembu, M., 1991. Pesticide use and misuse by small scale farmers in Kiambu. Kenyatta University
- Kaushal, J., Khatri, M., Arya, S.K., 2021. A treatise on Organophosphate pesticide pollution: Current strategies and advancements in their environmental degradation and elimination. *Ecotoxicol Environ Saf.* 1;207:111483.



- Kaushik, R., Rosenfeld, C.A., Sultatos, L.G. 2007. Concentration-dependent interactions of the organophosphates chlorpyrifos oxon and methyl paraoxon with human recombinant acetylcholinesterase. *Toxicol Appl Pharmacol.* 221:243-250.
- Kenya Law Reports, Pest Control Products Act, Chapter 346, Revised Edition, 2012.
- Kortenkamp, A., Backhaus, T., Faust, M.J.C., 2009. State of the Art Report on Mixture Toxicity, vol. 70307. pp. 94–103.
- Kunyanga, C. Amimo, J., Kingori L.N., Chemining'wa, G., 2018. Consumer Risk Exposure to Chemical and Microbial Hazards Through Consumption of Fruits and Vegetables in Kenya. *Food Science and Quality Management* [www.iiste.org](http://www.iiste.org). Vol.78, 2018
- Larsen, K.E., Lifschitz, A.L., Lanusse, C.E., Virkel, G.L., 2019. In vitro and in vivo effects of chlorpyrifos and cypermethrin on blood cholinesterases in sheep. *J Vet Pharmacol Ther.* 2019 Sep;42(5):548-555.
- Lee, K.-G., Lee, S.-K., 2012. Monitoring and risk assessment of pesticide residues in yuza fruits (*Citrus junos* Sieb. Ex Tanaka) and yuza tea samples produced in Korea. *Food Chem.* 135, 2930–2933
- Li B, Sedlacek M, Manoharan I, Boopathy R, Duysen EG, Masson P, and Lockridge O 2005. Butyrylcholinesterase, paraoxonase, and albumin esterase, but not carboxylesterase, are present in human plasma. *Biochem Pharmacol* 70:1673-1684.
- López-Tobón, A., Villa, C.E., Cheroni, C., Trattaro, S., Caporale, N., Conforti, P., Iennaco, R., Lachgar, M., Rigoli, M.T., de la Cruz, B.M., et al., 2018. Longitudinal dissection in brain organoids at single cell resolution uncovers the developmental role of GSK3 in human corticogenesis. *BioRxiv* 2018.

- Louisse, J., Beekmann, K., Rietjens, I.M., 2017. Use of physiologically based kinetic modeling-based reverse dosimetry to predict in vivo toxicity from in vitro data. *Chemical Research in Toxicology* 30(1): 114- 125.
- Louisse, J., Bosgra, S., Blaauboer, B.J., Rietjens, I.M.C.M., Verwei, M., 2015. Prediction of in vivo developmental toxicity of all-trans-retinoic acid based on in vitro toxicity data and in silico physiologically based kinetic modeling. *Arch Toxicol* 89:1135-1148.
- Louisse, J., de Jong, E., van de Sandt, J.J., Blaauboer, B.J., Woutersen, R.A., Piersma, A.H., Rietjens, I.M.C.M, Verwei, M., 2010. The use of in vitro toxicity data and physiologically based kinetic modeling to predict dose-response curves for in vivo developmental toxicity of glycol ethers in rat and man. *Toxicol Sci* 118:470-484
- Lozowicka, B., Kaczynski, P., Paritova, A.E., Kuzembekowa, G.B., Abzhaliyeva, A.B., Sarsembayeva, N.B., Alihan, K., 2014. Pesticide residues in grain from Kazakhstan and potential health risks associated with exposure to detected pesticides. *Food Chem. Toxicol.* 64, 238–248.
- Lu, C., Holbrook, C.M., Andres, L.M., 2010. The implications of using a physiologically based pharmacokinetic (PBPK) model for pesticide risk assessment. *Environ Health Perspect* 118:125-130.
- Lupu, D., Andersson, P., Bornehag, C.G., Demeneix, B., Fritsche, E, Gennings, C., Lichtensteiger, W., Leis, M., Leonards, P.E.G., Ponsonby, A.L., Scholze, M., Testa, G., Tresguerres, J.A.F., Westerink, R.H.S., Zalc, B., Rüegg, J., 2020. The ENDpoiNTs Project: Novel Testing Strategies for Endocrine Disruptors Linked to Developmental Neurotoxicity. *Int J Mol Sci.* 1;21(11):3978.

- Macharia, M., Kengne, A. P., Blackhurst, D. M., Erasmus, R. T., Matsha, T. E. 2014. "Paraoxonase1 Genetic Polymorphisms in a Mixed Ancestry African Population", *Mediators of Inflammation*, vol. 2014, Article ID 217019, 9 pages, 2014.
- Madden, J.C., et al., 2019. In silico resources to assist in the development and evaluation of physiologically-based kinetic models. *Comput. Toxicol. Elsevier* 11 (January), 33–49.
- Mansour, S.A., 2004. Pesticide exposure-Egyptian scene. *Toxicology* 2004; 198: 91-115
- Martin, T., Ochou, O. G., Vaissayre, M., Fournier, D. 2003. Organophosphorus insecticides synergize pyrethroids in the resistant strain of cotton bollworm, *Helicoverpa armigera* (Hübner).
- Maxwell, D.M., Lenz, D.E., Groff, W.A., Kaminskis, A., Froehlich, H.L., 1987. The effects of blood flow and detoxification on in vivo cholinesterase inhibition by soman in rats. *Toxicol Appl Pharmacol* 88: 66-76.
- Mohamed Ali, S., Chia, S.E., 2008. Interethnic variability of plasma paraoxonase (PON1) activity towards organophosphates and PON1 polymorphisms among Asian populations--a short review. *Ind Health*. 46(4):309-17.
- Mostafalou, S., Abdollahi, M., 2013. Pesticides and human chronic diseases: evidences, mechanisms, and perspectives. *Toxicol Appl Pharmacol* 268:157-177.
- Mosquin, P.L., Licata, A.C., Liu, B., Sumner, S.C., Okino, M.S., 2009. Reconstructing exposures from small samples using physiologically based pharmacokinetic models and multiple biomarkers. *J Expo Sci Environ Epidemiol* 19:284-297.
- Mutch, E., Daly, A.K., Williams, F.M., 2007. The Relationship between PON1 phenotype and PON1-192 genotype in detoxification of three oxons by human liver. *Drug Metab Dispos*. 2007 Feb;35(2):315-20.
- Muller-Vahl, K., Kolbe, H., Dengler R., 1999: Transient severe parkinsonism after acute organophosphate poisoning. *J Neurol Neurosurg Psychiatry* 1999;66:253–254.

- Mungai, J.K., Ouko, J., Heiden, M., 2000. "Processing of Fruits and Vegetables in Kenya", GTZ – Integration of tree crops into farming systems project, ICRAF House, Nairobi.
- Mutai, C., Inonda, R. Njage, E., Ngeranwa, J., 2015. Determination of Pesticide Residues in Locally Consumed Vegetables in Kenya. *African Journal of Pharmacology and Therapeutics* Vol. 4 No. 1 Pages 1-6, 2015
- Mundform, D.J., et al., 2011. Number of replications required in Monte Carlo simulation studies: a synthesis of four studies. *J. Modern Appl. Stat. Methods* 10 (1), 19–28.
- Naughton, S.X., Terry, A.V. Jr., 2018. Neurotoxicity in acute and repeated organophosphate exposure. *Toxicology* 408:101-112.
- Ngatia, S.C., Kabaara, A. M., 1976. The state of the Kenya coffee industry with reference to research and extension. *Kenya Coffee* 480: 94-99
- Ngigi, M., Njenga, M., Lagerkvist, C. J, Karanja, N., & Okello, J. 2011. *Measures to reduce food safety risks in urban and peri-urban leafy vegetables value chain in Nairobi, Kenya* [Feedback Workshop Report].
- Ngolo, P., Nawiri, M., Machochi, A., Oyieke, H., 2019. Pesticide Residue Levels in Soil, Water, Kales and Tomatoes in Ewaso Narok Wetland, Laikipia, County, Kenya. *Journal of Scientific Research and Reports*, 24(5):1-11.
- Nguyen, T. T., Rosello, C., Bélanger, R., & Ratti, C., 2020. Fate of Residual Pesticides in Fruit and Vegetable Waste (FVW) Processing. *Foods* (Basel, Switzerland), 9(10):1468.
- Ning, J., Rietjens, I.M.C.M., Strikwold, M., 2019. Integrating physiologically based kinetic (PBK) and Monte Carlo modelling to predict inter-individual and inter-ethnic variation in bioactivation and liver toxicity of lasiocarpine. *Arch Toxicol.* 93(10):2943-2960.
- NIP, (National Implication Plan for Stockholm convention on Persistent Organic Pollutants, NES.), 2006. Nairobi, Kenya: National Environmental Secretariat.

- Nishihama, Y., Nakayama, S.F., Isobe, T., Jung, C.-R., Iwai-Shimada, M., Kobayashi, Y., Michikawa, T., Sekiyama, M., Taniguchi, Y., Yamazaki, S., et al., 2021. Urinary Metabolites of Organophosphate Pesticides among Pregnant Women Participating in the Japan Environment and Children's Study (JECS). *Int. J. Environ. Res. Public Health* 18, 5929.
- Njuguna, S.M., Makokha, V.A., Yana, X., Gituru, R.W., Wanga, Q., Wanga, J., 2019. Health risk assessment by consumption of vegetables irrigated with reclaimed waste water: A case study in Thika (Kenya). *Journal of Environmental Management* 231(2019) 576–581
- Ntow, W. J., Gijzen, H. J., Kalderman, P., Drechesel, P., 2006. Farmer perceptions and pesticides use practices in vegetable production in Ghana. *Pesticide Management Science*, 62, 356–365.
- Okello, J. J., Lagerkvist, C.-J., Hess, S., Ngigi, M., Karanja, N., 2012. Choice of fresh vegetable retail outlets by developing- country urban consumers: The case of kale consumers in Nairobi, Kenya. *European Journal of Development Research*, 24, 434–449.
- Omwenga, I., Kanja, L., Nguta, J., Mbaria, J., Irungu, P., 2016. Organochlorine pesticide residues in farmed fish in Kiambu and Machakos Counties, Kenya. *Cogent Environmental Science*.
- Omwenga, I., Zhao, S., Kanja, L., Mol, H., Rietjens, I.M.C.M., Louisse, J., 2021. Prediction of dose-dependent in vivo acetylcholinesterase inhibition by profenofos in rats and humans using physiologically based kinetic (PBK) modeling-facilitated reverse dosimetry. *Arch Toxicol.* 2021 Apr;95(4):1287-1301
- Ortiz-Delgado, J.B., Funes, V., Sarasquete, C., 2019. The organophosphate pesticide -OP-

- malathion inducing thyroidal disruptions and failures in the metamorphosis of the Senegalese sole, *Solea senegalensis*. BMC Vet Res 15, 57 (2019).
- Paini, A., Leonard, J., Joossens, E., Bessems, J., Desalegn, A., Dorne, J., Gosling, J., Heringa, M., Klaric, M., Kliment, T., 2019. Next generation physiologically based kinetic (NG-PBK) models in support of regulatory decision making. Computational Toxicology 961-72.
- Pelekis, M., Nicolich, M.J., Gauthier, J.S., 2003. Probabilistic framework for the estimation of the adult and child toxicokinetic intraspecies uncertainty factors. Risk Anal 23:1239–1255.
- Pest control products Board of Kenya, 2019. accessed on 10/12/2019
- Pest control products Board of Kenya (PCPB), 2019.
- <http://www.pcpb.go.ke/list-of-registered-products/> accessed on 10/12/2019
- Pletz, J., Blakeman, S., Paini, A., Parissis, N., Worth, A., Andersson, A.M., Frederiksen, H., Sakhi, A.K., Thomsen, C., Bopp, S.K., 2020. Physiologically based kinetic (PBK) modelling and human biomonitoring data for mixture risk assessment. Environ Int. 2020 Oct;143:105978.
- Price, K., Haddad, S., Krishnan, K., 2003. Physiological modeling of age specific changes in the pharmacokinetics of organic chemicals in children. J Toxicol Environ Health Part A 66:417–433.
- Poet, T.S., Kousba, A.A., Dennison, S.L., Timchalk, C., 2004. Physiologically based pharmacokinetic/pharmacodynamic model for the organophosphorus pesticide diazinon. Neurotoxicology 25:1013-1030.
- Policy Department for External Relations, Directorate General for External Policies of the Union, 2012. The use of pesticides in developing countries and their impact on health and the right to food STUDY. <https://health.ec.europa.eu/food/docs/default-source/pesticides-study/20health%20and%20food.pdf> Accessed on 10/8/2021

- Punt, A., et al., 2016. Evaluation of interindividual human variation in bioactivation and DNA adduct formation of estragole in liver predicted by physiologically based kinetic/dynamic and Monte Carlo modeling. *Chem. Res. Toxicol.* 29 (4), 659–668.
- Pope, C.N., 1999. Organophosphorus pesticides: do they all have the same mechanism of toxicity? *J Toxicol Environ Health B Crit Rev.* 1999 Apr-Jun;2(2):161-81.
- Paul, K. C., Sinsheimer, J. S., Cockburn, M., Bronstein, J. M., Bordelon, Y., & Ritz, B. (2017). Organophosphate pesticides and PON1 L55M in Parkinson's disease progression. *Environment international*, 107, 75–81.
- Quistad, G.B., Sparks, S.E., Casida, J.E., 2001. Fatty acid amide hydrolase inhibition by neurotoxic organophosphorus pesticides. *Toxicol Appl Pharmacol* 173: 48-55.
- Quistad, G.B., Liang, S.N., Fisher, K.J., Nomura, D.K., Casida, J.E., 2006. Each lipase has a unique sensitivity profile for organophosphorus inhibitors. *Toxicol Sci* 91:166-172.
- Razzaghi, N., Ziarati, P., Rastegar, H., Shoeibi, S., Amirahmadi, M., Conti, G.O., Ferrante, M., Fakhri, Y., Mousavi Khaneghah, A., 2018. The concentration and probabilistic health risk assessment of pesticide residues in commercially available olive oils in Iran. *Food Chem Toxicol.* 2018 Oct;120:32-40.
- Reffstrup, T.K., Larsen, J.C., Meyer, O., 2010. Risk assessment of mixtures of pesticides. Current approaches and future strategies. *Regul Toxicol Pharmacol.* 2010 Mar;56(2):174-92.
- Research Solutions Africa, (RSA) Ltd, 2015. Report of a market study on fresh vegetables market in Kenya. Consumer's survey. December 2015. and future strategies. *Regul Toxicol Pharmacol* 56: 174-192.

- Richards, P.G., Johnson, M.K., Ray, D.E., 2000. Identification of acylpeptide hydrolase as a sensitive site for reaction with organophosphorus compounds and a potential target for cognitive enhancing drugs. *Mol Pharmacol* 58:577-583.
- Ridolfi, C., Hoffmann, V., Baral, S., Post-harvest Losses in Fruits and Vegetables: The Kenyan Context, Working Paper, Review, 2018.
- Risher, J., Navarro, H. A., 1997. Toxicological profile for chlorpyrifos. US Department of Health and Human Services. Agency for Toxic Substance and Disease Registry. <https://www.atsdr.cdc.gov/toxprofiles/tp84.pdf>. Accessed on 4/9/2021.
- Robb, E.L., Baker, M.B., 2020. Organophosphate Toxicity. 2020 In: StatPearls [Internet]. Treasure Island (FL): StatPearls Publishing; 2021 Jan-. PMID: 29261901.
- Saha, N., Zaman, M.R., 2012. Evaluation of possible health risks of heavy metals by consumption of foodstuffs available in the central market of Rajshahi City, Bangladesh. *Environ Monit Assessment*. 185(5):3867–78.
- Sapozhnikova, Y., 2014. Evaluation of low-pressure gas chromatography-tandem massspectrometry method for the analysis of >140 pesticides in fish. *J. Agric. FoodChem*. 62, 3684–3689
- Satoh, T., Hosokawa, M. 2006. Structure, function and regulation of carboxylesterases. *Chem Biol Interact* 162:195-211.
- Scacchi, R., Corbo, R.M., Rickards, O., Stefano, G.F., 2003. New data on the world distribution of paraoxonase (PON1 Gln192-Arg) gene frequencies. *Hum Biol* 75:365–373.
- Slob, W., 2006. Probabilistic dietary exposure assessment taking into account variability in both amount and frequency of consumption. *Food Chem. Toxicol*. 44 (7), 933–951.



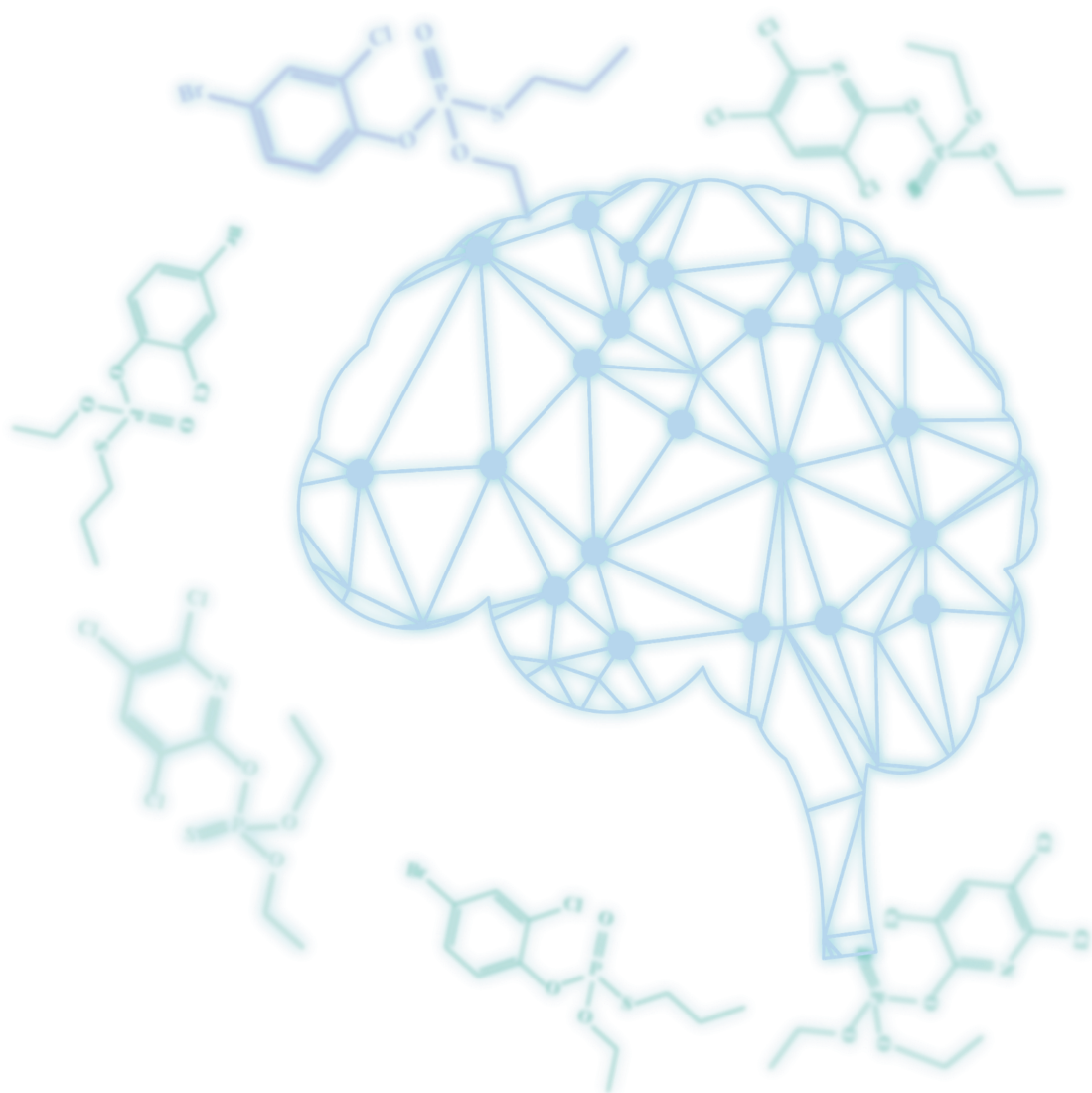
- Smegal, D. C. (2000). Revised human health risk assessment chlorpyrifos (pp. 1-131). Washington: EPA
- Schneider Medeiros, M., Reddy P.S, Socal, M., P, Schumacher-Schuh, A.F., Mello Rieder, C.R., 2020. Occupational pesticide exposure and the risk of death in patients with Parkinson's disease: an observational study in southern Brazil. *Environ Health.* 17;19(1):68.
- Sogorb, M.A., González-González, I., Pamies, D., Vilanova, E., 2010. An alternative in vitro method for detecting neuropathic compounds based on acetylcholinesterase inhibition and on inhibition and aging of neuropathy target esterase (NTE). *Toxicol In Vitro.* 24(3):942-52.
- Sprandel, K.A., et al., 2006. Population pharmacokinetic modeling and Monte Carlo simulation of varying doses of intravenous metronidazole. *Diagn. Microbiol. Infect. Dis.* 55 (4), 303–309.
- Strikwold, M., Spenkelink, B., de Haan, L.H.J., Woutersen, R.A., Punt, A., Rietjens, I.M.C.M. 2017. Integrating in vitro data and physiologically based kinetic (PBK) modelling to assess the in vivo potential developmental toxicity of a series of phenols. *Arch Toxicol* 91:2119-2133
- Strikwold, M., Spenkelink, B., Woutersen, R.A., Rietjens, I.M.C.M., Punt, A., 2013. Combining in vitro embryotoxicity data with physiologically based kinetic (PBK) modelling to define in vivo dose-response curves for developmental toxicity of phenol in rat and human. *Arch Toxicol* 87:1709-1723
- Suarez-Lopez, J.R., Himes, J.H., Jacobs, D.R. Jr., Alexander, B.H., Gunnar, M.R., 2013.

- Acetylcholinesterase activity and neurodevelopment in boys and girls. *Pediatrics*. 132(6):e1649-58. doi: 10.1542/peds.2013-0108. Epub 2013 Nov 18. PMID: 24249815; PMCID: PMC3838526.
- Sultatos, L.G. 1990. A physiologically based pharmacokinetic model of parathion based on chemical-specific parameters determined in vitro. *J Amer Coll Toxicol* 9:611-619.
- Suratman, S., Edwards, J.W., Babina, K., 2015. Organophosphate pesticides exposure among farmworkers: pathways and risk of adverse health effects. *Rev Environ Health*. 30(1):65-79. doi: 10.1515/reveh-2014-0072. PMID: 25741936
- Talk Africa – Association for Freelance Journalists, Agriculture Stakeholders Support Kenya Government’s Upgrade of Pesticide Legislation, online publication, 2019.
- te Biesebeek, J.D., Sam, M., Sprong, R.C., van Donkersgoed, G., Kruisselbrink, J.W., de Boer, W.J., van Lenthe, M., van der Voet, H., van Klaveren, J.D., 2021. Potential impact of prioritization methods on the outcome of cumulative exposure assessments of pesticides. EFSA supporting publication 2021:EN-6559. 91 pp. doi:10.2903/sp.efsa.2021.EN-6559
- Terry, A.V. Jr., 2012. Functional consequences of repeated organophosphate exposure: Potential noncholinergic mechanisms. *Pharmacol Ther*. Jun; 2012 134(3):355–65. [PubMed: 22465060]
- Timchalk, C., Nolan, R.J., Mendrala, A.L., Dittenber, D.A., Brzak, K.A., Mattsson, J.L., 2002. A physiologically based pharmacokinetic and pharmacodynamic (PBPK/PD) model for the organophosphate insecticide chlorpyrifos in rats and humans. *Toxicol Sci* 66:34-53.
- Timchalk, C., Poet, T.S., 2008. Development of a physiologically based pharmacokinetic and

- pharmacodynamic model to determine dosimetry and cholinesterase inhibition for a binary mixture of chlorpyrifos and diazinon in the rat. *Neurotoxicology*. 29(3):428-43.
- Voorhees, J. R., Rohlman, D. S., Lein, P. J., & Pieper, A. A., 2017. Neurotoxicity in Preclinical Models of Occupational Exposure to Organophosphorus Compounds. *Frontiers in neuroscience*, 10, 590.
- Wani, W. Y., Kandimalla, R. J. L., Sharma, D. R., Kaushal, A., Ruban, A., Sunkaria, A., Vallamkondu, J., Chiarugi, A., Reddy, P. H., and Gill, K. D., 2017. Cell cycle activation in p21 dependent pathway: An alternative mechanism of organophosphate induced dopaminergic neurodegeneration. *Biochim. Biophys. Acta* 1863, 1858–1866.
- Wang, A. ,Cockburn, M., Ly, T. T., Bronstein, J. M., and Ritz, B. 2014. The association between ambient exposure to organophosphates and Parkinson’s disease risk. *Occup. Environ. Med.* 71,275–281.doi:10.1136/oemed-2013-101394
- Wang, J, Chow W, Wong JW, Leung D, Chang J, Li M. Non-target data acquisition for target analysis (nDATA) of 845 pesticide residues in fruits and vegetables using UHPLC/ESI Q-Orbitrap. *Anal Bioanal Chem.* 2019 Mar;411(7):1421-1431.
- Williams, E.T., Bacon, J.A., Bender, D.M., Lowinger, J.J., Guo, W.K., Ehsani, M.E., Wang, X., Wang, H., Qian, Y.W., Ruterbories, K.J., Wrighton, S.A., Perkins, E.J. 2011. Characterization of the expression and activity of carboxylesterases 1 and 2 from the beagle dog, cynomolgus monkey, and human. *Drug Metab Dispos* 39: 2305-2313.
- WHO, 2003. GEMS/food Regional Diets (Regional Per Capita Consumption of Raw and Semi-Processed Agricultural Commodities). Retrieved from.[http://www.who.int/foodsafety/publications/chem/regional\\_diets/en/](http://www.who.int/foodsafety/publications/chem/regional_diets/en/)(accessed December2019)
- Wright, M. J., and Keller-Byrne, J., 2005. Environmental Determinants of Parkinson's

- Disease, Archives of Environmental & Occupational Health, 60:1, 32-38,
- Yang, F.W., Li, Y.X., Ren, F.Z., Luo, J., Pang, G.F., 2019. Assessment of the endocrine-disrupting effects of organophosphorus pesticide triazophos and its metabolites on endocrine hormones biosynthesis, transport and receptor binding in silico. Food Chem Toxicol. 133:110759.
- Zhao, S., Kamelia, L., Boonpawa, R., Wesseling, S., Spenkelink, B., Rietjens, I.M.C.M., 2019. Physiologically based kinetic modelling-facilitated reverse dosimetry to predict in vivo red blood cell acetylcholinesterase inhibition following exposure to chlorpyrifos in the Caucasian and Chinese population. Toxicol Sci 171: 69–83.
- Zhang, A., Luo, W., Sun, J., Xiao, H., Liu, W., 2015. Distribution and uptake pathways of organochlorine pesticides in greenhouse and conventional vegetables. Sci Total Environ 2015; 505: 1142-1147.
- Zhang, H., Wang, S., Zhou, Z., Pan, P., Zhang, J., Niu, W., 2008. Food Safety: Monitoring of Organophosphate Pesticide Residues in Crops and Food, Phosphorus, Sulfur, and Silicon, 183:2-3, 280-290,
- Zhao, S., Wesseling, S., Spenkelink, B., Rietjens, I.M.C.M., 2021. Physiologically based kinetic modelling based prediction of in vivo rat and human acetylcholinesterase (AChE) inhibition upon exposure to diazinon. Arch Toxicol. 2021 May;95(5):1573-1593.
- Zimmer, J., Kristensen, B. W., Jakobsen, B., Noraberg, J., 2000. Excitatory amino acid neurotoxicity and modulation of glutamate receptor expression in organotypic brain slice cultures. Amino Acids 19, 7–21.





# CHAPTER 7.

Summary

## Summary

The use of chemical pesticides is indispensable in Kenya due to the hot and humid tropical environmental conditions that are conducive to the development of pests, weeds, and disease vectors. Currently, OPs are among the most widely used pesticides in agriculture, and their residues have been found in various foods. Currently, PODs have been derived from data on OP-induced AChE inhibition from animal studies, and this is undesirable due to economical, ethical and scientific limitations. The main aim of this thesis was to develop non-animal approaches in OP risk assessment and application of these novel methods to predict the potential of the OPs to inhibit AChE *in vivo* upon acute exposure, also taking combined exposure into account. Furthermore, this thesis aimed to obtain data on the occurrence of OPs on commonly consumed vegetables in Kenya, as such data, and related estimations of human exposure, are lacking. **Chapter 1** of the thesis provides background information on OP use in agriculture, the exposure of non-target species to OPs and a description of the characteristics and toxicity of the OPs studied in this thesis, profenofos (PFF), and chlorpyrifos (CPF). This chapter also presents background information on the hazard assessments for PFF and CPF and presents the concepts of PBK modelling-based reverse dosimetry and approaches used to assess combined exposure. **Chapter 2** analyses the occurrence of OPs in commonly consumed vegetables in Kenya and assesses the accompanying exposure and health risks. A total of 90 samples were analysed by liquid chromatography/high-resolution tandem mass spectrometry. Residues of acephate, CPF, methamidophos, omethoate and PFF were found in 22% of the samples, at levels ranging from 10 to 1343 µg/kg. The EU MRL for these OPs was exceeded in 21%, 10%, 8% and 22% of the samples of French beans, kales, spinach, and tomatoes, respectively. CPF in spinach had an acute Health Quotient (HQ) of 3.3 and 2.2 for children and adults, respectively, implying that potential health risks with respect to acute dietary exposure cannot be excluded. For chronic



dietary exposure, all chronic HQs were below 1. The Health Index (HI) for the pesticides, i.e. the sum of the chronic HQs, was 0.54 and 0.34 for children and adults, respectively.

**Chapter 3** proposes a combined in vitro-in silico approach to predict AChE inhibition by the OP profenofos in rats and humans by applying PBK modelling-facilitated quantitative in vitro to in vivo extrapolation (QIVIVE). A PBK model was developed for both species. Parameter values for profenofos conversion to 4-bromo-2-chlorophenol (BCP) were derived from in vitro incubations with liver microsomes, liver cytosol, and plasma from rats and humans whereas other chemical-related parameter values were derived using in silico calculations. The PBK model predictions were evaluated by comparison to literature data on profenofos kinetics in rats following oral exposure (Cho et al., 2002). To facilitate PBK model based quantitative in vitro to in vivo extrapolation (QIVIVE), concentration-dependent inhibition of rat and human AChE was determined in vitro and these data were translated with the PBK models to predicted dose-dependent AChE inhibition curves in rats and humans in vivo. When the predicted dose-response curve for PFF-induced AChE inhibition in rats was compared to literature data, the prediction of the in vivo effect levels appeared accurate. Comparison of rat predictions (the BMDL10 of the predicted dose-response curve being 0.45 mg/kg bw) and human predictions (the BMDL10 of the predicted dose-response curve being 0.01 mg/kg bw) suggested humans to be more sensitive than rats. The PBK models revealed that this difference appeared to be mainly due to higher catalytic efficiencies for microsomal, cytosolic and plasma biotransformation of PFF to BCP in rats as compared to humans. Another possible reason for the differences in PFF detoxification may be related to quantitative differences in B-esterases in rats and humans, which may affect the metabolism and disposition of ester compounds including OPs. B-esterases, such as carboxylesterase (CaE), butyrylcholinesterase (BuChE) and acetylcholinesterase (AChE), detoxify oxons, but these enzymes are inhibited by the oxons as a consequence. In this way, B-esterases may play a protective role in rats but not humans. It has

been reported that rat plasma contains almost all types of esterases including CaE, PON1, BChE, and AChE, whereas humans are deficient of plasma CaE and plasma AChE. The absence of CaE in human plasma in addition to low PON1 activity may therefore be responsible for lower PFF clearance resulting in higher sensitivity of humans to PFF as compared to rodents . Altogether, the results demonstrate that in vivo AChE inhibition upon acute exposure to profenofos was closely predicted in rats, indicating the potential of this novel approach method in chemical hazard assessment.

**Chapter 4** investigates the combination effects of two selected OPs (PFF and CPF), by studying the combined effects of PFF and CPF's toxic metabolite chlorpyrifos oxon (CPO) on AChE inhibition in vitro, as well as the effects of CPF and CPO on PFF biotransformation (detoxification) by human liver microsomes, cytosol, and human plasma. The PFF physiologically based kinetic (PBK) model developed in chapter 3 was extended to include the description of CPF kinetics, using also in vitro kinetic data from the literature and in silico calculations. The PFF concentrations in the model are expressed as CPO-equivalents (i.e., using a TEF/RPF approach) allowing prediction of total internal CPO-equivalents (and related effects on AChE activity) upon combined exposure to PFF and CPF. AChE inhibition was shown to be 199-fold more potent by CPO than by PFF, and combined exposure to CPO and PFF resulted in effects that are in line with the principles of dose addition. CPF and CPO appeared to affect PFF detoxification to its main metabolite (BCP) in a non-competitive manner at high concentrations, with  $K_i$  values of 120, 256 and 473  $\mu\text{M}$  for CPF, and 80, 63 and 326  $\mu\text{M}$  for CPO, for liver microsomes, liver cytosol and plasma, respectively, concentrations far higher than in vivo relevant concentrations. The model adequately predicted the AChE inhibition in a hospitalized person with CPF poisoning as reported in the literature (Drevenkar et al., 1993). Combined exposure to PFF and CPF at their ARfD (0.005 mg/kg bw) was predicted to not affect AChE activity. Altogether, this study reveals that AChE inhibition upon combined

exposure to these OPs follows the concept of dose addition, and that at estimated exposure levels, no toxicokinetic interactions of CPF on PFF detoxification are expected

**Chapter 5** aimed to predict human interindividual differences in PFF detoxification based on a combined in vitro-in silico approach to account for human variability in toxicokinetics. To that end, PFF conversion to BCP was studied in in vitro incubations with S9 liver fractions of 25 different Caucasian donors and with plasma samples of 25 different Caucasian donors. The obtained information on the variation in the in vitro kinetic constants  $V_{max}$  and  $K_m$ , was applied in the PBK model developed in Chapter 3 using a Monte Carlo simulation modelling approach. Internal concentrations were estimated for the geometric mean (GM), the 90<sup>th</sup>, 95<sup>th</sup> and 99<sup>th</sup> percentiles of the simulated virtual population. The model was then used for reverse dosimetry of the in vitro data on PFF-induced AChE inhibition of Chapter 3. Also, the interindividual variability in PFF toxicokinetics was quantified by dividing the internal  $C_{max}$  concentrations of profenofos for the 90<sup>th</sup> or 99<sup>th</sup> percentile by that of the GM, which was compared to the default uncertainty factor for interindividual differences in kinetics (IPCS 2005). The predicted BMDL10 for the 99<sup>th</sup> percentile was compared to PODs of the regulatory bodies. Analysis of the predicted internal maximum concentrations of PFF in the simulated population indicated a 1.4-, 1.4- and 1.5-fold difference between the geometric mean (GM) and the 90<sup>th</sup>, 95<sup>th</sup> and 99<sup>th</sup> percentile, respectively, of the simulated population. These factors are below the default uncertainty factor accounting for human variability in toxicokinetics of 3.16. Concentration-response curves for inhibition of human AChE determined in vitro were translated with the PBK models to predicted dose-dependent AChE inhibition in humans in vivo. In line with the differences in  $C_{max}$  values, the 99<sup>th</sup> percentile of the population was predicted to be 1.5-fold more sensitive to PFF-induced AChE inhibition than the GM of the population based on the BMDL10 values of predicted dose-response data for the virtual populations. Comparing the predicted BMDL10 of 0.0057 mg/kg bw for the 99<sup>th</sup> percentile

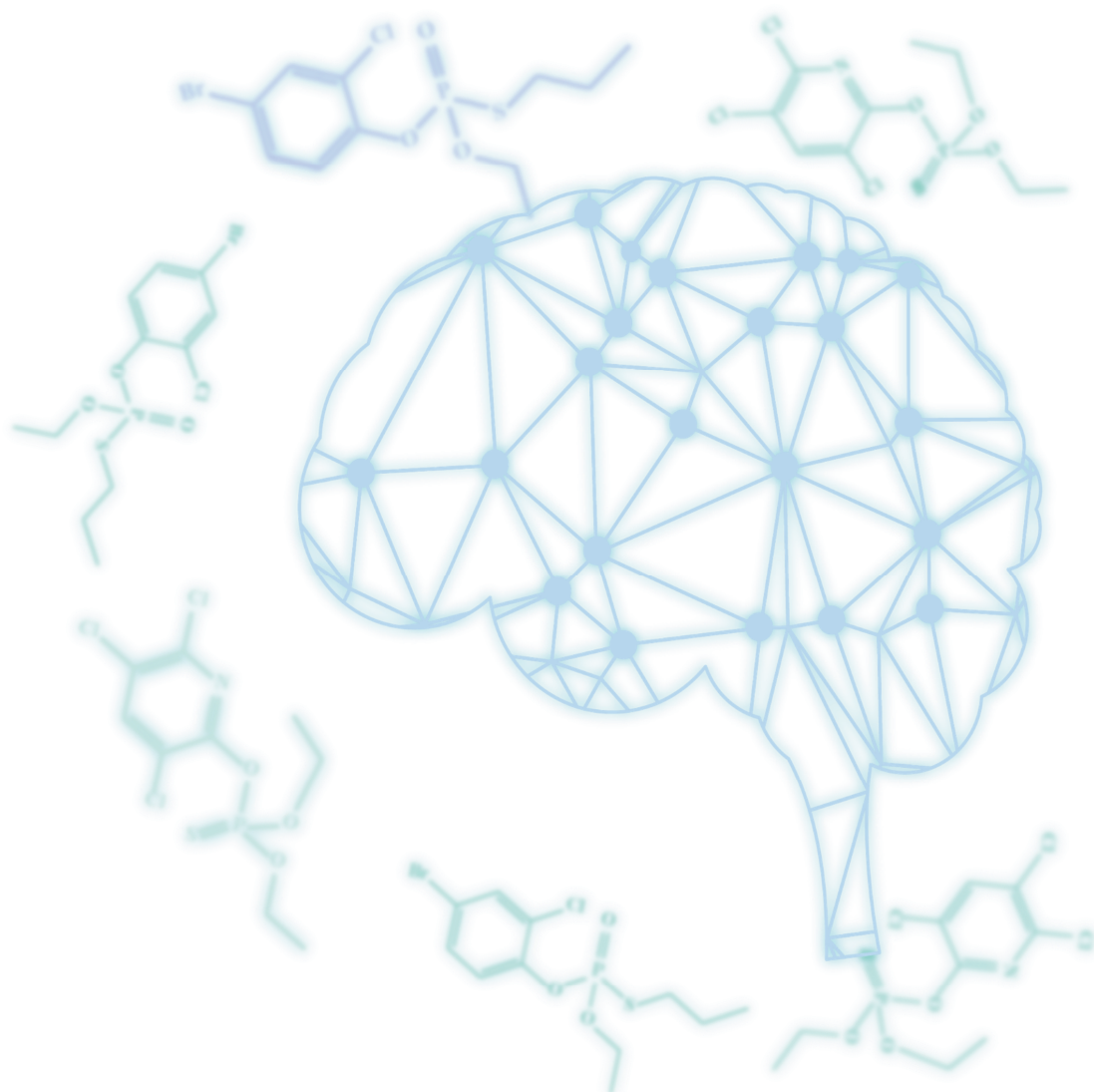
with health based guidance values proposed by the regulatory bodies reveals a close similarity to the ARfD reported by EFSA, (2019) of 0.005 mg/kg bw, based on a German evaluation, and being slightly higher than the ARfD adopted by EPA, (2016) of 0.002 mg/kg bw. It is, however, 200-fold lower than the ARfD of 1 mg/kg bw adopted by JMPR, (2007). The results from this thesis would support the use of the ARfD of 0.005 mg/kg bw rather than the ARfD of 1 mg/kg bw, as at 1 mg/kg bw clear PFF-induced AChE inhibition was predicted in humans. Altogether, the results obtained demonstrate that integrating PBK modelling with Monte Carlo simulations using human in vitro data provides a powerful strategy to quantify human interindividual variation in kinetics, which can be used to refine the hazard characterization of OPs.

Finally, **Chapter 6** of the present thesis discusses the general discussion of the results of the previous chapters and highlights on the future perspectives for research in the use of alternative methods in risk assessment of OPs.

In conclusion, the present thesis showed novel insights into hazards and risks following exposure to OPs via residues present in vegetables in Kenya. The assessment of the levels of OPs in vegetables in Kenya revealed that PFF and CPF were the most frequently encountered pesticide residues, and that CPF and PPF (when applying EFSA's latest ARfD) had for some situations an acute HQ higher than 1, implying that potential health risks with respect to acute dietary exposure cannot be excluded. Therefore, routine monitoring of OPs and carbamates in vegetables is recommended to minimize consumers' health risks.

Upon development of PFF PBK model adequate predictions were obtained for dose levels leading to in vivo AChE inhibition upon acute exposure to single or combined OPs, providing another proof-of-principle that with this new approach methodology (NAM) in vivo effects of chemicals can be predicted without the use of in vivo studies. In addition, the prediction of interindividual differences in PFF detoxification using PBK modelling linked to Monte Carlo simulation followed by PBK modelling based reverse dosimetry revealed a close similarity

between the predicted BMDL10 of the sensitive segment of the population and the latest ARfD reported by EFSA (2019) based on German evaluation. Finally, the present thesis has provided further proofs-of-principle that the PBK model-facilitated reverse dosimetry solely based on in vitro assays and in silico data, together with a relative potency factor methodology or Monte Carlo simulation, can be adequately used to derive PODs and provide data that may be used to derive a chemical specific adjustment factor (CSAF) value for defining inter-species and inter-individual differences in OP-induced RBC AChE inhibition resulting from the variability in toxicokinetics following acute oral exposure to an OP. The current and next generation human health risk assessors for OPs may utilize data generated in the present thesis on directly predicted PODs for the human situation based on the combined in vitro and in silico approach without the need for in vivo animal studies. Altogether, the current work supports the implementation of the 3Rs principle, the application of NAMs in next generation OP-human risk assessment and regulatory decision making.



# Appendices

Acknowledgements

Lists of Publications

About the author

Overview of Completed Training Activities

## Acknowledgements

I would like to express my sincere gratitude and appreciation to all people who encouraged and supported me throughout my PhD journey to get to where I am now. Without you, the journey would have been more difficult.

First I would like to sincerely thank you my promoter Prof. Dr. Ivonne Rietjens for your support, guidance and encouragement throughout the period of study. Thank you Ivonne for the opportunity to join the Division of Toxicology as a PhD student. Apart from the scientific knowledge, I have learnt many positive attributes, such as working in a smart and efficient way. I also highly appreciate your quick and constructive feedback during the writing process, especially at the last stage of my thesis. Despite the pandemic posing a new challenge last year, thank you Ivonne for your help in tackling one of the most critical and difficult moments of a PhD project. From you I learnt the meaning of a good scientist.

To my co-promoter Dr. Jochem Louisse, thank you so much for your dedicated support during the scholarship application process. We actually knew each other long before we met. I am grateful for your patience, guidance and critical comments throughout this journey. I appreciated and enjoyed the meetings we had and the discussions we had along the way, especially when we figured out the way forward after encountering challenges. I really appreciate your dedicated support and guidance on modelling. You challenged me to always learn more. All along, you were always ready and willing to help, and I highly appreciate you for that. I admired your thorough and diligent working style. I sincerely appreciate you for all you did to and the advice you provided.

To my co-promotor Dr. Hans Mol, thank you so much for your valuable advice and guidance throughout this journey. I really appreciate your critical comments on my publications and thesis. I am also grateful for the meetings we had to figure out risk assessment approach for my first paper. All your contributions are highly appreciated.



I would also like to thank the PhD thesis committee Prof. Dr. Violette Geissen, Dr. Jessica Broeders, Dr. Paul Scheepers and Dr. Remco Westerink, for the effort and time you expended to critically review this PhD thesis.

To everyone at TOX, thank you so much for your support and comradery. Sebas, thank you so much for your assistance and help in the ordering of products, setting up the methods of UPLC and being so patient to teach me how to use the machines. Thank you so much for the conversations we had about the Dutch lifestyle, family and your beautiful cat. I really appreciate you for your time, effort, and positive energy. Bert, thank you for helping me solve challenges related to the running of the UPLC. Thank you also for very well organized AChE practicals. I enjoyed the conversations we had in the lab and thank you for sharing your family pictures and stories of grandchildren me thank you for the great time! Nico and Hans, thanks for the nice talks during the coffee breaks/lunch, and the constructive questions during my research in progress presentations. Letty, thanks for your help in arranging PET courses. Laura, it was working with you in organizing for practical courses and for the chats from time to time. Lidy, thank you so much for all your help since my resumption of my studies until your last day at TOX. Carla and Gerda, thank you so much also for all your help with all administrative matters. To all the *Intoxicated PhDs* (old and new), I am so happy and grateful to have shared this time with you (birthdays, Sinterklaas, dinners, BBQs, etc). I'm grateful to all of my former and current office mates for the time we shared, I really had a wonderful time with you all. Felicia, Danlei, Bohan, Edit and Jing, thank you so much for being so cheerful, you made the office warm and a fun place be. I thank you for the good chats and encouragements during this journey. To all the former and current PhDs I have been privileged to meet;

Aafke, Akanksha, Annelies, Artem, Ashraf, Aziza, Biyao, Bohan, Chen, Danlei, Diana, Diego, Edith, Felicia, Frances, Gogo, Ixchel, Jia, Jiaqi, Jin Jing, Jing, Jingxuan, Katharina, Katja, Lenny, Liang, Lu, Maartje, Marta, Mebrahtom, Mengying, Menno, Merel, Miaoying, Nacho,

Nina, Orsolya, Pim, Qianrui, Qiuhui, Shensheng, Shuo, Suparmi, Tessa, Veronique, Weija, Yasser and Yiming, I wish you all a wonderful time and for those who already finished, all the success in the future! To Felicia, Diana, Annelies, Ixchel, Aziza, Menno, Mebrahtom, Shengsheng, Edith, Miaoying, and Diego, thanks for the friendship and it was great to have worked (and talked) with you. To all current, and new PhDs not included here, I wish you the best!

To Shensheng, thank you so much for the long hours of work we did together, for the enlightening discussions and laughs we had as we worked on our pet subject of pesticides. The constant support and encouragement we gave to each other was important.

To the Kenyans in WUR, Joshua, Faith, Shaphan, Asaph, Alex, Jared, Jane, Jasper, Kirina, Boit, Emma, Emily, Jackie, Hellen, Jasper, Mendi, Nyokabi, Shikuku, Ojos, Asaah, Migose, Richard, DK, Esther, Nathaniel, Mercy and Brian, thank you all for the hearty laughs, the chats, dinners, the BBQs and all the moments we shared, you are amazing! The constant support we gave to each other was important.

Finally, the most important to me, my family: My love and best friend Elcah, daughter Briella and son Omwenga junior, thank you for the love and the patience during this treacherous journey. To my all-time cheerleaders; Dad Samson Omwenga, Mom Marcellah Kemunto, brothers Ben and Andrew, sisters Judy and Evelyn, I love you all. Your constant prayers and support is highly appreciated. I couldn't have done all this without you!

## List of Publications

**Omwenga I**, Kanja L, Zomer P, Louisse J, Rietjens IMCM, Mol H. Organophosphate and carbamate pesticide residues and accompanying risks in commonly consumed vegetables in Kenya. Food Addit Contam Part B Surveill. 2021 Mar;14(1):48-58. doi: 10.1080/19393210.2020.1861661.

**Omwenga I**, Zhao S, Kanja L, Mol H, Rietjens IMCM, Louisse J. Prediction of dose-dependent in vivo acetylcholinesterase inhibition by profenofos in rats and humans using physiologically based kinetic (PBK) modeling-facilitated reverse dosimetry. Arch Toxicol. 2021 Apr; 95(4):1287-1301. doi: 10.1007/s00204-021-03004-4. Epub 2021 Mar 2.

**Omwenga I**, Zhao S, Mol H, Rietjens IMCM, Louisse J. Prediction of in vivo acetylcholinesterase inhibition upon acute combined exposure to profenofos and chlorpyrifos by using a combined in vitro and in silico approach. *(Submitted)*

**Omwenga I**, Zhao S, Mol H, Rietjens IMCM, Louisse J. Predicting interindividual differences in profenofos detoxification based on in vitro kinetic data and a physiologically based kinetic (PBK) and Monte Carlo modelling approach. *In preparation*

## About the Author

Isaac Omwenga was born on 31 December 1985 in Nyamira, Kenya. He studied Veterinary Medicine and Surgery at the University of Nairobi, Kenya. After obtaining his BVM in 2010, he was awarded a University of Nairobi scholarship to pursue his MSc studies in Pharmacology and Toxicology in the same university. Thereafter, he was awarded the Netherlands Universities Foundation for international Cooperation (NUFFIC) scholarship under the Netherlands fellowship program (NFP) to pursue a PhD in Toxicology at the Division of Toxicology, Wageningen University and Research under the supervision of Prof. Dr. Ivonne Rietjens, Dr. Jochem Louisse and Dr. Hans Mol. The results of the research program are presented in this thesis. During his PhD he followed a postgraduate education in Toxicology (PET) as part of the training required for the registration as European Toxicologist.

# Overview of Completed Training Activities

## Discipline specific courses

<b>Name of Course</b>	<b>Organising Institute and Year</b>
Mutagenesis and Carcinogenesis	Postgraduate Education in Toxicology (PET), 2019
Cell Toxicology	PET, 2019
Molecular Toxicology	PET, 2019
Pathobiology	PET, 2020
Organ Toxicology	PET, 2020
Introduction Laboratory Animal Science	PET, 2020
Medical and Forensic Toxicology	PET, 2019

## Conferences

Society of Toxicology 59 <sup>th</sup> Scientific conference (SOT) 2020 (Virtual)	California, 2020
SOT 60th Annual Meeting (Virtual)	2021

## General Courses

Risk assessment	Wageningen University and Research (WUR), 2018
Brain Training	WUR, 2019
Introduction to R	WUR, 2019
Scientific Writing	WUR, 2020
Start to teach	WUR, 2019
Philosophy and Ethics of Food Science and Technology	WUR, 2020

## Optional

General Toxicology	WUR, 2018
Food Toxicology	WUR, 2019
Environmental Toxicology	WUR, 2019
Preparation of Research proposal	WUR, 2015
Introduction to Epidemiology and public health	WUR, 2020
Scientific presentations at Division of Toxicology	WUR, 2018-2021

**Approved by Graduate School VLAG**





